World Journal of
Gastroenterology®

Volume 13 Number 20
May 28, 2007

National Journal Award
2005

The WJG Press

World Journal of Gastroenterology

www.wjgnet.com

Volume 13   Number 20   May 28   2007

WJG

World Journal of
Gastroenterology®

A Weekly Journal of Gastroenterology and Hepatology

World Journal of
Gastroenterology®

Volume 13 Number 20
May 28, 2007

National Journal Award
2005

The WJG Press

Contents

Contents

Contents

Responsible E-Editor for this issue: Gong-Jing Chen

C-Editor for this issue: Maria Isabel Torres, Professor

Responsible S-Editor for this issue: Ye Liu

Positron emission tomography/computer tomography: Challenge to conventional imaging modalities in evaluating primary and metastatic liver malignancies

Long Sun, Hua Wu, Yong-Song Guan

Long Sun, Hua Wu, Minnan PET Center, The First Hospital of Xiamen, Fujian Medical University, Xiamen 316003, Fujian Province, China
Yong-Song Guan, West China Hospital of Sichuan University, Chengdu 610041, Sichuan Province, China
Yong-Song Guan, State Key Laboratory of Biotherapy, West China Medical School, Sichuan University, Gaopeng Street, Keyuan Road 4, Chengdu 610041, Sichuan Province, China
Correspondence to: Yong-Song Guan, West China Hospital of Sichuan University, Chengdu 610041, China. yongsongguan@yahoo.com
Telephone: +86-28-85421008 Fax: +86-28-85538359
Received: 2007-03-21   Accepted: 2007-04-16

Abstract

Computer tomography (CT) and magnetic resonance imaging (MRI), as conventional imaging modalities, are the preferred methodology for tumor, nodal and systemic metastasis (TNM) staging. However, all the noninvasive techniques in current use are not sufficiently able to identify primary tumors and even unable to define the extent of metastatic spread. In addition, relying exclusively on macromorphological characteristics to make a conclusion runs the risk of misdiagnosis due mainly to the intrinsic limitations of the imaging modalities themselves. Solely based on the macromorphological characteristics of cancer, one cannot give an appropriate assessment of the biological characteristics of tumors. Currently, positron emission tomography/computer tomography (PET/CT) are more and more widely available and their application with ^{18}F-fluorodeoxyglucose (^{18}F-FDG) in oncology has become one of the standard imaging modalities in diagnosing and staging of tumors, and monitoring the therapeutic efficacy in hepatic malignancies. Recently, investigators have measured glucose utilization in liver tumors using ^{18}F-FDG, PET and PET/CT in order to establish diagnosis of tumors, assess their biologic characteristics and predict therapeutic effects on hepatic malignancies. PET/CT with ^{18}F-FDG as a radiotracer may further enhance the hepatic malignancy diagnostic algorithm by accurate diagnosis, staging, restaging and evaluating its biological characteristics, which can benefit the patients suffering from hepatic metastases, hepatocellular carcinoma and cholangiocarcinoma.

INTRODUCTION

Positron emission tomography (PET) is a noninvasive imaging technique that provides a functional or metabolic assessment of normal tissues or diseased conditions[1-3]. PET is now widely applied in clinical oncology. The development of the resolution and sensitivity of PET have been improved by the availability of newer scanners with a larger field of view and introduction of integral PET and computer tomography (CT) systems in 2000[4,5]. An additional factor is the decision by the Centers for Medicare and Medicaid Services to approve reimbursement for several oncologic clinical indications for PET, including the staging and restaging of non-small-cell lung, esophageal, colorectal, breast, and head and neck cancers, cervical cancer, as well as lymphoma and melanoma, and the monitoring of the response to treatment of breast cancer[6].

Asian and Western populations have their own characteristic disease spectrum and cancer incidence[7]. Hepatocellular carcinoma (HCC) and cholangiocarcinoma (CC) are the major primary hepatic malignancies in the world. In the United States, about 150 000 patients are diagnosed with colon cancer each year, and more than 50 000 of them will develop liver metastases[8]. HCC is one of the most common cancers in Asians and its mortality is just secondary to lung cancer in urban regions and gastric carcinoma in rural regions in China[9]. The incidence of CC is increasing worldwide and CC is a devastating malignancy with a high mortality that presents late and is difficult to diagnose[10]. At present, PET and PET/CT with ^{18}F-fluorodeoxyglucose (^{18}F-FDG) have joined the

team for the workup and management of selected patients suffering from hepatic colorectal metastases, HCC or CC[11]. This review focuses on the application of PET and PET/CT with ^{18}F-FDG as a radiotracer in the evaluation of hepatic malignancies, including their diagnosis, staging and restaging, evaluation of their biologic characteristics, making a treatment plan and monitoring their responses, detection of early recurrence and assessment of their prognosis.

PET AND PET/CT *VS* CONVENTIONAL IMAGING MODALITIES

Compared to conventional imaging technologies, including CT and conventional magnetic resonance imaging (MRI), PET provides information about functional or metabolic characteristics for detection of malignancies, characterization of tumor stage, assessment of therapeutic response, and tumor recurrence, whereas CT predominantly shows the anatomical or morphologic features of tumors (i.e. size, density, and shape, *etc*)[12,13]. Conventional imaging modalities reveal morphology of lesions with largely nonspecific features. Therefore, differentiation between malignant and benign lesions could be improved by PET with its metabolic assessment[14]. Furthermore, PET has a high sensitivity in identifying areas involving cancer at an early stage. In general, accelerated radiotracer activity occurs before changes occur in anatomical structure. In many circumstances, this specific feature permits more accurate assessment of treatment and enables early detection of cancerous lesions[15].

Several radiotracers have been used in detecting hepatic malignancies by PET or PET/CT, and provide insight into their physiologic features, including glucose consumption (assessed with ^{18}F-FDG) and lipid synthesis (^{11}C-acetate)[16], cell-membrane metabolism and tumor proliferation (^{18}F-fluorocholine)[17]. Of these radiotracers, ^{18}F-FDG is by far the most commonly used in oncologic PET and the only oncologic PET tracer approved by the Food and Drug Administration (FDA) for routine clinical use[18]. ^{18}F-FDG is transported into tumor cells by glucose transporter proteins on the cell surface and then phosphorylated by hexokinase to FDG-6-phosphate. FDG-6-phosphate cannot be further metabolized in most tumor cells, thereby it selectively accumulates in cancer tissues. The amount of tumoral ^{18}F-FDG uptake is often expressed as the standardized uptake value (SUV) with a semiquantitative measure. The SUV is calculated by dividing the tissue activity by the injected dosage of radioactivity per unit body weight. The SUV ratio is expressed as the tumor to non-tumor ratio. Iwata *et al*[19] found that the median SUV is significantly lower in HCC than in metastatic liver cancer or CC, and the median SUV ratio is significantly lower in HCC than in metastatic liver cancer or CC and significantly higher in multiple HCC than in single HCC, while the median SUV and median SUV ratio are significantly higher in the presence of portal vein thrombosis than in the absence of such thrombosis.

However, PET lacks anatomical landmarks for

Table 1 Characteristics of PET and its novel sister modalities in detecting liver malignancies

Modalities	Characteristics
PET	By detecting ^{18}F-FDG uptake, producing functional images but with very poor anatomical details
PET/CT	Integrated PET and CT system, locate ^{18}F-FDG in specific anatomical sites
PET/MDCT	Best to monitor response to treatment, especially early ones with fine details

topographic orientation, and it is difficult to identify the abnormal glucose metabolic activity in regions close to organs with variable physiological ^{18}F-FDG uptake. Thus combination with some other forms of imaging, such as CT, is desirable for differentiating normal from abnormal radiotracer uptake[20]. PET/CT is an integral combination of the cross-sectional anatomic information provided by CT and the metabolic information provided by PET. Anatomical and metabolic information is acquired during a single examination and images of the two series can be fused. ^{18}F-FDG PET/CT has several advantages over PET alone, the most important one is the ability to accurately localize increased ^{18}F-FDG activity to specific normal or abnormal anatomic locations, which can be difficult or even impossible with PET alone[21]. The main commercially available PET/CT systems in the world are PET with multi-detector computed tomography (MDCT), so that its most units can perform full dose diagnostic CT scan for selected patients who need additional CT scan after conventional ^{18}F-FDG PET/CT imaging. Comparison of several PET-derived imaging modalities with their features in detecting liver malignancies is shown in Table 1.

EVALUATION OF HEPATIC MALIGNANCIES
Diagnosis of hepatic metastases

PET has emerged as an important diagnostic tool in the evaluation of metastatic liver diseases[22-26]. A greater metabolic activity in malignant tissue is accompanied with a greater glucose uptake than that in surrounding normal tissue. This greater focal glucose uptake can be identified with ^{18}F-FDG PET, which allows for the identification of malignant tumor foci. Wiering *et al*[27] reported the results of a meta-analysis of the current literature about the usefulness of ^{18}F-FDG PET for the selection of patients to undergo resection of colorectal liver metastases. The sensitivity and specificity of ^{18}F-FDG PET in hepatic metastatic diseases were 79.9% and 92.3%, respectively, and 91.2% and 98.4% in extrahepatic diseases, respectively. The pooled sensitivity and specificity of CT were 82.7% and 84.1% in hepatic lesions, respectively, and 60.9% and 91.1% in extrahepatic lesions, respectively. ^{18}F-FDG PET results led to changes in clinical management from the first decision, with a percentage of 31.6% (range, 20.0%-58.0%). The combination of sensitivity with specificity in ^{18}F-FDG PET indicated that ^{18}F-FDG PET has an added value in the diagnostic workup of patients with colorectal liver metastases. ^{18}F-FDG PET can be considered as a useful tool in preoperative staging by
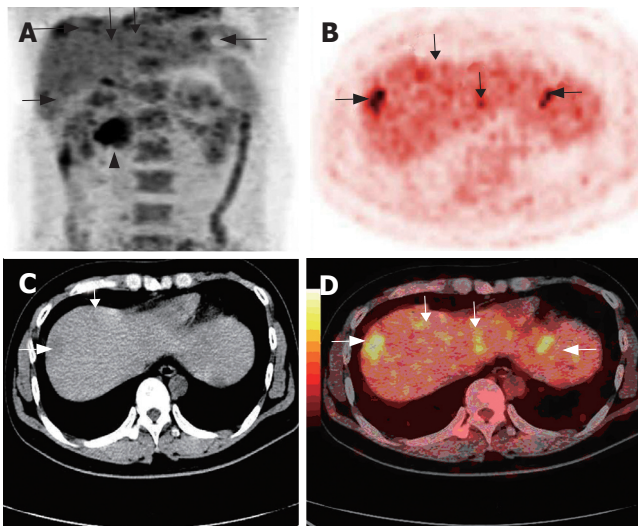
Figure 1 A 33-year-old man undergoing ascending colon cancer resection two years ago. Coronal PET image (**A**) also showing recurrent lesion (arrow head) at the root of mesentery, ^{18}F-FDG PET (**B**) and PET/CT fused imaging (**D**) demonstrating multiple hepatic metastases (arrow), and non-enhanced CT (**C**) detecting fewer lesions than PET/CT fused imaging (**D**).

producing superior results compared with conventional diagnostic modalities, especially in excluding or detecting extrahepatic metastatic disease.

Conventional PET scanning is associated with several shortcomings. The major drawback relates to its poor resolution and lack of concise anatomic illustration of PET images, making exact localization of ^{18}F-FDG uptake difficult. For example, a right adrenal gland metastasis might be misinterpreted as a liver metastasis[28,29]. Additionally, confirmation of a positive ^{18}F-FDG PET uptake by histology is sometimes impossible because of the lack of morphologic information. The new PET/CT technique allows exact identification of the lesions, which enables accurate biopsies and targeted surgery to be performed. Compared with contrast-enhanced CT, PET/CT provides comparable findings for the detection of primary liver metastases. However, PET/CT is more helpful than contrast-enhanced CT for detection of recurrent intrahepatic tumors after hepatectomy, extrahepatic metastases, and local recurrence at the site of the initial colorectal surgery[30]. Information provided by PET/CT results in a change from the initial decision on therapeutic strategies in about a fifth of the patients. Routinely performing PET/CT on all patients being evaluated for liver resection for metastatic colorectal cancer is recommended (Figure 1)[31]. To the patients with metastatic colorectal cancer, a routine PET/CT scan is recommended for making therapeutic decisions, such as liver resection.

Diagnosis of HCC

PET is an imaging technique reflecting cellular metabolism. However, the feasibility of PET in diagnosis of HCC is limited because of its vague images and high cost. Several investigators have reported controversial conclusions telling an inadequate sensitivity of PET (50%-55%)[32]. Shin *et al*[33] reported a group of 32 HCC patients verified

by surgical pathology or clinical course using imaging studies (CT, MRI or angiography) within 3 mo after PET. The sensitivity and specificity of ^{18}F-FDG PET were 65.5% and 33.3% respectively. The positive predictive value was 90.5%. The diagnostic accuracy was 62.5%. Chen *et al*[34] reported that the sensitivity, specificity and accuracy were 73.3%, 100% and 74.2%, respectively for detecting recurrence with ^{18}F-FDG PET in patients with unexplained rise of serum alpha-fetoprotein (AFP) levels after the treatment of HCC. Hanajiri[35] and Beadsmoore *et al*[36] found that ^{18}F-FDG PET is more sensitive than conventional CT and MRI in detecting suspected vein tumor thrombus in patients with HCC. The reported positive rate of perihepatic lymph node involvement in patients undergoing hepatic resection is approximately 5% for hepatocellular carcinoma. ^{18}F-FDG PET is useful in detecting distant metastases from a variety of malignancies and shows superior accuracy to conventional CT and MRI in identification of perihepatic lymph nodes and distant metastases[37,38]. ^{18}F-FDG PET could provide additional information and contribute to the management of HCC patients who are suspected of having extrahepatic metastases.

Of the noninvasive imaging techniques for studying HCC, triple-phase MDCT and contrast enhanced MRI have been widely applied[39,40]. PET/CT combines the advantages of CT with the functional studying ability of PET, through the fusion of PET and CT images acquired at the same time that may help accurately localize the focal metabolic activity. Currently available data indicate that PET/CT is more sensitive and specific than either of its constituent imaging methods alone and probably more so than images obtained separately from PET and CT and viewed side by side (Figure 2). However, ^{18}F-FDG PET/CT cannot replace separate diagnostic CT for HCC. Additional full dose enhanced triple-phase MDCT scan at the same time followed by ^{18}F-FDG PET/CT whole body scan may be needed to take in some suspected HCC patients, especially those at high risk[41].

Diagnosis of CC

Surgical resection is considered the only curative strategy for intrahepatic CC at present. Accurate staging is essential for appropriate management of patients with CC. MRI or CT combining endoscopic ultrasound and PET provide useful diagnostic information in certain patients[42]. In diagnosing malignant diseases in patients with biliary stricture, ^{18}F-FDG PET may give better sensitivity and specificity than CT, and is more sensitive than cytological examination of bile in sensitivity[43]. ^{18}F-FDG PET could be useful in cases of suspected hilar CC by radiological findings with non-confirmatory biopsy[44]. Anderson *et al*[45] reported that the sensitivity of ^{18}F-FDG is 85% in detecting nodular morphology, 65% in detecting metastases of CC, 78% in detecting gallbladder carcinoma, and 50% in detecting extrahepatic metastases. PET is accurate in predicting the presence of nodular CC (mass > 1 cm) but may be not helpful for the diagnosis of infiltrating type of CC. PET is also helpful for detecting residual gallbladder carcinoma following cholecystectomy and has led to a change in management of 30% of patients with CC.
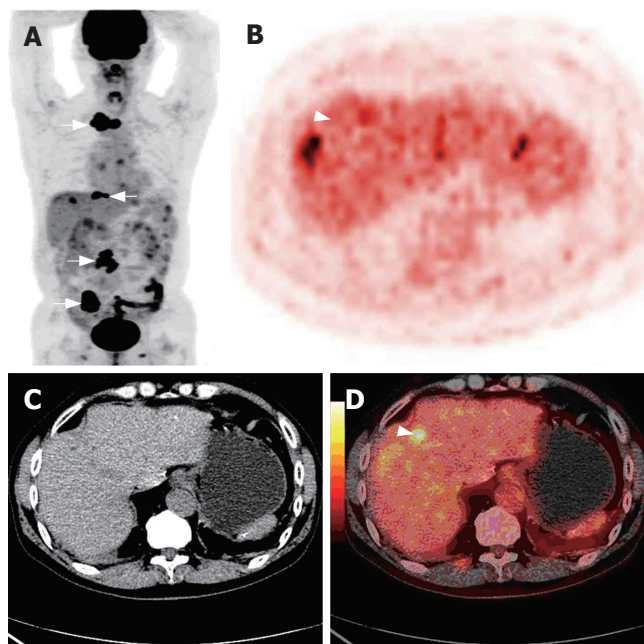
Figure 2 A 68-year-old male undergoing HCC resection 28-mo ago. Multiples bone metastases (arrow) on the image of whole body PET (**A**), non-enhanced CT (**C**) detecting no recurrence lesion in the liver, ^{18}F-FDG PET (**B**) and PET/CT fused imaging (**D**) showing a high metabolism recurrent lesion (arrow head).

Figure 3 A 68-year-old female complaining of uncomfortable left upper abdomen for one month with increasing of CA19-9 (> 700 μ/L) (**A**), non-enhanced CT (**C**) detecting a low density lesion in the left lobe of the liver (white arrow), ^{18}F-FDG PET (**B**) and fused imaging of PET/CT (**D**) showing necrosis (arrow head) in the center of the mass with a satellite lesion (black arrow). CC was confirmed by liver biopsy.

The number of metastatic lymph nodes is a significant prognostic factor for CC. The reported positive rate of perihepatic lymph node involvement ranges 30%-50% in patients with hilar CC[46], and 47%-58% in those with intrahepatic CC[47]. The involvement of paraaortic and regional nodes in advanced hilar cholangiocarcinoma is 14.4%. There is no consensus regarding the optimal technique for evaluating the status of perihepatic lymph nodes at the time of liver resection for intrahepatic CC. Some have advocated routine nodal sampling before resection, while others have advocated routine subhilar lymphadenectomy. Without liver resection, the optimal decision to sample lymph nodes can be only guided by information gathered from preoperative imaging studies and the intraoperative assessment of perihepatic nodes[48].

Petrowsky et al[49] reported that ^{18}F-FDG-PET/CT and contrast-enhanced CT may provide a comparable accuracy for the primary intra- and extra-hepatic CC. Regional lymph node metastases were detected with PET/CT and contrast-enhanced CT in only 12% vs 24%. All distant metastases were detected with ^{18}F-FDG PET/CT, while only 25% were detected with contrast-enhanced CT. PET/CT findings resulted in a change of management in 17% of patients deemed resectable after standard work-up. PET/CT is particularly valuable in detecting unsuspected distant metastases which have not been diagnosed with standard imaging. Thus, PET/CT staging has an important impact on selection of adequate therapy. However, false positive rates have been found in patients with inflammatory disease, such as primary sclerosing cholangitis and cholecystitis. Therefore, a multidisciplinary diagnostic approach using ^{18}F-FDG PET or PET/CT in conjunction with conventional modalities seems essential to a precise differential diagnosis.

EVALUATION OF HEPATIC MALIGNANT BIOLOGICAL CHARACTERISTICS

There is a dilemma that the five-year survival rate (ranging from 30% to 50%) of patients after curative resection of HCC almost does not increase in the past decade. The treatment procedures of cancer must face the core biological characteristics of cancer-aggressiveness and metastasis[50]. The diagnosis, treatment, prognosis standardizations of hepatic malignancies rely exclusively on the macromorphological characteristics, which is not enough to evaluate the biological characteristics of such malignancies. Molecular imaging in oncology is the noninvasive imaging of the key molecules and molecule-based events that are characteristic of the genotype and phenotype of human cancer. Since tumors with increased ^{18}F-FDG uptake are more metabolically active and more biologically aggressive[51,52], PET and PET/CT with ^{18}F-FDG would play a key role in evaluating the biological characteristics of hepatic malignancies (Figure 3).

It has been reported that the higher the glucose metabolism seen on ^{18}F-FDG PET imaging, the worse the prognosis of tumors, especially untreated tumors[53,54]. It is clear that a great deal of biological information is contained within the ^{18}F-FDG PET SUV that reflects the level of glycolysis, and strongly correlates to an adverse patient prognosis[50]. Although HCC accumulates ^{18}F-FDG to various degrees, a high positive rate of ^{18}F-FDG accumulation has been reported in patients with high-grade HCC[55] and in those with markedly elevated AFP levels. Preoperative ^{18}F-FDG uptake reflects tumor differentiation and P-glycoprotein expression and may be a good predictor of outcome in HCC[56]. The SUV ratio is related significantly to disease-related deaths as well as

other predictive factors, including the number, size and stage of tumors, involvement of vessels and the capsule, and provides information of prognostic relevance in patients with HCC before surgery[57]. A significant survival benefit is correlated with low ^{18}F-FDG uptake in patients with metastases of colorectal cancer[58].

Approximately 50% of patients with resected hepatic malignancy may have a tumor recurrence. Thus, it is of importance to predict the relapse and to tackle it with additional treatment. A better understanding of biological characteristics of hepatic malignancy could lead to adequate use of adjuvant surgical treatments and hopefully better treatment outcome[59]. For example, if patients at high risk of tumor recurrence could be identified before the resection, they would benefit from additional treatments, such as neoadjuvant and adjuvant therapy, biotherapy, or the three. It is not necessary for patients at a low risk of tumor recurrence to receive the above therapies.

SELECTION OF LIVER TRANSPLANTATION CANDIDATES

Liver transplantation is the only option capable of simultaneously curing both HCC and the underlying liver disease. Prevention of postoperative tumor recurrence to improve the patients' long-term survival remains the primary concern as well as the major difficulty in liver transplantation for HCC[60]. The key problem is thus the selection of patients who can benefit from liver transplantation, so that it is necessary to identify patients at low risk of recurrence. The stringent morphologic criteria (solitary nodule < 5 cm, 3 nodules < 3 cm each) have been implemented to list HCC patients for liver transplantation, leading to a big improvement in survival rate of transplanted HCC patients in the last 10 years. Nevertheless, several recent studies have shown the limitations of such criteria in prediction of prognosis[61,62]. All conventional imaging modalities in current use with the common HCC staging procedures (TNM, Milan criteria) have their own limits to identify primary tumors and may be even more limited in their ability to define the extent of metastatic spread[63]. Furthermore, relying exclusively on the macromorphological characteristics of tumors may result in misdiagnosis mainly due to the limits of imaging techniques. The macromorphological characteristics of cancer also give an imprecise estimate of the tumor's aggressiveness[64].

With the advantages of whole-body scanning and high sensitivity in tumor detection, ^{18}F-FDG PET/CT can be instrumental in preoperative evaluation of liver transplantation for HCC (such as modification of clinical staging) and early detection of postoperative recurrent tumors. Histological grade of differentiation and macroscopic vascular invasion are strong predictors of both survival and tumor recurrence in patients with cirrhosis who receive transplants because of HCC[65]. Cillo *et al*[66] reported that candidates for liver transplantation can be selected using HCC grades (G1 and G2) based on preoperative fine needle aspiration biopsy, which is

associated with an extremely low rate of tumor recurrence, comparable with that of incidentally detected HCC. Histological examination using percutaneous needle biopsy may be the most definite assessment of HCC grades. However, it is invasive and the specimen retrieved does not always represent the entire lesion owing to sampling errors[67]. Histological grade and vascular invasion cannot be determined preoperatively. PET and PET/CT with ^{18}F-FDG imaging could also be a good preoperative tool for estimating the post-liver transplantation risk of tumor recurrence, importantly, tumor recurrence can be highly anticipated for PET-imaging-positive HCC patients who satisfy the Milan criteria. Yang *et al*[68] supported that PET-imaging-positive HCC patients should be selected cautiously for liver transplantation.

SELECTION OF PATIENTS WITH HEPATIC COLORECTAL METASTASES FOR HEPATECTOMY

Hepatic resection, a potentially curative approach for patients with liver metastases from colorectal carcinoma, carries a 5-year survival rate of 30%-50%. The resection rate of hepatic metastases from colorectal carcinoma varies from 20% to 50%[69]. Some clinical and pathological factors have been identified as important prognostic determinants of survival after surgical resection of colorectal liver metastases, including sex and age of the patients, stage of tumor, the number and size as well as distribution of hepatic metastatic lesions, presence of extrahepatic distant metastases, type of hepatectomy, and adjuvant chemotherapy, *etc*[70]. Antoniou *et al*[71] reported that a repeated hepatectomy is safe and may provide survival benefit equal to that of the first liver resection based on their results from a meta-analysis of repeated hepatectomy for patients with colorectal cancer metastases.

^{18}F-FDG PET is a useful tool in preoperative staging. It may be better than conventional diagnostic modalities, especially for staging and re-staging after hepatectomy[72]. Kinkel *et al*[73] reported that the mean weighted sensitivity of ultrasonography, CT, MRI, and ^{18}F-FDG PET is 55%, 72%, 76% and 90% respectively, in the detection of hepatic metastases from colorectal, gastric, and esophageal cancers. Results of pair wise comparison between imaging modalities demonstrated a greater sensitivity of ^{18}F-FDG PET than ultrasonography, CT and MRI. At equivalent specificity, ^{18}F-FDG PET is the most sensitive noninvasive imaging modality for the diagnosis of hepatic metastases from colorectal, gastric, and esophageal cancers.

^{18}F-FDG PET/CT provides important additional information in patients with presumed resectable colorectal metastases to the liver, leading to a change of therapy in one fifth of patients[74]. The most significant additional information relates to the accurate detection of extrahepatic spread of tumor. ^{18}F-FDG PET/CT is particularly valuable in detecting local recurrence at the margin of a previous liver resection and at the site of the primary colorectal surgery[75]. It also increases the accuracy and certainty of locating lesions in colorectal cancer. More definitely normal and abnormal lesions could be identified

with PET/CT than with PET alone with an improved staging and restaging accuracy of 78%-89%[76]. This test should be used for patients at high risk for extrahepatic disease and evaluated prospectively for all patients under consideration for liver resection.

VIABLE TUMORS *VS* NECROSIS OR FIBROSIS AFTER TREATMENT

Less than 20% of patients with hepatic metastases, HCC and CC have been treated surgically. Palliative treatment of inoperable hepatic metastases, HCC and CC has been reported[77]. Despite initial resection or remission of hepatic malignancy, the survival benefits are not satisfactory because of frequent recurrences following the treatment[78]. Early detection of a residual or locally recurrent tumor after palliative treatment is critical to early successful retreatment. Conventional CT and MRI are disadvantageous in early evaluation of the local treatment efficacy and recurrent diseases[79].

An important contribution of restaging with PET among patients without any other clinical or biochemical evidence of disease is the possibility of distinguishing between viable tumors and necrosis or fibrosis in residual masses that may be present after treatment[78]. PET and PET/CT with ^{18}F-FDG are not affected by scar tissue and artificial materials. ^{18}F-FDG PET and PET/CT accurately monitor the local efficacy of radiofrequency ablation (RFA) for treatment of liver metastases and can recognize early incomplete tumor ablation, which may not be detectable on contrast-enhanced CT alone. Conversely, CT and MRI may be false-positive at the rim of the lesions because of hyperperfusion after RFA[80,81]. Zhao et al[82] reported that ^{18}F-FDG PET/CT is better than CT in judging tumor residue of HCC after treatment with transcatheter arterial chemo-embolization (TACE) combined with RFA or surgery and in guiding further treatment of HCC. Furthermore, integrated PET/CT can provide a value especially for the postoperatively distorted liver with scar tissue and artificial materials, where the sensitivity and specificity CT and MRI are relatively low.

PREDICTORS OF POSTOPERATIVE RECURRENCE IN ASYMPTOMATIC PATIENTS

An unexplained rise of tumor markers (e.g., among patients with colorectal cancer and elevated levels of serum carcinoembryonic antigen (CEA) or HCC patients with elevated serum AFP levels after the treatment) after the treatment of hepatic malignancy is an early indicator of tumor recurrence or extrahepatic metastases[83]. However, conventional imaging techniques have a limited sensitivity for detecting recurrent disease in such patients. ^{18}F-FDG PET has been proved to be an effective whole-body imaging technique that detects metabolic changes preceding structural findings. Several studies have persuasively demonstrated that tumor restaging with PET can detect and localize disease recurrence among patients

Table 2   Comparison between PET/CT and conventional imaging modalities of their values in examination of liver malignancies

Modalities	Specificity	Sensitivity	Accuracy
18F-FDG-PET/CT	+++	+++	+++
Ultrasound	+	++	-
CT	++	+++	+
MRI	++	++	++

- poor; + fair; ++ good; +++ excellent.

with no or mild symptoms and elevated tumor marker level. PET also can provide information about whether the detected disease is resectable[84,85].

Flamen et al[86] have reported the results of ^{18}F-FDG PET for unexplained rising CEA in postoperative colorectal cancer patients, showing that a patient-based analysis revealed that the sensitivity of ^{18}F-FDG PET in detecting tumor recurrence is 79%, and the positive predictive value is 89%, while a lesion-based analysis displayed that the sensitivity of ^{18}F-FDG PET in detecting tumor recurrence is 75%, and the positive predictive value is 79%. ^{18}F-FDG PET whole-body scan also provides a valuable imaging tool for detecting extrahepatic metastasis and contributes to the management of HCC patients suspected of having extrahepatic metastases[87]. ^{18}F-FDG PET/CT provides fused images demonstrating the complementary role of functional and anatomic assessment in the diagnosis of cancer recurrence through the precise localization of suspected ^{18}F-FDG uptake foci and their characterization as malignant or benign[88]. ^{18}F-FDG PET/CT is better than common CT in judging tumor residue of HCC after treatment, and in guiding further treatment of HCC.

EVALUATION OF PROGNOSIS OF HEPATIC MALIGNANCIES

At present, despite careful preoperative staging with conventional imaging modalities and colonoscopy, most patients with colorectal liver metastases have recurrence after liver resection. The overall 5-year survival rate is 30%, ranging 12%-41%. These results have not steadily improved over time[89,90]. Accordingly, to reduce the frequency of futile hepatic resections, more effective staging tools are needed. ^{18}F-FDG PET appears to define a new cohort of patients in whom tumor grade is a very important prognostic variable[91]. The current study focused on the prognostic value of pretreatment metabolic activity in metastases measured with ^{18}F-FDG PET, which was investigated as an indicator of survival in colorectal cancer.

The overall 5-year survival in patients screened with ^{18}F-FDG PET before hepatic resection for metastatic colorectal cancer is 58.6%, which is a substantial improvement in overall survival when compared with the results from a large number of historical series in which ^{18}F-FDG PET was not used[92]. A significant survival benefit has been shown in patients with low ^{18}F-FDG uptake in

metastases of colorectal cancer[93]. 18F-FDG PET is useful not only for the evaluation of malignancy of hepatocellular carcinoma but also for the prediction of outcome in patients with hepatocellular carcinoma[94]. The SUV of 18F-FDG PET in high-grade HCCs is significantly higher than that in low-grade HCCs. The SUV ratio is related significantly to disease-related deaths as well as other predictive factors, including the number, size and stage of tumors, and involvement of vessels as well as capsule[95]. Evaluation of examination results from these imaging modalities is illustrated in Table 2.

CONCLUSION

18F-FDG PET has advantages over conventional imaging techniques in designing and evaluating managements of hepatic malignancies with biological characteristics for an optimal patient outcome. With combined functional and anatomical image, PET/CT is more and more widely applied in clinical practice. It is more sensitive and specific than PET, with a lower false-positive and false-negative rate. Multiple avenues of investigation that can be used to improve the ability of PET and PET/CT with 18F-FDG to enhance the diagnostic algorithm of hepatic malignancies, which can benefit the patients suffering from hepatic metastases, HCC and CC by more accurate diagnosis, staging, restaging and further evaluation of their biologic characteristics.

REFERENCES

1   **Weissleder R**. Molecular imaging in cancer. *Science* 2006; **312**: 1168-1171
2   **Juweid ME**, Cheson BD. Positron-emission tomography and assessment of cancer therapy. *N Engl J Med* 2006; **354**: 496-507
3   **Maisey MN**. Overview of clinical PET. *Br J Radiol* 2002; **75** Spec No: S1-S5
4   **Beyer T**, Townsend DW, Brun T, Kinahan PE, Charron M, Roddy R, Jerin J, Young J, Byars L, Nutt R. A combined PET/CT scanner for clinical oncology. *J Nucl Med* 2000; **41**: 1369-1379
5   **Blodgett TM**, Meltzer CC, Townsend DW. PET/CT: form and function. *Radiology* 2007; **242**: 360-385
6   **Iglehart JK**. The new era of medical imaging--progress and pitfalls. *N Engl J Med* 2006; **354**: 2822-2828
7   **Ho CL**. Clinical PET imaging-an Asian perspective. *Ann Acad Med Singapore* 2004; **33**: 155-165
8   **Jemal A**, Siegel R, Ward E, Murray T, Xu J, Smigal C, Thun MJ. Cancer statistics, 2006. *CA Cancer J Clin* 2006; **56**: 106-130
9   **Qin LX, Tang ZY**. Hepatocellular carcinoma with obstructive jaundice: diagnosis, treatment and prognosis. *World J Gastroenterol* 2003; **9**: 385-391
10 **Khan SA**, Thomas HC, Davidson BR, Taylor-Robinson SD. Cholangiocarcinoma. *Lancet* 2005; **366**: 1303-1314
11 **von Schulthess GK**, Steinert HC, Hany TF. Integrated PET/CT: current applications and future directions. *Radiology* 2006; **238**: 405-422
12 **Yao FY**, Ferrell L, Bass NM, Watson JJ, Bacchetti P, Venook A, Ascher NL, Roberts JP. Liver transplantation for hepatocellular carcinoma: expansion of the tumor size limits does not adversely impact survival. *Hepatology* 2001; **33**: 1394-1403
13 **Kitagawa Y**, Nishizawa S, Sano K, Ogasawara T, Nakamura M, Sadato N, Yoshida M, Yonekura Y. Prospective comparison of 18F-FDG PET with conventional imaging modalities (MRI, CT, and 67Ga scintigraphy) in assessment of combined intraarterial chemotherapy and radiotherapy for head and neck carcinoma. *J Nucl Med* 2003; **44**: 198-206

14 **Adams S**, Baum RP, Stuckensen T, Bitter K, Hor G. Prospective comparison of 18F-FDG PET with conventional imaging modalities (CT, MRI, US) in lymph node staging of head and neck cancer. *Eur J Nucl Med* 1998; **25**: 1255-1260
15 **Avril NE**, Weber WA. Monitoring response to treatment in patients utilizing PET. *Radiol Clin North Am* 2005; **43**: 189-204
16 **Ho CL**, Yu SC, Yeung DW. 11C-acetate PET imaging in hepatocellular carcinoma and other liver masses. *J Nucl Med* 2003; **44**: 213-221
17 **Talbot JN**, Gutman F, Fartoux L, Grange JD, Ganne N, Kerrou K, Grahek D, Montravers F, Poupon R, Rosmorduc O. PET/CT in patients with hepatocellular carcinoma using (18)F fluorocholine: preliminary comparison with (18)F FDG PET/CT. *Eur J Nucl Med Mol Imaging* 2006; **33**: 1285-1289
18 **Food and Drug Administration (FDA)**: Positron Emission Tomography (PET) for Oncologic Applications. 1999, first edition, page 18
19 **Iwata Y**, Shiomi S, Sasaki N, Jomura H, Nishiguchi S, Seki S, Kawabe J, Ochi H. Clinical usefulness of positron emission tomography with fluorine-18-fluorodeoxyglucose in the diagnosis of liver tumors. *Ann Nucl Med* 2000; **14**: 121-126
20 **Fanti S**, Franchi R, Battista G, Monetti N, Canini R. PET and PET-CT. State of the art and future prospects. *Radiol Med* (Torino) 2005; **110**: 1-15
21 **Czernin J**, Allen-Auerbach M, Schelbert HR. Improvements in cancer staging with PET/CT: literature-based evidence as of September 2006. *J Nucl Med* 2007; **48** Suppl 1: 78S-88S
22 **Strasberg SM**, Dehdashti F, Siegel BA, Drebin JA, Linehan D. Survival of patients evaluated by FDG-PET before hepatic resection for metastatic colorectal carcinoma: a prospective database study. *Ann Surg* 2001; **233**: 293-299
23 **Ruers TJ**, Langenhoff BS, Neeleman N, Jager GJ, Strijk S, Wobbes T, Corstens FH, Oyen WJ. Value of positron emission tomography with [F-18] fluorodeoxyglucose in patients with colorectal liver metastases: a prospective study. *J Clin Oncol* 2002; **20**: 388-395
24 **Wiering B**, Ruers TJ, Oyen WJ. Role of FDG-PET in the diagnosis and treatment of colorectal liver metastases. *Expert Rev Anticancer Ther* 2004; **4**: 607-613
25 **Kantorova I**, Lipska L, Belohlavek O, Visokai V, Trubac M, Schneiderova M. Routine (18)F-FDG PET preoperative staging of colorectal cancer: comparison with conventional staging and its impact on treatment decision making. *J Nucl Med* 2003; **44**: 1784-1788
26 **Arulampalam TH**, Francis DL, Visvikis D, Taylor I, Ell PJ. FDG-PET for the pre-operative evaluation of colorectal liver metastases. *Eur J Surg Oncol* 2004; **30**: 286-291
27 **Wiering B**, Krabbe PF, Jager GJ, Oyen WJ, Ruers TJ. The impact of fluor-18-deoxyglucose-positron emission tomography in the management of colorectal liver metastases. *Cancer* 2005; **104**: 2658-2670
28 **Rohren EM**, Paulson EK, Hagge R, Wong TZ, Killius J, Clavien PA, Nelson RC. The role of F-18 FDG positron emission tomography in preoperative assessment of the liver in patients being considered for curative resection of hepatic metastases from colorectal cancer. *Clin Nucl Med* 2002; **27**: 550-555
29 **Teague BD**, Morrison CP, Court FG, Chin VT, Costello SP, Kirkwood ID, Maddern GJ. Role of FDG-PET in surgical management of patients with colorectal liver metastases. *ANZ J Surg* 2004; **74**: 646-652
30 **Selzner M**, Hany TF, Wildbrett P, McCormack L, Kadry Z, Clavien PA. Does the novel PET/CT imaging modality impact on the treatment of patients with metastatic colorectal cancer of the liver? *Ann Surg* 2004; **240**: 1027-1034; discussion 1035-1036
31 **Veit P**, Antoch G, Stergar H, Bockisch A, Forsting M, Kuehl H. Detection of residual tumor after radiofrequency ablation of liver metastasis with dual-modality PET/CT: initial results. *Eur Radiol* 2006; **16**: 80-87
32 **Yang SH**, Suh KS, Lee HW, Cho EH, Cho JY, Cho YB, Yi NJ, Lee KU. The role of (18)F-FDG-PET imaging for the selection of liver transplantation candidates among hepatocellular carcinoma patients. *Liver Transpl* 2006; **12**: 1655-1660

33 **Shin JA**, Park JW, An M, Choi JI, Kim SH, Kim SK, Lee WJ, Park SJ, Hong EK, Kim CM. Diagnostic accuracy of 18F-FDG positron emission tomography for evaluation of hepatocellular carcinoma. *Korean J Hepatol* 2006; **12**: 546-552

34 **Chen YK**, Hsieh DS, Liao CS, Bai CH, Su CT, Shen YY, Hsieh JF, Liao AC, Kao CH. Utility of FDG-PET for investigating unexplained serum AFP elevation in patients with suspected hepatocellular carcinoma recurrence. *Anticancer Res* 2005; **25**: 4719-4725

35 **Hanajiri K**, Mitsui H, Maruyama T, Kondo Y, Shiina S, Omata M, Nakagawa K. 18F-FDG PET for hepatocellular carcinoma presenting with portal vein tumor thrombus. *J Gastroenterol* 2005; **40**: 1005-1006

36 **Beadsmoore CJ**, Cheow HK, Sala E, Lomas DJ, Gibbs P, Save V, Alison ME, Balan KK. Hepatocellular carcinoma tumour thrombus in a re-canalised para-umbilical vein: detection by 18-fluoro-2-deoxyglucose positron emission tomography imaging. *Br J Radiol* 2005; **78**: 841-844

37 **Sugiyama M**, Sakahara H, Torizuka T, Kanno T, Nakamura F, Futatsubashi M, Nakamura S. 18F-FDG PET in the detection of extrahepatic metastases from hepatocellular carcinoma. *J Gastroenterol* 2004; **39**: 961-968

38 **Wudel LJ Jr**, Delbeke D, Morris D, Rice M, Washington MK, Shyr Y, Pinson CW, Chapman WC. The role of 18F fluorodeoxyglucose positron emission tomography imaging in the evaluation of hepatocellular carcinoma. *Am Surg* 2003; **69**: 117-124; discussion 124-126

39 **Lee KH**, O'Malley ME, Haider MA, Hanbidge A. Triple-phase MDCT of hepatocellular carcinoma. *AJR Am J Roentgenol* 2004; **182**: 643-649

40 **Kim YK**, Kim CS, Chung GH, Han YM, Lee SY, Chon SB, Lee JM. Comparison of gadobenate dimeglumine-enhanced dynamic MRI and 16-MDCT for the detection of hepatocellular carcinoma. *AJR Am J Roentgenol* 2006; **186**: 149-157

41 **Kuehl H**, Veit P, Rosenbaum SJ, Bockisch A, Antoch G. Can PET/CT replace separate diagnostic CT for cancer imaging? Optimizing CT protocols for imaging cancers of the chest and abdomen. *J Nucl Med* 2007; **48** Suppl 1: 45S-57S

42 **Khan SA**, Thomas HC, Davidson BR, Taylor-Robinson SD. Cholangiocarcinoma. *Lancet* 2005; **366**: 1303-1314

43 **Singh P**, Patel T. Advances in the diagnosis, evaluation and management of cholangiocarcinoma. *Curr Opin Gastroenterol* 2006; **22**: 294-299

44 **Kim YJ**, Yun M, Lee WJ, Kim KS, Lee JD. Usefulness of 18F-FDG PET in intrahepatic cholangiocarcinoma. *Eur J Nucl Med Mol Imaging* 2003; **30**: 1467-1472

45 **Anderson CD**, Rice MH, Pinson CW, Chapman WC, Chari RS, Delbeke D. Fluorodeoxyglucose PET imaging in the evaluation of gallbladder carcinoma and cholangiocarcinoma. *J Gastrointest Surg* 2004; **8**: 90-97

46 **Kitagawa Y**, Nagino M, Kamiya J, Uesaka K, Sano T, Yamamoto H, Hayakawa N, Nimura Y. Lymph node metastasis from hilar cholangiocarcinoma: audit of 110 patients who underwent regional and paraaortic node dissection. *Ann Surg* 2001; **233**: 385-392

47 **Yamamoto M**, Takasaki K, Yoshikawa T. Lymph node metastasis in intrahepatic cholangiocarcinoma. *Jpn J Clin Oncol* 1999; **29**: 147-150

48 **Grobmyer SR**, Wang L, Gonen M, Fong Y, Klimstra D, D'Angelica M, DeMatteo RP, Schwartz L, Blumgart LH, Jarnagin WR. Perihepatic lymph node assessment in patients undergoing partial hepatectomy for malignancy. *Ann Surg* 2006; **244**: 260-264

49 **Petrowsky H**, Wildbrett P, Husarik DB, Hany TF, Tam S, Jochum W, Clavien PA. Impact of integrated positron emission tomography and computed tomography on staging and management of gallbladder cancer and cholangiocarcinoma. *J Hepatol* 2006; **45**: 43-50

50 **Tang ZY**. Hepatocellular carcinoma surgery--review of the past and prospects for the 21st century. *J Surg Oncol* 2005; **91**: 95-96

51 **Larson SM**. Positron emission tomography-based molecular imaging in human cancer: exploring the link between hypoxia

and accelerated glucose metabolism. *Clin Cancer Res* 2004; **10**: 2203-2204

52 **Larson SM**, Schwartz LH. 18F-FDG PET as a candidate for "qualified biomarker": functional assessment of treatment response in oncology. *J Nucl Med* 2006; **47**: 901-903

53 **Miyamoto J**, Sasajima H, Owada K, Mineura K. Surgical decision for adult optic glioma based on 18F fluorodeoxyglucose positron emission tomography study. *Neurol Med Chir* (Tokyo) 2006; **46**: 500-503

54 **Jeong HJ**, Min JJ, Park JM, Chung JK, Kim BT, Jeong JM, Lee DS, Lee MC, Han SK, Shim YS. Determination of the prognostic value of (18)F fluorodeoxyglucose uptake by using positron emission tomography in patients with non-small cell lung cancer. *Nucl Med Commun* 2002; **23**: 865-870

55 **Hatano E**, Ikai I, Higashi T, Teramukai S, Torizuka T, Saga T, Fujii H, Shimahara Y. Preoperative positron emission tomography with fluorine-18-fluorodeoxyglucose is predictive of prognosis in patients with hepatocellular carcinoma after resection. *World J Surg* 2006; **30**: 1736-1741

56 **Seo S**, Hatano E, Higashi T, Hara T, Tada M, Tamaki N, Iwaisako K, Ikai I, Uemoto S. Fluorine-18 fluorodeoxyglucose positron emission tomography predicts tumor differentiation, P-glycoprotein expression, and outcome after resection in hepatocellular carcinoma. *Clin Cancer Res* 2007; **13**: 427-433

57 **Kong YH**, Han CJ, Lee SD, Sohn WS, Kim MJ, Ki SS, Kim J, Jeong SH, Kim YC, Lee JO, Cheon GJ, Choi CW, Lim SM. Positron emission tomography with fluorine-18-fluorodeoxyglucose is useful for predicting the prognosis of patients with hepatocellular carcinoma. *Korean J Hepatol* 2004; **10**: 279-287

58 **de Geus-Oei LF**, Wiering B, Krabbe PF, Ruers TJ, Punt CJ, Oyen WJ. FDG-PET for prediction of survival of patients with metastatic colorectal carcinoma. *Ann Oncol* 2006; **17**: 1650-1655

59 **Arriagada R**, Bergman B, Dunant A, Le Chevalier T, Pignon JP, Vansteenkiste J. Cisplatin-based adjuvant chemotherapy in patients with completely resected non-small-cell lung cancer. *N Engl J Med* 2004; **350**: 351-360

60 **Cha C**, Dematteo RP, Blumgart LH. Surgical therapy for hepatocellular carcinoma. *Adv Surg* 2004; **38**: 363-376

61 **Shetty K**, Timmins K, Brensinger C, Furth EE, Rattan S, Sun W, Rosen M, Soulen M, Shaked A, Reddy KR, Olthoff KM. Liver transplantation for hepatocellular carcinoma validation of present selection criteria in predicting outcome. *Liver Transpl* 2004; **10**: 911-918

62 **Leung JY**, Zhu AX, Gordon FD, Pratt DS, Mithoefer A, Garrigan K, Terella A, Hertl M, Cosimi AB, Chung RT. Liver transplantation outcomes for early-stage hepatocellular carcinoma: results of a multicenter study. *Liver Transpl* 2004; **10**: 1343-1354

63 **Mazzaferro V**, Regalia E, Doci R, Andreola S, Pulvirenti A, Bozzetti F, Montalto F, Ammatuna M, Morabito A, Gennari L. Liver transplantation for the treatment of small hepatocellular carcinomas in patients with cirrhosis. *N Engl J Med* 1996; **334**: 693-699

64 **Kirimlioglu H**, Dvorchick I, Ruppert K, Finkelstein S, Marsh JW, Iwatsuki S, Bonham A, Carr B, Nalesnik M, Michalopoulos G, Starzl T, Fung J, Demetris A. Hepatocellular carcinomas in native livers from patients treated with orthotopic liver transplantation: biologic and therapeutic implications. *Hepatology* 2001; **34**: 502-510

65 **Zavaglia C**, De Carlis L, Alberti AB, Minola E, Belli LS, Slim AO, Airoldi A, Giacomoni A, Rondinara G, Tinelli C, Forti D, Pinzello G. Predictors of long-term survival after liver transplantation for hepatocellular carcinoma. *Am J Gastroenterol* 2005; **100**: 2708-2716

66 **Cillo U**, Vitale A, Bassanello M, Boccagni P, Brolese A, Zanus G, Burra P, Fagiuoli S, Farinati F, Rugge M, D'Amico DF. Liver transplantation for the treatment of moderately or well-differentiated hepatocellular carcinoma. *Ann Surg* 2004; **239**: 150-159

67 **Guan YS**, Sun L, Zhou XP, Li X, Zheng XH. Hepatocellular carcinoma treated with interventional procedures: CT and MRI follow-up. *World J Gastroenterol* 2004; **10**: 3543-3548

68   **Yang SH**, Suh KS, Lee HW, Cho EH, Cho JY, Cho YB, Yi NJ, Lee KU. The role of (18)F-FDG-PET imaging for the selection of liver transplantation candidates among hepatocellular carcinoma patients. *Liver Transpl* 2006; **12**: 1655-1660

69   **Okano K**, Maeba T, Ishimura K, Karasawa Y, Goda F, Wakabayashi H, Usuki H, Maeta H. Hepatic resection for metastatic tumors from gastric cancer. *Ann Surg* 2002; **235**: 86-91

70   **Hirai I**, Kimura W, Fuse A, Isobe H, Hachiya O, Moriya T, Suto K, Mizutani M. Surgical management for metastatic liver tumors. *Hepatogastroenterology* 2006; **53**: 757-763

71   **Antoniou A**, Lovegrove RE, Tilney HS, Heriot AG, John TG, Rees M, Tekkis PP, Welsh FK. Meta-analysis of clinical outcome after first and second liver resection for colorectal metastases. *Surgery* 2007; **141**: 9-18

72   **Joyce DL**, Wahl RL, Patel PV, Schulick RD, Gearhart SL, Choti MA. Preoperative positron emission tomography to evaluate potentially resectable hepatic colorectal metastases. *Arch Surg* 2006; **141**: 1220-1226; discussion 1227

73   **Kinkel K**, Lu Y, Both M, Warren RS, Thoeni RF. Detection of hepatic metastases from cancers of the gastrointestinal tract by using noninvasive imaging methods (US, CT, MR imaging, PET): a meta-analysis. *Radiology* 2002; **224**: 748-756

74   **Selzner M**, Hany TF, Wildbrett P, McCormack L, Kadry Z, Clavien PA. Does the novel PET/CT imaging modality impact on the treatment of patients with metastatic colorectal cancer of the liver? *Ann Surg* 2004; **240**: 1027-1034; discussion 1035-1036

75   **Nakamoto Y**, Sakamoto S, Okada T, Senda M, Higashi T, Saga T, Togashi K. Clinical value of manual fusion of PET and CT images in patients with suspected recurrent colorectal cancer. *AJR Am J Roentgenol* 2007; **188**: 257-267

76   **Cohade C**, Osman M, Leal J, Wahl RL. Direct comparison of (18)F-FDG PET and PET/CT in patients with colorectal carcinoma. *J Nucl Med* 2003; **44**: 1797-1803

77   **Donckier V**, Van Laethem JL, Goldman S, Van Gansbeke D, Feron P, Ickx B, Wikler D, Gelin M. F-18 fluorodeoxyglucose positron emission tomography as a tool for early recognition of incomplete tumor destruction after radiofrequency ablation for liver metastases. *J Surg Oncol* 2003; **84**: 215-223

78   **Veltri A**, Moretto P, Doriguzzi A, Pagano E, Carrara G, Gandini G. Radiofrequency thermal ablation (RFA) after transarterial chemoembolization (TACE) as a combined therapy for unresectable non-early hepatocellular carcinoma (HCC). *Eur Radiol* 2006; **16**: 661-669

79   **Torizuka T**, Nakamura F, Kanno T, Futatsubashi M, Yoshikawa E, Okada H, Kobayashi M, Ouchi Y. Early therapy monitoring with FDG-PET in aggressive non-Hodgkin's lymphoma and Hodgkin's lymphoma. *Eur J Nucl Med Mol Imaging* 2004; **31**: 22-28

80   **Blokhuis TJ**, van der Schaaf MC, van den Tol MP, Comans EF, Manoliu RA, van der Sijp JR. Results of radio frequency ablation of primary and secondary liver tumors: long-term follow-up with computed tomography and positron emission tomography-18F-deoxyfluoroglucose scanning. *Scand J Gastroenterol Suppl* 2004; 93-97

81   **Veit P**, Antoch G, Stergar H, Bockisch A, Forsting M, Kuehl H. Detection of residual tumor after radiofrequency ablation of liver metastasis with dual-modality PET/CT: initial results. *Eur Radiol* 2006; **16**: 80-87

82   **Zhao M**, Wu PH, Zeng YX, Zhang FJ, Huang JH, Fan WJ, Gu YK, Zhang L, Tan ZB, Lin YE. Evaluating efficacy of transcatheter arterial chemo-embolization combined with radiofrequency ablation on patients with hepatocellular carcinoma by 18FDG-PET/CT. *Ai Zheng* 2005; **24**: 1118-1123

83   **Liu FY**, Chen JS, Changchien CR, Yeh CY, Liu SH, Ho KC, Yen TC. Utility of 2-fluoro-2-deoxy-D-glucose positron emission tomography in managing patients of colorectal cancer with unexplained carcinoembryonic antigen elevation at different levels. *Dis Colon Rectum* 2005; **48**: 1900-1912

84   **Park YA**, Lee KY, Kim NK, Baik SH, Sohn SK, Cho CW. Prognostic effect of perioperative change of serum carcinoembryonic antigen level: a useful tool for detection of systemic recurrence in rectal cancer. *Ann Surg Oncol* 2006; **13**: 645-650

85   **Israel O**, Mor M, Guralnik L, Hermoni N, Gaitini D, Bar-Shalom R, Keidar Z, Epelbaum R. Is 18F-FDG PET/CT useful for imaging and management of patients with suspected occult recurrence of cancer? *J Nucl Med* 2004; **45**: 2045-2051

86   **Flamen P**, Hoekstra OS, Homans F, Van Cutsem E, Maes A, Stroobants S, Peeters M, Penninckx F, Filez L, Bleichrodt RP, Mortelmans L. Unexplained rising carcinoembryonic antigen (CEA) in the postoperative surveillance of colorectal cancer: the utility of positron emission tomography (PET). *Eur J Cancer* 2001; **37**: 862-869

87   **Anderson GS**, Brinkmann F, Soulen MC, Alavi A, Zhuang H. FDG positron emission tomography in the surveillance of hepatic tumors treated with radiofrequency ablation. *Clin Nucl Med* 2003; **28**: 192-197

88   **Israel O**, Kuten A. Early detection of cancer recurrence: 18F-FDG PET/CT can make a difference in diagnosis and patient care. *J Nucl Med* 2007; **48** Suppl 1: 28S-35S

89   **Metcalfe MS**, Mullin EJ, Maddern GJ. Choice of surveillance after hepatectomy for colorectal metastases. *Arch Surg* 2004; **139**: 749-754

90   **Takahashi S**, Inoue K, Konishi M, Nakagouri T, Kinoshita T. Prognostic factors for poor survival after repeat hepatectomy in patients with colorectal liver metastases. *Surgery* 2003; **133**: 627-634

91   **Strasberg SM**, Dehdashti F, Siegel BA, Drebin JA, Linehan D. Survival of patients evaluated by FDG-PET before hepatic resection for metastatic colorectal carcinoma: a prospective database study. *Ann Surg* 2001; **233**: 293-299

92   **Fernandez FG**, Drebin JA, Linehan DC, Dehdashti F, Siegel BA, Strasberg SM. Five-year survival after resection of hepatic metastases from colorectal cancer in patients screened by positron emission tomography with F-18 fluorodeoxyglucose (FDG-PET). *Ann Surg* 2004; **240**: 438-447; discussion 447-450

93   **de Geus-Oei LF**, Wiering B, Krabbe PF, Ruers TJ, Punt CJ, Oyen WJ. FDG-PET for prediction of survival of patients with metastatic colorectal carcinoma. *Ann Oncol* 2006; **17**: 1650-1655

94   **Shiomi S**, Nishiguchi S, Ishizu H, Iwata Y, Sasaki N, Tamori A, Habu D, Takeda T, Kubo S, Ochi H. Usefulness of positron emission tomography with fluorine-18-fluorodeoxyglucose for predicting outcome in patients with hepatocellular carcinoma. *Am J Gastroenterol* 2001; **96**: 1877-1880

95   **Iwata Y**, Shiomi S, Sasaki N, Jomura H, Nishiguchi S, Seki S, Kawabe J, Ochi H. Clinical usefulness of positron emission tomography with fluorine-18-fluorodeoxyglucose in the diagnosis of liver tumors. *Ann Nucl Med* 2000; **14**: 121-126

REVIEW

Survivin: Potential role in diagnosis, prognosis and targeted therapy of gastric cancer

Ting-Ting Wang, Xiao-Ping Qian, Bao-Rui Liu

Ting-Ting Wang, Xiao-Ping Qian, Bao-Rui Liu, Department of Oncology, Affiliated Gulou Hospital, Medical School of Nanjing University, Nanjing, 210008, Jiangsu Province, China
Correspondence to: Bao-Rui Liu, Department of Oncology, Affiliated Drum Tower Hospital, Medical School of Nanjing University, Nanjing, 210008, Jiangsu Province, China. baoruiliu@nju.edu.cn
Telephone: +86-25-83304616 Fax: +86-25-83304616
Received: 2007-01-27   Accepted: 2007-02-14

Abstract

Survivin is a protein that is highly expressed in a vast number of malignancies, but is minimally expressed in normal tissues. It plays a role as an inhibitor of cell death in cancer cells, thus facilitating the growth of these cells. In the case of gastric cancer, survivin is over-expressed in tumor cells and plays a role in the carcinogenesis process. Several studies on gastric cancer have indicated that there is a relationship between survivin expression and the ultimate behavior of the carcinoma. Since the expression pattern of survivin is selective to cancer cells, it has been described as an "ideal target" for cancer therapy. Currently, several pre-clinical and clinical trials are on-going to investigate the effects of interfering with survivin function in cancer cells as a biologic therapy. Survivin is a potentially significant protein in the diagnosis, prognosis and treatment of gastric tumors.

INTRODUCTION

Carcinomas in the upper gastrointestinal (GI) tract constitute a major health problem world wide. It is estimated that approximately 36 830 new cases of upper GI carcinomas and 25 200 deaths due to upper GI carcinomas occurred in the United States in 2006[1]. This fact emphasizes the importance of identifying useful diagnostic and prognostic markers in the earliest stage of the disease. As to the treatment of gastric cancer, surgical therapy is the primary treatment, with combination of adjuvant chemotherapy. Most anticancer drugs in use today were discovered based on the ability to kill rapidly dividing cancer cells *in vitro*. Predictably, when administered to patients, many of these drugs also injure rapidly dividing normal cells, such as bone-marrow haematopoietic precursors and gastrointestinal mucosal epithelial cells. In addition, many of these drugs are toxic to normal cells that are not rapidly dividing[2]. The need for effective targeted treatment strategies is evident.

Survivin is an inhibitor of apoptosis protein (IAP) and is expressed in a large number of malignancies[3]. Its expression levels correlate with more aggressive disease and poor clinical outcome. Since its expression is restricted in normal differentiated tissues, it has become of great interest as both a tumor diagnostic, prognostic marker and as a potential biologic target for future anticancer therapies. Recently the use of survivin has been described in bladder cancer[4] and other cancers, but not in gastric cancer. For example, urine testing for survivin has been used as a diagnostic tool for an early detection of bladder cancer[5].

This review will provide a brief introduction about the structure of the survivin gene and protein and survivin expression and function in apoptosis will be discussed. The significance of survivin in gastric cancer will be discussed in two sections: the possible diagnostic and prognostic importance of its expression, and the possibility of modulating survivin function for therapeutic gain. Survivin can be considered as a potentially significant protein in the diagnosis, prognosis and treatment of gastric tumor.

BIOLOGY OF SURVIVIN

Structure and function

Survivin belongs to the apoptosis inhibitor gene family[6], in which the proteins are characterized by a domain of about 70 amino acids, termed baculovirus IAP repeat (BIP), which is evolutionarily conserved. The human survivin gene, spanning 14.7 kb on the telomeric position of chromosome 17, contains 4 exons and 3 introns and produces a 16.5-kDa protein (Figure 1). Unlike other IAPs, survivin is small and has only a single N-terminal BIR domain, a long C-terminal alpha-helix coiled region, and forms a stable dimmer in solution. The BIR domain is thought to be critical for anti-apoptotic function, whereas the coiled domain probably interacts with tubulin structures[7]. The survivin gene locus encodes multiple genetic splice variants with unique properties and functions. These isoforms include survivin,
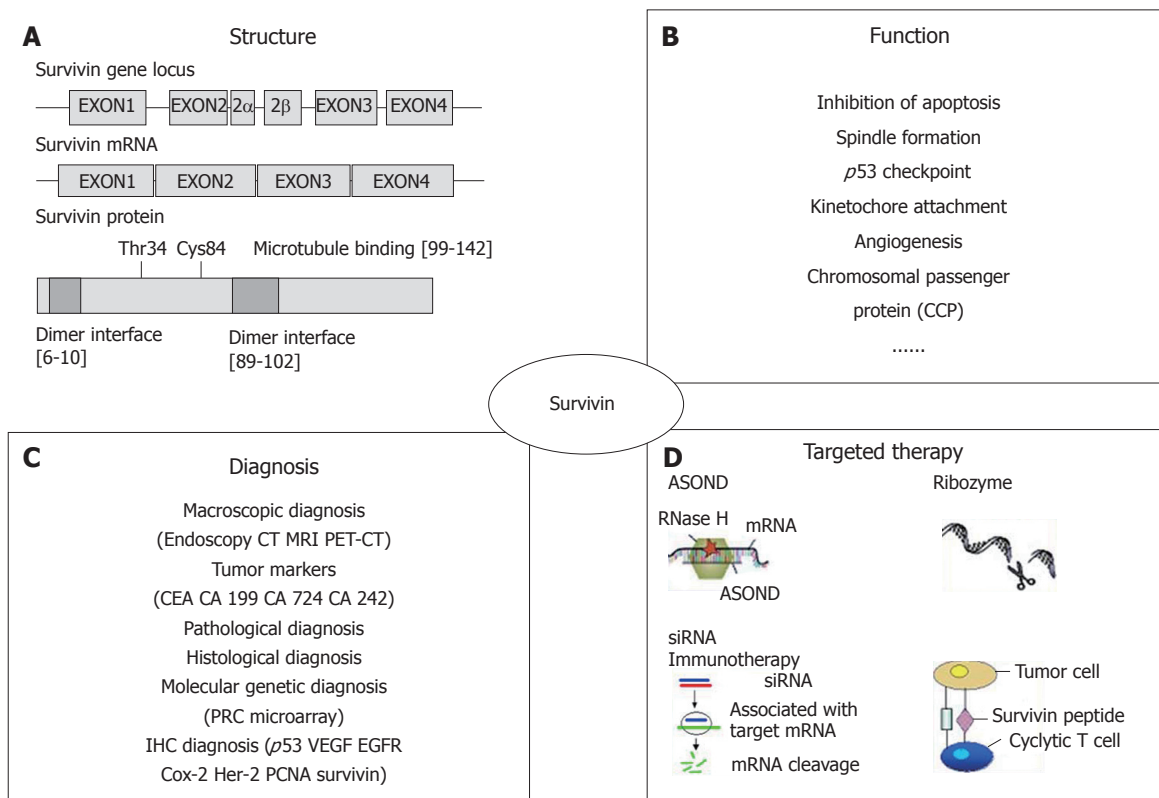
Figure 1 Survivin: from basic knowledge to clinicl application. **A**: the structure of surviving gene, mRNA and protein. The survivin gene is composed of exons 1-4, and produces a 16.5 kDa protein. **B**; Survivin has a dual function in apoptosis and mitotic progression; **C**: the proposal of modern gastric cancer diagnostic methodology and marker panel, with combination of the conventional diagnostic procedure and the new diagnostic methods. The latter was based on the examination of further molecular markers in less advanced stages of tumor and can be used for super-early diagnosis; **D**: the targeted therapy based on survivin nowadays.

survivin-2B, survivin-ΔEx-3, survivin-3B, and survivin-2alpha. Transcription and translation of these isoforms have been demonstrated by several groups of investigators[8-10]. In malignant cells, all of these isoforms are expressed at very high levels, when compared with normal tissues. Survivin has a dual function, playing a roll in cell death regulation and mitotic progression.

Survivin inhibits apoptosis, *via* its BIR domain, by either directly or indirectly interfering with the function of caspase-3 and caspase-7. It also counteracts cell death by interfering with caspase-9 processing, the upstream inhibitor in the intrinsic pathway of apoptosis[11]. Preferentially expressed at mitosis in a cell cycle-dependent manner and physically associated with the mitotic apparatus, survivin is essential for proper completion of various stages of cell division, from centrosomal functions to proper kinetochore attachment to spindle formation, potentially via regulation of microtubule dynamics (Figure 1).

Expression characteristics

The expression of survivin is tissue specific and cell cycle specific. During human development, survivin is expressed in fetal lung, heart, liver, kidney, gastrointestinal tract and in other fetal tissues where apoptosis occurs, such as the stem cell layer of stratified epithelia, endocrine pancreas and thymic medulla. Survivin was strongly expressed in the most common solid tumors of adults, including those of the lung, breast, colon, brain, stomach, esophagus, pancreas, liver, prostate, uterus, and ovaries, but it was not found in normal, adult tissues[12]. These findings suggest that the cell division and anti-apoptosis functions of survivin could be important not only during early development but also during cancer progression. In actively proliferating cells, survivin expression is cell cycle regulated, being virtually undetectable in G1 and S phases, with a peak level in G2/M[13].

SURVIVIN EXPRESSION AND DIAGNOSIS IN GASTRIC CANCER

Approximately 50% of patients have gastric carcinoma that extends beyond the locoregional confines at diagnosis. In addition, approximately 50% of patients with locoregional gastric carcinoma cannot undergo a curative resection (R0). About 70% to 80% of resected gastric carcinoma specimens have metastases in the regional lymph nodes[1]. Based on these facts, gastric carcinoma is often diagnosed at an advanced stage, and continues to pose a major challenge for healthcare professionals. Now, with the development of expression microarray technology, a large number of genes and molecules have been studied regarding the relationship between the development, progression, and metastasis of gastric cancer[14]. These genes include oncogenes, tumor suppressor genes, genes controlling apoptosis (e.g., survivin), cell cycle control genes, DNA synthesis genes, cell division genes, and genes for transcription and translation factors. They offer opportunities not only for early cancer diagnosis but for molecular-based, histological, exact diagnosis of tumors.

Figure 1 shows a proposal for modern gastric cancer.

Development of gastric cancer, like many other malignancies, is a multi-step process involving the accumulation of mutations and changes in cell cycle regulatory mechanisms. The detection of these alterations in the early stage of cancer development may shed new light on the gastric carcinogenesis process. In the gastrointestinal tract, there are indications that activation of survivin may be required for carcinogenesis. Yu et al[15] showed that survivin expression is frequently (68%) present in gastric cancer tissues and is also present, albeit at lower frequency (27%), in gastric mucosa of first-degree relatives. Survivin expression was also found in 22% of the non-cancerous tissues adjacent to gastric cancer tissues, but was not detectable in all of the normal, non-adjacent gastric mucosal tissues. Survivin expression is found in cancerous tissue, as well as in normal adult tissues that are predisposed to malignancy, indicating that survivin function may be required for carcinogenesis itself.

As we have already mentioned, survivin shows significant differential expression between malignant and normal adult cells, with very low to absent levels in normal adult tissue but increased levels in a wide variety of tumors. Therefore, the detection of survivin in body fluids could serve as a diagnostic marker that allows the early detection of malignancy. Such a study was firstly performed by Smith et al[5]. They measured survivin protein in urine samples from patients with bladder cancer and controls. Using a novel detection method for survivin, urine samples were filtered onto nitrocellulose membranes and probed with an anti-survivin antibody. Its presence in urine has been used to diagnose bladder cancer and to differentiate neoplastic lesions from inflammatory conditions with a sensitivity of 100% and specificity of 95%. This result suggests that survivin can be measured in samples easily obtained from patients and can be used to screen for the presence of malignancy. Furthermore, the result suggests that survivin expression can identify the lesions at highest risk for malignant transformation and invasion. As to gastric cancer, Wang et al[16] studied the expression of survivin in the peritoneal lavage fluid from 48 patients with gastric carcinoma using RT-PCR. They found survivin expression in the peritoneal cavity significantly correlated with depth of cancer invasion, lymph node metastasis, and TNM stage. Ninety two percent of clinically evident peritoneal metastasis cases showed detectable survivin expression. This result suggests that survivin can serve as a molecular marker for detecting peritoneal micrometastasis. Its ubiquitous expression in peritoneal cancer cells and metastatic nodules also suggests a promising future therapeutic strategy based on survivin inhibition for cases of gastric cancer involving peritoneal metastasis. This application, however, has not been tested in clinical trial.

SURVIVIN EXPRESSION AND PROGNOSIS IN GASTRIC CANCER

The outcome of gastric cancer depends on the initial stage of the cancer at diagnosis. Surgical therapy is the standard treatment for gastric carcinoma, and patients who can undergo a curative resection of the tumor may have a better outcome. However, even with surgery, recurrence rates range from 30%-60% depending on the pathologic stage, and five-year survival rate is only 20%. With the emergence of partially effective but potentially toxic (neo-) adjuvant chemotherapy, it has become increasingly important to discover biomarkers that will identify those patients who have the highest likelihood of recurrence and who might benefit most from adjuvant chemotherapy.

Numerous papers have appeared over the past several decades proposing a variety of molecular markers or proteins that may have prognostic significance in gastric cancer. Although no single marker has yet been shown to be perfect in predicting patient outcome, a profile based on survivin may be helpful in directing patient therapy[17-19]. The prognostic importance of survivin expression at both the level of the message and protein has been demonstrated in multiple studies (Table 1). Clinical studies correlating survivin expression with disease aggression in adult cancer have shown that survivin is a reliable marker of unfavorable disease and decreased survival. High survivin expression by neoplasms correlates with more aggressive behavior and invasive clinical phenotype, decreased response to chemotherapeutic agents, increased rates of relapse and shortened survival times. For example, in a study of 106 patients with gastric tumors, survivin mRNA expression in the tumor was associated with tumor size, depth of invasion, lymph node metastasis, tumor stage and decreased overall survival[30]. In addition to its level of expression, the localization of survivin may also be prognostically important. In a study of 84 patients with esophageal carcinoma, increased nuclear survivin expression correlated with reduced overall survival (estimated mean survival of 28 mo for patients with nuclear survivin versus 108 mo for patients with no nuclear survivin), but cytoplasmic levels of survivin were not predictive of outcome[31]. This discrepancy between nuclear and cytoplasmic survivin highlights the different anti-apoptotic functions of survivin and suggests that the role of survivin as a cell cycle regulator may be a more important determinant of patient outcome than its role as a caspase inhibitor. This phenomenon has not been detected in gastric cancer, and needs further investigation. High expression of survivin also revealed a decreased responsiveness to chemotherapeutic agents. Gastric carcinoma is one of the most intractable cancers and is known for resistance to various chemotherapeutic agents. Although cisplatin demonstrated better clinical efficacy against gastric cancer than other anti-neoplastic drugs, the overall response rate to CDDP-based treatment was only 33%. The mechanism of CDDP includes inducing apoptosis via caspase-3 activation, and therefore, survivin may mediate the drug resistance. Nakamura et al[32] transfected wild-type and dominant-negative mutants of the survivin gene into gastric cancer cells using a lipofection method. Overexpression of survivin protected MKN45 cells from CDDP-induced apoptosis. Expression of the dominant-negative mutant of the survivin gene sensitized NUGC-3 cells to drug-induced apoptosis. These results indicate that survivin may be central for exhibition of not only intrinsic resistance, but also acquired resistance to CDDP, and could be a predictive marker for response

Table 1 Expression of survivin in gastric cancer in association with cancer progression and malignancy

Author /Year	Number of patients	Diagnostic technique	Survivin expression	Correlation with (*P* value)	References
LUCD /1998	174	IHC	60 (34.5%)	Apoptotic index (< 0.001)	20
Okada E /2001	133	IHC	60 (82.0%)	–	21
Krieg A /2002	30	RT-PCR	30 (100.0%)	Tumor stage (0.033)	22
Yu J /2002	50	RT-PCR/IHC	34 (68.0%)	Apoptotic index (0.02), Cox-2 overexpression (0.001)	15
Tsuburaya A /2002	25	RT-PCR	16 (64.0%)	Depth of tumor (< 0.05) peritoneal metastasis (< 0.05)	23
Wakana Y /2002	42	RT-PCR/IHC	–	Apoptotic index (< 0.05), histological type (< 0.001)	24
Miyachi /2003	107	RT-PCR	105 (98.1%)	Lymph node metastasis (< 0.01)	25
Yao XQ /2004	120	IHC	59 (49.2%)	Histological subtypes, lymph node metastasis apoptotic index (< 0.05)	26
Wang ZN /2004	48	RT-PCR	32 (66.7%)	Depth of cancer invasion, peritoneal lavage fluid, lymph node metastasis, TNM stage (< 0.05)	16
Meng H /2005	77	RT-PCR	77 (100.0%)	Survival rate (< 0.01)	27
				Docetaxel-resistance (< 0.05)	28
Sun YS /2006	96	IHC	55 (57.2%)	Serosal infiltration, lymphatic invasion, regional lymph node metastasis, TNM stage, distant metastasis, survival rate (< 0.05), VEGF-C (< 0.001)	29
Lee GH /2006	106	IHC	53 (50.0%)	Tumor size (0.011), tumor stage (0.002), depth of invasion (0.004), poor survival (0.046), lymph node metastasis (0.020)	30

IHC: Immunohistochemistry; RT-PCR: Reverse transcriptase PCR.

to CDDP-based treatment. Given these compelling data, survivin should be considered as a potentially key biological marker in gastric cancer. In addition, with the emergence of survivin-targeted therapies that are known to be effective in pre-clinical trials, survivin could be used as a marker to identify patients that might be good candidates for therapies. The prognostic importance of survivin in gastric tumor has been demonstrated repeatedly, but the challenge remains how to incorporate these molecular markers into clinical algorithms. Perhaps patients with elevated survivin could be offered more intensive or novel therapies at diagnosis. However, such investigational approaches need to be done in a properly controlled trial.

TARGETED THERAPY

Because survivin is preferentially expressed in malignant cells and is prognostically important, it acts as an attractive therapeutic target. Efforts are under way to develop surviving inhibitors for clinical use with the dual aim to inhibit tumor growth through an increase in spontaneous apoptosis and to enhance tumor cell response to apoptosis-inducing agents[12]. Different kinds of survivin molecular antagonists, including antisense oligonucleotides, ribozymes, small interfering RNAs (siRNAs), as well as cancer vaccines, have been used (Figure 1).

Antisense Oligonucleotides

One therapeutic strategy to inhibit survivin uses antisense oligonucleotides (ASONDs) to decrease the target survivin mRNA and subsequently decrease the protein. ASONDs inhibit survivin by forming duplexes with intracellular native mRNA. The duplexes disrupt ribosome assembly and inhibit protein translation. More importantly, the mRNA-ASONDs complex recruits RNase H enzymes that cleave the native mRNA strand while leaving the ASOND intact. The ASOND is then released back into the cytosol, where it is capable of inhibiting additional native mRNA. ASONDs have been actively developed against survivin in gastric cancer. The efficacy of survivin ASONDs has been demonstrated both *in vitro* and *in vivo*. *In vitro*, several ASONDs that target different regions of survivin were designed[33], and one of them (ASOND3) caused a statistically significant loss of survivin mRNA, reduction of cell viability to 60.6% and inhibition of cell growth. The protein level was significantly decreased 48 h after survivin ASODN transfection compared with untreated controls. This result shows survivin antisense molecules directly induce apoptosis in gastric cancer cell lines overexpressing survivin. *In vivo*, antisense survivin oligonucleotides, administered by transfecting tumor cells with plasmids encoding survivin antisense before tumor implantation, reduced tumor growth in xenograft models of gastric carcinoma[34]. Clinical grade antisense surviving oligonucleotides (LY2181308) are currently under development by Isis Pharmaceuticals and Lily Pharmaceuticals in the United Kingdom as a single agent in patients with refractory malignancies. In preclinical studies, LY2181308 demonstrated activity in multiple *in vivo* models of cancer. In November 2004[35], Lilly initiated phase 1 clinical trials in cancer patients. Given the current developmental status of survivin, antisense oligonucleotides against survivin will likely be used in clinical practice before chemical inhibitors. Furthermore, a synergistic effect was noted when tumor cells were treated with ASOND and the chemotherapeutic agent. Targeting of the survivin pathway in cancer, alone or in conjunction with chemo-therapeutic agents, has potential as a novel therapeutic regimen.

Survivin ribozyme approach

As an alternative strategy for survivin inhibition, ribozymes directed against different portions of survivin mRNA were developed. Ribozymes are small RNA molecules that possess specific endonucleolytic activity and catalyse the

hydrolysis of specific phosphodiester bonds[36], resulting in the cleavage of the RNA target sequences. In particular, the hammerhead ribozyme consists of a highly conserved catalytic core, which cleaves substrate RNA at NHH triplets 3' to the second H, where N is any nucleotide and H is any nucleotide but guanidine. Pennati et al[37] have done several studies in this area. They found ribozyme-mediated inhibition of survivin expression increases spontaneous and drug-induced apoptosis and decreases the tumorigenic potential of human prostate cancer cells, and it also causes chemosensitization and radiosensitization of human melanoma cells[38,39]. This may be an effective alternative tool for research purposes but appears to be unsuitable for clinical treatment of cancer.

Survivin RNA interference approach

Recently, studies suggest that RNA interference (RNAi) technology is a powerful approach to silence mammalian gene expression for gene function studies[40]. Two approaches can effectively inhibit expression of the targeted genes in mammalian cells without activation of the nonspecific interferon response. These approaches are the in vitro synthesized 21-25 nucleotide (nt) double-stranded RNAs (small inhibitory RNA, siRNA) or the 21-29 nt short hairpin double-stranded RNAs (shRNA). Several studies on experimental human tumor models have demonstrated the feasibility of this technology for the inhibition of cancer-related genes including survivin[41-43]. Carvalho et al[44] first used RNA interference to specifically repress survivin in HeLa cells. These authors showed that survivin was no longer detectable in cultures 60 h after transfection with specific siRNA and that survivin-depleted cells were delayed in mitosis and accumulated in prometaphase with misaligned chromosomes. Moreover, siRNA-mediated survivin knock down caused radio-sensitization, which was paralleled by an increased activity of caspase-3 and caspase-7, in wt-p53 but not in mutant-p53 sarcoma cells[45]. It is widely accepted that RNAi provides a powerful tool for targeted inhibition of gene expression, with respect to conventional antisense strategies presumably, because it relies on a natural process. Ribozymes as well as siRNAs can lead to nonsequence specific effects (off-target effects) that are strongly dependent on the concentration of oligomers. Until recently, there were no studies focused on gastric tumor cells and further research is needed in this field.

Survivin-derived cancer immunotherapy

Immunotherapy also appears to be a plausible approach for treating survivin-positive tumors. Current research suggests that tumors of different origin appear to be able to present the same set of survivin-derived peptide epitopes. CD8+ T cells and monocyte-derived DCs can home to the primary solid tumor site, which provides the feasibility for cancer cells to act as survivin-antigen presenting cells to prime CD8+ T cells. Metastatic tumor cells can act as survivin antigen presenting cells to mature CD8+ T cells in the immune system (lymph node) into CTL, and these can be released into the circulation system and home to the primary tumor site[46,47].Spontaneous cytotoxic T lymphocyte response to survivin, in a major histocompatibility complex class I restricted manner, has been detected in patients with chronic lymphocytic leukemia, melanoma, and breast cancer. In addition, in vitro cytolytic T-cell induction against a survivin epitope results in cytolytic activity against a wide variety of human tumors, including gastric cancer[48]. Hence, survivin appears to be a universal tumor antigen and immunotherapy is a conceivable approach to treating survivin-positive tumors. Survivin-directed immunotherapy has been quickly moved to the clinic, and several phase I trials with administration of survivin peptides or survivin-directed autologous CTL generated ex vivo have been recently completed. In a phase study[49], an HLA-A24-restricted antigenic peptide, Survivin-2B80-88, which is recognized by CD8+ cytotoxic T-lymphocytes, was used to vaccinate patients with recurrent colorectal cancer. Results showed a decrease in expression of tumor markers in 40% of patients and a reduction in tumor size in one of fifteen patients. An open phase I/II cancer vaccine study is evaluating the toxicity and efficacy of HLA-A1, -A2, and -B35 restricted survivin epitopes in patients with tumors other than gastric cancer[50]. When used as an oral DNA vaccine, the survivin-directed immune response affected both tumor cells and tumor-associated angiogenesis, eradicating pulmonary metastases without toxicity in preclinical studies[51]. Survivin-based vaccination was found to be safe, devoid of significant side effects, and frequently associated with antigen-specific immunologic responses.

Others therapies

There are many other anti-survivin therapies, for example, the dominant negative (DN) mutant approach and approaches using small organic compounds or other small antagonists such as small peptides. As to dominant negative mutant, plasmid constructs expressing survivin antisense and DN mutant replacing the cysteine residue at amino acid 84 with alanine (Cys84Ala) were prepared and introduced into BCG-823 and MKN-45 gastric cancer cells[52], with a result of decreased cell growth and increased rate of apoptosis and mitotic catastrophe. This result was found also in nude mice xenografts. This approach is a good tool for research on demonstrating the principles of the survivin pathway, but it is not suitable for direct cancer therapy. While use of small antagonists will be a very exciting area of research in the coming years, it also appears to be the most practical way towards suitable approaches for clinical application. The potential small chemical molecules include those that either transcriptionally or post-transcriptionally inhibit survivin expression or abrogate survivin function, such as disruption of survivin-caspase interactions. For example, tetra-O-methyl nordihydroguaiaretic acid was shown to function by directly suppressing Sp1-dependent surviving gene expression, resulting in activation of mitochondrial apoptosis in tumor cells[53]. These phase I trials with small-molecule inhibitors that directly target survivin are approaching completion. Several small-molecule antagonists indirectly affect survivin levels include cyclin-dependent kinase inhibitors[54], antagonists of STAT3[55], T-cell factor[56], Hsp90[57], and ErbB2[58]. These compounds

reduce survivin levels by different mechanisms. Molecules that target survivin will initially be used as single agents or in combination with low-dose chemotherapy in patients with relapsed or refractory disease. As more experience is gained, these targeted therapies will be used upfront in the treatment of disease in combination with standard chemotherapy. In the future, when more small molecules that modulate the apoptosis cascade are developed, they will be used together to simultaneously target different molecular defects.

In summary, survivin is a potent caspase inhibitor, but it also inhibits cell death by modulating cell cycle progression, cell division, and signal transduction pathways. The vast difference in expression patterns of survivin between normal tissues and cancer cells has identified survivin as an exciting molecule to consider in the study of the underlying biology of tumorigenesis and to provide a platform to design molecules that can specifically target and eliminate cancer cells[11]. Despite its relatively recent discovery in 1997, survivin has attracted considerable interest from several viewpoints in the biochemical sciences. Our basic understanding of the structure and function of survivin is now being translated into clinical practice. Survivin-positive neoplasms are often more aggressive and less responsive to chemotherapeutic agents making survivin an independent negative prognostic parameter in gastric tumors. Survivin is also a potential therapeutic target for development of new anti-cancer therapies. However, mechanisms by which survivin suppresses apoptosis are still under considerable debate, and it is not yet known how survivin is upregulated in neoplastic cells. The challenge in all of these studies will be to prove that survivin based therapies are both efficacious and are, indeed, less toxic for normal human proliferating cells than standard therapies.

REFERENCES

1   **Jemal A**, Siegel R, Ward E, Murray T, Xu J, Smigal C, Thun MJ. Cancer statistics, 2006. *CA Cancer J Clin* 2006; **56**: 106-130
2   **Kaelin WG Jr**. The concept of synthetic lethality in the context of anticancer therapy. *Nat Rev Cancer* 2005; **5**: 689-698
3   **Altieri DC**. Survivin, versatile modulation of cell division and apoptosis in cancer. *Oncogene* 2003; **22**: 8581-8589
4   **Akhtar M**, Gallagher L, Rohan S. Survivin: role in diagnosis, prognosis, and treatment of bladder cancer. *Adv Anat Pathol* 2006; **13**: 122-126
5   **Smith SD**, Wheeler MA, Plescia J, Colberg JW, Weiss RM, Altieri DC. Urine detection of survivin and diagnosis of bladder cancer. *JAMA* 2001; **285**: 324-328
6   **Salvesen GS**, Duckett CS. IAP proteins: blocking the road to death's door. *Nat Rev Mol Cell Biol* 2002; **3**: 401-410
7   **Wheatley SP**, McNeish IA. Survivin: a protein with dual roles in mitosis and apoptosis. *Int Rev Cytol* 2005; **247**: 35-88
8   **Badran A**, Yoshida A, Ishikawa K, Goi T, Yamaguchi A, Ueda T, Inuzuka M. Identification of a novel splice variant of the human anti-apoptopsis gene survivin. *Biochem Biophys Res Commun* 2004; **314**: 902-907
9   **Caldas H**, Honsey LE, Altura RA. Survivin 2alpha: a novel Survivin splice variant expressed in human malignancies. *Mol Cancer* 2005; **4**: 11
10   **Yamada Y**, Kuroiwa T, Nakagawa T, Kajimoto Y, Dohi T, Azuma H, Tsuji M, Kami K, Miyatake S. Transcriptional expression of survivin and its splice variants in brain tumors in humans. *J Neurosurg* 2003; **99**: 738-745
11   **Altieri DC**. Targeted therapy by disabling crossroad signaling

networks: the survivin paradigm. *Mol Cancer Ther* 2006; **5**: 478-482
12   **Altieri DC**. Validating survivin as a cancer therapeutic target. *Nat Rev Cancer* 2003; **3**: 46-54
13   **Reed JC**, Bischoff JR. BIRinging chromosomes through cell division--and survivin' the experience. *Cell* 2000; **102**: 545-548
14   **Galamb O**, Sipos F, Fischer K, Tulassay Z, Molnar B. The results of the expression array studies correlate and enhance the known genetic basis of gastric and colorectal cancer. *Cytometry B Clin Cytom* 2005; **68**: 1-17
15   **Yu J**, Leung WK, Ebert MP, Ng EK, Go MY, Wang HB, Chung SC, Malfertheiner P, Sung JJ. Increased expression of survivin in gastric cancer patients and in first degree relatives. *Br J Cancer* 2002; **87**: 91-97
16   **Wang ZN**, Xu HM, Jiang L, Zhou X, Lu C, Zhang X. Expression of survivin mRNA in peritoneal lavage fluid from patients with gastric carcinoma. *Chin Med J* (Engl) 2004; **117**: 1210-1217
17   **Shariat SF**, Lotan Y, Saboorian H, Khoddami SM, Roehrborn CG, Slawin KM, Ashfaq R. Survivin expression is associated with features of biologically aggressive prostate carcinoma. *Cancer* 2004; **100**: 751-757
18   **Span PN**, Sweep FC, Wiegerinck ET, Tjan-Heijnen VC, Manders P, Beex LV, de Kok JB. Survivin is an independent prognostic marker for risk stratification of breast cancer patients. *Clin Chem* 2004; **50**: 1986-1993
19   **Kajiwara Y**, Yamasaki F, Hama S, Yahara K, Yoshioka H, Sugiyama K, Arita K, Kurisu K. Expression of survivin in astrocytic tumors: correlation with malignant grade and prognosis. *Cancer* 2003; **97**: 1077-1083
20   **Lu CD**, Altieri DC, Tanigawa N. Expression of a novel antiapoptosis gene, survivin, correlated with tumor cell apoptosis and p53 accumulation in gastric carcinomas. *Cancer Res* 1998; **58**: 1808-1812
21   **Okada E**, Murai Y, Matsui K, Isizawa S, Cheng C, Masuda M, Takano Y. Survivin expression in tumor cell nuclei is predictive of a favorable prognosis in gastric cancer patients. *Cancer Lett* 2001; **163**: 109-116
22   **Krieg A**, Mahotka C, Krieg T, Grabsch H, Muller W, Takeno S, Suschek CV, Heydthausen M, Gabbert HE, Gerharz CD. Expression of different survivin variants in gastric carcinomas: first clues to a role of survivin-2B in tumour progression. B*r J Cancer* 2002; **86**: 737-743
23   **Tsuburaya A**, Noguchi Y, Yoshikawa T, Saito A, Doi C, Okamoto T, Fukuzawa K. An anti-apoptosis gene, survivin and telomerase expression in gastric cancer. *Hepatogastroenterology* 2002; **49**: 1150-1152
24   **Wakana Y**, Kasuya K, Katayanagi S, Tsuchida A, Aoki T, Koyanagi Y, Ishii H, Ebihara Y. Effect of survivin on cell proliferation and apoptosis in gastric cancer. *Oncol Rep* 2002; **9**: 1213-1218
25   **Miyachi K**, Sasaki K, Onodera S, Taguchi T, Nagamachi M, Kaneko H, Sunagawa M. Correlation between survivin mRNA expression and lymph node metastasis in gastric cancer. *Gastric Cancer* 2003; **6**: 217-224
26   **Yao XQ**, Liu FK, Qi XP, Wu B, Yin HL, Ma HH, Shi QL, Zhou XJ, Li JS. Expression of survivin in human gastric adenocarcinomas: correlation with proliferation and apoptosis. *Zhonghua Waike Zazhi* 2004; **42**: 145-148
27   **Meng H**, Dai DJ, Lu CD. Prognostic significance of survivin splicing variants in expression gastric cancer. *Zhonghua Weichang Waike Zazhi* 2005; **8**: 234-236
28   **Meng H**, Lu CD, Dai DJ, Sun YL, Tanigawa N. Elevated expression level of wild-type survivin in gastric cancer promotes in vitro docetaxel-resistance. *Zhonghua Yixue Zazhi* 2004; **84**: 2060-2063
29   **Sun YS**, Ye ZY, Zhao ZS, Shi D, Zou SC. Expression of vascular endothelial growth factor C and survivin in gastric carcinoma and their clinical implications. *Zhonghua Wei chang Waike Zazhi* 2006; **9**: 264-267
30   **Lee GH**, Joo YE, Koh YS, Chung IJ, Park YK, Lee JH, Kim HS, Choi SK, Rew JS, Park CS, Kim SJ. Expression of survivin in gastric cancer and its relationship with tumor angiogenesis.

Eur J Gastroenterol Hepatol 2006; **18**: 957-963

31   **Grabowski P**, Kuhnel T, Muhr-Wilkenshoff F, Heine B, Stein H, Hopfner M, Germer CT, Scherubl H. Prognostic value of nuclear survivin expression in oesophageal squamous cell carcinoma. *Br J Cancer* 2003; **88**: 115-119

32   **Nakamura M**, Tsuji N, Asanuma K, Kobayashi D, Yagihashi A, Hirata K, Torigoe T, Sato N, Watanabe N. Survivin as a predictor of cis-diamminedichloroplatinum sensitivity in gastric cancer patients. *Cancer Sci* 2004; **95**: 44-51

33   **Yang JH**, Zhang YC, Qian HQ. Survivin antisense oligodeoxynucleotide inhibits growth of gastric cancer cells. *World J Gastroenterol* 2004; **10**: 1121-1124

34   **Tu SP**, Jiang XH, Lin MC, Cui JT, Yang Y, Lum CT, Zou B, Zhu YB, Jiang SH, Wong WM, Chan AO, Yuen MF, Lam SK, Kung HF, Wong BC. Suppression of survivin expression inhibits in vivo tumorigenicity and angiogenesis in gastric cancer. *Cancer Res* 2003; **63**: 7724-7732

35   **Schimmer AD**. Inhibitor of apoptosis proteins: translating basic knowledge into clinical practice. *Cancer Res* 2004; **64**: 7183-7190

36   **Zaffaroni N**, Pennati M, Daidone MG. Survivin as a target for new anticancer interventions. *J Cell Mol Med* 2005; **9**: 360-372

37   **Pennati M**, Binda M, Colella G, Zoppe' M, Folini M, Vignati S, Valentini A, Citti L, De Cesare M, Pratesi G, Giacca M, Daidone MG, Zaffaroni N. Ribozyme-mediated inhibition of survivin expression increases spontaneous and drug-induced apoptosis and decreases the tumorigenic potential of human prostate cancer cells. *Oncogene* 2004; **23**: 386-394

38   **Pennati M**, Binda M, De Cesare M, Pratesi G, Folini M, Citti L, Daidone MG, Zunino F, Zaffaroni N. Ribozyme-mediated down-regulation of survivin expression sensitizes human melanoma cells to topotecan in vitro and in vivo. *Carcinogenesis* 2004; **25**: 1129-1136

39   **Pennati M**, Binda M, Colella G, Folini M, Citti L, Villa R, Daidone MG, Zaffaroni N. Radiosensitization of human melanoma cells by ribozyme-mediated inhibition of survivin expression. *J Invest Dermatol* 2003; **120**: 648-654

40   **Izquierdo M**. Short interfering RNAs as a tool for cancer gene therapy. *Cancer Gene Ther* 2005; **12**: 217-227

41   **Uchida H**, Tanaka T, Sasaki K, Kato K, Dehari H, Ito Y, Kobune M, Miyagishi M, Taira K, Tahara H, Hamada H. Adenovirus-mediated transfer of siRNA against survivin induced apoptosis and attenuated tumor cell growth in vitro and in vivo. *Mol Ther* 2004; **10**: 162-171

42   **Beltrami E**, Plescia J, Wilkinson JC, Duckett CS, Altieri DC. Acute ablation of survivin uncovers p53-dependent mitotic checkpoint functions and control of mitochondrial apoptosis. *J Biol Chem* 2004; **279**: 2077-2084

43   **Caldas H**, Holloway MP, Hall BM, Qualman SJ, Altura RA. Survivin-directed RNA interference cocktail is a potent suppressor of tumour growth in vivo. *J Med Genet* 2006; **43**: 119-128

44   **Carvalho A**, Carmena M, Sambade C, Earnshaw WC, Wheatley SP. Survivin is required for stable checkpoint activation in taxol-treated HeLa cells. *J Cell Sci* 2003; **116**: 2987-2998

45   **Kappler M**, Taubert H, Bartel F, Blumke K, Panian M, Schmidt H, Dunst J, Bache M. Radiosensitization, after a combined treatment of survivin siRNA and irradiation, is correlated with the activation of caspases 3 and 7 in a wt-p53 sarcoma cell line, but not in a mt-p53 sarcoma cell line. *Oncol Rep* 2005; **13**: 167-172

46   **Li F**, Ling X. Survivin study: an update of "what is the next wave"? *J Cell Physiol* 2006; **208**: 476-486

47   **Reed JC**, Wilson DB. Cancer immunotherapy targeting survivin: commentary re: V. Pisarev et al., full-length dominant-negative survivin for cancer immunotherapy. Clin. Cancer Res., 9: 6523-6533, 2003. *Clin Cancer Res* 2003; **9**: 6310-6315

48   **Schmidt SM**, Schag K, Muller MR, Weck MM, Appel S, Kanz L, Grunebach F, Brossart P. Survivin is a shared tumor-associated antigen expressed in a broad variety of malignancies and recognized by specific cytotoxic T cells. *Blood* 2003; **102**: 571-576

49   **Tsuruma T**, Hata F, Torigoe T, Furuhata T, Idenoue S, Kurotaki T, Yamamoto M, Yagihashi A, Ohmura T, Yamaguchi K, Katsuramaki T, Yasoshima T, Sasaki K, Mizushima Y, Minamida H, Kimura H, Akiyama M, Hirohashi Y, Asanuma H, Tamura Y, Shimozawa K, Sato N, Hirata K. Phase I clinical study of anti-apoptosis protein, survivin-derived peptide vaccine therapy for patients with advanced or recurrent colorectal cancer. *J Transl Med* 2004; **2**: 19

50   **Otto K**, Andersen MH, Eggert A, Keikavoussi P, Pedersen LO, Rath JC, Bock M, Brocker EB, Straten PT, Kampgen E, Becker JC. Lack of toxicity of therapy-induced T cell responses against the universal tumour antigen survivin. *Vaccine* 2005; **23**: 884-889

51   **Xiang R**, Mizutani N, Luo Y, Chiodoni C, Zhou H, Mizutani M, Ba Y, Becker JC, Reisfeld RA. A DNA vaccine targeting survivin combines apoptosis with suppression of angiogenesis in lung tumor eradication. *Cancer Res* 2005; **65**: 553-561

52   **Tu SP**, Jiang XH, Lin MC, Cui JT, Yang Y, Lum CT, Zou B, Zhu YB, Jiang SH, Wong WM, Chan AO, Yuen MF, Lam SK, Kung HF, Wong BC. Suppression of survivin expression inhibits in vivo tumorigenicity and angiogenesis in gastric cancer. *Cancer Res* 2003; **63**: 7724-7732

53   **Chang CC**, Heller JD, Kuo J, Huang RC. Tetra-O-methyl nordihydroguaiaretic acid induces growth arrest and cellular apoptosis by inhibiting Cdc2 and survivin expression. *Proc Natl Acad Sci USA* 2004; **101**: 13239-13244

54   **Shapiro GI**. Preclinical and clinical development of the cyclin-dependent kinase inhibitor flavopiridol. *Clin Cancer Res* 2004; **10**: 4270s-4275s

55   **Turkson J**. STAT proteins as novel targets for cancer drug discovery. *Expert Opin Ther Targets* 2004; **8**: 409-422

56   **Emami KH**, Nguyen C, Ma H, Kim DH, Jeong KW, Eguchi M, Moon RT, Teo JL, Kim HY, Moon SH, Ha JR, Kahn M. A small molecule inhibitor of beta-catenin/CREB-binding protein transcription (corrected). *Proc Natl Acad Sci USA* 2004; **101**: 12682-12687

57   **Sausville EA**, Tomaszewski JE, Ivy P. Clinical development of 17-allylamino, 17-demethoxygeldanamycin. *Curr Cancer Drug Targets* 2003; **3**: 377-383

58   **Xia W**, Gerard CM, Liu L, Baudson NM, Ory TL, Spector NL. Combining lapatinib (GW572016), a small molecule inhibitor of ErbB1 and ErbB2 tyrosine kinases, with therapeutic anti-ErbB2 antibodies enhances apoptosis of ErbB2-overexpressing breast cancer cells. *Oncogene* 2005; **24**: 6213-6221

Alteration of nuclear matrix-intermediate filament system and differential expression of nuclear matrix proteins during human hepatocarcinoma cell differentiation

Jian Tang, Jing-Wen Niu, Dong-Hui Xu, Zhi-Xing Li, Qi-Fu Li, Jin-An Chen

Jian Tang, Jing-Wen Niu, Zhi-Xing Li, Qi-Fu Li, Jin-An Chen, The Key Laboratory of Chinese Ministry of Education for Cell Biology and Tumor Cell Engineering, School of Life Sciences, Xiamen University, Xiamen 361005, Fujian Province, China
Dong-Hui Xu, Department of Hepatic Biliary Pancreatic Vascular Surgery, 1st Hospitalof Xiamen, Fujian Medical University, Xiamen 361003, Fujian Province, China
Correspondence to: Dr Qi-Fu Li, Laboratory of Cell Biology, School of Life Sciences,Xiamen University, Xiamen 361005, Fujian Province, China. chifulee@xmu.edu.cn
Telephone: +86-592-2185363 Fax: +86-592-2181015

Abstract

AIM: To investigate the association between the configurational and compositional changes of nuclear matrix and the differentiation of carcinoma cells.

METHODS: Cells cultured with or without 5×10^{-3} mmol/L of hexamethylene bisacetamide (HMBA) on Nickel grids were treated by selective extraction and prepared for whole mount observation under electron microscopy. The samples were examined under transmission electron microscope. Nuclear matrix proteins were selectively extracted and subjected to subcellular proteomics study. The protein expression patterns were analyzed by PDQuest software. Spots of differentially expressed nuclear matrix proteins were excised and subjected to *in situ* digestion with trypsin. The peptides were analyzed by matrix-assisted laser-desorption/ionization time of flight mass spectrometry (MALDI-TOF-MS). Data were submitted for database searching using Mascot tool (www.matrixscience.com).

RESULTS: The nuclear matrix (NM) and intermediate filament (IF) in SMMC-7721 hepatocarcinoma cells were found relatively sparse and arranged irregularly. The nuclear lamina was non-uniform, and two kinds of filaments were not tightly connected. After induction for differentiation by HMBA, the NM-IF filaments were concentrated and distributed uniformly. The heterogeneous population of filaments, including highly branched utrathin filaments could also be seen in the regular meshwork. The connection between the two kinds of filaments and the relatively thin, condensed and sharply demarcated lamina composed of intermediate-sized filaments was relatively fastened. Meanwhile, 21 NM proteins changed remarkably during SMMC-7721 cell differentiation. Four proteins, i.e. mutant Pyst1, hypothetical protein, nucleophosmin1, and LBP were downregulated, whereas four other proteins, eIF6, p44 subunit, β-tubulin, and SIN3B were upregulated with the last one, SR2/ASF found only in the differentiated SMMC-7721 cells.

CONCLUSION: The induced differentiation of SMMC-7721 cells by HMBA is accompanied by the configurational changes of nuclear matrix-intermediate filament (NM-IF) system and the compositional changes of nuclear matrix protein expression. These changes may be important morphological or functional indications of the cancer cell reversion.

Tang J, Niu JW, Xu DH, Li ZX, Li QF, Chen JA. Alteration of nuclear matrix-intermediate filament system and differential expression of nuclear matrix proteins during human hepatocarcinoma cell differentiation. *World J Gastroenterol* 2007; 13(20): 2791-2797

INTRODUCTION

The nuclear matrix not only plays an important role in the process of DNA replication, hRNA processing and steroid hormone action, but also has direct effect on cell division and proliferation through constructing the architecture of higher order chromatin[1-3]. Moreover, it is often the important binding site of expression and regulation of oncogenes[4,5]. Previous researches have proved that the ultrastructural change of cytoskeleton and nuclear matrix was closely related to cell proliferation and differentiation[6]. The nuclear matrix or nuclear matrix associatied proteins have strong effects on the regulation of signal transduction, mRNA modification

or translation, and more important, on the expression of oncogenes or tumor suppressor genes such as rb, $p21$, $p53$, which is extremely significant in the cell cycle processing and cell differentiation[7-11]. The nuclear matrix in cancer cells is not only abnormal in morphology, but also apparently different in its composition[12]. Our early studies showed distinct changes of the morphology or protein composition of nuclear matrix during differentiation of several cell lines treated with different reagents[13,14]. It is implied that those differentially expressed nuclear matrix proteins not only have direct association with regulators of cell cycle and signal transduction, but also are important during the cancerization and its reversion of the cell. Based on our former research of the effect on differentiation of SMMC-7721 cells with HMBA inducement[15], we studied the features and protein alternations of the nuclear matrix-intermediate filament (NM-IF) system in human hepatocarcinoma cell line SMMC-7721 during its differentiation induced by hexamethylamine bisacetamide (HMBA). It is helpful for further exploration and illustrating the relationship between the nuclear matrix and the cancerization and malignant phenotypic reversion of cancer cells.

MATERIALS AND METHODS

Materials
HMBA (Sigma Chemical Company) was used to induce the differentiation of SMMC-7721 cells. Sequence grade, modified trypsin (Promega) and iodoacetamide (Sigma) were used in the in-gel digestion. ReadyStrip IPG strips (pH 3-10, 11 cm) and IPG buffer pH 3-10 were obtained from Amersham Biosciences. Other reagents used in 2-D gel electrophoresis and Coomassie blue R250 were from Shanghai Sangon Biological Engineering Technology and Service Co., Ltd.

Cell culture and experimental treatment
SMMC-7721 human hepatocarcinoma cells were cultured at 37℃ in RPMI-1640 medium (pH 7.2) supplemented with 10% newborn calf serum, 100 U/mL penicillin, 100 U/mL streptomycin and 50 μg/mL kanamycin. Cells of experimental group were cultured at the same medium added with 5×10^{-3} mol/L HMBA (Sigma). SMMC-7721 cells and the treated cells were seeded in small culture flasks with cover slip strips on which some nickel grids were covered with formvar and carbon film was sticked with polylysine, and grown in the normal medium and the medium containing 5×10^{-3} mol/L HMBA respectively. Fresh culture media were added to the cells every 48 h, and cells were harvested at subconfluency. The obtained cells were then stored at -80℃.

Cell selective extraction
The cells were selectively extracted as described in our previous article[13]. Cover slip strips were removed from the culture medium and rinsed in phosphate-buffered saline at 4℃. Then they were placed in high ionic strength extraction medium [10 mmol/L PIPES (pH 6.8), 250 mmol/L $(NH_4)_2SO_4$, 300 mmol/L sucrose, 3 mmol/L

MgCl₂, 1.2 mmol/L PMSF, 0.5% Triton X-100; CSK-AS] 4℃ for 3 min. The extracted cells were rinsed briefly in digestion medium [10 mmol/L PIPES (pH 6.8), 50 mmol/L NaCl, 300 mmol/L sucrose, 3 mmol/L MgCl₂, 1.2 mmol/L PMSF, 0.5% Triton X-100] without enzymes. Grids with anchored skeletons were placed in the digestion medium and appropriate enzymes (400 mg/L DNase I and 400 mg/L RNase A) and were incubated for 20 min at 23℃. The grids were then placed in high ionic strength extraction medium CSK-AS for 5 min at 23℃. Thus, only the nuclear matrix-intermediate filament structure remained intact.

Sample preparation for whole mount electron microscopy
The NM-IF samples on the grids after the selective extraction were prefixed in 2% glutaraldehyde at 4℃ for 30 min, followed by 1% OsO4 in 0.1 mol/L sodium cacodylate (pH 7.2) for 5 min at 4℃. The cells, still attached to grids, were dehydrated in ethanol, dried through the CO₂ critical point and examined under a JEM-100CXII/S transmission electron microscopy.

Purification of nuclear matrix proteins
The SMMC-7721 cells were washed with PBS and extracted with cytoskeleton buffer (CSK100) (10 mmol/L PIPES pH 6.8, 300 mmol/L sucrose, 100 mmol/L NaCl, 4 mmol/L CaCl₂, 1.0 mmol/L PMSF, 0.5% Triton X-100) at 0℃ for 10 min, and subjected to centrifugation for 5 min at 400 r/min. The deposition was washed twice with CSK50 (10 mmol/L PIPES pH 6.8, 300 mmol/L sucrose, 50 mmol/L NaCl, 4 mmol/L CaCl₂, 1.0 mmol/L PMSF, 0.5% Triton X-100) and digested for 30 min at 25℃ in the same buffer containing 300 U/mL DNase I. One mole per liter ammonium sulfate was added dropwise to a final concentration of 0.25 mmol/L. After incubation for 15 min, the nuclear matrix proteins were pelleted by centrifugation at 1000 r/min for 5 min, and washed once with the CSK50 buffer, then stored at -80℃. Protein concentrations were determined by the method of Bradford.

Two-dimensional gel electrophoresis
To solubilize nuclear matrix proteins, the pellet of purified nuclei was resuspended in 2-D buffer containing 7 mol/L urea, 2 mol/L thiourea, 4% CHAPS, 50 mmol/L DTT and ultrasonicated for 2 min. The supernatant was centrifuged for 30 min at $16\,000 \times g$ at 4℃. IEF was performed in ReadyStrip IPG strips. ReadyStrip IPG strips were rehydrated overnight in a reswelling tray with 2-D buffer containing 0.5% IPG buffer pH 3-10 and nuclear matrix proteins in a final volume of 250 μL (200 μg). IEF was carried out on a Protean IEF cell (Investigator) at 19℃ with a maximum current setting of 80 mA/strip. Focusing was performed for a total of 70 000 V × h. Before carrying out the second dimensional SDS-PAGE, the strips were equilibrated in an equilibration buffer consisting of 20% glycerol, 2% SDS, 65 mmol/L Tris-HCl, pH 6.8 and 20 mmol/L DTT for 10 min at room temperature, then transferred into the second equilibration buffer containing 20% glycerol, 2% SDS, 65 mmol/L Tris-

HCl, pH 6.8 and 2.5% iodoacetamide. The strips were transferred onto 1-mm thick SDS-PAGE gels and sealed in place with 1% agarose. SDS-PAGE was performed on a 12.5% acrylamide/bisacrylamide gel at 50 V for 30 min followed by 170 V for 8 h. The gels were run in the following electrode buffer: 25 mmol/L Tris, 192 mmol/L glycine, 0.1% SDS. SDS-PAGE standards were used for gel calibration.

Silver staining

The gel was fixed (50% methanol and 10% glacial acetic acid) for more than 40 min, sensitized (70 mL of methanol, 10 mL of 10% Sodium thiosulfate, 17 g of NaAC, bringing up to 250 mL with dH_2O) for 30 min and rinsed in dH_2O 3 times for 5 min each. The gel was stained in stain solution (25 mL of 5% $AgNO_3$, 0.1 mL of formaldehyde, then increasing to 250 mL with dH_2O) for 30 min rinsed in dH_2O 3 times 1 min each and placed in developer (250 mL of dH_2O, 6.25g Na_2CO_3, 50 μL of formaldehyde) until spots were almost as dark as desired. Development was stopped (3.75 g EDTA in 250 mL dH_2O) and scanned using Magicscan. 2-DE maps of nuclear matrix proteins were subjected to analysis with PDQuest (Bio Rad) software.

In-gel trypsin digestion of proteins

Silver-stained spots were excised and washed with 50 mL fresh bleaching liquid (100 mmol/L $Na_2S_2O_3$: 30 mmol/L $K_3Fe (CN)_6$ = 1:1). Gel spots were dried in a vacuum centrifuge and reswelled in 50 mL of solution containing 10 mol/L DTT/100 mol/L NH_4HCO_3 and incubated at 57℃ for 1 h. This solution was subsequently replaced with 50 mL of solution containing 55 mol/L IAA, 100 mol/L NH_4HCO_3 and incubated at room temperature for 30 min. The gel spots were dried again and digested with TPCK-trypsin at 37℃ overnight. After the incubation, the liquid was removed from the gel piece and the liquid was transferred to a new-labeled tube. This solution contains the extracted tryptic peptides.

MALDI-TOF-MS analysis of tryptic peptide

For MALDI-TOF-MS analysis, samples were dissolved in 2 μL 0.1% TFA. Mass measurements were carried out on a Brucker ULTRAFLEXTM TOF/TOF mass spectrometer. This instrument was used at a maximum accelerating potential of 20 kV (in positive mode) and was operated in reflector mode. And 0.5 μL of saturated solution of α-cyano-4-hydroxy cinnamic acid in 0.1% TFA/30% acetonitrile was mixed with 0.5 μL sample solution, and added to the target. Internal calibration was performed with tryptic peptides coming from autodigestion of trypsin (monoisotopic masses at m/z 842.51, and m/z 2 211.10). Monoisotopic peptide masses were assigned and used for database search.

Database searching and identification of proteins

Peptide mass fingerprints obtained by the MALDI-TOF-MS were used to search nonredundant protein sequence database using Mascot software from Matrix Science. Search parameters included a maximum allowed peptide mass error of 100 ppm with consideration of one incomplete cleavage per peptide. Accepted modifications included carbamidomethylation of cysteine residues (from iodoacetamide exposure) and methionine oxidation, a common modification occurring during SDS-PAGE. The criteria for positive identification of proteins were set as follows: (1) Statistical significance ($P < 0.05$) of the match when tested by Mascot; (2) The matched peptides covered at least 17% of the whole protein sequence; (3) Concordance ($\pm$ 15%) with the molecular weight and pI of the parent 2-D PAGE protein spot; and (4) Protein identifications not fulfilling criterion 2 were still assigned, if criteria 1 and 3 were fulfilled and no other homo-sapiens proteins with peptide mass-matched. $P < 0.05$ was identified by Mascot and identified protein wasinferred.

RESULTS

Effect of HMBA on configurational changes of NM-IF system under transmission electron microscopy

Selective extraction technique revealed cytoplasmic and nuclear meshworks in SMMC-7721 cells. The nuclear matrix was mainly composed of thick filaments. The peripheral region of the nucleus was demarcated by the wide band of densely packed filaments. This structure, representing nuclear lamina, was attached to the surrounding intermediate filaments (IF) of cytoskeleton. The nuclear matrix filaments in SMMC-7721 cells were relatively few and scattered, not well distributed and arranged irregularly within the nucleus region, and there were few single filaments while most of the nuclear matrix filaments were quite thick in bundle-like form and interweaved into an irregular meshwork (Figure 1A). The nuclear lamina was composed of densely packed fibrils, and it was ununiformly thick and compact. The inner nuclear lamina was connected with some thick nuclear matrix filament bundles or thin and short filaments. The intermediate filaments which terminated on the out nuclear lamina were few, always in thick bundles or in strip-rope-like structure, and arranged irregularly, too (Figure 1C and 1E). Nevertheless, in the SMMC-7721 cells induced by HMBA, the nuclear matrix filaments were abundant and well-distributed, different in slender and thick form in the nucleus region. The single filaments increased, and interweaved into a regular network (Figure 1B). The wide nuclear lamina turned into a thin and compact fibroid structure, the inner nuclear lamina was connected closely with the nuclear matrix filaments, and many long and slender intermediate filament bundles were terminated directly on the outer nuclear lamina. Both the nuclear matrix filaments and the intermediate filaments connected to the nuclear lamina increased and appeared quite dense. Moreover, the intermediate filaments in the treated cells were abundant and well-distributed in the cytoplasmic region (Figure 1D and 1F).

2-D gel map and image analysis

Samples of nuclear matrix proteins extracted from SMMC-7721 cells treated with or without 5 mmol/L HMBA were subjected to 2-D gel electrophoresis for at
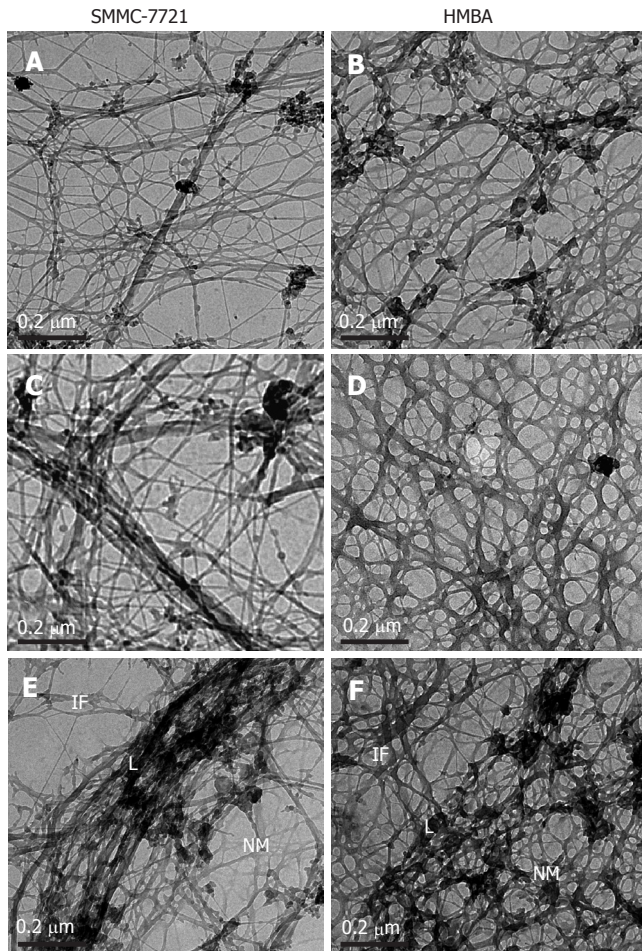
Figure 1 **A**: TEM observation of nuclear matrix filaments in SMMC-7721 cells; **B**: TEM observation of nuclear matrix filaments in SMMC-7721 cells treated with HMBA; **C**: TEM observation of intermediate filaments in SMMC-7721 cells; **D**: TEM observation of intermediate filaments in SMMC-7721 cells treated with HMBA; **E**: TEM observation of NM-IF system in SMMC-7721 cells. L: lamina; NM: Nuclear matrix; IF: intermediate filament; **F**: TEM observation of NM-IF system in SMMC-7721 cells treated with HMBA. Bar = 0.2 μm.
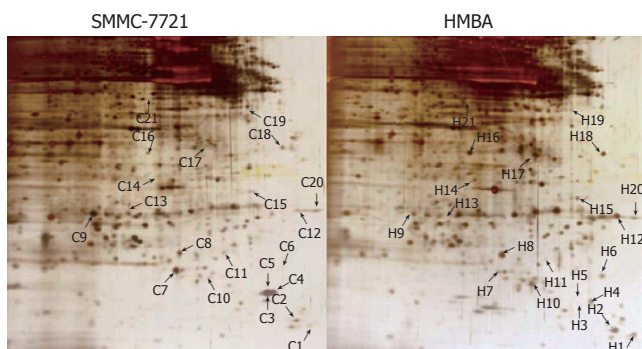
Figure 2 2-D PAGE gels of nuclear matrix proteins from SMMC-7721 cells, silver stained.

least three repeats per experimental condition. Analysis of proteins was based on evaluation of at least two gels. Twenty-one protein spots were changed remarkably, whereas most of the spots were similar to the control in the expression patterns of nuclear matrix proteins from differentiated SMMC-7721 cell. Among the changed
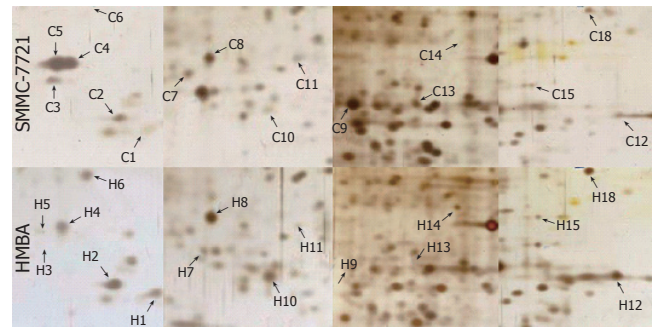
Figure 3 Enlarged maps of changed nuclear matrix proteins from SMMC-7721 cells.
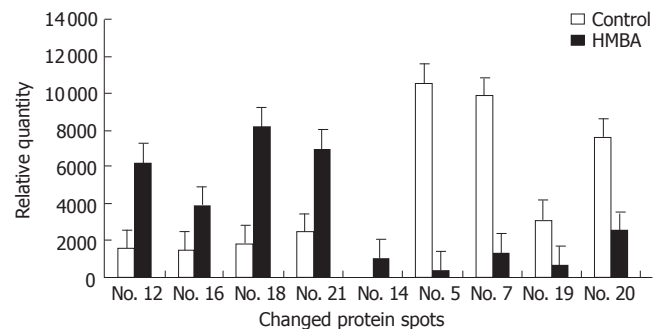
Figure 4 Relative expression level of changed nuclear matrix proteins.

spots, 8 spots (C4, C5, C7, C9, C11, C13, C19, C20) were downregulated, one spot disappeared in the differentiated SMMC-7721 cells, whereas 11 spots (C1, C2, C6, C8, C10, C12, C15, C16, C17, C18, C21, C3) were upregulated, and 1 spot (C14) emerged as a new protein spot in the differentiated cells (Figures 2 and 3). Relative expression levels of the changed proteins were shown using Melanie software (Figure 4), relative volume (% vol) of spot was employed to make data independent of uninteresting variation between gels, such as differences in protein loading or staining.

MALDI-TOF-MS analysis and protein identification
These 22 protein spots were cut out from the gels and analyzed with MALDI-TOF-MS. Peptide mass fingerprint (PMF) of each protein spot was then generated (data not shown). By searching the Mascot database, we identified 9 proteins combined with the searching results. The characteristics of the protein, the number and intensity of peptide matching peak, the sequence coverage of matching peptide, the theoretical and approximate values of Mr and pI, the identified protein names, accession numbers, the sequence coverages, and the theoretical Mr and pI values for each protein spot are listed in Table 1.

DISCUSSION
The abnormality of NM-IF system is closely associated with the canceration of cells. Previous studies showed that the nuclear matrix in cancer cells had some distinctive irregular morphology which differed from those of

Table 1 Proteins identified by MALDI-TOF-MS

Spot No.	NCBInr entry	Protein name	Mw/pI	Sequence coverage (%)	Biological function
Up-regulated					
No. 12	gi13785574	p27^{BBP} protein/eIF6	26 845/4.56	27	β4 integrin interactor, a component of NM filaments escorts 60S ribosome subunit from nuclear to cytoplasm
No. 16	gi88983724	Similar to TFIIH	36 539/6.79	23	Basic transcriptin factor 2 44 kDa subunit (BTF2-p44) (General transcription factor)
		Basal transcription factor complex p44 subunit			
No. 18	gi14043898	Tubulin, beta 2C	50 255/4.79	17	Tubulin β subunit, with GTPase activity
	gi27368062	Class IVb beta tubulin	50 177/4.82	17	
No. 21	gi13477279	SIN3B protein	49 609/6.56	23	Interact with the Mad components of the Myc/Max/Mad network of cell growth regulators
New protein					
No. 14	gi45708738	SFRS1 protein	22560/7.72	25	arginine/serine-rich 1 alternate splicing factor
Down-regulated					
No. 5	gi5822131	Crystal structure of an active site mutant of the pyst1	16364/5.31	47	ERK-specific MAP kinase phosphatase PYST1/MKP3
No. 7	gi62088338	Hypothetical protein: DKFZp434K1815 variant	26 864/5.64	24	From Deutches Krebs-Forschungszentrum cancer research centre (German)
No. 19	gi34234	Laminin-binding protein	31 888/4.84	28	Laminin-binding protein, LBP
	gi250127	67 kDa laminin receptor	32 860/4.83	27	
	gi17939541	Integrin beta 4 binding protein	27 095/4.56	26	
No. 20	gi83641870	Nucleophosmin1 Isoform 3	28 497/4.56	23	Also known as NPM, numatrin, No38, B23 protein
	gi40353734	Nucleophosmin 1 Isoform 2	29 617/4.47	23	A major nucleolus phosphoprotein, a component of NM

normal cells obviously[16,17]. HMBA could inhibit the malignant proliferation of SMMC-7721 cells, change the expression activity of hepatocarcinoma cell-associated enzyme or antigen such as Gamma Glutamyl Transferase (γ-GT), α-fetoprotein (AFP), proliferating cell nuclear antigen (PCNA), and arrest the cells in G_0/G_1 phase. Furthermore, HMBA could up-regulate the expression of *p*21$^{WAF1/CIP1}$ and *p*16 genes, down-regulate the activity of Cyclin D1-CDK4 and the transcription of c-myc gene which were necessary for cells entering into S phase, arrest the cells in G_0/G_1 phase, and induce the differentiation of SMMC-7721 cells[15,18]. This study further displayed that, after selective extraction, filaments of NM-IF system in SMMC-7721 cells were relatively few, not well-distributed and arranged irregularly, and the single filaments were few, the thick nuclear lamina was not closely associated with the nuclear matrix and intermediate filaments. It exhibited the rapid proliferation and the typical configuration characteristics of NM-IF system in malignant tumor cells. While in SMMC-7721 cells induced with HMBA, the nuclear matrix filaments and intermediate filaments interweaved into a regular and well-distributed meshwork in which the quantity of single filaments increased and differed in slender and thick form, moreover, the nuclear matrix filaments and intermediate filaments firmly fastened to the thin and compact fiber-like nuclear lamina. This morphology of NM-IF system was significantly different from those of rapidly proliferating SMMC-7721 cells but similar to those of some previously reported epithelial or normal cells[16,19], and was consistent with our previous studies in which we treated the human osteosarcoma cell line MG-63 and human gastric adenocarcinoma cell

line MGC80-3 with retinotic acid (RA) respectively[13,20]. It showed that the morphology and function of NM-IF system in SMMC-7721 cells during its differentiation had undergone a reverse alteration. This alteration is not only important for the reversion of hepatocarcinoma cells, but also the indication of the differential expression of nuclear matrix proteins.

Through 2-D gel electrophoresis and analysis of MALDI-TOF-MS, we found 21 nuclear matrix proteins that were differentially expressed during the differentiation process. Among the changed spots, 8 were downregulated, one disappeared in the differentiated SMMC-7721 cells, whereas 11 spots were upregulated, and 1 emerged as a new protein spot that appeared in the differentiated cells. Nine of the 21 changed proteins were identified. Four proteins-mutant Pyst1, hypothetical protein, nucleophosmin1 and LBP were downregulated, whereas four proteins-eIF6, p44 subunit, β-tubulin and SIN3B were upregulated, and the SR2/ASF was only found in the differentiated SMMC-7721 cells. Previous researches showed that the composition of nuclear matrix in other cell lines varied apparently in the different stages of cell differentiation[21,22]. Our early studies also confirmed that the induced differentiation of human osteosarcoma cell line MG-63 and human gastric adenocarcinoma cell line MGC80-3 with HMBA was accompanied with changes of nuclear matrix proteins[14]. In this study, we proved for the first time that specific nuclear matrix proteins were accompanied with the differentiation of SMMC-7721 cells.

The identified differentially expressed proteins could be grouped into three classes: The first group was the important transcription factor that regulated the tumor

cell proliferation associated gene expression, such as the basal transcription factor complex p44 subunit, the SIN3B protein which regulated the activation of Myc through interaction with Mad[23], the nucleophosmin which regulated gene transcription by binding with many factors of signal transduction[24-26], and the Pyst1 protein which played an important role in the MAPK signling[27]. The second was the splicing factor that reflected post-transcription level of the cell differentiation associated gene expression, such as the SFRS1 protein[28]. The third group was a kind of proteins that affected the synthesization, processing, and nuclear exportion of the ribosome, such as the multifuctional nucleophosmin, P27BBP/eIF6, and the LBP/P40[29,30]. Besides, one unknown protein (hypothetical protein) was found in this study and its function needs to be further illustrated. These identified nuclear matrix proteins were not only significant in the nuclear region, but also could influence the cell proliferation and differentiation through regulating the gene expression at transcriptional, mRNA processional or post-transcriptional level. Further characterization of those proteins and their interaction with the nuclear matrix network is important for revealing the mechanism of cancerization and understanding of the phenotypic reversion of tumor cells.

COMMENTS

Background

Previous studies showed that different stages of cell differentiation were characterized by different morphology of nuclear matrix. However, the relationship between alteration of morphology and function of nuclear matrix-intemediate filament system in cancer cells and its phenotypic reversion has not been well illustrated. The functions of important nuclear matrix proteins which influence the cancer cell differentiation have not been investigated in detail.

Research frontiers

To identify differentially expressed nuclear matrix proteins and analyze their function in cancer cell differentiation is one of the most interesting hotspots in current studies of nuclear matrix.

Innovations and breakthroughs

The authors showed for the first time that the induced differentiation of human hepatocarcinoma cells had not only the morphological changes of nuclear matrix-intermediate filament system, but also the differential expressed nuclear matrix proteins which might be essential for cancer cell reversion.

Applications

Differentially expressed nuclear matrix proteins can be used as potential targets in both diagnosis and treatment of tumors.

Terminology

Nuclear matrix: The residual proteinaseous structure that remains after the nuclei are depleted of the nuclear membranes, histones, soluble nuclear proteins and nucleic acids. The structures that remain in matrix preparations are the nuclear lamina, the residual nucleolus and the fibrillogranular network.

Peer review

This is an interesting paper that links morphological and proteomical techniques in the study of nuclear matrix. The results are important for subsequent research on the function of those differentially expressed proteins.

REFERENCES

1   Tsutsui KM, Sano K, Tsutsui K. Dynamic view of the nuclear matrix. *Acta Med Okayama* 2005; **59**: 113-120

2   Radichev I, Parashkevova A, Anachkova B. Initiation of DNA replication at a nuclear matrix-attached chromatin fraction. *J Cell Physiol* 2005; **203**: 71-77

3   Iarovaia OV, Akopov SB, Nikolaev LG, Sverdlov ED, Razin SV. Induction of transcription within chromosomal DNA loops flanked by MAR elements causes an association of loop DNA with the nuclear matrix. *Nucleic Acids Res* 2005; **33**: 4157-4163

4   Girard-Reydet C, Gregoire D, Vassetzky Y, Mechali M. DNA replication initiates at domains overlapping with nuclear matrix attachment regions in the xenopus and mouse c-myc promoter. *Gene* 2004; **332**: 129-138

5   Okorokov AL, Rubbi CP, Metcalfe S, Milner J. The interaction of p53 with the nuclear matrix is mediated by F-actin and modulated by DNA damage. *Oncogene* 2002; **21**: 356-367

6   Gniadecki R, Olszewska H, Gajkowska B. Changes in the ultrastructure of cytoskeleton and nuclear matrix during HaCaT keratinocyte differentiation. *Exp Dermatol* 2001; **10**: 71-79

7   Samaniego R, Jeong SY, de la Torre C, Meier I, Moreno Diaz de la Espina S. CK2 phosphorylation weakens 90 kDa MFP1 association to the nuclear matrix in Allium cepa. *J Exp Bot* 2006; **57**: 113-124

8   Munarriz E, Barcaroli D, Stephanou A, Townsend PA, Maisse C, Terrinoni A, Neale MH, Martin SJ, Latchman DS, Knight RA, Melino G, De Laurenzi V. PIAS-1 is a checkpoint regulator which affects exit from G1 and G2 by sumoylation of p73. *Mol Cell Biol* 2004; **24**: 10593-10610

9   Okorokov AL, Rubbi CP, Metcalfe S, Milner J. The interaction of p53 with the nuclear matrix is mediated by F-actin and modulated by DNA damage. *Oncogene* 2002; **21**: 356-367

10   Taniura H, Kobayashi M, Yoshikawa K. Functional domains of necdin for protein-protein interaction, nuclear matrix targeting, and cell growth suppression. *J Cell Biochem* 2005; **94**: 804-815

11   Ben-Yehoyada M, Ben-Dor I, Shaul Y. c-Abl tyrosine kinase selectively regulates p73 nuclear matrix association. *J Biol Chem* 2003; **278**: 34475-34482

12   Bosman FT. The nuclear matrix in pathology. *Virchows Arch* 1999; **435**: 391-399

13   Li QF. Effect of retinoic acid on the changes of nuclear matrix in termediate filament system in gastric carcinoma cells. *World J Gastroenterol* 1999; **5**: 417-420

14   Zhao CH, Li QF, Zhao Y, Niu JW, Li ZX, Chen JA. Changes of nuclear matrix proteins following the differentiation of human osteosarcoma MG-63 cells. *Geno Prot Bioinfo* 2006; **4**: 10-17

15   Ouyang GL, Li QF, Peng XX, Hong SG. Differentiation of human hepatocarcinoma SMMC-7721 cells induced by HMBA. *Shiyan Shengwu Xuebao* 2001; **34**: 269-273

16   Fey EG, Wan KM, Penman S. Epithelial cytoskeletal framework and nuclear matrix-intermediate filament scaffold: three-dimensional organization and protein composition. *J Cell Biol* 1984; **98**: 1973-1984

17   He DC, Nickerson JA, Penman S. Core filaments of the nuclear matrix. *J Cell Biol* 1990; **110**: 569-580

18   Ouyang GL, Li QF, Peng XX, Hong SG. Effects of HMBA on the expression of cell-cycle-associated genes in human hepatocarcinoma SMMC-7721 cells. *Shiyan Shengwu Xuebao* 2002; **35**: 173-178

19   Fey EG, Penman S. Tumor promoters induce a specific morphological signature in the nuclear matrix-intermediate filament scaffold of Madin-Darby canine kidney (MDCK) cell colonies. *Proc Natl Acad Sci USA* 1984; **81**: 4409-4413

20   Zhao Y, Tang J, Zhao CH, Shi SL, Li QF. Observation of the effects of retinoic acid on the configurational changes of the NM-IF system and the alteration of nuclear matrix proteins in human osteosarcoma cell line MG-63. *Xiamen Daxue Xuebao* 2006; **45**: 6-10

21   Alberti I, Barboro P, Barbesino M, Sanna P, Pisciotta L, Parodi S, Nicolo G, Boccardo F, Galli S, Patrone E, Balbi C. Changes in the expression of cytokeratins and nuclear matrix proteins are correlated with the level of differentiation in human prostate cancer. *J Cell Biochem* 2000; **79**: 471-485

22   Jin ML, Zhang P, Ding MX, Yun JP, Chen PF, Chen YH, Chew

YQ. Altered expression of nuclear matrix proteins in etoposide induced apoptosis in HL-60 cells. *Cell Res* 2001; **11**: 125-134

23   **van Ingen H**, Lasonder E, Jansen JF, Kaan AM, Spronk CA, Stunnenberg HG, Vuister GW. Extension of the binding motif of the Sin3 interacting domain of the Mad family proteins. *Biochemistry* 2004; **43**: 46-54

24   **Colombo E**, Marine JC, Danovi D, Falini B, Pelicci PG. Nucleophosmin regulates the stability and transcriptional activity of p53. *Nat Cell Biol* 2002; **4**: 529-533

25   **Korgaonkar C**, Hagen J, Tompkins V, Frazier AA, Allamargot C, Quelle FW, Quelle DE. Nucleophosmin (B23) targets ARF to nucleoli and inhibits its function. *Mol Cell Biol* 2005; **25**: 1258-1271

26   **Lambert B**, Buckle M. Characterisation of the interface between nucleophosmin (NPM) and p53: potential role in p53 stabilisation. *FEBS Lett* 2006; **580**: 345-350

27   **Smith TG**, Karlsson M, Lunn JS, Eblaghie MC, Keenan ID, Farrell ER, Tickle C, Storey KG, Keyse SM. Negative feedback predominates over cross-regulation to control ERK MAPK activity in response to FGF signalling in embryos. *FEBS Lett* 2006; **580**: 4242-4245

28   **Huang Y**, Steitz JA. SRprises along a messenger's journey. *Mol Cell* 2005; **17**: 613-615

29   **Ceci M**, Offenhauser N, Marchisio PC, Biffo S. Formation of nuclear matrix filaments by p27(BBP)/eIF6. *Biochem Biophys Res Commun* 2002; **295**: 295-299

30   **Sato M**, Kong CJ, Yoshida H, Nakamura T, Wada A, Shimoda C, Kaneda Y. Ribosomal proteins S0 and S21 are involved in the stability of 18S rRNA in fission yeast, Schizosaccharomyces pombe. *Biochem Biophys Res Commun* 2003; **311**: 942-947

S- Editor Liu Y   L- Editor Ma JY   E- Editor Lu W

Effect of hydroxyapatite nanoparticles on the growth and p53/c-Myc protein expression of implanted hepatic VX₂ tumor in rabbits by intravenous injection

Jun Hu, Zhi-Su Liu, Sheng-Li Tang, Yue-Ming He

Jun Hu, Zhi-Su Liu, Sheng-Li Tang, Yue-Ming He, Department of General Surgery, Zhongnan Hospital, Wuhan University, Wuhan 430071, Hubei Province, China
Supported by National Science Funds, No. 30471689
Correspondence to: Zhi-Su Liu, Department of General Surgery, Zhongnan Hospital, Wuhan University, Wuhan 430071, Hubei Province, China. liuzs53@sina.com
Telephone: +86-27-67813007 Fax: +86-27-67813052
Received: 2006-12-05   Accepted: 2007-03-08

Abstract

AIM: To evaluate the effect of hydroxyapatite nano-particles (Nano HAP) by intravenous injection on the inhibition of implanted hepatic VX₂ tumor growth in rabbits and cell p53/c-Myc protein expression.

METHODS: 60 hepatic VX₂ tumor-bearing rabbits was randomly divided into five groups. Nano HAP collosol 20 mg/kg, 40 mg/kg, 5-FU solutions 20 mg/mL, mixed liquor of 5-FU solution 20 mg/mL and Nano HAP collosol 20 mg/kg were infused by vein, normal saline conducted as the control. The general state, weight, liver function and gross tumor volume were detected dynamically. The expression of p53 and c-Myc gene protein in tumor tissue was detected by immunohistochemistry methods.

RESULTS: The growth of implanted hepatic VX₂ tumors was significantly inhibited in all therapy groups, 3 wk after the injection, the tumor control rates in Nano HAP collosol groups were 25.5% and 32.5% respectively, and the gross tumor volumes were obviously less than that of control group. (24.81 ± 5.17 and 22.73 ± 4.23 *vs* 33.32 ± 5.26, *P* < 0.05). The tumor control rate of 5-FU group was 43.7% (18.74 ± 4.40 *vs* 33.32 ± 5.26, *P* < 0.05), but the general state of the animals after injection aggravated; and the adverse reaction in the drug combination group obviously decreased. Due to the effect of Nano HAP, the positive expression of tumor associated the mutated p53 and c-Myc in tumor tissue was decreased obviously compared with the control group.

CONCLUSION: Nano HAP has evident inhibitory action on rabbit implanted hepatic VX₂ tumor *in vivo*, which may be the result of decreasing the expression of the mutated p53 and c-myc, and drug combination can obviously decrease the adverse reaction of 5-FU.

INTRODUCTION

As the nanometer technique continuous to develop, its application in medical area has became a hot spot of current investigation. Hydroxyapatite (HAP), the molecular formula of which is $Ca_{10}(PO4)_6(OH)_2$, is the essential component of inorganic composition in human bone. It has been found to have obvious inhibitory function on growth of many kinds of tumor cells, and its nanoparticle has stronger anti-tumor effect than macromolecule microparticles. *In vitro*, HAP has been demonstrated to have obvious apoptosis induction and growth inhibition effects[1]. Based on the above, we examined the effect of HAP on growth inhibition of implanted hepatic VX₂ tumor in rabbits and cell p53/c-Myc protein expression in tumor tissue *in vivo*.

MATERIALS AND METHODS

Materials

New Zealand rabbits, female or male, weighing 2.5-3.5 kg, were obtained from the Laboratory Animal Center of Wuhan University Medical School; tumor bearing rabbits were presented by Tangdu Hospital of the Fourth Military Medical University; Nano HAP and 0.2% CMC-Na were provided by Biomaterial Center of East China University of Science and Technology; 5-FU injection was produced by Shanghai Xudong Haipu Medicine Company Ltd.; rat anti rabbit c-Myc, P53 monoclonal antibody and the immunohistochemistry kit were purchased from Fuzhou Maixin Biologic Product Company. 20 mg/mL and 40 mg/mL solutions were prepared with normal saline and Nano HAP powder, and 20 mg/mL Nano HAP and

20 mg/mL 5-FU were mixed in vol. proportion 1:1, 0.2% CMC-Na was separately added as dispersion stabilizer, then dispersed to suspending-stable Nano HAP sol and mix injection in Sonic V130 ultrasonic cell pulverizer; 5-FU injection was diluted with normal saline to 20 mg/mL.

Animal model

VX₂ tumor fragments were implanted in rabbit thigh muscle, and were taken out when their diameter extended to 1.0-1.5 cm. Having removed the connective tissue, we cut the tumor tissue, like flesh of a fish into small cubes about 1 mm³ in size and implanted it in the left lobe visceral surface of healthy rabbit liver, with a depth exceeding 1 cm. Ultrasound detection was taken 7 d after the implantation, and the tumor growth state was recorded. If the tumor doesn't have ectopia implantation, colliquation or cystoid degeneration, the animal implantation model is considered successful. The selected 60 tumor bearing rabbits were randomly divided into five groups: A, B, C, D and E. The drug began to be injected through dorsal ear vein 3 wk after the implantation every other day. Group A was given normal saline, 2 mL every time; group B was given Nano HAP sol 20 mg/kg; group C was given Nano HAP sol 40 mg/kg; group D was given 5-FU 20 mg/kg; group E was given the mixed liquor of Nano HAP sol 20 mg/mL and 5 Fu 20 mg/mL, the doses were both 20 mg/kg.

Monitoring the growth state of tumor-bearing rabbits

The tumor-bearing rabbits were fed in the standard cleaning level lab, the general state changes of the animals, such as color pattern, food-intake, water-drinking, activity, oral and nasal discharge were followed up daily. The weight of the animals were taken before feeding in the early morning every 3 d, and the liver function (ALT) was detected by extracting venous blood of experimental rabbits every week.

Tissue and sample disposal

3 wk after the injection, rabbits were intravenously anesthetized and their abdominal cavities were opened, integrate liver were taken out, abdominal and thoracic cavities were examined. tumor volume was calculated by the formula $V = 0.5 \times a \times b^2$ (a: maximum diameter, b: maximum transverse diameter), growth inhibition rate of tumor (GIR) = (tumor volume of control group-tumor volume of therapy group)/tumor volume of control group × 100%.

HE and Immunohistochemistry staining

The samples were labeled, numbered and placed in 10% formalin solution for fixation. Then the tissue was embedded in paraffin and serially sectioned (4 μm) for HE staining. The final diagnosis of tumor depended on pathology. Immunohistochemistry staining was made using SABC assay, PBS was used as negative control instead of first antibody, and existing P53 and c-Myc positive liver tumor slides (provided by pathology division of Wuhan University Zhongnan Hospital) were used as positive control.

Table 1 Change of average weight of animals in each group mean ± SD

Group	n	Weight (kg)		
		Before injection	One week after injection	Three weeks after injection
A (Control)	12	2.73 ± 0.21	2.67 ± 0.21	2.32 ± 0.14
B (HAP)	11	2.66 ± 0.15	2.59 ± 0.14	2.46 ± 0.19^a,d
C (HAP)	12	2.70 ± 0.16	2.61 ± 0.14	2.52 ± 0.12^a,d
D (5-FU)	11	2.70 ± 0.17	2.47 ± 0.17^a	1.95 ± 0.14^b
E (5-FU + HAP)	12	2.78 ± 0.19	2.60 ± 0.18	2.23 ± 0.22^d

[a]$P < 0.05$, [b]$P < 0.01$, *vs* group A; [d]$P < 0.01$, *vs* group D.

Judgement of immunohistochemistry staining result

The mutated p53 positive staining area was located in the nuclei, and c-Myc positive staining was mainly located in the plasma, but part of the nuclei can also be stained. 5 high power lens fields were chosen and stained uniformly to count positive cells. The immunostaining of the mutated p53 and c-Myc had 4 grades according to the staining intensity or positive cell rate: negative (-): no positive staining or positive cell rate < 5%; Weakly positive (+): staining yellow or 6%-20% positive tumor cells; positive (++): staining buffy or 21%-60% tumor cell staining; strongly positive (+++): buffy particles or > 61% tumor cells staining.

Statistical analysis

All Data were expressed as means ± standard deviation (SD). Means between multi-groups were compared using a one-way ANOVA with LSD test and Student-Newman-Keuls *q* test. Rates between groups were compared using Fisher's exact propability test. Statistical analysis was performed using SPSS 12.0.

RESULTS

Change of general state and weight of tumor-bearing rabbits

The general health state of rabbits was fine before drug injection in each groups , and the rabbit hair was smooth and glossy, food intake and activity were normal, weight between groups had no significant difference. The animals in control group began to have symptoms of gradual failure 2 wk after injection, the activity and food intake worsened, stools got loose, oral and nasal discharge increased. The time when two Nano HAP groups had failure symptom were later than the control group, and the weight of the rabbits was also higher than that in control group ($P < 0.05$) (Table 1). After 3 continuous drug injections, the food intake and activity of the animals decreased obviously, and at 1 wk after injection, the weight of the rabbits was lower than that in control group ($P < 0.05$), and at 3 wk after injection, the weight of animals was lower than other groups ($P < 0.01$). The weight in the drug combination group lowered after injection, but had no (do they mean no or do they mean "were significantly different") significant difference compared with 5-FU group.

Table 2 ALT level before and after treatment in each group mean ± SD

Group	n	ALT (U/L)		
		Before injection	One week after injection	Three weeks after injection
A (Control)	12	43.56 ± 7.24	45.33 ± 8.29	75.33 ± 12.51
B (Nano HAP)	11	39.29 ± 6.52	42.73 ± 10.05[d]	59.55 ± 15.40[a,d]
C (Nano HAP)	12	40.38 ± 6.88	43.75 ± 6.30[d]	62.00 ± 14.49[a,d]
D (5-FU)	11	42.70 ± 7.08	74.64 ± 15.55[b]	99.73 ± 14.70[b]
E (5-FU + HAP)	12	42.86 ± 6.79	59.67 ± 12.66[b,c]	86.42 ± 11.54[a,c]

[a]$P < 0.05$, [b]$P < 0.01$, vs A group; [c]$P < 0.05$, [d]$P < 0.01$, vs D group.

Table 3 Tumor volume and tumor growth inhibition rate of each group 3 wk after treatment mean ± SD

Group	Gross tumor volume (cm^3)	Inhibition ratio (%)	t value (vs group)
A (control)	33.32 ± 5.26	—	—
B (Nano HAP)	24.81 ± 5.17[b,d]	25.53	3.91
C (Nano HAP)	22.73 ± 4.23[b,d]	32.52	5.29
D5-FU	18.74 ± 4.40[b,d]	43.7	7.17
E (5-FU + HAP)	13.10 ± 2.48[b]	60.97	12.05

[b]$P < 0.01$ vs group A; [d]$P < 0.01$ vs group E.

Table 4 P53 and c-Myc positive staining in groups

Group	n	P53				Positive (%)	c-Myc				Positive (%)
		-	+	++	+++		-	+	++	+++	
A	12	2	4	5	1	83.3	3	5	3	1	75.0
B	23	13	6	4	0	43.5[a]	12	5	5	1	47.8
D	11	6	2	3	0	45.5	5	2	3	1	54.5
E	12	7	3	2	0	41.7	6	3	3	0	50.0

[a]$P = 0.034$ vs group A.

Result of liver function level detection

Differences in the ALT level of each group was not statistically significant. One week after injection , ALT in 5-FU group became significantly higher than other groups (Table 2, $P < 0.05$), and ALT in drug combination group increased obviously compared with control group ($P < 0.05$), but lower than that in 5-FU group ($P < 0.05$). Three weeks after injection, the liver function got worse in control group, displaying an obvious rise in ALT. ALT in two Nano HAP group increased slightly, but obviously lower than that in control group ($P < 0.05$). ALT in 5-FU group was higher than other groups. ALT in drug combination group increased compared with control group, but lower than that in 5-FU group ($P < 0.05$).

Tumor pathology

Before treatment, the tumor size of each group was not statistically significant. Table 3 shows the average tumor volume and tumor growth inhibition rate 3 wk after injection. The tumor growth inhibition rate of each group were 25.5%, 32.5%, 43.7% and 60.9% respectively, and the tumor volume had significant differences compared with that in control group ($P < 0.01$). The tumor volume of drug combination group also showed significant deference
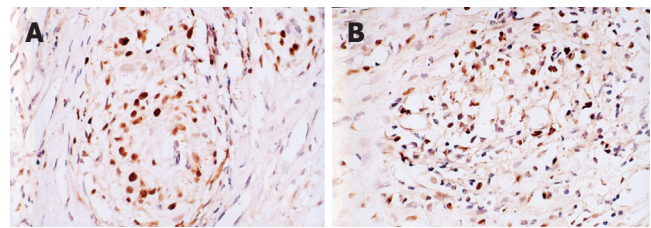
Figure 1 A: The mutated p53 positive expression in tumor tissue (× 200); **B**: c-myc positive expression in tumor tissue (× 200).
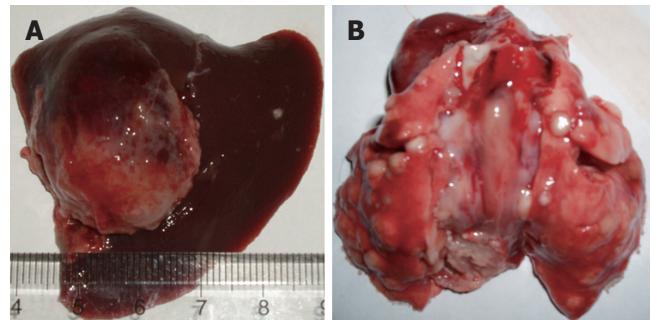
Figure 2 A: The outward appearance of VX$_2$ liver tumor the metastatic carcinoma on lung in control group; **B**: The metastatic carcinoma on lung in control group.

compared with B, C and D group ($P < 0.05$).

Result of Immunohistochemistry Staining

Table 4 shows the result of immunohistochemistry staining: Figure 1 show the results of mutated P53 and c-Myc positive staining. In this result 2 groups that injected HAP combined to B group, and other groups did not change. The mutated P53 and c-Myc both expressed strongly in tumor tissue, and positive cell rates were 83.3% and 75.0%, through the Nano HAP treatment, the positive expression rates of these two protein were 43.5% and 47.8%, lower than the control group, in which expression rate of mutated P53 has statistical significant difference, but there was no significant difference of the two proteins between therapy groups. In tumor tissue of control group, positive expression rate of both mutated P53 and c-Myc was 75.0%, which in Nano HAP group decreased to 39.1%.

Simple observation and histological studies

VX$_2$ liver tumor tissue was gray and had clear borderline with liver tissue, it had no envelope, and the section turned like the flesh of fish (Figure 2A). The VX$_2$ liver tumors in control group were much larger than that in therapy group, and grew to the surface of liver, adhering with surrounding tissue, most of them had chest and abdominal wall metastasis, moreover two cases had lung metastasis, showing many lesser tubercles on the surface of lung (Figure 2B), as diagnosed by histology. Few animals in other groups had abdominal cavity and wall metastasis, but did not have lung metastasis. Observed in light microscope after HE staining, tumor cells turned to be round, and fusiform shape or irregular shape, and the size was large, irregular shape, less endochylema, Karyomegaly and dense
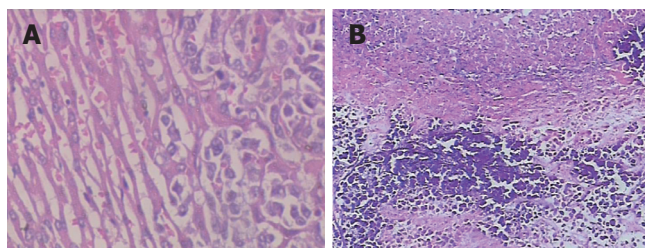
Figure 3 **A**: There are apparent morphological differences between VX₂ liver tumor tissue and the normal liver tissue (× 200); **B**: There are lots of calcified points in tumor tissue in group treated by nano-HAP (× 100).

staining. The cells ranked abnormally, and initial infiltrative hepatic cords distributed at the edge of cancer nest (Figure 3A), some centers of tumors occurred colliquation and necrosis. At the edge of necrotic tumor tissue in HAP group, many microcalcification focuses were observed (Figure 3B), however tumor tissure in control group and normal liver tissue did not have same calcification focus.

DISCUSSION

Liver cancer is one of the most common malignant tumors in China, and the incidence of disease has continuously increased, its integral & clinical therapy effect is not still ideal due to features of difficulty in early diagnosis, high malignancy and easy relapse etc. Therefore, it is imperative to speed-up the research of biological medicine, to look for a highly efficient, low poison chemotherapy medicine which is one of the main directions of our present study.

HAP has a good issue compatibility both inside and outside the body[2-7], it has been widely used as the biological material for bone damage and oral cavity medicine, simultaneously used as in body medicine carrier[8,9], moreover Nano HAP had a very small excitation on blood vessel, feeding medicine can be made by intravenous injection[5,10]. Nano HAP used for this research is synthesized by sol-coagel method having a good dispersive effect, its particle size with about 50 nm is very uniform, which meets the requirement for Nano meter grade (0.1 nm-100 nm), having advantage of high surface energy etc., that can not exist for the large particle size of HAP. During early out-body experiment Nano HAP has been proved to have obvious inhibition function for multi-kinds of tumors.

This research has proved that Nano HAP had obvious inhibition effect on the growth on the implanted tumor in VX₂ liver of rabbit through its intravenous injection into rabbit body. During these experiments the early model was selected for implanted tumor of VX₂ liver, different concentrations of Nano HAP have been injected after 3 wk, their inhibition rates of tumors reached separately to 25.3% and 32.5%, which indicated that it could inhibit the growth of tumors. Moreover, liver function on the experimental rabbits has also proved that Nano HAP had a little effect of physiological function on the organism. Inhibition function for tumor growth in 5-FU group was stronger than that in Nano HAP group, but the poisonous side effect has also been indicated obviously, after being continuously injected of 5-FU, the food-intake & activity

of animals were obviously decreased; their body weights were obviously lower than that of other groups; the degree of liver function damaged was obviously higher than that of other groups. These results indicated that Nano HAP has no obvious in body adverse reaction.

Through experiment, it was also discovered that not only did Nano HAP have an anti-tumor function by itself, but also it had very strong cooperation effect with other anti-tumor medicines. The inhibition rate of tumor is the highest in the combinative therapy group in experiments. Moreover after having been injected into tumor-bearing rabbit with same dosage of 5-FU, the indication of two groups of animals was quite different. The general situation for animal of combinative therapy group was obviously better than that in 5-FU group. Dynamic supervision on body weight & liver function indicated also that the effect of 5-FU on the animal physiological function of combinative therapy group is obviously less than that in 5-FU group.

In combination with feature of Nano HAP having large surface & high surface energy, it, may be, has played a role of its carrier after being mixed of Nano HAP with 5-FU. This adsorption of carrier[11] could obviously reduce first blood-medicine concentration of 5-FU, and reach to a relaxation effect, it was also reported in the literature that Nano HAP could produce a complex with blood serum protein in biological body[12,13], it was inferred that the Nano HAP-5-FU protein compound could be formed in animal blood after mixing of Nano HAP with 5-FU, therefore not only the poisonous by-effect of high concentration free 5-FU in body could be reduced, but also the blood solubility of Nano HAP could be increased.

The present researches for various Nano HAP anti-tumors mechanism indicate the anti-tumor effect can be reached through effecting the end grain enzyme of cancer cell, cell skeleton, Ca^{2+} concentration and immunity function. In experiment the expression product in tumor tissue was detected after reaction of gene mutated P53 and c-Myc with Nano HAP. The result indicates that the positive expression rates of two kinds of proteins are separately 43.5%, 47.8% after reaction of Nano HAP, which are obviously lower than that in comparison control group. p53 and c-Myc are the important genes for controlling proliferation and withering of tumors cells, of which c-Myc protein positive expression can lead to directional development of non-function, originalization of cells. Low differentiation of cells with high toxicity is early accident occurring malignant tumor, so c-Myc protein positive expression was mainly distributed at the edge of tumor. Nano HAP can lower positive expression of these two kinds of protein, it was prompted it could prevent the malignant cell proliferation of tumor through effecting control of cancer cell gene, to reach anti-tumor effect. But it has to be further researched carefully for the detail mechanism.

To sum up, not only the Nano HAP has expressed obvious anti-tumor effect *in vivo* of animal, but also, its poisonous by-effect was low, and it could bring very strong cooperation effect with using other chemotherapy medicine, reduce toxicity of other chemotherapy medicine. It might become new clinical anti-tumor medicine.

REFERENCE

1   **Liu ZS**, Tang SL, Ai ZL. Effects of hydroxyapatite nanoparticles on proliferation and apoptosis of human hepatoma BEL-7402 cells. *World J Gastroenterol* 2003; **9**: 1968-1971

2   **Aoki H**, Aoki H, Kutsuno T, Li W, Niwa M. An in vivo study on the reaction of hydroxyapatite-sol injected into blood. *J Mater Sci Mater Med* 2000; **11**: 67-72

3   **Tachibana Y**, Ninomiya S, Kim YT, Sekikawa M. Tissue response to porous hydroxyapatite ceramic in the human femoral head. *J Orthop Sci* 2003; **8**: 549-553

4   **Huang J**, Best SM, Bonfield W, Brooks RA, Rushton N, Jayasinghe SN, Edirisinghe MJ. In vitro assessment of the biological response to nano-sized hydroxyapatite. *J Mater Sci Mater Med* 2004; **15**: 441-445

5   **Pezzatini S**, Solito R, Morbidelli L, Lamponi S, Boanini E, Bigi A, Ziche M. The effect of hydroxyapatite nanocrystals on microvascular endothelial cell viability and functions. *J Biomed Mater Res A* 2006; **76**: 656-663

6   **Fu Q**, Zhou N, Huang W, Wang D, Zhang L, Li H. Effects of nano HAP on biological and structural properties of glass bone cement. *J Biomed Mater Res A* 2005; **74**: 156-163

7   **Wahl DA**, Czernuszka JT. Collagen-hydroxyapatite composites for hard tissue repair. *Eur Cell Mater* 2006; **11**: 43-56

8   **Kunieda K**, Seki T, Nakatani S, Wakabayashi M, Shiro T, Inoue K, Sougawa M, Kimura R, Harada K. Implantation treatment method of slow release anticancer doxorubicin containing hydroxyapatite (DOX-HAP) complex. A basic study of a new treatment for hepatic cancer. *Br J Cancer* 1993; **67**: 668-673

9   **Rauschmann MA**, Wichelhaus TA, Stirnal V, Dingeldein E, Zichner L, Schnettler R, Alt V. Nanocrystalline hydroxyapatite and calcium sulphate as biodegradable composite carrier material for local delivery of antibiotics in bone infections. *Biomaterials* 2005; **26**: 2677-2684

10   **Mizushima Y**, Ikoma T, Tanaka J, Hoshi K, Ishihara T, Ogawa Y, Ueno A. Injectable porous hydroxyapatite microparticles as a new carrier for protein and lipophilic drugs. *J Control Release* 2006; **110**: 260-265

11   **Zhu S**, Zhou K, Huang B, Huang S, Liu F, Li Y, Xue Z, Long Z. Hydroxyapatite nanoparticles: a novel material of gene carrier. *Shengwu Yixue Gongchengxue Zazhi* 2005; **22**: 980-984

12   **Kandori K**, Masunari A, Ishikawa T. Study on adsorption mechanism of proteins onto synthetic calcium hydroxyapatites through ionic concentration measurements. *Calcif Tissue Int* 2005; **76**: 194-206

13   **Niwa M**, Li W, Sato T, Daisaku T, Aoki H, Aoki H. The adsorptive properties of hydroxyapatite to albumin, dextran and lipids. *Biomed Mater Eng* 1999; **9**: 163-169

Correlation of N-myc downstream-regulated gene 1 expression with clinical outcomes of colorectal cancer patients of different race/ethnicity

Minori Koshiji, Kensuke Kumamoto, Keiichirou Morimura, Yasufumi Utsumi, Michiko Aizawa, Masami Hoshino, Shinji Ohki, Seiichi Takenoshita, Max Costa, Thérèse Commes, David Piquemal, Curtis C Harris, Kam-Meng Tchou-Wong

Minori Koshiji, Kam-Meng Tchou-Wong, Department of Environmental Medicine, New York University School of Medicine, 57 Old Forge Road, Tuxedo, NY 10987, United States
Kensuke Kumamoto, Shinji Ohki, Seiichi Takenoshita, Second Department of Surgery, Fukushima Medical University, 1 Hikarigaoka, Fukushima 960-1295, Japan
Kensuke Kumamoto, Curtis Harris, National Institutes of Health, National Cancer Institute, Building 37, Bethesda, MD 20892, United States
Keiichirou Morimura, Department of Pathology, Osaka City University, Osaka, Japan
Yasufumi Utsumi, Michiko Aizawa, Department of Pathology, Ohara General Hospital, 6-11 Ohmachi, Fukushima 960-8611, Japan
Masami Hoshino, Department of Surgery, Ohara General Hospital, 6-11 Ohmachi, Fukushima 960-8611, Japan
Therese Commes, David Piquemal, University Montpellier II, Montpellier, France
Supported by grant numbers ES00260 (Costa and Tchou-Wong), ES05512 (Costa), ES10344 (Costa), and T32-ES07324 (Costa and Tchou-Wong) from the National Institutes of Environmental Health Sciences and CA16087 (Costa) from the National Cancer Institute, as well as DK63603 (Tchou-Wong) and CA101234 (Tchou-Wong) from the National Institutes of Health
Correspondence to: Dr. Kam-Meng Tchou-Wong, Department of Environmental Medicine, New York University School of Medicine, 57 Old Forge Road, Tuxedo, NY 10987, United States. tchouk02@med.nyu.edu
Telephone: +1-845-7313504 Fax: +1-845-3512218
Received: 2007-02-02   Accepted: 2007-03-01

Abstract

AIM: To evaluate the role of N-myc downstream-regulated gene 1 (NDRG1) expression in prognosis and survival of colorectal cancer patients with different ethnic backgrounds.

METHODS: Because NDRG1 is a downstream target of p53 and hypoxia inducible factor-1α (HIF-1α), we examined NDRG1 expression together with p53 and HIF-1α by immunohistochemistry. A total of 157 colorectal cancer specimens including 80 from Japanese patients and 77 from US patients were examined. The correlation between protein expression with clinicopathological features and survival after surgery was analyzed.

RESULTS: NDRG1 protein was significantly increased in colorectal tumor compared with normal epithelium in both Japanese and US patient groups. Expression of NDRG1 protein was significantly correlated with lymphatic invasion, venous invasion, depth of invasion, histopathological type, and Dukes' stage in Japanese colorectal cancer patients. NDRG1 expression was correlated to histopathological type, Dukes' stage and HIF-1α expression in US-Caucasian patients but not in US-African American patients. Interestingly, Kaplan-Meier survival analysis demonstrated that NDRG1 expression correlated significantly with poorer survival in US-African American patients but not in other patient groups. However, in p53-positive US cases, NDRG1 positivity correlated significantly with better survival. In addition, NDRG1 expression also correlated significantly with improved survival in US patients with stages Ⅲ and Ⅳ tumors without chemotherapy. In Japanese patients with stages Ⅱ and Ⅲ tumors, strong NDRG1 staining in p53-positive tumors correlated significantly with improved survival but negatively in patients without chemotherapy.

CONCLUSION: NDRG1 expression was correlated with various clinicopathological features and clinical outcomes in colorectal cancer depending on the race/ethnicity of the patients. NDRG1 may serve as a biological basis for the disparity of clinical outcomes of colorectal cancer patients with different ethnic backgrounds.

INTRODUCTION

N-myc downstream-regulated gene 1 (NDRG1) was first

discovered by two groups under differing physiological conditions[1,2]. NDRG1, also termed CAP43, DRG1, NDR1, RIT42, and RTP, has been mapped to human chromosome 8q24 and encodes for a 394-amino acid cytoplasmic protein with a molecular weight of 43 kDa[2-5]. Transcription of the NDRG1 gene is negatively regulated by the MYC family proteins including N-MYC and c-MYC[6]. The expression of NDRG1 could be induced by diverse agents including metals that mimic hypoxia, homocysteine, calcium ionophore, okadaic acid, and androgens[3,4,7-10]. The induction of NDRG1 expression by carcinogenic nickel and hypoxia is mediated by hypoxia inducible factor-1α (HIF-1α)[7,8,11]. DNA damaging agents induced NDRG1 expression in a p53-dependent manner[12,13] and a putative p53 binding site had been reported within the NDRG1 promoter region[13].

Earlier publications had reported down regulation of NDRG1 expression in colon, breast, and prostate cancers[2,14-16]. In contrast, recent studies reported increased expression of NDRG1 protein in malignancy including skin, brain, lung, colon, breast and prostate cancers[17-19]. The expression of NDRG1 in colon cancer has also been controversial. Wang et al[19] reported that the level of NDRG1 protein was gradually increased in colorectal cancers and immunohistochemical staining of NDRG1 was correlated with lymph node metastasis in a Chinese patient population. In contrast, Shah et al[20] stated that NDRG1 staining in the primary colorectal tumor was always less than adjacent normal colon in a US patient population. They examined NDRG1 expression in colorectal liver metastases and demonstrated a trend for unilobar metastases with high NDRG1 expression and a suggestion of improved 2-years survival[20].

It has been reported that African Americans have a higher incidence and mortality from colorectal cancer than Caucasians[21]. Another recent study reported that African American patients received less adjuvant chemotherapy than Caucasian patients, providing a plausible reason for the higher mortality in African Americans[22]. However, a biological basis for the existence of a more aggressive colorectal cancer in African American patients remains to be determined. Similarly, disparity in the incidence and clinical progression of prostate cancer between African Americans and Caucasians had also been reported. When access to care as a possible confounding variable in disease outcome was controlled for, Caruso et al[23] demonstrated that African American patients presented with a significantly worse clinicopathological profile than Caucasian patients and that ethnicity was an independent factor in disease recurrence after surgical treatment. Interestingly, different expression patterns of the NDRG1 protein might reflect differences in the response of prostatic epithelium to hypoxia and androgens in African Americans compared with Caucasians, revealing a possible biological basis underlying the disparity in clinical outcomes of prostate cancer patients with different ethnic background[23]. We hypothesized that NDRG1 expression in colorectal cancers, similar to that in prostate cancer, might reflect different race/ethnic backgrounds and underlie the disparity in clinical outcomes of colorectal cancer patients with different race/ethnic backgrounds.

MATERIALS AND METHODS

Patients

The study population consisted of 157 consecutive patients (103 male, 54 female; age range, 37 to 85 years; average 66.5 years) observed between January 1995 and December 2003, with histologically proven colorectal adenocarcinoma. Tumors that met the Bethesda guidelines for hereditary nonpolyposis colorectal cancer and/or carcinomas associated with inflammatory bowel disease were excluded from this study. Patient selection was primarily based on the availability of both adequate clinical follow-up and representative specimens for immunohistochemical analysis. Out of a total of 157 colorectal cancer specimens, 80 were from Japanese patients and 77 were from US patients. Among the 80 Japanese patients, 44 received oral 5-fluorouracil chemotherapy in addition to surgery. The number of stage III and IV US patients totaled 42, among which 19 patients had chemotherapy and 23 patients did not receive chemotherapy.

Immunohistochemical staining and pathological evaluation

Immunohistochemical (IHC) staining was performed by using serial sections of paraffin-embedded tumor specimens. Antigen retrieval and immunochemical staining were performed as described[24]. Sections were incubated with a 1:100 dilution of polyclonal anti-NDRG1 antibody[5], polyclonal anti-HIF-1α antibody (Santa Cruz), and a 1:200 dilution of monoclonal anti-p53 antibody (DAKO). Slides were examined by three independent pathologists blinded to each other's work and with no prior knowledge of clinical and pathological features of tumors. For assessment of IHC staining, the following criteria were used: 0 represented negative staining while positive staining was scored from +1 to +3 (+1, weak staining or moderate to intense staining in the peripheral region of < 10% of the cancer nests; +2, moderate staining in most of the cancer cells or intense staining in the peripheral regions in 10%-40% of the cancer nests; +3, intense staining in almost all the cancer cells). NDRG1 negative staining means 0 while positivity means +1 to +3.

Statistical analysis

Statistical comparisons for significance between protein expression patterns and clinicopathological features were evaluated by Mann Whitney U-test and χ^2 test. Multivariate analyses were performed according to a logistic regression analysis. The survival curves were estimated by the Kaplan-Meier method, and the resulting curves were compared using the log-rank test. Statistical analysis was performed using StatMate (ATMS Co. Ltd., Tokyo, Japan) and $P < 0.05$ was considered statistically significant.

RESULTS

NDRG1 expression in colon cancer

Immunohistochemical analysis demonstrated that NDRG1 was expressed in the cytoplasm and membranes of epithelial cells of colorectal adenocarcinoma from a
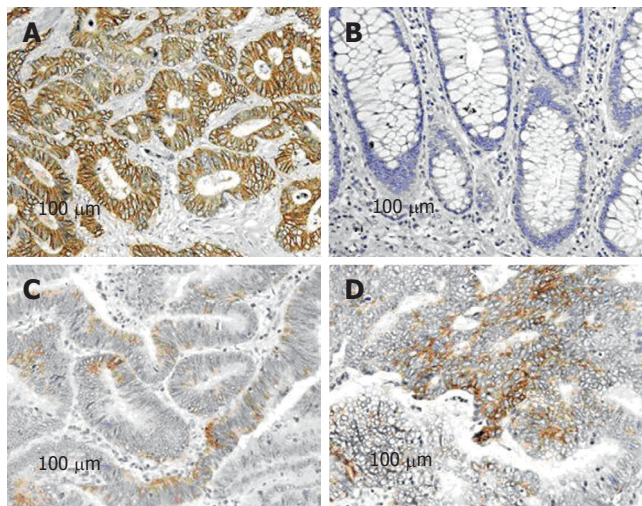
Figure 1 Expression of NDRG1 in colorectal cancer as analyzed by immunohistochemistry. **A**: Moderately differentiated colorectal adenocarcinoma from a Japanese patient demonstrating membranous and cytoplasmic staining with NDRG1 antibody; **B**: No NDRG1 expression was detected in normal adjacent colon mucosa; **C**: Well differentiated colorectal adenocarcinoma from US patient; **D**: Moderately differentiated colorectal adenocarcinoma form US patient.

Table 1A Correlation of NDRG1 expression with clinicopathologic variables in Japanese cases

	Total cases (%) $n = 80$	Positive $n = 55$	Negative $n = 25$	*P* value
Age (yr)				0.622
> 66	48 (60.0)	34	14	
< 66	32 (40.0)	21	11	
Gender				0.649
Male	45 (56.3)	30	15	
Female	35 (43.7)	25	10	
Tumor location				0.164
Right-hemicolon	28 (35.0)	22	6	
Left-hemicolon	52 (65.0)	33	19	
Histopathological Type				0.067
Well	39 (48.8)	22	17	0.017
Moderate	38 (47.6)	31	7	
Poor	1 (1.2)	1	0	
Mucinous	1 (1.2)	1	0	
Sig	1 (1.2)	0	1	
Dukes' stage				0.036
A	22 (27.5)	11	11	
B	21 (26.3)	14	7	
C	27 (33.7)	20	7	
D	10 (12.5)	10	0	
Liver metastasis				0.062
Negative	73 (91.3)	48	25	
Positive	7 (8.7)	7	0	
Lymph node metastasis				0.14
Negative	48 (60.0)	30	18	
Positive	32 (40.0)	25	7	
Lymphatic invasion				0.021
Negative	19 (23.8)	9	10	
Positive	61 (76.2)	46	15	
Venous invasion				0.0077
Negative	15 (18.8)	6	9	
Positive	65 (81.2)	49	16	
Depth of invasion				0.01
m	5 (6.3)	1	4	
sm	8 (10.0)	4	4	
mp	14 (17.5)	10	4	
ss, a1	29 (36.3)	23	6	
se, a2	23 (28.7)	16	7	
si, ai	1 (1.2)	1	0	

P < 0.05 is considered significant.

Japanese patient (Figure 1A) but not in normal adjacent colon mucosa (Figure 1B). Non-epithelial cells including stroma, muscle, and invading lymphocytes were also negative for NDRG1 expression. NDRG1 expression was also detected in well-differentiated (Figure 1C) and moderately differentiated (Figure 1D) colorectal adenocarcinomas from US patients. The correlation of NDRG1 expression with clinicopathologic variables in Japanese and US cases was shown in Table 1A and B. In Japanese colorectal cancer patients, positive NDRG1 expression was correlated with histopathological type ($P = 0.017$), Dukes' stage ($P = 0.036$), lymphatic invasion ($P = 0.021$), venous invasion ($P = 0.0077$), and depth of invasion ($P = 0.01$) (Table 1A).

Because of the smaller sizes of surgical specimens available from the US patients, pathological information relating lymphatic invasion, venous invasion and depth of invasion could not be obtained. Since the US patient population consisted of two race/ethnic groups, namely, Caucasian and African American, analysis of NDRG1 expression and clinicopathological variables was also performed based on race/ethnicity. As shown in Table 1B, while there was a trend in the correlation of NDRG1 expression with Dukes' stage in the overall US cases ($P = 0.056$), NDRG1 expression was only significantly correlated to Dukes' stage in Caucasians ($P = 0.0063$) but not in African Americans ($P = 0.88$). Similarly, when comparing well versus moderate differentiated tumors, significant correlation with NDRG1 positivity was also only observed in Caucasians but not in other populations.

Expression of other biomarkers in colon cancer

Next, we examined the frequency of NDRG1 expression relative to that of p53 and HIF-1α (Table 2A). Normal colonic epithelium showed negative to weak nuclear staining of p53 while HIF-1α was not detected in normal colonic mucosa. As shown in Table 2B, while there was a trend in the correlation of NDRG1 expression with HIF-1α expression in colorectal tumors from Japanese patients ($P = 0.061$), the correlation was significant in the overall US patients ($P = 0.036$). Similar to that observed with Dukes' staging, when analysis was performed based on race/ethnicity, significant correlation between NDRG1 and HIF-1α was only observed in Caucasian patients ($P = 0.015$) but not in African American patients ($P = 0.73$). On the other hand, no significant correlation between NDRG1 and p53 expression was observed in all three groups.

Clinical outcomes of colorectal patients

As shown in Table 1A and B, NDRG1 expression was significantly correlated with advanced Dukes' stages in Japanese and Caucasian colorectal cancer patients ($P = 0.036$ and 0.0063, respectively), but not in African American patients ($P = 0.88$). As expected, Kaplan-Meier survival curves revealed that prognosis was associated with Dukes' stage in both Japanese and US groups (Figure 2A). To examine if NDRG1 expression correlated with survival

Table 1B Correlation of NDRG1 expression with clinicopathologic variables in U.S. (Caucasian and African American) cases

	All U.S. cases (n = 77) NDRG1				Caucasian (n = 43) NDRG1				African American (n = 34) NDRG1			
	Total (%)	+	-	P value	Total (%)	+	-	P value	Total (%)	+	-	P value
Age (yr)				0.079				0.092				0.464
> 66	45 (58.4)	19	26		26 (60.5)	10	16		19 (55.9)	9	10	
< 66	32 (41.6)	20	12		17 (39.5)	11	6		15 (44.1)	9	6	
Gender				0.074				0.255				0.153
Male	58 (75.3)	26	32		32 (74.4)	14	18		26 (76.5)	12	14	
Female	19 (24.7)	13	6		11 (25.6)	7	4		8 (23.5)	6	2	
Histopathological type				0.31				0.21				0.18
Well	47 (61.0)	20	27	0.15[a]	28 (65.1)	11	17	0.049[a]	19 (55.9)	9	10	0.88[a]
Moderate	23 (29.9)	14	9		14 (32.6)	10	4		9 (26.5)	4	5	
Poor	2 (2.6)	1	1		0 (0)	0	0		2 (5.9)	1	1	
Mucinous	5 (6.5)	4	1		1 (2.3)	0	1		4 (11.8)	4	0	
Dukes' stage				0.056				0.0063				0.88
A	7 (9.1)	1	6		4 (9.3)	0	4		3 (8.8)	1	2	
B	28 (36.4)	14	14		16 (37.2)	8	8		12 (35.3)	6	6	
C	23 (29.9)	16	7		14 (32.6)	11	3		9 (26.5)	5	4	
D	19 (24.6)	8	11		9 (20.9)	2	7		10 (29.4)	6	4	
Liver metastasis				0.39				0.072				0.59
Negative	58 (75.3)	31	27		34 (79.1)	19	15		24 (70.6)	12	12	
Positive	19 (24.7)	8	11		9 (20.9)	2	7		10 (29.4)	6	4	
Lymph node metastasis				0.212				0.28				0.52
Negative	35 (45.5)	15	20		20 (46.5)	8	12		15 (44.1)	7	8	
Positive	42 (54.5)	24	18		23 (53.5)	13	10		19 (55.9)	11	8	

[a]P < 0.05 vs moderate.

Table 2A Frequency of expression of p53 and HIF-1α in Japanese and U.S. patients n (%)

	p53		HIF-1α	
	Positive	Negative	Positive	Negative
Japanese (n = 80)	43 (54.0)	37 (46.0)	42 (52.5)	38 (47.5)
All U.S. cases (n = 77)	48 (62.3)	29 (37.7)	18 (23.4)	59 (76.6)
Caucasian (n = 43)	28 (65.1)	15 (34.9)	13 (30.2)	30 (69.8)
African American (n = 34)	20 (58.8)	14 (41.2)	5 (14.7)	29 (85.3)

Table 2B Correlation of expression of NDRG1 with p53 and HIF-1α

		NDRG1		P value
		Positive	Negative	
Japanese (n = 80)				
p53	+	31	12	0.49
	-	24	13	
HIF-1α	+	25	17	0.061
	-	30	8	
All U.S. cases (n = 77)				
p53	+	28	20	0.083
	-	11	18	
HIF-1α	+	13	5	0.036
	-	26	33	
Caucasian (n = 43)				
p53	+	16	12	0.14
	-	5	10	
HIF-1α	+	10	3	0.015
	-	11	19	
African American (n = 34)				
p53	+	12	8	0.32
	-	6	8	
HIF-1α	+	3	2	0.73
	-	15	14	

P < 0.05 is considered significant.

of patients after surgery, Kaplan-Meier analysis was performed comparing NDRG1-positive with NDRG1-negative tumors from Japanese and US patients. As depicted in Figure 2B, no significant correlation between NDRG1 expression and survival was observed in Japanese patients (Log rank, $P = 0.36$) while NDRG1 positivity was significantly correlated with poorer survival compared to NDRG1 negativity in US patients (Log rank, $P = 0.025$). To examine if there was differential correlation based on race/ethnicity, NDRG1 expression was further examined in Caucasian and African American populations. Interestingly, NDRG1 positivity was significantly correlated with poorer survival only in African Americans but not Caucasians ($P = 0.035$ and $P = 0.31$, respectively) (Figure 3A). Since NDRG1 is a possible downstream target of p53, survival was further correlated with expression of the p53 protein, generally indicative of p53 mutations leading to a longer protein half-life. In p53-negative tumors in US cases, NDRG1 expression had no correlation with survival (Figure 3B). In contrast, in p53-positive tumors, NDRG1 positivity was significantly correlated with better survival ($P = 0.005$), suggesting that p53 and NDRG1 could potentially be used as biomarkers for prognosis in

US colorectal cancer patients.

When similar studies were performed on Japanese cases, survival was not significantly correlated with NDRG1 and p53 expression. Hence, we analyzed NDRG1 expression in various stages of colorectal cancer in Japanese patients. As shown in Figure 4A, no significance in correlation of NDRG1 expression with survival was observed in stages Ⅱ and Ⅲ colorectal cancers. However, when NDRG1 expression was re-classified as weak
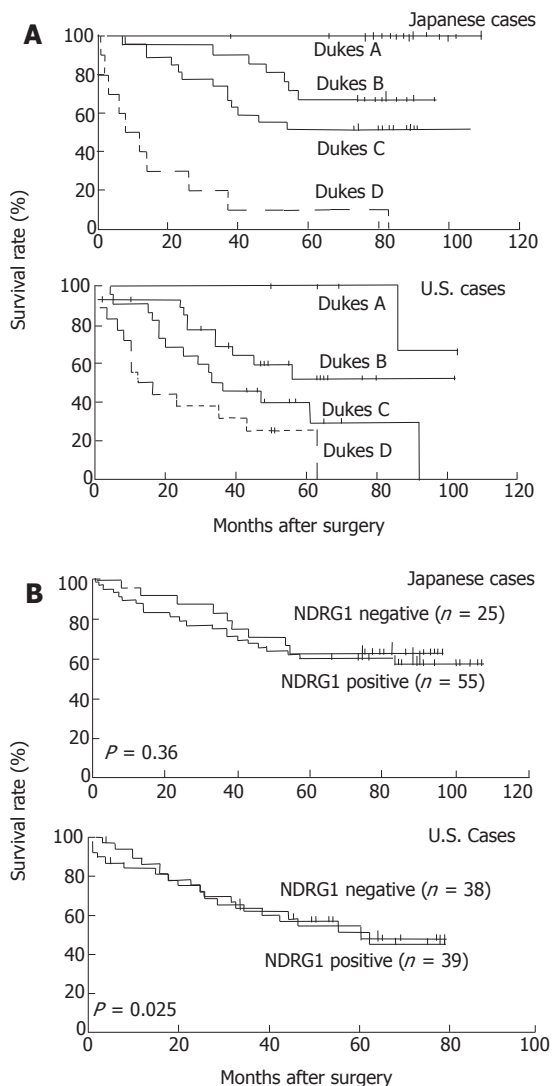
Figure 2 Kaplan-Meier survival analysis of colorectal cancer patients. **A**: Survival (months after surgery) of Japanese and US patients stratified according to Dukes' staging; **B**: Correlation of NDRG1 expression (negative, 0; positive, +1 to +3) with survival in Japanese patients and US patients (including Caucasians and African Americans).

Figure 3 Kaplan-Meier survival analysis of US colorectal cancer patients according to NDRG1 expression. **A**: Comparison of survival according to race/ethnicity, i.e., Caucasian and African American; **B**: Correlation of survival in p53-negative and p53-positive staining tumors.

staining (0, +1) and strong staining (+2, +3), strong NDRG1 staining was significantly correlated with better survival in patients with stage Ⅱ and Ⅲ colorectal cancers ($P = 0.036$). In combination with p53-positive staining, strong NDRG1 staining (+2, +3) also significantly correlated with improved survival ($P = 0.013$) (Figure 4B). Since high NDRG1 expression in patients with colorectal liver metastases was associated with relative resistance to irinotecan [20], NDRG1 expression and survival was compared in patients with or without chemotherapy. Interestingly, despite the small sample size, strong NDRG1 staining was significantly correlated with poorer survival in stages Ⅱ and Ⅲ colorectal cancer patients without chemotherapeutic treatment ($P = 0.019$) (Figure 4C).

When stages Ⅱ and Ⅲ colorectal cancer patients from the US were similarly evaluated, no significance was observed between weak or strong NDRG1 staining with survival (data not shown). We therefore evaluated if NDRG1 expression correlated with survival of US patients with stages Ⅲ and Ⅳ colorectal cancers. As shown

in Figure 5A, although it was not statistically significant ($P = 0.058$), a trend for improved survival was observed with NDRG1-positive staining. Interestingly, when these stages Ⅲ and Ⅳ tumors were analyzed based on the status of chemotherapy, NDRG1 positivity was significantly correlated with improved survival in stages Ⅲ and Ⅳ patients without chemotherapeutic treatment ($P = 0.04$) while no significant correlation was observed in patients who had received chemotherapy (Figure 5B).

DISCUSSION

Despite NDRG1 upregulation in many other tumor types[10,17,18,23], NDRG1 expression in colorectal cancer has been controversial[2,19,20]. Wang *et al*[19] demonstrated that NDRG1 expression was increased in colorectal carcinogenesis and correlated with lymph node metastasis in a Chinese population and suggested that NDRG1 might be a possible marker for prediction of early metastasis of colorectal cancers. Consistent with the latter, we
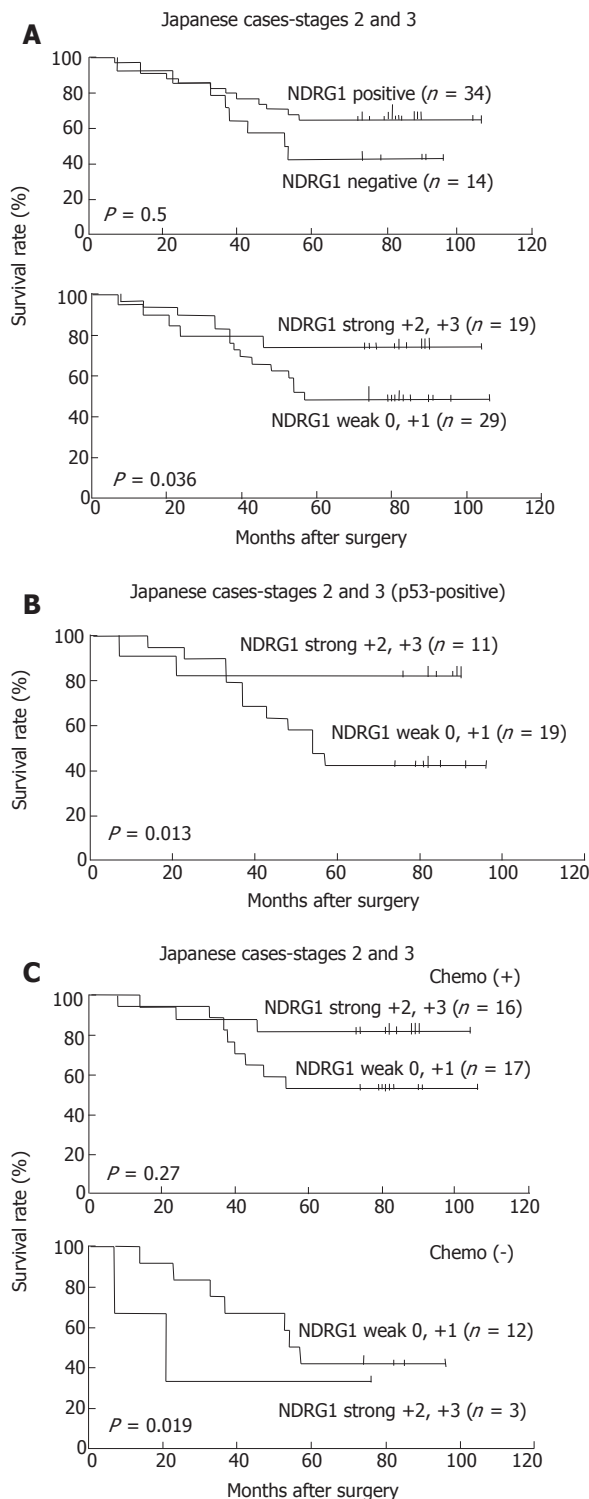
Figure 4 Kaplan-Meier survival analysis of NDRG1 expression in Japanese patients with stages II and III colorectal cancers. **A**: Correlation of survival with NDRG1 expression stratified as negative (0) or positive (+1 to +3) and weak (0, +1) or strong (+2, +3); **B**: Correlation of survival with weak or strong NDRG1 staining in p53-positive tumors; **C**: Correlation of survival with weak or strong NDRG1 staining in patients with or without chemotherapeutic treatment, chemo (+) or chemo (-), respectively.

Figure 5 Kaplan-Meier survival analysis of NDRG1 expression in US with stages III and IV colorectal cancers. **A**: Correlation of survival with NDRG1 expression stratified as negative (0) or positive (+1 to +3); **B**: Correlation of survival with weak or strong NDRG1 staining in patients with or without chemotherapeutic treatment, chemo (+) or chemo (-), respectively.

demonstrated that NDRG1 expression was significantly correlated to lymphatic invasion, venous invasion, depth of invasion, and histopathological type, and Dukes' stage in Japanese colorectal cancer patients (Table 1A), suggesting that NDRG1 expression might be correlated with more aggressive phenotypes in both Japanese and Chinese populations[19]. Although we did not have a significant number of Japanese cases with liver metastasis for the analysis of the correlation between NDRG1 expression and hepatic metastasis, NDRG1 was expressed in the tumors of all 7 Japanese patients that developed liver metastasis (Table 1A). On the other hand, compared with Japanese and Chinese patients, the opposite trend was observed in Caucasian patients with NDRG1 expression correlated negatively with liver metastasis (Table 1B). The latter was consistent with a previous report suggesting that NDRG1 suppressed colon cancer metastasis, possibly by inducing colon cancer cell differentiation[25]. In addition, Shah et al[20] demonstrated NDRG1 expression in all 131 colorectal liver metastases from US patients and observed a trend for unilobar metastases with high NDRG1 expression which was associated with relative resistance to irinotecan. However, the race/ethnicity of the US patient population was not analyzed in these studies.

Although NDRG1 expression is inducible by hypoxia and its mimetic and is responsive to p53 in vitro[7,8,12,13], there was no significant correlation of NDRG1 expression with p53 expression but significant correlation was observed with HIF-1α expression in US patients, attributed to Caucasian patients, while a trend for association was observed in Japanese patients (Table 2B). On the other

hand, no significant correlation was observed between NDRG1 and HIF-1α expression in African American patients, suggesting that there may be other hypoxia-independent pathway(s) contributing to NDRG1 expression in African American patients. Nevertheless, NDRG1 expression in African Americans but not Caucasians was significantly correlated with poorer prognosis in African American patients (Figure 3A). However, when the overall US cases were analyzed based on p53 and NDRG1 positivity, patients with p53-positive and NDRG1-positive tumors have improved survival independent of race/ethnicity (Figure 3B). In p53-negative tumors, no significant correlation of NDRG1 expression with survival was observed, suggesting the potential use of both NDRG1 and p53 as prognostic markers for US colorectal cancer patients. Because of the limitation in small sample sizes, the latter was not further analyzed in Caucasian and African American patients. Future studies with a larger cohort will be needed to determine if NDRG1 and p53 expression can serve reliably as prognostic factors for survival after surgery for US patients, especially in African American patients. Moreover, NDRG1 inducibility may provide a biological basis underlying the ethnic disparity in clinical outcomes between African American and Caucasian patients.

Interestingly, when we analyzed NDRG1 expression in US patients with various stages of colorectal cancers including stages I and Ⅱ, stages Ⅱ and Ⅲ, and stages Ⅲ and Ⅳ, we only observed a trend for NDRG1 expression with improved survival (Figure 5A) while significant association of NDRG1 positivity with better survival was observed in US patients who had not undergone chemotherapy (Figure 5B). Since adjuvant chemotherapy for stage Ⅲ colon cancer had been associated with a 5-year survival of 16% but the benefits of adjuvant chemotherapy seemed to be lower in African American patients[26], future studies with larger sample sizes are needed for determining the utility of NDRG1 expression either alone or in combination with p53 expression as prognostic marker(s) for adjuvant therapies including chemotherapy or radiotherapy to improve survival.

In Japanese patients with stage Ⅱ and Ⅲ colorectal cancers, significant positive association of survival with NDRG1 expression was only observed when the latter was analyzed as weak (0, +1) or strong (+2, +3) staining (Figure 4A). Similar to US cases, strong NDRG1 staining and p53 positivity in stages Ⅱ and Ⅲ Japanese tumors correlated significantly with improved survival (Figures 3B and 4B). However, unlike US stages Ⅲ and Ⅳ patients without chemotherapy, strong NDRG1 staining was significantly correlated with poorer survival in Japanese patients with stages Ⅱ and Ⅲ colorectal cancers without chemotherapy (Figures 4C and 5B). These differences can be due to differences in stages and or race/ethnicity. Nevertheless, NDRG1 expression may potentially be used as a clinical marker for prognosis and adjuvant therapies.

In summary, the correlation of NDRG1 expression with various clinicopathological features and clinical outcomes in colorectal cancers from patients with different race/ethnicity suggested that it may serve not only as a potential prognostic marker but may provide a biological basis underlying the disparity of clinical outcomes among different race/ethnic groups.

REFERENCES

1 **Kokame K**, Kato H, Miyata T. Homocysteine-respondent genes in vascular endothelial cells identified by differential display analysis. GRP78/BiP and novel genes. *J Biol Chem* 1996; **271**: 29659-29665

2 **van Belzen N**, Dinjens WN, Diesveld MP, Groen NA, van der Made AC, Nozawa Y, Vlietstra R, Trapman J, Bosman FT. A novel gene which is up-regulated during colon epithelial cell differentiation and down-regulated in colorectal neoplasms. *Lab Invest* 1997; **77**: 85-92

3 **Zhou D**, Salnikow K, Costa M. Cap43, a novel gene specifically induced by Ni2+ compounds. *Cancer Res* 1998; **58**: 2182-2189

4 **Kokame K**, Kato H, Miyata T. Nonradioactive differential display cloning of genes induced by homocysteine in vascular endothelial cells. *Methods* 1998; **16**: 434-443

5 **Piquemal D**, Joulia D, Balaguer P, Basset A, Marti J, Commes T. Differential expression of the RTP/Drg1/Ndr1 gene product in proliferating and growth arrested cells. *Biochim Biophys Acta* 1999; **1450**: 364-373

6 **Shimono A**, Okuda T, Kondoh H. N-myc-dependent repression of ndr1, a gene identified by direct subtraction of whole mouse embryo cDNAs between wild type and N-myc mutant. *Mech Dev* 1999; **83**: 39-52

7 **Park H**, Adams MA, Lachat P, Bosman F, Pang SC, Graham CH. Hypoxia induces the expression of a 43-kDa protein (PROXY-1) in normal and malignant cells. *Biochem Biophys Res Commun* 2000; **276**: 321-328

8 **Salnikow K**, Blagosklonny MV, Ryan H, Johnson R, Costa M. Carcinogenic nickel induces genes involved with hypoxic stress. *Cancer Res* 2000; **60**: 38-41

9 **Salnikow K**, Kluz T, Costa M, Piquemal D, Demidenko ZN, Xie K, Blagosklonny MV. The regulation of hypoxic genes by calcium involves c-Jun/AP-1, which cooperates with hypoxia-inducible factor 1 in response to hypoxia. *Mol Cell Biol* 2002; **22**: 1734-1741

10 **Ulrix W**, Swinnen JV, Heyns W, Verhoeven G. The differentiation-related gene 1, Drg1, is markedly upregulated by androgens in LNCaP prostatic adenocarcinoma cells. *FEBS Lett* 1999; **455**: 23-26

11 **Cangul H**. Hypoxia upregulates the expression of the NDRG1 gene leading to its overexpression in various human cancers. *BMC Genet* 2004; **5**: 27

12 **Kurdistani SK**, Arizti P, Reimer CL, Sugrue MM, Aaronson SA, Lee SW. Inhibition of tumor cell growth by RTP/rit42 and its responsiveness to p53 and DNA damage. *Cancer Res* 1998; **58**: 4439-4444

13 **Stein S**, Thomas EK, Herzog B, Westfall MD, Rocheleau JV, Jackson RS 2nd, Wang M, Liang P. NDRG1 is necessary for p53-dependent apoptosis. *J Biol Chem* 2004; **279**: 48930-48940

14 **van Belzen N**, Dinjens WN, Eussen BH, Bosman FT. Expression of differentiation-related genes in colorectal cancer: possible implications for prognosis. *Histol Histopathol* 1998; **13**: 1233-1242

15 **Bandyopadhyay S**, Pai SK, Gross SC, Hirota S, Hosobe S, Miura K, Saito K, Commes T, Hayashi S, Watabe M, Watabe K. The Drg-1 gene suppresses tumor metastasis in prostate cancer. *Cancer Res* 2003; **63**: 1731-1736

16 **Bandyopadhyay S**, Pai SK, Hirota S, Hosobe S, Takano Y, Saito K, Piquemal D, Commes T, Watabe M, Gross SC, Wang Y, Ran S, Watabe K. Role of the putative tumor metastasis suppressor gene Drg-1 in breast cancer progression. *Oncogene* 2004; **23**: 5675-5681

17 **Gomez-Casero E**, Navarro M, Rodriguez-Puebla ML, Larcher F, Paramio JM, Conti CJ, Jorcano JL. Regulation of the differentiation-related gene Drg-1 during mouse skin carcinogenesis. *Mol Carcinog* 2001; **32**: 100-109

18 **Cangul H**, Salnikow K, Yee H, Zagzag D, Commes T, Costa M. Enhanced expression of a novel protein in human cancer cells:

a potential aid to cancer diagnosis. *Cell Biol Toxicol* 2002; **18**: 87-96

19   **Wang Z**, Wang F, Wang WQ, Gao Q, Wei WL, Yang Y, Wang GY. Correlation of N-myc downstream-regulated gene 1 overexpression with progressive growth of colorectal neoplasm. *World J Gastroenterol* 2004; **10**: 550-554

20   **Shah MA**, Kemeny N, Hummer A, Drobnjak M, Motwani M, Cordon-Cardo C, Gonen M, Schwartz GK. Drg1 expression in 131 colorectal liver metastases: correlation with clinical variables and patient outcomes. *Clin Cancer Res* 2005; **11**: 3296-3302

21   **Polite BN**, Dignam JJ, Olopade OI. Colorectal cancer and race: understanding the differences in outcomes between African Americans and whites. *Med Clin North Am* 2005; **89**: 771-793

22   **Baldwin LM**, Dobie SA, Billingsley K, Cai Y, Wright GE, Dominitz JA, Barlow W, Warren JL, Taplin SH. Explaining black-white differences in receipt of recommended colon cancer treatment. *J Natl Cancer Inst* 2005; **97**: 1211-1220

23   **Caruso RP**, Levinson B, Melamed J, Wieczorek R, Taneja S, Polsky D, Chang C, Zeleniuch-Jacquotte A, Salnikow K, Yee H, Costa M, Osman I. Altered N-myc downstream-regulated gene 1 protein expression in African-American compared with caucasian prostate cancer patients. *Clin Cancer Res* 2004; **10**: 222-227

24   **Plaschke J**, Kruger S, Pistorius S, Theissig F, Saeger HD, Schackert HK. Involvement of hMSH6 in the development of hereditary and sporadic colorectal cancer revealed by immunostaining is based on germline mutations, but rarely on somatic inactivation. *Int J Cancer* 2002; **97**: 643-648

25   **Guan RJ**, Ford HL, Fu Y, Li Y, Shaw LM, Pardee AB. Drg-1 as a differentiation-related, putative metastatic suppressor gene in human colon cancer. *Cancer Res* 2000; **60**: 749-755

26   **Jessup JM**, Stewart A, Greene FL, Minsky BD. Adjuvant chemotherapy for stage III colon cancer: implications of race/ethnicity, age, and differentiation. *JAMA* 2005; **294**: 2703-2711

Mechanisms involved in Korean mistletoe lectin-induced apoptosis of cancer cells

Lee-Yong Khil, Wi Kim, Suyun Lyu, Won Bong Park, Ji-Won Yoon, Hee-Sook Jun

Lee-Yong Khil, Wi Kim, Department of Microbiology and Infectious Diseases, Faculty of Medicine, University of Calgary, Calgary, Alberta, T2N 4N1, Canada
Suyun Lyu, Immune Modulation Group, Boots Science Building, School of Pharmacy, University of Nottingham, University Park, Nottingham, NG7 2RD, United Kingdom
Won Bong Park, College of Natural Science, Seoul Women's University, Seoul 139-774, Korea
Ji-Won Yoon, Hee-Sook Jun, Department of Pathology, Chicago Medical School, North Chicago, IL, 60064, United States
Sadly, Dr. Ji-Won Yoon passed away on April 6, 2006
Supported by the International Innovative Biotechnology Institute
Correspondence to: Hee-Sook Jun, Department of Pathology, Chicago Medical School, North Chicago, IL, 60064, United States. hee-sook.jeon@rosalindfranklin.edu
Telephone: +1-847-5788341 Fax: +1-847-5783432
Received: 2006-12-16   Accepted: 2007-03-19

Abstract

AIM: To investigate the anti-cancer mechanisms of Korean mistletoe lectin (*Viscum album coloratum* agglutinin, VCA) using a human colon cancer cell line (COLO).

METHODS: Cytotoxic effects of VCA on COLO cells were determined by 3-(4,5-dimethylthiazol-2-yl)-2,5-diphenyltetrazolium bromide (MTT) assay *in vitro* and tumor-killing effects *in vivo*. To study the mechanisms involved, the expression of various pro-caspases, anti-apoptotic proteins, and death receptors was determined by western blot. To determine which death receptor is involved in VCA-induced apoptosis of COLO cells, cytotoxicity was examined by MTT assay after treatment with agonists or antagonists of death receptors.

RESULTS: VCA killed COLO cells in a time- and dose-dependent manner and induced complete regression of tumors in nude mice transplanted with COLO cells. Treatment of COLO cells with VCA activated caspase-2, -3, -8, and -9 and decreased expression of anti-apoptotic molecules including receptor interacting protein, nuclear factor-κB, X-linked inhibitor of apoptosis protein, and Akt/protein kinase B. We then examined the involvement of death receptors in VCA-induced apoptosis. Only tumor necrosis factor receptor 1, among the death receptors examined, was involved in apoptosis of COLO cells, evidenced by inhibition of VCA-induced apoptosis and decreased activation of caspases, particularly caspase-8, by tumor necrosis factor receptor 1 antagonizing antibody.

CONCLUSION: VCA-induced apoptotic COLO cell death is due to the activation of caspases and inhibition of anti-apoptotic proteins, in part through the tumor necrosis factor receptor 1 signaling pathway.

Khil LY, Kim W, Lyu S, Park WB, Yoon JW, Jun HS. Mechanisms involved in Korean mistletoe lectin-induced apoptosis of cancer cells. *World J Gastroenterol* 2007; 13(20): 2811-2818

http://www.wjgnet.com/1007-9327/13/2811.asp

INTRODUCTION

Extracts from European white berry mistletoe (*Viscum album* L, Family Viscaceae) have been used in adjuvant chemotherapy[1]. Lectins were identified as one of the therapeutically active molecules in mistletoe extracts[2-4]. European mistletoe lectins (*Viscum album* agglutinins, VAAs) showed cytotoxic effects on tumor cells by apoptotic cell death[3]. Korean mistletoe (*Viscum album* var. *coloratum* Kom.), a subspecies of European mistletoe, has been used as a medicinal herb and has also been shown to be cytotoxic against tumor cells[5]. It was reported that a lectin isolated from Korean mistletoe (*Viscum album* var. *coloratum* agglutinin, VCA) was different from VAAs in molecular weight, N-terminal amino acid sequence, and structure. VCA has a molecular mass of 60 kDa, consisting of a 31 kDa A chain and a 34 kDa B chain, and binds preferentially to galactose and N-acetyl-D-galactosamine[6-9]. VCA showed strong cytotoxic activity against human and murine tumor cells[10]. VCA inhibited telomerase activity, resulting in DNA fragmentation and tumor cell apoptosis[11-13].

There are two major pathways for apoptosis: the death receptor-induced pathway and the mitochondria-apoptosome-mediated pathway. The death receptor-induced apoptotic pathway includes ligands such as Fas, tumor necrosis factor (TNF), and death receptor (DR)3 and their receptors and downstream molecules such as caspases[14,15]. The mitochondria-apoptosome-mediated pathway includes apoptotic stimuli induced by radiation

or chemotherapy. The caspase cascade is activated by the release of cytochrome c, which is initiated by the formation of apoptosomes[15]. Cross-talk between these two apoptotic pathways also exists[15,16]. Both VAAs and VCA were shown to induce apoptosis of tumor cells through the mitochondria-mediated pathway[17,18]. However, it is not known whether the death receptor-mediated apoptosis pathway is also involved in the killing of tumor cells by VCA.

In this study, it was found that VCA treatment showed a strong killing effect on COLO 320HSR (COLO) cells both *in vitro* and *in vivo*. VCA treatment of COLO cells resulted in the activation of caspase-2, -3, -8, and -9, induced the degradation of Akt/protein kinase B (PKB) and poly(ADP) ribose polymerase, and decreased the expression of anti-apoptotic proteins such as receptor-interacting protein (RIP) and X-linked inhibitor of apoptosis (XIAP). Antagonizing anti-tumor necrosis factor receptor (TNFR)1 antibody treatment partially inhibited the activation of caspases and apoptosis induced by VCA. These results suggest that TNFR1, a component of the death receptor-mediated apoptosis pathway, may be involved, in part, in activating caspases, resulting in the apoptosis of colon cancer cells by VCA.

MATERIALS AND METHODS

VCA and antibodies

VCA was extracted from *Viscum album L. coloratum* and the biochemical properties were characterized as described elsewhere[6,7]. Anti-phospho-Akt/PKB (Ser-473), anti-Akt/PKB, anti-caspase-8, anti-caspase-9, and anti-XIAP antibodies were purchased from New England Biolabs (Beverly, CA). Anti-caspase-2, anti-RIP, anti-FasL, anti-Fas, and anti-caspase-3 antibodies were purchased from BD Pharmingen (San Diego, CA). Anti-nuclear factor (NF)-κB, and anti-TNFR2 antibodies were purchased from Santa Cruz Biotechnology (Santa Cruz, CA). Anti-β-actin antibody was purchased from Sigma Chemicals (St. Louis, MO). Anti-DR3 and anti-TNFR1 antibodies were purchased from Stressgen Biotechnologies Corp. (Victoria, BC, Canada). Activating anti-Fas antibody (clone CH11) was purchased from Upstate Biotechnology (Charlottesville, VA). Antagonizing anti-TNFR1 antibody and DR3/Fc chimeric protein were purchased from R & D Systems (Minneapolis, MN).

Cell culture

The COLO 320HSR colon cancer cell line (COLO), human epidermoidal cancer cell line (A253), and human diploid cell line from normal embryonic lung tissue (WI-38) were obtained from American Type Culture Collection (Rockville, MD). COLO cells and A253 cells were maintained in RPMI 1640 medium supplemented with 10% fetal bovine serum (FBS) and gentamycin (50 μg/mL). WI-38 cells were cultured in Minimum Eagle's essential medium containing 2 mmol/L L-glutamine, Earle's balanced salts, 0.1 mmol/L non-essential amino acids, 1 mmol/L sodium pyruvate and 10% FBS with antibiotics as above. Cells were cultured at 37℃ in a

humidified atmosphere containing 5% CO_2.

Viability test

3- (4, 5-Dimethylthiazol-2-yl) -2, 5-diphenyltetrazolium bromide (MTT; Sigma Chemicals) was used to measure the cytotoxic effect of VCA. Cells (2×10^4/well) were seeded and cultured in 96-well plates for 24 h and treated with various reagents. After treatment, 20 μL MTT (5 mg/mL) was added and cells were incubated for 4 h at 37℃. After removing the supernatant, the produced formazan crystals were dissolved in dimethyl sulfoxide, and optical density was measured at A570 nm and at A670 nm as reference with a microplate reader (Thermo Labsystems, Helsinki, Finland). The viability of the cells was calculated as: % viability = (absorbance of treated cells)/(absorbance of untreated cells) × 100.

FACS analysis

COLO cells were cultured with or without VCA for 9 h, harvested, washed twice with PBS, and fixed with cold 70% ethanol at 4℃ overnight. Fixed cells were stored in absolute alcohol until staining with propidium iodide. Cells were washed twice with PBS and incubated with a propidium iodide mixture containing 100 μg/mL RNase A (Sigma Chemicals) and 50 μg/mL propidium iodide (Sigma Chemicals) in PBS at 37℃ for 30 min in the dark. The numbers of cells in various phases of the cell cycle or undergoing apoptosis were determined by flow cytometry.

In vivo tumor-killing effect

Male CD1 nu/nu nude mice (5 wk old) were purchased from Charles River (Wilmington, MA). Mice were adapted for 1 wk before experiments and were allowed food and water ad libitum during the experiments. COLO cells (1 $\times 10^7$ cells/mouse) were subcutaneously injected into the neck of nude mice. After 5 wk, the tumor-bearing mice were injected with VCA (10 μg/kg in PBS; 30 μL/mouse) around the tumor mass every 2 d for 5 wk. The use and care of the animals in this study were approved by the Animal Care Committee, Faculty of Medicine, University of Calgary.

Western blot analysis

Cells cultured under various experimental conditions were washed twice with ice-cold PBS and lysed in lysis buffer containing 50 mmol/L Tris-HCl, pH 7.5, 150 mmol/L NaCl, 1 mmol/L EDTA, 0.5 mmol/L dithiothreitol, 1% NP-40, 0.05 mmol/L phenylmethylsulfonyl fluoride, phosphatase inhibitor cocktail, and proteinase inhibitor cocktail (Sigma Chemicals). After incubation for 30 min on ice, cell lysates were centrifuged at 18 300 × *g* at 4℃ for 20 min. Protein concentrations were determined using a protein assay kit (Bio-Rad, Richmond, CA). Samples of cell lysate containing 50 μg of total protein were separated by 10%-12% SDS-PAGE and transferred onto a polyvinylidene fluoride membrane (Amersham Pharmacia Biotech, Buckinghamshire, UK). After blocking with 5% skim milk in Tris-buffered saline (50 mmol/L Tris-HCl, pH 7.6, 150 mmol/L NaCl, 0.05% Tween-20), the membranes were incubated overnight at 4℃ with various primary antibodies and further incubated with

horseradish peroxidase-conjugated secondary antibodies (Santa Cruz). The membranes were visualized by an enhanced chemiluminescence detection kit (Amersham Pharmacia Biotech).

Statistical analysis

The statistical significance of differences between groups was analyzed by Student's t-test. A level of $P < 0.05$ was accepted as significant.

RESULTS

Ability of VCA to kill human colon cancer cells in vitro and in vivo

To determine the cytotoxic effects of VCA on cancer cells, COLO (colon cancer), A253 (epidermal cancer), and WI-38 (normal) cells were treated with VCA for 24 h and cell viability was examined by MTT assay. VCA showed a strong killing effect on COLO cells, significantly less on A253 cells, and no effect on WI-38 cells (Figure 1A). COLO cells were treated with various doses of VCA for various times and cell viability was examined by MTT assay. A dose- and time-dependent killing effect could be seen between 10 ng/mL and 100 ng/mL VCA, with 100 ng/mL showing the maximum effect (Figure 1B). Propidium iodide staining and FACS analysis of VCA-treated COLO cells showed apoptosis in 64.7% of the cells (Figure 1C). To determine whether VCA shows a tumor-killing effect on colon cancer cells *in vivo*, COLO cells were subcutaneously injected into the neck of 6-wk-old male CD1 nu/nu mice. Five weeks later when tumors developed, VCA or PBS, as a control, was injected into the tumor every 2 d for 5 wk. We found that treatment with VCA for 5 wk resulted in the killing of tumors (Figure 2A). All of the tumors treated with VCA disappeared and were replaced by scar tissue, and this scar tissue healed in mice kept for an additional 2 mo without further treatment (Figure 2B). However, tumors remained in PBS-treated mice (data not shown).

Activation of caspase and inhibition of anti-apoptotic proteins in COLO cells by VCA treatment

To examine the apoptosis of COLO cells by VCA, COLO cells were treated with VCA for 12 h and the amount of procaspase was examined by western blot. Treatment of COLO cells with VCA decreased the amount of procaspases-2, -3, -8, and -9 as compared with untreated COLO cells, whereas VCA treatment of control WI38 cells did not change the amount of these procaspases (Figure 3A), indicating that VCA treatment activates caspases specifically in COLO tumor cells. To determine the time-dependent activation of caspases, COLO cells were treated with VCA and harvested at 0.5, 1, 3, 6, 9, and 12 h after treatment and western blots were performed using antibodies specific for each procaspase. It was found that cleaved products from procaspase-2, -3, -8, and -9 were detected from 6 h after VCA treatment and the corresponding procaspase bands were almost completely absent at 12 h after treatment (Figure 3B). These results indicate that VCA treatment activated caspase-2, -3, -8,
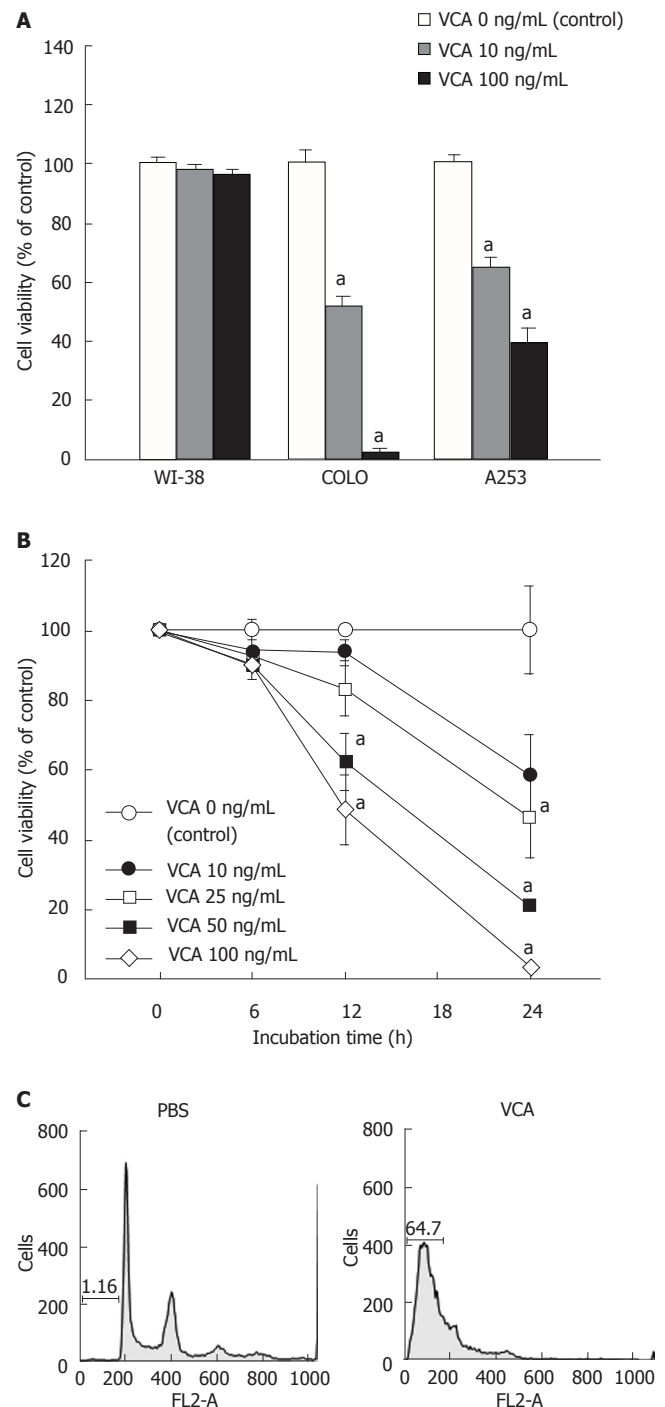
Figure 1 Cytotoxic effects of VCA on COLO cells *in vitro*. **A**: Cells were treated with VCA for 24 h and cell viability was determined by MTT assay. Values are mean ± SE; $n = 4$/group; **B**: COLO cells were incubated with the indicated amounts of VCA for various times and cell viability was determined by MTT assay. Values are mean ± SE, $n = 5$/group. $^{a}P < 0.05$ *vs* control group; **C**: COLO cells were treated with or without VCA (100 ng/mL) for 9 h. Cells were harvested, fixed in ethanol, and stained with propidium iodide in the presence of RNase A. The stained cells were analyzed by flow cytometry.

and -9 in a time-dependent manner.

To further determine the mechanisms of the apoptotic pathway involved in VCA-induced killing of COLO cells, we examined the expression of adaptor molecules of death receptors and their downstream molecules, including

Figure 2 Tumor-killing effect of VCA *in vivo*. COLO cells (1×10^7 cells/mouse) were injected into the neck of CD1 nude mice. Five weeks later, VCA was injected around the developed tumors every 2 d for 5 wk. (**A**) The tumors were measured at 0, 1, 3 and 5 wk after VCA treatment and (**B**) were photographed at the end of experiment. The size of the tumors decreased (**a-c**) at 5 wk of treatment and eventually disappeared at 2 mo after the termination of VCA treatment (**d**).

Figure 3 Activation of caspases in COLO cells treated with VCA. **A**: COLO and WI-38 cells were treated without (-) or with (+) VCA (100 ng/mL) for 12 h. Cell lysates were prepared and western blots were performed using antibodies specific for each pro-caspase (PCas). Immunoreactive bands were visualized by chemiluminescence. Representative western blots are shown (left panel). Each band was quantified and normalized against the internal control (β-actin). Normalized values were used to calculate the relative expression of each procaspase as a percentage of PBS-treated WI-38 cells. WP: WI-38 cells treated with PBS, WV: WI-38 cells treated with VCA, CP: COLO cells treated with PBS, CV: COLO cells treated with VCA. Values are mean±SE of three independent experiments (right panel). $^aP < 0.05$ *vs* WP. $^cP < 0.05$ *vs* CP; B: COLO cells were treated without (-) or with (+) VCA (100 ng/mL) for various times and western blots were performed and quantified as described for (A). Representative western blots of three independent experiments are shown (left panel). Each band was quantified and normalized against the internal control (β-actin). Normalized values were used to calculate the relative expression of each procaspase as a percentage of COLO cells without VCA treatment at each time point (right panel).

RIP, Fas-associated death domain (FADD), NF-κB, Akt/PKB, and XIAP, by western blot. The expression of RIP and FADD started to decrease after 6 h of VCA treatment and was correlated with a decreased expression of NF-κB, Akt/PKB, and XIAP in COLO cells (Figure 4).

Involvement of TNFR1 in VCA-induced killing of COLO cells

To determine whether death receptors are involved in VCA-induced apoptosis of COLO cells, we examined the expression of the death receptors TNFR1, TNFR2, DR3,

Fas, and FasL in COLO and WI-38 cells by western blot. The expression of TNFR1, TNFR2, DR3, and FasL was higher in COLO cells as compared with WI-38 cells. Fas expression was not detected in either cell type (data not shown). Treatment of COLO cells with VCA significantly decreased the expression of TNFR2, but not TNFR1, DR3, or FasL. Treatment of WI-38 cells with VCA did not change the expression of these molecules (Figure 5A).

To determine which death receptor is involved in VCA-induced apoptosis of COLO cells, the killing effect of VCA on COLO cells was examined in the

A

B
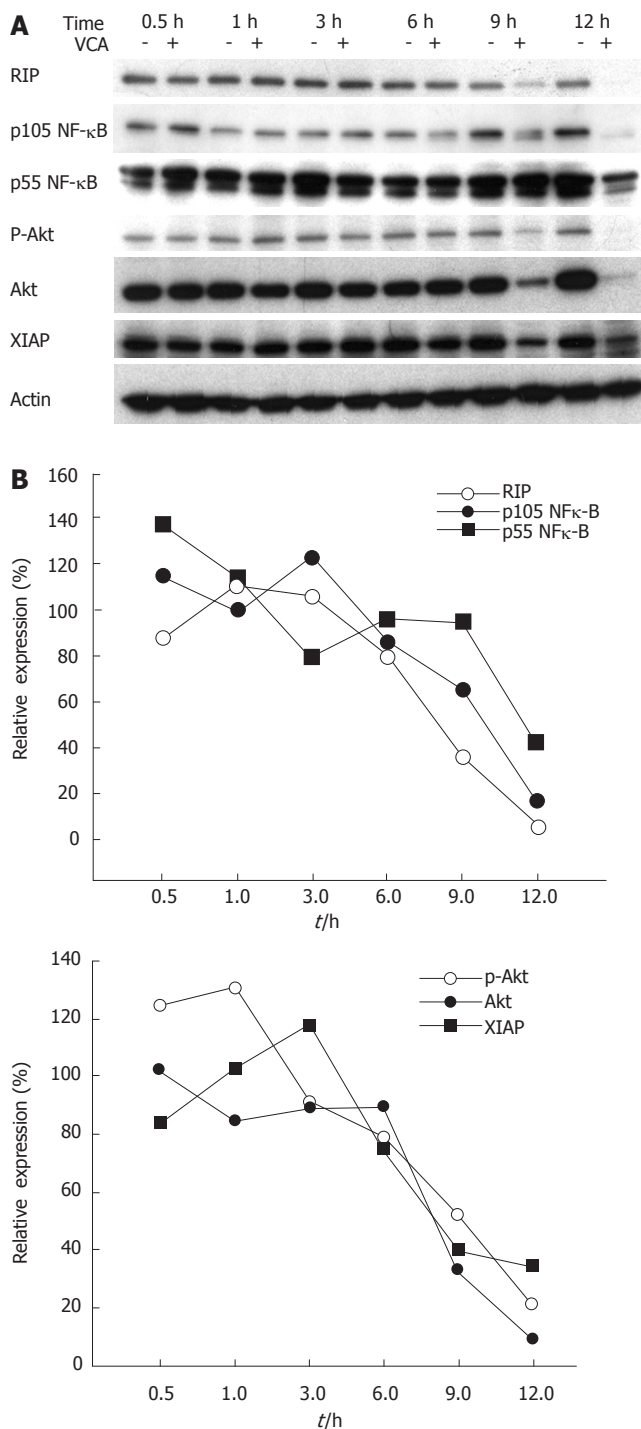
Figure 4 Decreased expression of anti-apoptotic molecules in COLO cells treated with VCA. COLO cells were treated without (-) or with (+) VCA (100 ng/mL) for the indicated times. Cell lysates were prepared and western blots were performed using specific antibodies. Immunoreactive bands were visualized by chemiluminescence. Representative western blots are shown (**A**). Each band was quantified and normalized against the internal control (®-actin). Normalized values were used to calculate the relative expression as a percentage of COLO cells without VCA treatment at each time point (**B**). p-Akt: phosphorylated Akt. Results are representative of three independent experiments.

presence or absence of agonists or antagonists of death receptors. Treatment of COLO cells with activating anti-Fas antibody did not induce cell death or affect the killing effect of VCA, which was expected as Fas is not expressed in COLO cells (data not shown). In addition, anti-Fas antibody did not affect the killing effects of VCA on

COLO cells. Treatment with DR3-Fc chimeric protein, which inhibits the activation of DR3, did not affect the cytotoxic effect of VCA on COLO cells (data not shown). Treatment with antagonizing anti-TNFR1 antibody, which blocks TNF-α-induced apoptosis, inhibited the killing effect of VCA on COLO cells (Figure 5B).

Inhibition of caspase activation and subsequent apoptosis in COLO cells by treatment with antagonizing TNFR1 antibody

To determine whether blocking TNFR1 inhibits VCA-induced activation of caspase-2, -3, -8, and -9, resulting in the inhibition of apoptotic death of COLO cells, the expression of the respective procaspases in VCA-treated COLO cells was determined in the presence or absence of antagonizing anti-TNFR1 antibody by western blot. Anti-TNFR1 antibody significantly inhibited the activation of caspase-8 and caspase-2, as shown by the inhibition of the decrease of their respective procaspase, but not caspase -3 or -9 (Figure 6A). VCA treatment of COLO cells decreased the expression of anti-apoptotic molecules, such as Akt/PKB and XIAP, and treatment with antagonizing anti-TNFR1 antibody significantly inhibited this decrease (Figure 6B).

DISCUSSION

It was previously reported that *Viscum album* var. *coloratum* agglutinin (VCA) had cytotoxic effects on cancer cells such as hepatocarcinoma and HL-60 leukemia cells by inducing apoptosis[12,18]. Consistent with this, it was found that VCA selectively killed colon cancer cells (COLO 320HSR) *in vitro* and *in vivo*, but not normal human diploid cells (WI-38). However, the detailed molecular mechanisms involved in the killing of tumor cells by VCA have not been clearly elucidated. In this study, it was found that VCA-induced apoptosis of colon cancer cells is due to the activation of caspases and inhibition of anti-apoptotic proteins partly through the TNFR1 signaling pathway.

Apoptotic morphological and biochemical changes, including chromatin condensation, degradation of chromosomal DNA, and membrane blebbing[19-21], occur after a cascade of cell signaling and caspase-mediated events that regulate pro-apoptotic and anti-apoptotic proteins[14,22,23]. Apoptosis is triggered by two major pathways: the death-receptor-induced apoptotic pathway and the mitochondria-apoptosome-mediated apoptotic pathway[14]. Both of these pathways lead to caspase activation and cleavage of specific cellular substrates[14,15]. Inhibitors of apoptotic proteins such as XIAP, cellular inhibitor of apoptosis proteins, phosphatidylinositol 3-kinase, Akt/PKB, NF-κB, and heat shock proteins can interact with caspases and inhibit apoptosis[15]. We examined the activation of caspases in VCA-treated COLO cells and found that caspase-2, -3, -8, and -9 were activated as compared with PBS-treated COLO cells.

While the activation of caspases is critical for the induction of apoptosis[23,24]. The degradation of anti-apoptotic proteins such as RIP, Akt/PKB, and XIAP can accelerate the death of cancer cells. Consistent with previous work[14], the present study found that treatment of
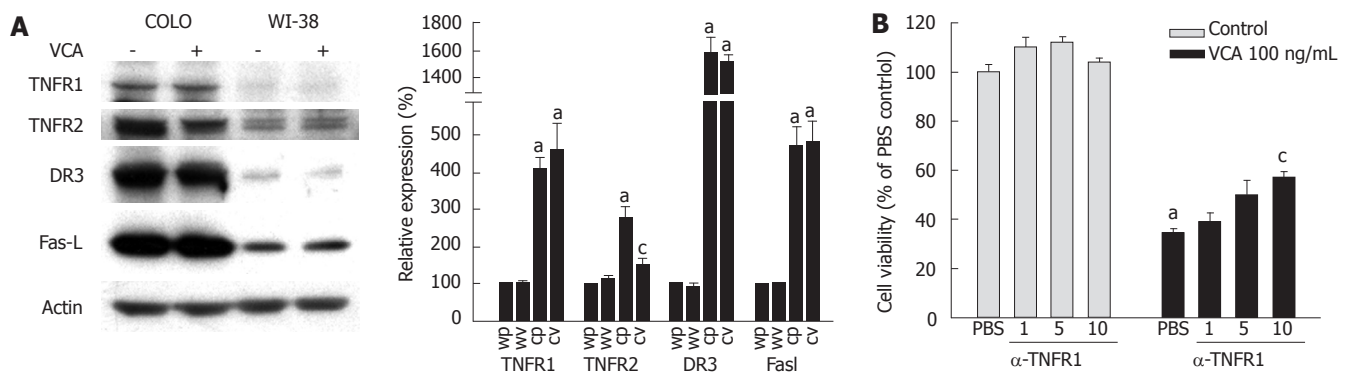
Figure 5 Inhibition of VCA-induced cytotoxicity of COLO cells by antagonizing anti-TNFR1 antibody (**A**) COLO and WI-38 cells were treated without (-) or with (+) VCA (100 ng/mL) for 12 h, cell lysates were prepared, and western blots were performed using specific antibodies. Immunoreactive bands were visualized by chemiluminescence. Representative western blot is shown (left panel). Each band was quantified and normalized against the density of the internal control (®-actin). Normalized values were used to calculate the relative expression as a percentage of PBS-treated WI-38 cells. WP: WI-38 cells treated with PBS, WV: WI-38 cells treated with VCA, CP: COLO cells treated with PBS, CV: COLO cells treated with VCA. Values are mean±SE of three independent experiments (right panel). [a]$P < 0.05$ *vs* WP. [c]$P < 0.05$ *vs* CP. (**B**) COLO cells were treated without (Control) or with VCA (100 ng/mL) in the absence (PBS) or presence of the indicated amounts of antagonizing TNFR1 antibody (®-TNFR1) for 12 h. Cell viability was determined by MTT assay. Values are mean ± SE ($n = 4$). [a]$P < 0.05$ *vs* the PBS-treated control group. [c]$P < 0.05$ *vs* the PBS/VCA-treated group.
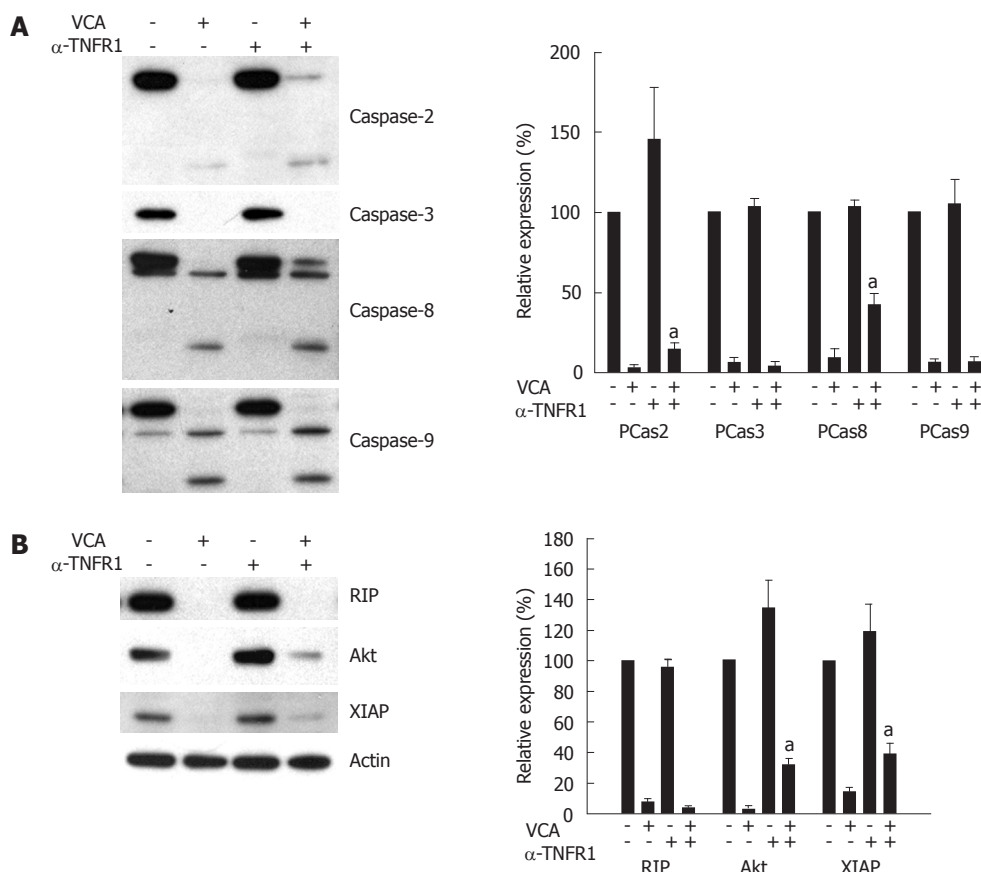
Figure 6 Inhibition of VCA-induced caspase activation and VCA-induced decrease of anti-apoptotic molecules in COLO cells treated with anti-TNFR1 antibody. COLO cells were treated without (-) or with (+) VCA (100 ng/mL) for 12 h in the presence (+) or absence (-) of anti-TNFR1 antibody (α-TNFR1, 10 μg/mL). Cell lysates were prepared and western blot was performed using specific antibodies for (**A**) various procaspases (PCas) and (**B**) anti-apoptotic molecules. Immunoreactive bands were visualized by chemiluminescence. Representative western blot is shown (left panels). Each band was quantified and normalized against the density of the internal control (actin). Normalized values were used to calculate the relative expression as a percentage of COLO cells without VCA or anti-TNFR1 antibody treatment. Values are mean ± SE of three independent experiments (right panels). [a]$P < 0.05$ *vs* VCA-treated cells without anti-TNFR1.

COLO cells with VCA significantly decreased the amount of RIP, Akt/PKB, and XIAP. The cytotoxic effects of VCA on COLO cells was more rapid and intense in serum-free media (data not shown), probably due to the absence of survival signals mediated by the Akt/PKB pathway by growth factors in serum-containing media. These results support the hypothesis that degradation of anti-apoptotic proteins by VCA treatment contributes to the induction of apoptosis in COLO cells.

It was previously reported that the activation of caspase-8 by VAAs, European mistletoe lectins, was not mediated by death receptors[17]. Transfection of a dominant-negative FADD into BJAB cells did not affect the induction of apoptosis by VAAs, suggesting that VAAs trigger a mitochondria-mediated apoptotic pathway[17]. In our study, it was found that VCA treatment activated caspase-2, -3 and -8, which are mediated by death receptors[15,16,25], and caspase-2 and -9, which are mediated by the mitochondrial pathway[25-27]. Therefore, VCA appears to induce activation of caspases by both mitochondria-mediated and death receptor-mediated pathways. VCA, from Korean mistletoe, and mistletoe

lectin (ML) Ⅱ, an isotype of VAAs from European mistletoe, have the same sugar-binding characteristics; however, the structures of these lectins are different. Variations in VAAs (ML Ⅰ, ML Ⅱ, and ML Ⅲ) result from different degrees of glycosylation[28], whereas variations in VCA result from amino acid sequence variation in the A and B chains, which are 10%-27% different from ML[29]. These differences in amino acid sequence may result in different cytotoxic mechanisms between VCA and VAAs.

COLO cells were found to express a high level of the death receptors TNFR1, TNFR2, and DR3, but did not express Fas. The expression of FasL was also high in COLO cells, probably as a mechanism to escape immune attack[30]. The expression of TNFR2 was decreased in COLO cells by VCA treatment, suggesting that VCA may inhibit survival signals through TNFR2, since TNFR2 mediates both survival and apoptotic signals[25,31]. However, this should be addressed further. To determine if any of these death receptors is involved in VCA-induced apoptosis of COLO cells, we activated or inhibited their signaling pathways in VCA-treated COLO cells using antibodies. Activating anti-Fas antibody did not affect the viability of COLO cells, as expected by the absence of Fas in these cells. Since DR3 is expressed on COLO cells, VCA may bind to DR3 and trigger apoptotic signals, resulting in cell death. Thus, DR3-Fc chimeric protein, which binds to the DR3 ligand and inhibits DR3-mediated apoptosis, was used to determine whether VCA-mediated apoptosis could be inhibited by blocking the interaction between VCA and DR3. DR3-Fc chimeric protein did not affect the cytotoxic effect of VCA on COLO cells.

TNF-α induced apoptosis of COLO cells sensitized with actinomycin D (data not shown)[32], indicating a role for TNFR in apoptosis of COLO cells. In our study, antagonizing anti-TNFR1 inhibited the cytotoxicity of VCA in COLO cells, suggesting that the TNFR1 pathway is involved in VCA-induced cell death. This antibody also inhibited VCA-induced apoptosis and activation of caspase-8 and -2, confirming the involvement of TNFR1 in VCA-induced apoptosis. This finding is supported by previous reports that TNFR1 induces both receptor-mediated (activation of caspase -3 and -8) and mitochondria-mediated (activation of caspase -2 and -9) apoptosis[16,25]. The exact mechanism by which VCA activates TNFR1 is not known; however, VCA was co-precipitated when TNFR1 was immunoprecipitated with TNFR1 antibody in VCA-treated COLO cells (unpublished data). Thus, we speculate that VCA might bind to TNFR1 and trigger cell death. This mechanism needs further investigation. Based on the results obtained in this study, we suggest that VCA may induce the activation of the TNFR1 signal transduction pathway, which contributes, in part, to the activation of caspases and degradation of anti-apoptotic molecules, resulting in the death of colon cancer cells.

ACKNOWLEDGMENTS

REFERENCES

1   **Steuer-Vogt MK**, Bonkowsky V, Ambrosch P, Scholz M, Neiss A, Strutz J, Hennig M, Lenarz T, Arnold W. The effect of an adjuvant mistletoe treatment programme in resected head and neck cancer patients: a randomised controlled clinical trial. *Eur J Cancer* 2001; **37**: 23-31

2   **Holtskog R**, Sandvig K, Olsnes S. Characterization of a toxic lectin in Iscador, a mistletoe preparation with alleged cancerostatic properties. *Oncology* 1988; **45**: 172-179

3   **Stauder H**, Kreuser ED. Mistletoe extracts standardised in terms of mistletoe lectins (ML I) in oncology: current state of clinical research. *Onkologie* 2002; **25**: 374-380

4   **Mengs U**, Gothel D, Leng-Peschlow E. Mistletoe extracts standardized to mistletoe lectins in oncology: review on current status of preclinical research. *Anticancer Res* 2002; **22**: 1399-1407

5   **Khwaja TA**, Varven JC, Pentecost S, Pande H. Isolation of biologically active alkaloids from Korean mistletoe Viscum album, coloratum. *Experientia* 1980; **36**: 599-600

6   **Lyu SY**, Park SM, Choung BY, Park WB. Comparative study of Korean (Viscum album var. coloratum) and European mistletoes (Viscum album). *Arch Pharm Res* 2000; **23**: 592-598

7   **Park WB**, Han SK, Lee MH, Han KH. Isolation and characterization of lectins from stems and leaves of Korean mistletoe (Viscum album var. coloratum) by affinity chromatography. *Arch Pharm Res* 1997; **20**: 306-312

8   **Hajto T**, Hostanska K, Frei K, Rordorf C, Gabius HJ. Increased secretion of tumor necrosis factors alpha, interleukin 1, and interleukin 6 by human mononuclear cells exposed to beta-galactoside-specific lectin from clinically applied mistletoe extract. *Cancer Res* 1990; **50**: 3322-3326

9   **Peumans WJ**, Verhaert P, Pfuller U, Van Damme EJ. Isolation and partial characterization of a small chitin-binding lectin from mistletoe (Viscum album). *FEBS Lett* 1996; **396**: 261-265

10 **Yoon TJ**, Yoo YC, Kang TB, Shimazaki K, Song SK, Lee KH, Kim SH, Park CH, Azuma I, Kim JB. Lectins isolated from Korean mistletoe (Viscum album coloratum) induce apoptosis in tumor cells. *Cancer Lett* 1999; **136**: 33-40

11 **Kim MS**, Lee J, Lee KM, Yang SH, Choi S, Chung SY, Kim TY, Jeong WH, Park R. Involvement of hydrogen peroxide in mistletoe lectin-II-induced apoptosis of myeloleukemic U937 cells. *Life Sci* 2003; **73**: 1231-1243

12 **Lyu SY**, Park WB, Choi KH, Kim WH. Involvement of caspase-3 in apoptosis induced by Viscum album var. coloratum agglutinin in HL-60 cells. *Biosci Biotechnol Biochem* 2001; **65**: 534-541

13 **Choi SH**, Lyu SY, Park WB. Mistletoe lectin induces apoptosis and telomerase inhibition in human A253 cancer cells through dephosphorylation of Akt. *Arch Pharm Res* 2004; **27**: 68-76

14 **Debatin KM**. Apoptosis pathways in cancer and cancer therapy. *Cancer Immunol Immunother* 2004; **53**: 153-159

15 **Kim R**, Tanabe K, Uchida Y, Emi M, Inoue H, Toge T. Current status of the molecular mechanisms of anticancer drug-induced apoptosis. The contribution of molecular-level analysis to cancer chemotherapy. *Cancer Chemother Pharmacol* 2002; **50**: 343-352

16 **Nunez G**, Benedict MA, Hu Y, Inohara N. Caspases: the proteases of the apoptotic pathway. *Oncogene* 1998; **17**: 3237-3245

17 **Bantel H**, Engels IH, Voelter W, Schulze-Osthoff K, Wesselborg S. Mistletoe lectin activates caspase-8/FLICE independently of death receptor signaling and enhances anticancer drug-induced apoptosis. *Cancer Res* 1999; **59**: 2083-2090

18 **Lyu SY**, Choi SH, Park WB. Korean mistletoe lectin-induced apoptosis in hepatocarcinoma cells is associated with inhibition of telomerase via mitochondrial controlled pathway independent of p53. *Arch Pharm Res* 2002; **25**: 93-101

19 **Green DR**, Reed JC. Mitochondria and apoptosis. *Science* 1998; **281**: 1309-1312

20 **Gross A**, McDonnell JM, Korsmeyer SJ. BCL-2 family

members and the mitochondria in apoptosis. *Genes Dev* 1999; **13**: 1899-1911

21   **Kerr JF**, Wyllie AH, Currie AR. Apoptosis: a basic biological phenomenon with wide-ranging implications in tissue kinetics. *Br J Cancer* 1972; **26**: 239-257

22   **Evan G**, Littlewood T. A matter of life and cell death. *Science* 1998; **281**: 1317-1322

23   **Thornberry NA**, Lazebnik Y. Caspases: enemies within. *Science* 1998; **281**: 1312-1316

24   **Kumar S**, Vaux DL. Apoptosis. A cinderella caspase takes center stage. *Science* 2002; **297**: 1290-1291

25   **Gaur U**, Aggarwal BB. Regulation of proliferation, survival and apoptosis by members of the TNF superfamily. *Biochem Pharmacol* 2003; **66**: 1403-1408

26   **Robertson JD**, Enoksson M, Suomela M, Zhivotovsky B, Orrenius S. Caspase-2 acts upstream of mitochondria to promote cytochrome c release during etoposide-induced apoptosis. J Biol Chem 2002; **277**: 29803-29809

27   **Guo Y**, Srinivasula SM, Druilhe A, Fernandes-Alnemri T, Alnemri ES. Caspase-2 induces apoptosis by releasing

proapoptotic proteins from mitochondria. *J Biol Chem* 2002; **277**: 13430-13437

28   **Zimmerman R**, Pfuller U. Glycosylation pattern of mistletoe lectins. In: Bardocz S, Pfuller U, Pusztai A. COST 98: Effects of antinutrients on the nutritional value of legume diets. Luxembourg: European Commission, 1998: 55-62

29   **Park CH**, Lee DW, Kang TB, Lee KH, Yoon TJ, Kim JB, Do MS, Song SK. cDNA cloning and sequence analysis of the lectin genes of the Korean mistletoe (Viscum album coloratum). *Mol Cells* 2001; **12**: 215-220

30   **Houston A**, Bennett MW, O'Sullivan GC, Shanahan F, O'Connell J. Fas ligand mediates immune privilege and not inflammation in human colon cancer, irrespective of TGF-beta expression. *Br J Cancer* 2003; **89**: 1345-1351

31   **Gupta S**. A decision between life and death during TNF-alpha-induced signaling. *J Clin Immunol* 2002; **22**: 185-194

32   **Powell CB**, Mutch DG, Massad LS, Kao MS, Collins JL. Common expression of a tumor necrosis factor resistance mechanism among gynecological malignancies. *Cancer Immunol Immunother* 1990; **32**: 131-136

S- Editor Liu Y   **L- Editor** Alpini GD   **E- Editor** Zhou T

Liver biochemistry profile, significance and endoscopic management of biliary tract complications post orthotopic liver transplantation

Yogesh M Shastri, Nicolas M Hoepffner, Bora Akoglu, Christina Zapletal, Wolf O Bechstein, Wolfgang F Caspary, Dominik Faust

Yogesh M Shastri, Nicolas M Hoepffner, Bora Akoglu, Wolfgang F Caspary, Dominik Faust, Department of Medicine I, J.W. Goethe-University Hospital, Theodor-Stern-Kai 7, D - 60590 Frankfurt am Main, Germany

Christina Zapletal, Wolf O Bechstein, Department of Surgery, Theodor-Stern-Kai 7, D-60590, J.W. Goethe University Hospital, Frankfurt am Main, Germany

Co-first-authors: Nicolas M Hoepffner

Correspondence to: Dr. Dominik Faust, Medizinische Klinik I, J.W. Goethe-University Hospital, Theodor-Stern-Kai 7, D-60590 Frankfurt am Main, Germany. d.faust@em.uni-frankfurt.de

Telephone: +49-69-63015212 Fax: +49-69-63014807

Received: 2007-03-01   Accepted: 2007-03-28

Abstract

AIM: To correlate the significance of liver biochemical tests in diagnosing post orthotopic liver transplantation (OLT) biliary complications and to study their profile before and after endoscopic therapy.

METHODS: Patients who developed biliary complications were analysed in detail for the clinical information, laboratory tests, treatment offered, response to it, follow up and outcomes. The profile of liver enzymes was determined. The safety, efficacy and outcomes of endoscopic retrograde cholangiography (ERC) were also analysed.

RESULTS: 40 patients required ERC for 70 biliary complications. GGT was found to be > 3 times (388.1 ± 70.9 U/mL *vs* 168.5 ± 34.2 U/L, *P* = 0.007) and SAP > 2 times (345.1 ± 59.1 U/L *vs* 152.7 ± 21.4 U/L, *P* = 0.003) the immediate post OLT values. Most frequent complication was isolated anastomotic strictures in 28 (40%). Sustained success was achieved in 26 (81%) patients.

CONCLUSION: Biliary complications still remain an important problem post OLT. SAP and GGT can be used as early, non-invasive markers for diagnosis and also to assess the adequacy of therapy. Endoscopic management is usually effective in treating the majority of these biliary complications.

Key words: Liver biochemistry; Biliary lesion; Ischemic type biliary lesions; Endoscopic therapy; Orthotopic liver transplantation

INTRODUCTION

Chronic liver diseases are an important cause of morbidity and mortality, the impact of which can be judged by the mortality rates due to these diseases. The highest deaths rates per 100 000 populations (in Europe) from chronic liver disease have been reported from Austria (37.9) while the lowest are those from Iceland (0.9)[1].

Only a small fraction of these patients with end stage liver disease end up obtaining a suitable liver transplant. Despite standardization of biliary reconstruction, biliary complications after orthotopic liver transplantation (OLT) occur in 7% to 51% of cases and are an important cause of early and late postoperative morbidity and mortality[2-11]. The commonest are bile duct strictures and biliary leaks. The biliary anastomosis has been rightly termed the 'Achilles' heel' of the OLT. Early diagnosis, followed by prompt and adequate treatment of biliary complications will not only reduce the unnecessary diagnostic procedures but will also be necessary to reduce hospital stays, morbidity, mortality and to improve outcomes related to OLT. Some of these patients may ultimately experience graft loss. Diagnosing and localizing these obstructive biliary complications post OLT could be very challenging to the clinician because of following reasons: (1) hepatic denervation leading to right upper quadrant abdominal pain, which is normally a feature of Charcot's triad is usually not seen in these patients[12], (2) clinical symptoms that may be non-specific like fever, anorexia etc., (3) recurrence of the underlying pretransplant liver illnesses (like HBV, HCV reactivation, PSC recurrence etc.) or graft rejection which could lead to the elevation of liver biochemical parameters and can be misleading, (4)

epithelial casts fill up the biliary system thus making its visualization difficult by indirect imaging e.g. USG/CT scan, (5) the time for the biliary system to dilate upstream after being obstructed as compared to that of native biliary system.

Direct cholangiography by endoscopic retrograde cholangiography (ERC) or PTC still remains the gold standard to diagnose biliary complications; however it is an invasive procedure associated with morbidity. There are multitudes of studies reporting the role of endoscopy in diagnosis and management of biliary complications. Shah, et al[13] demonstrated ERC to have a sensitivity and specificity of 53% and 98%; respectively in predicting overall biliary complications post OLT. But there is a scarcity of information in the literature evaluating the significance of serum levels of liver biochemistry panels, i.e. AST (aspartate aminotransferase), ALT (alanine aminotransferase), gamma glutamyl transferase (GGT), and serum alkaline phosphatase (SAP) in diagnosing these biliary complications. The present study had the primary aim to analyse the significance of deranged liver biochemistry for early suspicion of biliary complications, and also to study their profile during post endoscopic therapy and follow up.

Biliary complications post OLT are usually evaluated and treated now-a-days by ERC or by percutaneous transhepatic biliary drainage (PTBD); surgical intervention (including placement of T tube drainage)[14] is reserved for lesions not managed by the above 2 techniques. ERC being the less invasive and safer intervention is generally the preferred mode of management[2,3,15,16]. The secondary aim of this study was to study the efficacy, safety and outcomes of ERC in diagnosing and managing biliary complications post OLT from our centre.

MATERIALS AND METHODS

This study included 162 patients (109 males, age 52 ± 10 years; 53 females, age 49 ± 14 years) who underwent OLT between 1994 and 2004, 84 of these patients were transplanted between January 2002 through December 2004, and who were followed up regularly at Frankfurt Liver Transplantation Center. The mean time since OLT was 3 ± 2 years. Indications for OLT were as depicted in Figure 1. 154 patients received biliary continuity by choledocho-choledochostomy (40 with side-to-side technique and 114 with end to side technique). Eight patients underwent OLT with primary biliary reconstruction by Roux-en-Y choledocho-jejunostomy.

Routine measurements for liver biochemistry (ALT, AST, GGT, AP, and bilirubin) were performed in all patients being followed up post OLT at our centre, and also before and after initial ERC and on subsequent visits thereafter. Rise in values of these liver biochemical tests were further evaluated by doing ultrasonography (USG). All these patients except for those with obvious biliary leak underwent liver biopsy to exclude rejection and or reinfection of graft with hepatitis B or C virus. This was followed by cholangiography which was performed through the T tube, if present at the time of occurrence of biliary complications (as usually it is removed 6 wk post transplantation), ERC or PTC (if ERC had
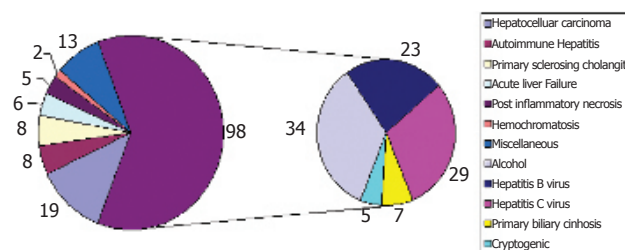
Figure 1 Indications of OLT.

failed or was not technically feasible e.g. patients with cholecystojejeunostomy). ERC was carried out under standard conditions with Propofol and midazolam sedation. All the patients received preprocedure antibiotic prophylaxis 30 min before ERC with intravenous infusion of 500 mg ciprofloxacin. The diagnosis made by ERC, methods of therapeutic intervention, success rates and complications were analyzed. Centre practice of endoscopic treatment for post OLT biliary complications has been biliary sphincterotomy, balloon dilatation, placement of single or multiple (if indicated) plastic biliary endoprosthesis [routinely 10 French (F)]. Balloon dilatation of the stricture was done using 6-8 mm biliary balloon dilator (Maxforce; Microvasive Boston Scientific, Ireland). Fluoroscopic image of duodenoscope was used as the rough guide to assess the diameter of bile duct and the stricture. Dilatation is started with a 6 mm balloon and was upsized until attainment of adequate dilatation which is judged by disappearance of waist of dilating balloon under fluoroscopy control. The pressure used for dilation was 6-8 ATM/BAR for 2 min. Before placing all 10 F biliary endoprosthesis (stent), standard endoscopic biliary sphincterotomy was performed. On individual basis, patient's biliary strictures (anastomotic and non anastomotic e.g. ITBL) were treated sequentially with balloon dilation and/or consecutive stent placement. Those patients with biliary stents underwent elective biliary stent exchange every 10-12 wk for 12 mo. All patients were followed up regularly (every 3 mo) for signs and symptoms suggesting recurrence of biliary tract complications and other relevant issues associated with liver transplant throughout the study period. Success of the therapy performed was primarily assessed by evaluating the serum levels of liver biochemistry panel and secondarily on cholangiography of these biliary lesions before and after endoscopic treatment. PTBD was resorted to in cases of ERC failures (inability to reach the papilla endoscopically), which were performed by the endoscopists themselves.

Statistical analysis

Continuous variables are reported as medians and ranges. Categorical and continuous variables were compared by using the Fisher's exact test and Wilcoxon rank-sum test as appropriate[17]. P values of 0.05 or less were considered as significant.

RESULTS

Out of all patients undergoing OLT, 40 (24.7%) underwent ERC to diagnose and treat biliary complications. The

Table 1 Liver biochemical profile in 40 Patients with biliary complications post OLT depending on time of presentation [Median, (range); mean ± SD]

Liver biochemical parameters	Post OLT / before any biliary complication	On the day of presentation	Ist Follow-up (avg-1 mo) after endoscopic therapy	IInd Follow-up (avg-3 mo) after endoscopic therapy
Bilirubin, mg/dL (< 1.3)	1.3	1.3	0.9	1
	(0.5-13.7)	(0.4-35.0)	(0.3-29.0)	(0.4-26.2)
	2.8 ± 0.6	5.1 ± 1.3	2.8 ± 1.0	3.0 ± 1.0
< 30 d	3.3	4.2	1.2	1.4
1-3 mo	1.1	1	0.7	0.7
4-12 mo	1.1	1.2	0.9	0.7
> 12 mo	0.8	1	1.2	1.1
AST, U/L (< 32)	22.5	48.5	20.5	29.5
	(6.0-378.0)	(8.0-313.0)	(4.0-179.0)	(12.0-142.0)
	54.4 ± 14.1	75.4 ± 12.2	38.8 ± 6.5	42.3 ± 5.7
< 30 d	37	64	18	25
1-3 mo	19	40	18	20
4-12 mo	20	46	20	25
> 12 mo	17	40	34	38
ALT, U/L (< 31)	26.5	90.5	30	24
	(4.0-126.0)	(4.0-891.0)	(4.0-216.0)	(5.0-142.0)
	98.8 ± 22.0	145.7 ± 33.1	46.1 ± 8.0	37.2 ± 5.7
< 30 d	125	102	23	25
1-3 mo	97	89	32	23
4-12 mo	26	97	24	24
> 12 mo	19	58	37	30
GGT, U/L (< 38)	74.5	236	123	117
	(14.0-182.0)	(19.0-1748.0)	(9.0-1697.0)	(9.0-1294.0)
	168.5 ± 34.2	388.1 ± 70.9	282.2 + 63.9	233.4 ± 60.4
< 30 d	152	296	123	54
1-3 mo	82	157	96	38
4-12 mo	45	367	103	63
> 12 mo	39	182	235	266
Alkaline phosphatase, U/L (< 104)	107	242	141	127.5
	(24.0-671.0)	(32.0-1799.0)	(47.0-1435.0)	(46.0-1267.0)
	152.7 ± 21.4	345.1 ± 59.1	270.7 ± 51.3	287.3 ± 53.8
< 30 d	107	240	144	120
1-3 mo	130	100	138	117
4-12 mo	75	244	125	110
> 12 mo	107	263	286	423

median time between OLT and the first suspicion of biliary complications was 10 mo (range-1 to 54 mo).

The relevant liver biochemistry panel along with its time profile is summarized in Table 1. The initially elevated values of bilirubin, AST and ALT might be caused by ongoing reperfusion injury after OLT and/or early viral re-infection of the transplant or rejection (which was ruled out by performing liver biopsy). In patients presenting with biliary complications it was found that GGT values were found to be > 3 times (388.1 ± 70.9 U/mL *vs* 168.5 ± 34.2 U/L, $P = 0.007$) and SAP values > 2 times (345.1 ± 59.1 U/L *vs* 152.7 ± 21.4 U/L, $P = 0.003$) the immediate post OLT values. In the subgroup of patients with an early onset (≤ 3 mo) of biliary complications a normalisation of GGT and SAP at the end of treatment could be achieved. In contrast the group of patients with late onset (> 3 mo) of biliary complications showed no normalisation in SAP and GGT, although sufficient decrease in laboratory values was obvious as compared to these values before treatment. 70 different biliary tract complications were identified in these 40 patients. 20 (50%) patients developed only one biliary complication post OLT whereas in 14 (35%) patients two types of complications were seen and the remaining 6 (15%) patients had more than two complications. The number and type of complications are

Table 2 Type and number of complications in patients post OLT (*n* = 40)

No. of complications	No. of patients	Type of complication
1	20	10 biliary leakage (50%), 7 anastomotic strictures(35%), 1 vanishing bile duct syndrome,ITBL, and abscess (5%) each
2	14	5 anastomotic strictures and biliary leakage (36%), 5 anastomotic strictures and ITBL (36%), 4 other combinations (28%)
> 2	6	2 anastomotic strictures and stones and secondary chonlangitis (33%), 4 other combinations (66%)

shown in Table 2.

Due to our experience and with regard to ERC findings, spectrum of biliary tract complications along with their treatment is classified as shown in Table 3. The most frequently diagnosed complication was isolated anastomotic stricture (IAS) in 24 (40%) of the patients. Upon analysing the complications on time profile, maximum number 22 (31.4%) were seen between 4-12

Table 3 Spectrum of biliary tract complications (n = 70) and their treatment post OLT

Classification	No. of complications n (%)	Type of treatment
Isolated bile leak	17 (24.3)	Stent +/- Stent exchange
		PTBD (2 patients)
		Primary re-operation (3 patients)
Isolated anastomotic stricture	28 (40)	Stent +/- Stent exchange
		Multiple stenting
		Bougienage, Balloon dilatation
		PTBD (2 patients)
		Primary re-operation (1 patients)
Ischemic type biliary lesion (ITBL)	6 (8.6)	Stent +/- Stent exchange
		Bougienage, Balloon dilatation
Miscellaneous	19 (27.1)	Stent +/- Stent exchange
Stones	7 (10)	Multiple stenting
Vanishing bile duct Syndrome	2 (2.8)	Bougienage, Balloon dilatation
		Stone extraction
Ductopenic rejection	1 (1.4)	
Absecss	5 (7.1)	
Secondary cholangitis	2 (2.8)	
Ampullary dyskinesia (SOD)	2 (2.8)	

SOD: sphincter of Oddi; PTBD: percutaneous transhepatic biliary drainage.

Table 4 Type of complications related to time post OLT

Time elapsed between OLD & complication	No. of complication	Type of complication (%)			
		IBL	IAS	ITBL	Misc.
≤ 30 d	20	11 (55.0)	7 (35.0)	1 (5.0)	1 (5.0)
1-3 mo	13	5 (38.5)	4 (30.1)	1 (7.7)	3 (23.0)
4-12 mo	22	1 (4.5)	11 (50.0)	2 (9.0)	8 (36.4)
> 12 mo	15	-	6 (40.0)	2 (13.3)	7 (46.7)
Total	70	17 (24.3)	28 (40.0)	6 (8.6)	19 (27.1)

IBL: isolated bile leak; IAS: isolated anastomotic stricture; ITBL: ischemic type biliary lesion; Misc.: miscellaneous.

Figure 2 Type of complications related to time post OLT.
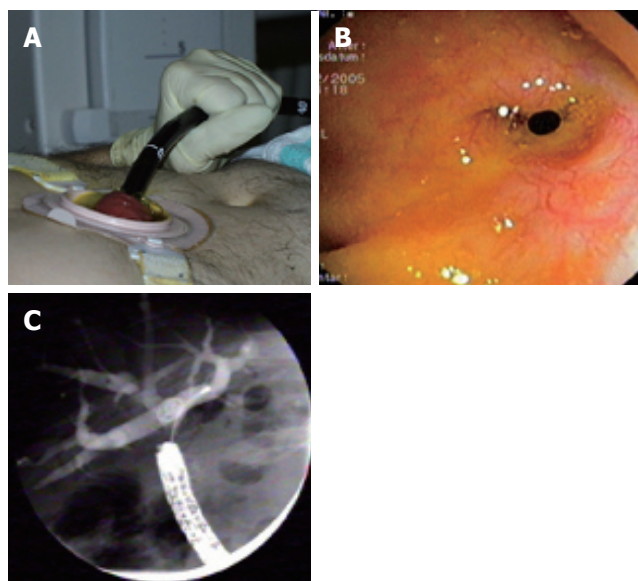
Figure 3 A patient with recurrent intrahepatic stones had a jejunal stoma made so as to reach the bilio-enteric anastomosis endoscopically. **A**: Jejunal stoma; **B**: Endoscopic view of the bilioenteric anastomosis; **C**: Fluoroscopic film after stone extraction.

mo post OLT and amongst them IAS was the commonest one (Table 4 and Figure 2). Out of 6 ITBL patients 2 had hepatic artery thrombosis.

32 patients were treated endoscopically, 4 patients were treated via the percutaneous route while 4 patients had to be referred back for surgery. Nasobiliary drain (NBD) was placed in 4 patients and in 7 patients we had to resort to multiple 10 F biliary stent placements (2 stents).

Out of 32 endoscopically treated patients sustained success was achieved in 26 (81%) of cases and failure in 6 (19%). From this failed group, 3 patients needed to be re-operated upon with surgical revision of anastomosis, one died while waiting for retransplantation (because of intracerebral bleed), two are still under endoscopic treatment and out of these, 1 young patient with severe ITBL had a co-existent development of advanced lung carcinoma and therefore is unfit for retransplantation. To date, none of these patients had undergone retransplantation.

Total numbers of ERC performed were 302. Number of ERCs performed per patient ranged from 2 to 35, in 23 (72%) patients up to 4 ERCs were needed, and in the remaining 9 (28%) patients more than 4 ERCs were

needed to achieve sustained success. There were 5 (1.65%) ERC related complications, 2 patients had mild pancreatitis i.e. abdominal pain with elevation of amylase and lipase (3 times the upper limit of normal) and only required conservative management including intravenous fluid and bowel rest. 3 patients presented with gastrointestinal bleeding from biliary sphincterotomy, out of which 1 required 2 units of blood transfusion whereas other 2 settled with endoscopic injection of epinephrine. There was no procedure related death.

31 (27.1%) out of 114 patients with end to end anastomosis, 4 (10%) of 40 patients with side to side anastomosis and 5 (62.5%) out of 8 with Roux en Y anastomosis developed biliary complications. All the 3 patients with total thrombosis of hepatic artery later developed IAS.

Late bile leaks are quite rare and we encountered only 1 patient presenting with this complication in the 5th month post OLT. Patient developed abscess and secondary cholangitis for which hepaticojejunostomy had to be performed.

7 (10%) patients had choledocholithiasis, most of

which was late complication developing mean 11.1 mo (range 3-26 mo) post OLT. 6 of these had anastomotic stricture distal to the stone which was dilated prior to stone extraction.

1 patient presenting with biliary abscess had bile leak communicating with biliary system so was managed with ERC sphincterotomy and drainage. Another 3 patients with liver abscess underwent CT-guided drainage while the one with late bile leak needed hepaticojejunostomy.

DISCUSSION

Various serum cholestasis indicating liver enzymes have been used to predict early outcomes post OLT[18]. However there are mixed results about their utility in predicting biliary complications. One study reported that these non-invasive blood tests are often not sensitive and accurate enough to detect any biliary complications post OLT[12]. While Hintze, *et al*[19] had shown in 1999 that ITBLs may be diagnosed using alkaline phosphatase levels. Zoepf *et al*[20] found that liver biochemical values do provide a clue towards the existence of post transplant biliary strictures but they further stated that it is of no help in differentiating various lesions like IAS or ITBLs. The drawback of their study design was that they performed biochemical values at the point of presentation of complications and it was not a continuum like in the present study in which these tests were performed immediately after OLT and thereafter regularly on every follow up and also before and after endoscopic interventions. In fact, ours is the first study in which such a detailed and systematic analysis of liver biochemical values have been reported in post OLT patients.

Contrary to the understanding we found GGT and SAP to be quite sensitive in predicting biliary complications on the other hand liver transaminases (AST\ALT) and bilirubin were not of any clinical significance in diagnosing these complications. Also there was significant fall in serum levels of SAP and GGT following endoscopic therapy to about 0.5 and 0.6 times the preprocedure levels respectively but not that of serum bilirubin. This was also reported by Mahajani *et al*[21]. Thus GGT and SAP can be used as early, non-invasive and inexpensive markers for diagnosing biliary complications post OLT and can also be used to assess adequacy of endoscopic treatment in the group of patients presenting early (≤ 3 mo).

Abdominal USG is a non invasive, easily available, portable and an economical modality for imaging. However it has low sensitivity (59%-68%)[20] and specificity; and also it has been shown to be a poor diagnostic technique to detect biliary obstruction post transplant unlike in non transplant population. It has been shown to have a sensitivity of around 50% in diagnosing biliary congestion[22-24]. Various reasons, like acute onset occlusion not allowing sufficient time to allow dilatation of prestenotic biliary duct[22-24], inability to assess biliary dimensions secondary to their filling with epithelial casts[20] etc. have been implicated in this shortcoming of USG.

Although MRI and MRCP are highly sensitive and specific[25] modalities to diagnose biliary complications and have been shown to be the most accurate indirect

techniques to do so[20]. However they have certain drawbacks; expensive, not available at all the centres, will not be practically feasible to repeat during each follow up, contraindicated in certain patient groups (metallic implants, pacemakers etc.) and last but not the least, inability to perform any therapeutic intervention.

One of the studies has reported the occurrence of one third of all biliary complications within a month post OLT[4] which was 28.5% in our study.

IBL has been reported to occur in the range of 1%-25% of patients post OLT[9,26]. It has been arbitrarily subdivided in the literature in to, early-presenting within 1-3 mo and late- beyond 3 mo. IBL was found in 17 (24.3%) of our patients, 11 (64.7%) presented early within 1 mo while 5 (35.3%) manifested within 3 mo post OLT. ERC plus placement of biliary endoprosthesis with or without endoscopic sphincterotomy has been shown to achieve a success rate of over 90%[7,27,28] in treating IBL. We failed to treat bile leakage in 1 patient (success rate 95.5%) while 3 other patients were shown to have complete dissociation and necrosis of common bile duct on ERC, hence were not considered for endoscopic therapy. These patients were managed with wide surgical debridement of necrotic and infected tissue and conversion to bilio-enteric anastomosis, similar to the management done in previous studies also[26,29,30].

Placement of T tube during OLT is still a controversial issue. There are conflicting results about it in 3 different studies. Two of them demonstrated nearly double the rate of complications in the T tube group as against those without it (33% *vs* 15.5%)[31,32]. However the third one showed that T tube prevented development of anastomotic strictures, 3.3% *vs* 20% in the group with and without T tube respectively[33]. Pending this issue we still use a T tube in all of our patients undergoing OLT.

IAS are the most common late complications of OLT and usually follow IBL in chronology[4,28]. Biliary strictures are usually seen in about 3-14% of all OLT and could constitute up to 40% of total biliary complications[4,9,34,35]. It constituted 28 (40%) of biliary complications in our patient group and half of these presented between 4-12 mo post OLT. Use of ERC for treating anastomotic stricture in older studies had been disappointing[36,37], however newer studies have reported the efficacy of endoscopic and percutaneous approaches in managing these complications[5,36,38-40]. 2 failures of endoscopic treatment for anastomotic stricture in the present study had to undergo hepaticojejunostomy after 7 and 8 mo of OLT. Our success rate of 81% lies between 70%-100% as has been reported in previous studies[21,39,41].

The severity and number of these anastomotic strictures will increase in coming times as more and more complex biliary anastomoses are being performed (living donor, split liver transplant, etc)[42-45], mainly because of widening gap of demand and supply of the organ. This would pose tougher challenges to endoscopists in future. Though there are reports of placement of self expandable metal stents[46,47] we did not place it in any of our patient as it is a controversial therapy in present scenario. It may lead to difficulties in performing surgeries later, if required and also usually undergoes stent blockages which are difficult

to manage. Recently one of the studies has reported placement of T-tube drainage for biliary strictures in patients with failed endoscopic or percutaneous therapy[14].

Though the exact cause for ITBL is not known but has been postulated to be secondary to microcirculatory problems like ischemia-reperfusion injury. It was a late complication occurring after a mean time period of 33.8 mo (range-1 to 95 mo) post OLT and was observed in 6 (8.6%) which is comparable to the quoted figure of 2.5-19% in the literature[19,48]. They have been found difficult to treat endoscopically or by PTC[26,29] so was the case in our experience. Out of 6 patients with ITBL, 4 (66%) could be treated successfully, 1 had to undergo surgery while another one had an interesting clinical course. After 5 ERC with balloon dilatation and biliary stent placement with only partial relief, the patient underwent hepaticojejunostomy. This patient had excessively lithogenic bile and presented within few months with intrahepatic stones and secondary cholangitis. To prevent repeated surgeries for the same, a jejunal stoma (Figure 3) was created so as to reach the biliary-enteric anastomosis easily using the endoscope. Presently the patient gets routine endoscopy through the stoma for removal of biliary stones and sludge and for thorough flushing of the biliary tree every 3-4 mo and thus is saved from retransplantation and has undergone 74 endoscopic procedures till date in last 14 years.

Two (1.4 %) of all patients undergoing OLT manifested with significant dilatation of the bile duct, elevated liver biochemistry but no evidence of obvious obstruction on cholangiography which responded to endoscopic sphincterotomy. This was most probably papillary dyskinesia or sphincter of Oddi dysfunction. It has been reported to occur in 0-7% of patients[12,49,50]. We did not perform biliary manometry in any of these patients to prove it. 1 patient had partial biliary cast.

In conclusion, biliary complications still remain an important problem in liver transplant recipients. A multidisciplinary approach is required to manage them. Serum GGT and SAP should be closely monitored and can be used as an early, non invasive and cheap markers for diagnosing post OLT biliary complications. They can also be of great help during follow up after endoscopic therapy and correlate with adequacy of therapy in patients presenting with early onset (< 3 mo) biliary complications post OLT. Endoscopic therapy is usually effective in managing majority of these complications but may require multiple procedures especially to treat strictures. Surgical intervention is required only in a few selected cases. There is a definite need of prospective multicenter studies to further evaluate the role of liver biochemical markers in predicting biliary complications post OLT.

REFERENCES

1   Burroughs A, McNamara D. Liver disease in Europe. *Aliment Pharmacol Ther* 2003; **18** Suppl 3: 54-59
2   Catalano MF, Van Dam J, Sivak MV Jr. Endoscopic retrograde cholangiopancreatography in the orthotopic liver transplant patient. *Endoscopy* 1995; **27**: 584-588
3   Gholson CF, Zibari G, McDonald JC. Endoscopic diagnosis and management of biliary complications following orthotopic liver transplantation. *Dig Dis Sci* 1996; **41**: 1045-1053
4   Greif F, Bronsther OL, Van Thiel DH, Casavilla A, Iwatsuki S, Tzakis A, Todo S, Fung JJ, Starzl TE. The incidence, timing, and management of biliary tract complications after orthotopic liver transplantation. *Ann Surg* 1994; **219**: 40-45
5   Pfau PR, Kochman ML, Lewis JD, Long WB, Lucey MR, Olthoff K, Shaked A, Ginsberg GG. Endoscopic management of postoperative biliary complications in orthotopic liver transplantation. *Gastrointest Endosc* 2000; **52**: 55-63
6   Sherman S, Jamidar P, Shaked A, Kendall BJ, Goldstein LI, Busuttil RW. Biliary tract complications after orthotopic liver transplantation. Endoscopic approach to diagnosis and therapy. *Transplantation* 1995; **60**: 467-470
7   Stratta RJ, Wood RP, Langnas AN, Hollins RR, Bruder KJ, Donovan JP, Burnett DA, Lieberman RP, Lund GB, Pillen TJ. Diagnosis and treatment of biliary tract complications after orthotopic liver transplantation. *Surgery* 1989; **106**: 675-683; discussion 683-684
8   Theilmann L, Kuppers B, Kadmon M, Roeren T, Notheisen H, Stiehl A, Otto G. Biliary tract strictures after orthotopic liver transplantation: diagnosis and management. *Endoscopy* 1994; **26**: 517-522
9   Tung BY, Kimmey MB. Biliary complications of orthotopic liver transplantation. *Dig Dis* 1999; **17**: 133-144
10   Colonna JO 2nd, Shaked A, Gomes AS, Colquhoun SD, Jurim O, McDiarmid SV, Millis JM, Goldstein LI, Busuttil RW. Biliary strictures complicating liver transplantation. Incidence, pathogenesis, management, and outcome. *Ann Surg* 1992; **216**: 344-350; discussion 350-352
11   Abt P, Crawford M, Desai N, Markmann J, Olthoff K, Shaked A. Liver transplantation from controlled non-heart-beating donors: an increased incidence of biliary complications. *Transplantation* 2003; **75**: 1659-1663
12   Thuluvath PJ, Pfau PR, Kimmey MB, Ginsberg GG. Biliary complications after liver transplantation: the role of endoscopy. *Endoscopy* 2005; **37**: 857-863
13   Shah SR, Dooley J, Agarwal R, Patch D, Burroughs AK, Rolles K, Davidson BR. Routine endoscopic retrograde cholangiography in the detection of early biliary complications after liver transplantation. *Liver Transpl* 2002; **8**: 491-494
14   Hashimoto M, Sugawara Y, Tamura S, Kishi Y, Matsui Y, Kaneko J, Makuuchi M. T-tube drainage for biliary stenosis after living donor liver transplantation. *Transplantation* 2006; **81**: 293-295
15   Sossenheimer M, Slivka A, Carr-Locke D. Management of extrahepatic biliary disease after orthotopic liver transplantation: review of the literature and results of a multicenter survey. *Endoscopy* 1996; **28**: 565-571
16   Wolfsen HC, Porayko MK, Hughes RH, Gostout CJ, Krom RA, Wiesner RH. Role of endoscopic retrograde cholangiopancreatography after orthotopic liver transplantation. *Am J Gastroenterol* 1992; **87**: 955-960
17   Armitage P. Statistical methods in medical research. Oxford: Blackwell Scientific, 1971
18   Ben-Ari Z, Weiss-Schmilovitz H, Sulkes J, Brown M, Bar-Nathan N, Shaharabani E, Yussim A, Shapira Z, Tur-Kaspa R, Mor E. Serum cholestasis markers as predictors of early outcome after liver transplantation. *Clin Transplant* 2004; **18**: 130-136
19   Hintze RE, Abou-Rebyeh H, Adler A, Veltzke W, Langrehr J, Wiedenmann B, Neuhaus P. Endoscopic therapy of ischemia-type biliary lesions in patients following orthotopic liver transplantation. *Z Gastroenterol* 1999; **37**: 13-20
20   Zoepf T, Maldonado-Lopez EJ, Hilgard P, Dechene A, Malago M, Broelsch CE, Schlaak J, Gerken G. Diagnosis of biliary strictures after liver transplantation: which is the best tool? *World J Gastroenterol* 2005; **11**: 2945-2948
21   Mahajani RV, Cotler SJ, Uzer MF. Efficacy of endoscopic management of anastomotic biliary strictures after hepatic transplantation. *Endoscopy* 2000; **32**: 943-949
22   Zemel G, Zajko AB, Skolnick ML, Bron KM, Campbell WL. The role of sonography and transhepatic cholangiography in the diagnosis of biliary complications after liver transplantation. *AJR Am J Roentgenol* 1988; **151**: 943-946

23   **Shaw AS**, Ryan SM, Beese RC, Sidhu PS. Ultrasound of non-vascular complications in the post liver transplant patient. *Clin Radiol* 2003; **58**: 672-680

24   **Kok T**, Van der Sluis A, Klein JP, Van der Jagt EJ, Peeters PM, Slooff MJ, Bijleveld CM, Haagsma EB. Ultrasound and cholangiography for the diagnosis of biliary complications after orthotopic liver transplantation: a comparative study. *J Clin Ultrasound* 1996; **24**: 103-115

25   **Boraschi P**, Braccini G, Gigoni R, Sartoni G, Neri E, Filipponi F, Mosca F, Bartolozzi C. Detection of biliary complications after orthotopic liver transplantation with MR cholangiography. *Magn Reson Imaging* 2001; **19**: 1097-1105

26   **Jagannath S**, Kalloo AN. Biliary Complications After Liver Transplantation. *Curr Treat Options Gastroenterol* 2002; **5**: 101-112

27   **Moser MA**, Wall WJ. Management of biliary problems after liver transplantation. *Liver Transpl* 2001; **7**: S46-S52

28   **Porayko MK**, Kondo M, Steers JL. Liver transplantation: late complications of the biliary tract and their management. *Semin Liver Dis* 1995; **15**: 139-155

29   **Pascher A**, Neuhaus P. Bile duct complications after liver transplantation. *Transpl Int* 2005; **18**: 627-642

30   **Verran DJ**, Asfar SK, Ghent CN, Grant DR, Wall WJ. Biliary reconstruction without T tubes or stents in liver transplantation: report of 502 consecutive cases. *Liver Transpl Surg* 1997; **3**: 365-373

31   **Scatton O**, Meunier B, Cherqui D, Boillot O, Sauvanet A, Boudjema K, Launois B, Fagniez PL, Belghiti J, Wolff P, Houssin D, Soubrane O. Randomized trial of choledochocholedochostomy with or without a T tube in orthotopic liver transplantation. *Ann Surg* 2001; **233**: 432-437

32   **Shimoda M**, Saab S, Morrisey M, Ghobrial RM, Farmer DG, Chen P, Han SH, Bedford RA, Goldstein LI, Martin P, Busuttil RW. A cost-effectiveness analysis of biliary anastomosis with or without T-tube after orthotopic liver transplantation. *Am J Transplant* 2001; **1**: 157-161

33   **Vougas V**, Rela M, Gane E, Muiesan P, Melendez HV, Williams R, Heaton ND. A prospective randomised trial of bile duct reconstruction at liver transplantation: T tube or no T tube? *Transpl Int* 1996; **9**: 392-395

34   **Klein AS**, Savader S, Burdick JF, Fair J, Mitchell M, Colombani P, Perler B, Osterman F, Williams GM. Reduction of morbidity and mortality from biliary complications after liver transplantation. *Hepatology* 1991; **14**: 818-823

35   **Vallera RA**, Cotton PB, Clavien PA. Biliary reconstruction for liver transplantation and management of biliary complications: overview and survey of current practices in the United States. *Liver Transpl Surg* 1995; **1**: 143-152

36   **Mosca S**, Militerno G, Guardascione MA, Amitrano L, Picciotto FP, Cuomo O. Late biliary tract complications after orthotopic liver transplantation: diagnostic and therapeutic role of endoscopic retrograde cholangiopancreatography. *J Gastroenterol Hepatol* 2000; **15**: 654-660

37   **Testa G**, Malago M, Broelseh CE. Complications of biliary tract in liver transplantation. *World J Surg* 2001; **25**: 1296-1299

38   **Bourgeois N**, Deviere J, Yeaton P, Bourgeois F, Adler M, Van De Stadt J, Gelin M, Cremer M. Diagnostic and therapeutic endoscopic retrograde cholangiography after liver transplantation. *Gastrointest Endosc* 1995; **42**: 527-534

39   **Rossi AF**, Grosso C, Zanasi G, Gambitta P, Bini M, De Carlis L, Rondinara G, Arcidiacono R. Long-term efficacy of endoscopic stenting in patients with stricture of the biliary anastomosis after orthotopic liver transplantation. *Endoscopy* 1998; **30**: 360-366

40   **Rizk RS**, McVicar JP, Emond MJ, Rohrmann CA Jr, Kowdley KV, Perkins J, Carithers RL Jr, Kimmey MB. Endoscopic management of biliary strictures in liver transplant recipients: effect on patient and graft survival. *Gastrointest Endosc* 1998; **47**: 128-135

41   **Rerknimitr R**, Sherman S, Fogel EL, Kalayci C, Lumeng L, Chalasani N, Kwo P, Lehman GA. Biliary tract complications after orthotopic liver transplantation with choledochocholedochostomy anastomosis: endoscopic findings and results of therapy. *Gastrointest Endosc* 2002; **55**: 224-231

42   **Sugawara Y**, Makuuchi M, Sano K, Ohkubo T, Kaneko J, Takayama T. Duct-to-duct biliary reconstruction in living-related liver transplantation. *Transplantation* 2002; **73**: 1348-1350

43   **Settmacher U**, Steinmuller TH, Schmidt SC, Heise M, Pascher A, Theruvath T, Hintze R, Neuhaus P. Technique of bile duct reconstruction and management of biliary complications in right lobe living donor liver transplantation. *Clin Transplant* 2003; **17**: 37-42

44   **Testa G**, Malago M, Valentin-Gamazo C, Lindell G, Broelsch CE. Biliary anastomosis in living related liver transplantation using the right liver lobe: techniques and complications. *Liver Transpl* 2000; **6**: 710-714

45   **Hisatsune H**, Yazumi S, Egawa H, Asada M, Hasegawa K, Kodama Y, Okazaki K, Itoh K, Takakuwa H, Tanaka K, Chiba T. Endoscopic management of biliary strictures after duct-to-duct biliary reconstruction in right-lobe living-donor liver transplantation. *Transplantation* 2003; **76**: 810-815

46   **Lake JR**. Long-term management of biliary tract complications. *Liver Transpl Surg* 1995; **1**: 45-54

47   **Petersen BD**, Maxfield SR, Ivancev K, Uchida BT, Rabkin JM, Rosch J. Biliary strictures in hepatic transplantation: treatment with self-expanding Z stents. *J Vasc Interv Radiol* 1996; **7**: 221-228

48   **Sanchez-Urdazpal L**, Gores GJ, Ward EM, Maus TP, Buckel EG, Steers JL, Wiesner RH, Krom RA. Diagnostic features and clinical outcome of ischemic-type biliary complications after liver transplantation. *Hepatology* 1993; **17**: 605-609

49   **Douzdjian V**, Abecassis MM, Johlin FC. Sphincter of Oddi dysfunction following liver transplantation. Screening by bedside manometry and definitive manometric evaluation. *Dig Dis Sci* 1994; **39**: 253-256

50   **Richards RD**, Yeaton P, Shaffer HA Jr, Pambianco DJ, Pruett TL, Stevenson WC, Mittal RK, McCallum RW. Human sphincter of Oddi motility and cholecystokinin response following liver transplantation. *Dig Dis Sci* 1993; **38**: 462-468

CLINICAL RESEARCH

Anti-inflammatory properties of the short-chain fatty acids acetate and propionate: A study with relevance to inflammatory bowel disease

Sofia Tedelind, Fredrik Westberg, Martin Kjerrulf, Alexander Vidal

Sofia Tedelind, Fredrik Westberg, Martin Kjerrulf, Alexander Vidal, Department of Molecular Pharmacology, AstraZeneca R&D, Mölndal, Sweden
Correspondence to: Alexander Vidal, PhD, Department of Molecular Pharmacology, AstraZeneca R&D Mölndal, SE-431 83 Mölndal, Sweden. alexander.vidal@astrazeneca.com
Telephone: +46-31-7762926 Fax: +46-31-7763761
Received: 2007-02-09   Accepted: 2007-03-15

Abstract

AIM: To compare the anti-inflammatory properties of butyrate with two other SCFAs, namely acetate and propionate, which have less well-documented effects on inflammation.

METHODS: The effect of SCFAs on cytokine release from human neutrophils was studied with ELISA. SCFA-dependent modulation of NF-κB reporter activity was assessed in the human colon adenocarcinoma cell line, Colo320DM. Finally, the effect of SCFAs on gene expression and cytokine release, measured with RT-PCR and ELISA, respectively, was studied in mouse colon organ cultures established from colitic mice.

RESULTS: Acetate, propionate and butyrate at 30 mmol/L decreased LPS-stimulated TNFα release from neutrophils, without affecting IL-8 protein release. All SCFAs dose dependently inhibited NF-κB reporter activity in Colo320DM cells. Propionate dose-dependently suppressed IL-6 mRNA and protein release from colon organ cultures and comparative studies revealed that propionate and butyrate at 30 mmol/L caused a strong inhibition of immune-related gene expression, whereas acetate was less effective. A similar inhibition was achieved with the proteasome inhibitor MG-132, but not the p38 MAPK inhibitor SB203580. All SCFAs decreased IL-6 protein release from organ cultures.

CONCLUSION: In the present study propionate and butyrate were equipotent, whereas acetate was less effective, at suppressing NF-κB reporter activity, immune-related gene expression and cytokine release *in vitro*. Our findings suggest that propionate and acetate, in addition to butyrate, could be useful in the treatment of inflammatory disorders, including IBD.

INTRODUCTION

Inflammatory bowel diseases (IBD), Crohn's disease and ulcerative colitis, are chronic inflammatory disorders of the gastrointestinal tract which withstand strong influence from both genetic and environmental factors[1]. A dysfunctional mucosal barrier combined with an aberrant mucosal tolerance to pathogens and/or components of the endogenous intestinal flora, is suggested to be an important cause of IBD.

The chronic inflammation that is a hallmark of IBD results from the recruitment and activation of immune cells from the circulation. These in turn release pro-inflammatory cytokines locally in the submucosa, including members of the interleukin (IL) family and tumour necrosis factor-alpha (TNFα), which play a key role in the pathogenesis of IBD[2,3]. Cytokine signalling leads to the activation of two major inflammatory signalling pathways, the nuclear factor kappa B (NF-κB) and mitogen activated protein kinase (MAPK) pathways, which both have been found to be active in mucosal biopsy specimens from patients with IBD[4,5]. As expected, these signalling pathways are important down-stream targets for current therapies including steroids and immunomodulating drugs such as azathioprine and 6-mercaptopurine. However, these current therapies are also associated with side effects and accordingly, there is a great need for alternative remedies.

Dietary fibres are complex carbohydrates, which serve as substrates for anaerobic fermentation by bacteria in the colon. Fermentation gives rise to three major luminal Short-Chain Fatty Acids (SCFAs): acetate, propionate, and butyrate[6]. SCFAs readily reach millimolar concentrations in the colonic lumen[7,8] from which they are absorbed by

passive and active transport over the epithelium[7]. Butyrate is considered to be the preferred source of energy for colonocytes[9], and is to a major extent metabolized by these cells[7,10,11]. Butyrate is, by far, the most extensively studied SCFA, and its anti-inflammatory capacity is well documented both *in vitro* and *in vivo*. Importantly, several clinical studies demonstrate beneficial effects of butyrate in IBD[12-14]. The exact mechanism of action of butyrate on inflammation is only partially understood. Recently, several reports have been published describing inhibitory effects of butyrate on NF-κB, one of the key transcription factors regulating genes implicated in innate immunity, cell cycle control and apoptosis[15,16].

The production of acetate, propionate and butyrate occurs in the molar ratio of approximately 60: 20: 20[17]. Thus, acetate can be considered the predominant SCFA in the colon. However, with regard to inflammation, little is known about acetate and propionate relative to the well-established anti-inflammatory properties of butyrate. The purpose of this study was therefore to investigate and compare the *in vitro* anti-inflammatory properties of SCFAs in model systems relevant to IBD.

MATERIALS AND METHODS

Cell culture

Human neutrophils were isolated from whole blood of healthy donors through density gradient separation with Polymorphprep™ according to the manufacturer's instructions (AXIS-SHIELD PoC AS, Oslo, Norway). Briefly, fresh citrate-anticoagulated blood was layered over an equal volume of Polymorphprep™ and centrifuged at $500 \times g$ for 30 min. The granulocyte fraction was selected and washed with PBS (Sigma) followed by removal of erythrocytes through hypotonic lysis. Immunophenotyping of the isolated cells was done with a FACSCalibur flow cytometer (BectonDickinson, Erembodegem, Belgium). Greater than 95% of the cells were identified as neutrophils, confirmed by side and forward scatter diagrams; CD66b positivity (Acris, Hiddenhausen, Germany) and CD14 negativity (Pharmingen, San Diego, CA, USA). The neutrophils were cultured in RPMI 1640 (Invitrogen) supplemented with 0.5% fetal bovine serum (FBS; Nordic Biolabs AB) and 1% penicillin/streptomycin (PEST; Invitrogen) in 12-well plates at 37°C in 5% CO2. Culture viability was 98.1% determined by a Cedex HiRes Analyzer (Innovatis AG, Bielefeld, Germany).

Colo320DM cells (American Type Culture Collection, Rockville, MD, USA) were cultured in RPMI 1640 supplemented with 10% FBS and 1% PEST.

Transfection and luciferase assay

COLO320DM cells, seeded 24 h prior to transfection, were transiently transfected using FuGENE6 transfection agent (Roche) and 0.5 μg/mL of a luciferase reporter vector containing three tandem copies of the NF-κB binding consensus sequence fused to firefly luciferase. The cells were co-transfected with 25 ng/mL *Renilla* luciferase-positive control vector (pRL-SV40: Promega) to normalize for transfection efficiency. Five hours post-transfection the cells were seeded into a 96 well plate (white/clear bottom,

Wallac) at a density of 6×10^4 cells/well in assay medium (phenol-free RPMI 1640, 10% FBS dextran/charcoal stripped serum and 1% L-Glutamine) containing 10 ng/mL TNFα with or without 1 nmol/L to 100 mmol/L acetate, propionate or butyrate. After 24 h of treatment the cells were lysed and the luciferase activity was measured using the Dual-Luciferase Reporter Assay Systems reagent kit (Promega) in a Viktor luminometer plate reader (Wallac). The firefly luciferase activity was divided by *Renilla* luciferase activity and presented as per cent inhibition with TNFα treatment alone representing 0% inhibition and assay medium without TNFα as 100% inhibition.

Animals

Female C57BL/6J mice (Harlan Nederlands B.V.) at 7-9 wk of age were used. 5% (w/v) dextran sulphate sodium (DSS, T&D consulting, Uppsala, Sweden) was given in the drinking water for five days in order to induce colonic inflammation. Water was given one day prior to ending the experiment.

All mice were kept under standard conditions of temperature and light, and were fed with standard laboratory chow and water *ad libitum*. All experiments were approved by the Animal Ethics Committee at Gothenburg University.

Organ culture

Mice were sacrificed and colons were collected and placed in ice-cold Dulbecco's modified Eagle's medium (DMEM). Transverse 1 mm sections were cut longitudinally and placed in 12-well Transwell™ plates (Costar), containing medium with 1% PEST and compounds. Organ cultures were maintained at 37°C in 5% CO2. After six hours the medium was replaced with fresh medium containing compounds. Cultures were then further incubated 18 h, after which medium was collected and frozen until further processing. Tissue was placed in Collection microtubes (Qiagen) containing stainless steel beads (Qiagen) followed by homogenisation in RLT lysis buffer (RNeasy Kit, Qiagen) with a TissueLyser (Qiagen) at 30 Hz for 10 min. Total RNA was isolated according to the manufacturer's instructions and cDNA was prepared from purified total RNA with the iScript cDNA synthesis kit (Bio-Rad).

Real-time PCR arrays

TaqMan™ Low Density mouse immune-arrays (Micro Fluidic Cards, Applied Biosystems) were used to assess the regulation of immune-related genes in organ cultures established from non-inflamed and colitic mouse colon. Samples were assayed in quadruplicate and the expression levels were determined with an ABI Prism 7900HT Sequence Detector (Applied Biosystems). Data was normalized to GAPDH mRNA levels and subsequently expressed as the fold change relative to non-inflamed or colitic vehicle controls.

ELISA

The levels of TNFα, IL-8 or IL-6 in conditioned medium from neutrophil or organ cultures were determined with commercial ELISA kits (human TNFα, BD OptEIA, BD Biosciences; human IL-8, QuantiGlo ELISA, R&D
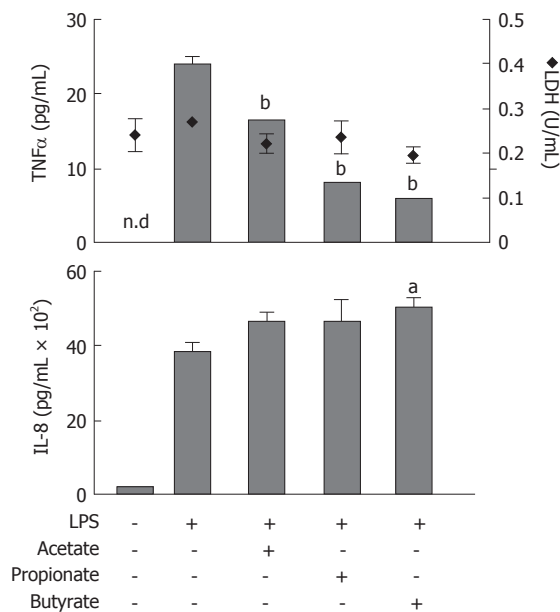
Figure 1 Effects of Short-Chain Fatty Acids on LPS-stimulated TNFα and IL-8 release, and lactate dehydrogenase (LDH) activity in conditioned medium from neutrophil cultures. Cells were exposed to LPS (1 μg/mL) concomitant with acetate, propionate or butyrate (all 30 mmol/L) for 6 h followed by analysis of TNFα (upper panel, bars) and IL-8 (lower panel) protein levels and LDH activity (upper panel, diamonds). n.d: not detectable. mean ± SEM (n = 3), [a]P < 0.05, [b]P < 0.01.

systems; mouse IL-6, Quantikine ELISA, R&D systems), according to the manufacturer's instructions.

Lactate dehydrogenase activity

Lactate dehydrogenase (LDH) activity was determined with a commercial kit (Cytotoxicity Detection Kit, Roche), according to the manufacturer's instructions.

Statistical analysis

Values are expressed as mean ± SEM and tested for statistical significance using Student´s t-test.

RESULTS

SCFAs suppress LPS-induced release of TNFα from neutrophils

Protein levels of TNFα and IL-8, released from lipopolysaccharide (LPS)-stimulated (1 μg/mL) human neutrophils, were determined with ELISA (Figure 1). Acetate, propionate and butyrate (all 30 mmol/L) decreased LPS-stimulated TNFα release to the culture medium from 24 ± 1 pg/mL to 16 ± 0.1 pg/mL (P < 0.01), 8 ± 0.2 pg/mL (P < 0.01) and 6 ± 0.2 (P < 0.01), respectively (Figure 1; upper panel, bars). The LPS-stimulated increase in IL-8 protein levels from 190 ± 21 pg/mL to 3753 ± 152 pg/mL was not affected by SCFAs (Figure 1; lower panel). Furthermore, SCFAs did not have an effect on LDH activity (Figure 1; upper panel, diamonds).

SCFA-induced inhibition of the NF-κB pathway in Colo320DM cells

Colo320DM cells were transiently transfected with a NF-
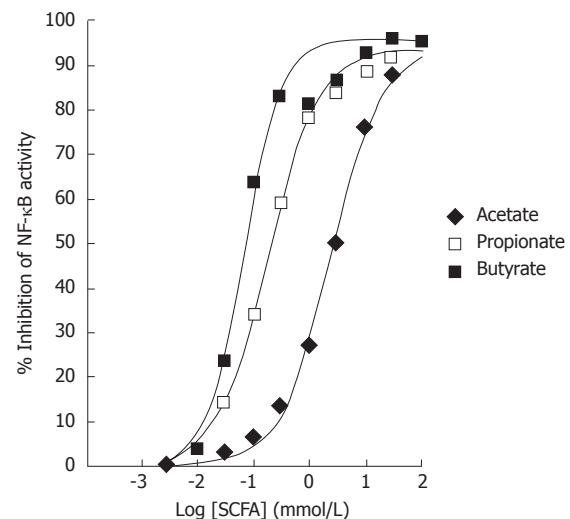
Figure 2 Effects of Short-Chain Fatty Acids on TNFα-induced NF-κB reporter activity in Colo320DM cells. Cells were exposed to TNFα (10 ng/mL) along with acetate (diamonds), propionate (open squares) or butyrate (closed squares) for 24 h. Data is presented as the mean % inhibition of NF-κB activity after normalization to *Renilla* Luciferase (n = 3).

κB luciferase reporter. TNFα at 10 ng/mL was used to induce NF-κB activity in the presence of varying concentrations of SCFAs. All SCFAs dose dependently inhibited the TNFα-stimulated NF-κB luciferase activity in Colo320DM cells (Figure 2). The EC50 values for inhibition of NF-κB were as follows: acetate 2.4 mmol/L (diamonds), propionate 120 μmol/L (open squares) and butyrate 64 μmol/L (filled squares). Data points represent the mean of triplicate values.

Anti-inflammatory effects of propionate in colon organ cultures

In order to study the anti-inflammatory properties of SCFAs in the context of intestinal inflammation, we established an organ culture protocol where pieces of colitic mouse colon were cultured *in vitro* in the absence or presence of SCFAs. Exposure of organ cultures to 0.3-30 mmol/L propionate caused a dose dependent decrease in IL-6 mRNA levels from 7.5 ± 1.3 fold (relative to non-inflamed colon) to 1.7 ± 0.2 fold (P < 0.01) at the highest propionate concentration (30 mmol/L) (Figure 3; upper panel). This was paralleled by a decrease in IL-6 protein levels in the culture medium from 253 ± 65 pg/mL per mg to 75 ± 31 pg/mL per mg (30 mmol/L propionate; P < 0.05) (Figure 3; lower panel, bars). Consistent with the results obtained in the previous cell experiments, the effect of propionate was not a result of SCFA-induced cytotoxicity as determined by LDH activity in the culture medium (Figure 3; lower panel, diamonds).

SCFAs inhibit immune-related gene expression in colon organ cultures

Quantitative Real-time PCR was used to determine the transcriptional regulation of immune-related genes in colon organ cultures (Figure 4). As shown in Figure 4A, IL-1α, IL-6 and inducible nitric oxide synthetase (iNOS) mRNA levels were strongly induced in colon organ cultures established from mice treated with 5%
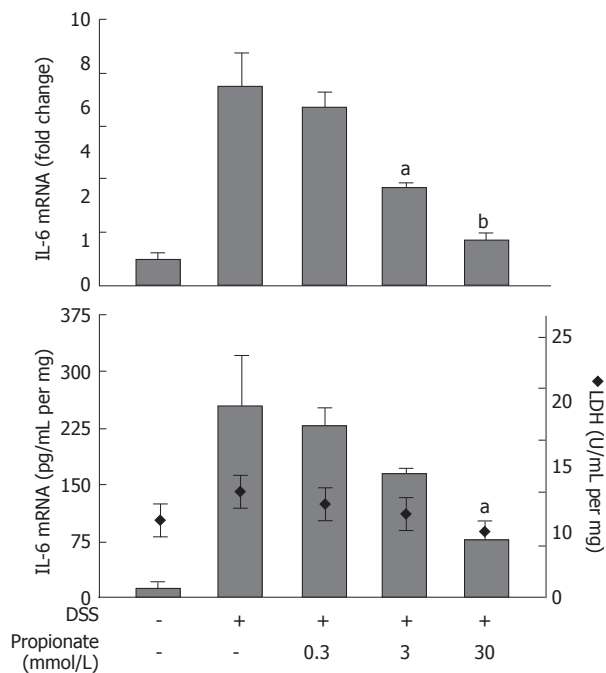
Figure 3 Dose-dependent effects of propionate in organ cultures from inflamed mouse colon. Dextran sulphate sodium (DSS) was used to induce colonic inflammation. Upper panel: IL-6 mRNA expression (data is shown as changes relative to the expression value obtained in non-inflamed organ cultures). Lower panel: IL-6 protein levels (bars) and lactate dehydrogenase (LDH) activity (diamonds) in culture medium. Organ cultures were exposed to various concentrations of propionate for 24 h. Mean ± SEM (n = 4), [a]P < 0.05, [b]P < 0.01.

dextran sulphate sodium, compared to non-colitic organ culture. This induction was heavily suppressed by SCFA treatment (all at 30 mmol/L). In order to compare effects of compounds with known anti-inflammatory activity to the immune suppressive effects of SCFAs, the expression levels of twelve selected genes (increased > 3-fold in colitis vs. non-inflamed colon) were compiled as a heat map representation showing the effect of treatments relative to control levels (Figure 4B). MG-132 (a proteasome and NF-κB inhibitor) at 10 μmol/L, acetate, propionate and butyrate (all at 30 mmol/L) potently decreased the mRNA levels of selected gene transcripts. In addition, MG-132 was clearly more potent than SB203580 (a p38 MAPK inhibitor) at suppressing transcription of the selected genes at the same dose (Figure 4B).

SCFAs suppress IL-6 release from colon organ cultures

The effects of SCFAs on IL-6 protein release from colon organ cultures were studied (Figure 5). Acetate, propionate and butyrate (all 30 mmol/L) decreased the IL-6 levels in conditioned medium from colon organ cultures from 507 ± 84 pg/mL per mg to 169 ± 16 pg/mL per mg (P < 0.01), 39 ± 14 pg/mL per mg (P < 0.01) and 87 ± 11 pg/mL per mg (P < 0.01), respectively (Figure 5; bars). SCFA-treatment did not cause any significant change in LDH activity (Figure 5; diamonds).

DISCUSSION

SCFAs represent a major constituent of the luminal contents of the colon. Among SCFAs butyrate is believed
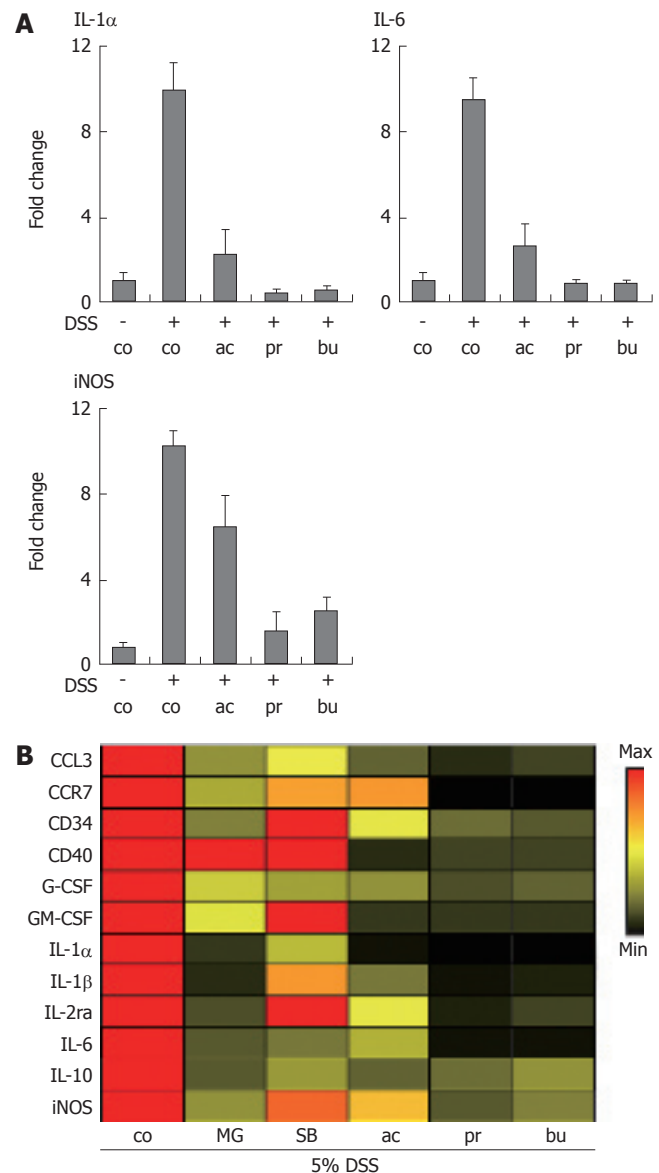
Figure 4 Transcriptional profiling of gene expression in Short-Chain Fatty Acid-treated organ cultures. Dextran sulphate sodium (DSS) was used to induce colonic inflammation. (**A**) Organ cultures were incubated with acetate, propionate or butyrate (all 30 mmol/L) for 24 h followed by analysis of IL-1α, IL-6 and iNOS mRNA levels. Data was normalized to GAPDH mRNA levels and presented as fold change relative to control levels. Mean ± SEM (n = 4). (**B**) Heat map representation of gene expression changes induced by MG-132, SB203580 (both 10 μmol/L); acetate, propionate and butyrate (all 30 mmol/L). Data was normalized to GAPDH and expressed as the ratio between treatment and control. control (co), acetate (ac), propionate (pr), butyrate (bu), MG-132 (MG), SB203580 (SB).

to play an important role for epithelial homeostasis[18]. Solutions containing butyrate[12-14] or mixtures of SCFAs[19-23] have been used for treatment of active IBD. Unfortunately these studies do not discriminate between actions of individual SCFAs, with the exception of butyrate.

To our knowledge the present study is the first aimed at comparing the effects of acetate, propionate and butyrate on markers of inflammation (i.e., NF-κB activity and cytokine production). The findings of the present study substantiate previous findings, relating to butyrate and its anti-inflammatory properties. For the first time it is also clearly demonstrated that acetate and propionate
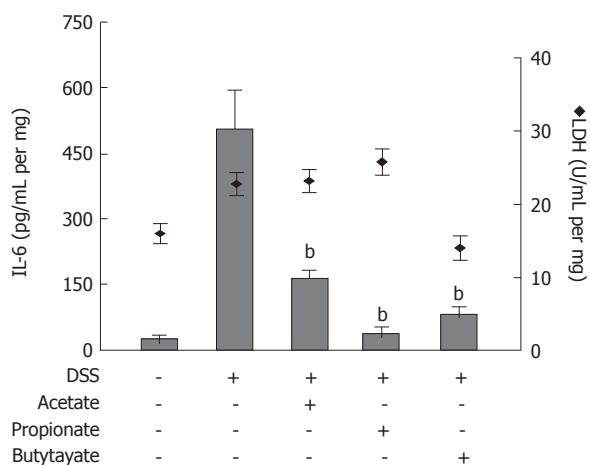
Figure 5 Effects of Short-Chain Fatty Acids on IL-6 release and lactate dehydrogenase (LDH) activity in organ cultures from inflamed mouse colon. Dextran sulphate sodium (DSS) was used to induce colonic inflammation. Organ cultures were exposed to acetate, propionate or butyrate (all 30 mmol/L) for 24 h followed by analysis of IL-6 level (bars) and LDH activity (diamonds) in culture medium. Mean ± SEM ($n = 4$), [b]$P < 0.01$.

ameliorate an ongoing inflammatory response at the cellular level and thus acetate and propionate may also contribute to the anti-inflammatory properties of SCFA mixtures *in vivo*.

Because leukocytes are considered the primary effector cells in IBD, the properties of acetate, propionate and butyrate, were first investigated in human blood-derived neutrophils. Several studies in the past have analysed the effects of SCFAs on neutrophils[24]. Propionic acid has been shown to stimulate superoxide generation in human neutrophils[25] and recently it has been demonstrated that propionate also stimulates neutrophil chemotaxis[26]. However, it is not clear how SCFAs influence the response to inflammatory mediators, such as LPS in neutrophils. We demonstrate that SCFAs strongly inhibit the LPS-stimulated release of TNFα in human neutrophils. Interestingly, our findings also show that SCFAs do not affect LPS-induced release of IL-8, indicating that LPS stimulates TNFα and IL-8 release by separate mechanisms in neutrophils.

The colonic epithelium is considered an important target for the beneficial effects of butyrate[18]. Furthermore, butyrate has anti-inflammatory activity in colon adenocarcinoma cells, which is mediated by inhibition of the NF-κB pathway[15,27]. We therefore next compared the anti-inflammatory actions of acetate, propionate and butyrate on TNFα-induced NF-κB reporter activity in the colon adenocarcinoma cell line Colo320DM. Our results demonstrate that SCFAs inhibit NF-κB activity in Colo320DM cells with the rank order of potency being butyrate > propionate > acetate. Previous studies have suggested that butyrate inhibits the NF-κB pathway by interfering with proteasome-mediated degradation of IκBα in colonocytes[27]. It is possible that acetate and propionate also act via this mechanism.

In animal models of colitis butyrate reduces the ulcer index and myeloperoxidase (MPO) activity[28,29]. The effect of other SCFAs in experimental colitis is less clear. There are, for example, contrasting results of propionate-treatment in trinitrobenzene sulfonic acid (TNBS)-induced colitis, demonstrating either a reduced ulcer index[30], or an aggravated inflammation[31]. In order to compare the effect of different SCFAs on intestinal inflammatory responses in the absence of confounding factors, such as inappropriate uptake or metabolism of SCFAs, we developed an organ culture protocol where colitis is established by administering dextran sulphate sodium to mice in the drinking water. The inflamed colonic tissue is then collected and the effect of anti-inflammatory agents is studied *in vitro*. A dose finding study with propionate revealed a dose dependent suppression of IL-6 mRNA and protein in colon organ cultures with an IC50 of approximately 1 mmol/L, without any sign of cytotoxicity. Furthermore, acetate and propionate, along with butyrate at 30 mmol/L were shown to reduce the expression levels of selected immune-related genes in colon organ cultures. Acetate was less potent than the two other SCFAs at this dose, a finding in line with the results in neutrophils and in Colo320DM cells. SCFA treatment of organ cultures suppressed a majority of genes decreased also by MG-132, a proteasome and NF-κB inhibitor. Interestingly, at 10 μmol/L MG-132 was far more potent than the p38 MAPK inhibitor SB203580 in suppressing immune-related gene expression, indicating a central role for the NF-κB pathway in DSS-mediated inflammation. Finally, SCFAs potently reduced IL-6 protein release from colon organ cultures with the rank order being propionate > butyrate > acetate.

The mechanism whereby SCFAs mediate their anti-inflammatory effects is currently poorly understood. As discussed above the NF-κB pathway is an important target for butyrate, and possible mechanisms for this could involve inhibition of IκBα kinase activity or proteasome function. Interestingly, our findings in Colo320DM cells suggest a positive correlation between potency and carbon chain length, which may possibly reflect the preferential utilization of larger SCFAs in a specific metabolic pathway. One illustrating example of a component of intermediary metabolism with anti-inflammatory properties is pyruvate which has well-documented immune suppressive activities *in vitro* and *in vivo*[32,33]. Thus, it is likely that the metabolism of SCFAs may give rise to metabolites with activity comparable to that of pyruvate. Alternatively, the rank order potency of SCFAs may result from an affinity relationship with a specific receptor. Recently, several independent groups have characterized SCFAs as ligands for the G-protein coupled receptors, GPR41 and GPR43[26,34,35]. The transcript for GPR43 is readily detectable with real-time PCR in neutrophils as well as in the colon (authors unpublished observation), thus it is possible that receptor dependent mechanisms may underlie some of the anti-inflammatory effects of SCFAs described in this study. GPR43 deficient mice may become an important tool for the understanding of SCFA signalling during inflammatory conditions in future studies.

As mentioned before, there are few and inconclusive studies regarding the ameliorating effects of acetate and propionate on inflammation, hence it is difficult to predict the outcome of treatment with these SCFAs in IBD. However, some interesting observations have been

published which provide indirect evidence that acetate and propionate may exhibit immune suppressive activity *in vivo*. Ethanol-intake, which is associated with elevated plasma acetate[36], was recently shown to prevent the development of destructive arthritis in rats[37]. In addition lactulose, a polysaccharide that is rapidly converted into acetate by colonic fermentation[38], ameliorates DSS-induced colitis in mice[39]. Noteworthy is also the observation that elevated systemic levels of propionate, due to mutations in the propionyl-CoA carboxylase enzyme, are associated with progressive immune suppression[40].

In conclusion, the present study demonstrates that acetate and propionate have anti-inflammatory properties, which are comparable to those of butyrate. It is demonstrated for the first time that SCFAs inhibit LPS-induced TNFα release, but not IL-8 secretion, from human blood-derived neutrophils. Furthermore, we show that acetate and propionate, similar to butyrate, inhibit TNFα-mediated activation of the NF-κB pathway in a human colon adenocarcinoma cell line with the rank order of potency being, butyrate > propionate > acetate. Finally anti-inflammatory activity, comparable to that of butyrate, was demonstrated for acetate and propionate in an *in vitro* model of murine experimental colitis. Taken together these findings suggest that propionate and acetate, in addition to butyrate, could be efficacious in the treatment of inflammatory conditions such as IBD.

ACKNOWLEDGMENTS

REFERENCES

1   **Hanauer SB**. Inflammatory bowel disease: epidemiology, pathogenesis, and therapeutic opportunities. *Inflamm Bowel Dis* 2006; **12** Suppl 1: S3-S9

2   **Brynskov J**, Nielsen OH, Ahnfelt-Ronne I, Bendtzen K. Cytokines (immunoinflammatory hormones) and their natural regulation in inflammatory bowel disease (Crohn's disease and ulcerative colitis): a review. *Dig Dis* 1994; **12**: 290-304

3   **Fuss IJ**. Cytokine network in inflammatory bowel disease. *Curr Drug Targets Inflamm Allergy* 2003; **2**: 101-112

4   **Schreiber S**, Nikolaus S, Hampe J. Activation of nuclear factor kappa B inflammatory bowel disease. *Gut* 1998; **42**: 477-484

5   **Waetzig GH**, Seegert D, Rosenstiel P, Nikolaus S, Schreiber S. p38 mitogen-activated protein kinase is activated and linked to TNF-alpha signaling in inflammatory bowel disease. *J Immunol* 2002; **168**: 5342-5351

6   **Wong JM**, de Souza R, Kendall CW, Emam A, Jenkins DJ. Colonic health: fermentation and short chain fatty acids. *J Clin Gastroenterol* 2006; **40**: 235-243

7   **Cook SI**, Sellin JH. Review article: short chain fatty acids in health and disease. *Aliment Pharmacol Ther* 1998; **12**: 499-507

8   **Topping DL**, Clifton PM. Short-chain fatty acids and human colonic function: roles of resistant starch and nonstarch polysaccharides. *Physiol Rev* 2001; **81**: 1031-1064

9   **Roediger WE**. Role of anaerobic bacteria in the metabolic welfare of the colonic mucosa in man. *Gut* 1980; **21**: 793-798

10 **Clausen MR**, Mortensen PB. Kinetic studies on the metabolism of short-chain fatty acids and glucose by isolated rat colonocytes. *Gastroenterology* 1994; **106**: 423-432

11 **Cummings JH**, Macfarlane GT. Role of intestinal bacteria in nutrient metabolism. *JPEN J Parenter Enteral Nutr* 1997; **21**: 357-365

12 **Scheppach W**, Sommer H, Kirchner T, Paganelli GM, Bartram P, Christl S, Richter F, Dusel G, Kasper H. Effect of butyrate enemas on the colonic mucosa in distal ulcerative colitis. *Gastroenterology* 1992; **103**: 51-56

13 **Steinhart AH**, Hiruki T, Brzezinski A, Baker JP. Treatment of left-sided ulcerative colitis with butyrate enemas: a controlled trial. *Aliment Pharmacol Ther* 1996; **10**: 729-736

14 **Di Sabatino A**, Morera R, Ciccocioppo R, Cazzola P, Gotti S, Tinozzi FP, Tinozzi S, Corazza GR. Oral butyrate for mildly to moderately active Crohn's disease. *Aliment Pharmacol Ther* 2005; **22**: 789-794

15 **Luhrs H**, Gerke T, Boxberger F, Backhaus K, Melcher R, Scheppach W, Menzel T. Butyrate inhibits interleukin-1-mediated nuclear factor-kappa B activation in human epithelial cells. *Dig Dis Sci* 2001; **46**: 1968-1973

16 **Segain JP**, Raingeard de la Bletiere D, Bourreille A, Leray V, Gervois N, Rosales C, Ferrier L, Bonnet C, Blottiere HM, Galmiche JP. Butyrate inhibits inflammatory responses through NFkappaB inhibition: implications for Crohn's disease. *Gut* 2000; **47**: 397-403

17 **Cummings JH**, Hill MJ, Bone ES, Branch WJ, Jenkins DJ. The effect of meat protein and dietary fiber on colonic function and metabolism. II. Bacterial metabolites in feces and urine. *Am J Clin Nutr* 1979; **32**: 2094-2101

18 **Cuff MA**, Shirazi-Beechey SP. The importance of butyrate transport to the regulation of gene expression in the colonic epithelium. *Biochem Soc Trans* 2004; **32**: 1100-1102

19 **Breuer RI**, Buto SK, Christ ML, Bean J, Vernia P, Paoluzi P, Di Paolo MC, Caprilli R. Rectal irrigation with short-chain fatty acids for distal ulcerative colitis. Preliminary report. *Dig Dis Sci* 1991; **36**: 185-187

20 **Breuer RI**, Soergel KH, Lashner BA, Christ ML, Hanauer SB, Vanagunas A, Harig JM, Keshavarzian A, Robinson M, Sellin JH, Weinberg D, Vidican DE, Flemal KL, Rademaker AW. Short chain fatty acid rectal irrigation for left-sided ulcerative colitis: a randomised, placebo controlled trial. *Gut* 1997; **40**: 485-491

21 **Patz J**, Jacobsohn WZ, Gottschalk-Sabag S, Zeides S, Braverman DZ. Treatment of refractory distal ulcerative colitis with short chain fatty acid enemas. *Am J Gastroenterol* 1996; **91**: 731-734

22 **Scheppach W**, Muller JG, Boxberger F, Dusel G, Richter F, Bartram HP, Christl SU, Dempfle CE, Kasper H. Histological changes in the colonic mucosa following irrigation with short-chain fatty acids. *Eur J Gastroenterol Hepatol* 1997; **9**: 163-168

23 **Vernia P**, Marcheggiano A, Caprilli R, Frieri G, Corrao G, Valpiani D, Di Paolo MC, Paoluzi P, Torsoli A. Short-chain fatty acid topical treatment in distal ulcerative colitis. *Aliment Pharmacol Ther* 1995; **9**: 309-313

24 **Niederman R**, Zhang J, Kashket S. Short-chain carboxylic-acid-stimulated, PMN-mediated gingival inflammation. *Crit Rev Oral Biol Med* 1997; **8**: 269-290

25 **Nakao S**, Moriya Y, Furuyama S, Niederman R, Sugiya H. Propionic acid stimulates superoxide generation in human neutrophils. *Cell Biol Int* 1998; **22**: 331-337

26 **Le Poul E**, Loison C, Struyf S, Springael JY, Lannoy V, Decobecq ME, Brezillon S, Dupriez V, Vassart G, Van Damme J, Parmentier M, Detheux M. Functional characterization of human receptors for short chain fatty acids and their role in polymorphonuclear cell activation. *J Biol Chem* 2003; **278**: 25481-25489

27 **Yin L**, Laevsky G, Giardina C. Butyrate suppression of colonocyte NF-kappa B activation and cellular proteasome activity. *J Biol Chem* 2001; **276**: 44641-44646

28 **Butzner JD**, Parmar R, Bell CJ, Dalal V. Butyrate enema therapy stimulates mucosal repair in experimental colitis in the rat. *Gut* 1996; **38**: 568-573

29 **Okamoto T**, Sasaki M, Tsujikawa T, Fujiyama Y, Bamba T, Kusunoki M. Preventive efficacy of butyrate enemas and oral administration of Clostridium butyricum M588 in dextran sodium sulfate-induced colitis in rats. *J Gastroenterol* 2000; **35**: 341-346

30   **Uchida M**, Mogami O. Milk whey culture with Propionibacterium freudenreichii ET-3 is effective on the colitis induced by 2,4,6-trinitrobenzene sulfonic acid in rats. *J Pharmacol Sci* 2005; **99**: 329-334

31   **Tarrerias AL**, Millecamps M, Alloui A, Beaughard C, Kemeny JL, Bourdu S, Bommelaer G, Eschalier A, Dapoigny M, Ardid D. Short-chain fatty acid enemas fail to decrease colonic hypersensitivity and inflammation in TNBS-induced colonic inflammation in rats. *Pain* 2002; **100**: 91-97

32   **Gupta SK**, Rastogi S, Prakash J, Joshi S, Gupta YK, Awor L, Verma SD. Anti-inflammatory activity of sodium pyruvate--a physiological antioxidant. *Indian J Physiol Pharmacol* 2000; **44**: 101-104

33   **Fink MP**. Ethyl pyruvate: a novel anti-inflammatory agent. *Crit Care Med* 2003; **31**: S51-S56

34   **Nilsson NE**, Kotarsky K, Owman C, Olde B. Identification of a free fatty acid receptor, FFA2R, expressed on leukocytes and activated by short-chain fatty acids. *Biochem Biophys Res Commun* 2003; **303**: 1047-1052

35   **Brown AJ**, Goldsworthy SM, Barnes AA, Eilert MM, Tcheang L, Daniels D, Muir AI, Wigglesworth MJ, Kinghorn I, Fraser NJ, Pike NB, Strum JC, Steplewski KM, Murdock PR, Holder JC, Marshall FH, Szekeres PG, Wilson S, Ignar DM, Foord SM, Wise A, Dowell SJ. The Orphan G protein-coupled receptors GPR41 and GPR43 are activated by propionate and other short chain carboxylic acids. *J Biol Chem* 2003; **278**: 11312-11319

36   **Siler SQ**, Neese RA, Hellerstein MK. De novo lipogenesis, lipid kinetics, and whole-body lipid balances in humans after acute alcohol consumption. *Am J Clin Nutr* 1999; **70**: 928-936

37   **Jonsson IM**, Verdrengh M, Brisslert M, Lindblad S, Bokarewa M, Islander U, Carlsten H, Ohlsson C, Nandakumar KS, Holmdahl R, Tarkowski A. Ethanol prevents development of destructive arthritis. *Proc Natl Acad Sci USA* 2007; **104**: 258-263

38   **Pouteau E**, Vahedi K, Messing B, Flourie B, Nguyen P, Darmaun D, Krempf M. Production rate of acetate during colonic fermentation of lactulose: a stable-isotope study in humans. *Am J Clin Nutr* 1998; **68**: 1276-1283

39   **Rumi G**, Tsubouchi R, Okayama M, Kato S, Mozsik G, Takeuchi K. Protective effect of lactulose on dextran sulfate sodium-induced colonic inflammation in rats. *Dig Dis Sci* 2004; **49**: 1466-1472

40   **Feliz B**, Witt DR, Harris BT. Propionic acidemia: a neuro-pathology case report and review of prior cases. *Arch Pathol Lab Med* 2003; **127**: e325-e328

Effects of glutamine supplementation on gut barrier, glutathione content and acute phase response in malnourished rats during inflammatory shock

Liliana Belmonte, Moïse Coëffier, Florence Le Pessot, Olga Miralles-Barrachina, Martine Hiron, Antony Leplingard, Jean-François Lemeland, Bernadette Hecketsweiler, Maryvonne Daveau, Philippe Ducrotté, Pierre Déchelotte

Liliana Belmonte, Moïse Coëffier, Olga Miralles-Barrachina, Antony Leplingard, Bernadette Hecketsweiler, Philippe Ducrotté, Pierre Déchelotte, Appareil Digestif Environnement Nutrition, ADEN EA3234, Institut Hospitalo-Universitaire de Recherche Biomédicale et Institut Fédératif de Recherches Multidisciplinaires sur les Peptides, Faculté de Médecine-Pharmacie, Rouen, France

Florence Le Pessot, Service d'Anatomie Pathologique, Centre Hospitalier Universitaire, Rouen, France

Martine Hiron, Maryvonne Daveau, INSERM unit 519, Institut Hospitalo-Universitaire de Recherche Biomédicale and Institut Fédératif de Recherches Multidisciplinaires sur les Peptides, Faculté de Médecine-Pharmacie, Rouen, France

Jean-François Lemeland, Groupe de Recherche sur les Antimicrobiens et les Microorganismes, GRAM EA2656, Institut Hospitalo-Universitaire de Recherche Biomédicale and Institut Fédératif de Recherches Multidisciplinaires sur les Peptides, Faculté de Médecine-Pharmacie, Rouen, France

Correspondence to: Professor Pierre Déchelotte, ADEN - Faculté de Médecine-Pharmacie de Rouen, 22 Bld Gambetta, 76183 Rouen, France. pierre.dechelotte@chu-rouen.fr

Telephone: +33-2-32886465 Fax: +33-2-32888332

Received: 2007-03-02   Accepted: 2007-03-28

Abstract

AIM: To evaluate the effect of glutamine on intestinal mucosa integrity, glutathione stores and acute phase response in protein-depleted rats during an inflammatory shock.

METHODS: Plasma acute phase proteins (APP), jejunal APP mRNA levels, liver and jejunal glutathione concentrations were measured before and one, three and seven days after turpentine injection in 4 groups of control, protein-restricted, protein-restricted rats supplemented with glutamine or protein powder. Bacterial translocation in mesenteric lymph nodes and intestinal morphology were also assessed.

RESULTS: Protein deprivation and turpentine injection significantly reduced jejunal villus height, and crypt depths. Mucosal glutathione concentration significantly decreased in protein-restricted rats. Before turpentine oil, glutamine supplementation restored villus heights and glutathione concentration (3.24 ± 1.05 *vs* 1.72 ± 0.46 µmol/g tissue, *P* < 0.05) in the jejunum, whereas in the liver glutathione remained low. Glutamine markedly increased jejunal α1-acid glycoprotein mRNA level after turpentine oil but did not affect its plasma concentration. Bacterial translocation in protein-restricted rats was not prevented by glutamine or protein powder supplementation.

CONCLUSION: Glutamine restored gut glutathione stores and villus heights in malnourished rats but had no preventive effect on bacterial translocation in our model.

INTRODUCTION

Sepsis and endotoxemia impair gut glutamine metabolism[1]. This impairment may contribute to the weakening of the gut mucosal barrier and to the development of bacterial translocation[1,2]. The tripeptide glutathione is an active free radical scavenging compound[3]. Glutathione has been shown to play an important role in the protection of intestinal mucosa against exogenous injury both *in vitro*[4,5] and *in vivo*[6]. Intestinal mucosa glutathione content falls markedly following a period of protein restriction[7] and also in patients with inflammatory bowel disease[8,9]. The depletion of reduced glutathione content in the mucosa could therefore favor oxidative stress within the mucosa. In addition to the liver, intestine also contributes to the systemic inflammatory response and acute phase proteins expression[10] and this intestinal acute phase response may be influenced by protein malnutrition[11,12].

Although glutamine has traditionally been recognized as a nonessential amino acid, recent studies have demon-

strated that glutamine plays a major role in the response to injury[13], in the enterocyte oxidative metabolism[14], and in the maintenance of the intestinal epithelium[15,16]. Glutamine supplementation may prevent gut mucosal damage and bacterial translocation in various experimental models of gut injury[13,17]. Moreover, glutamine could with stand systemic[18] but also gut-associated[19,20] immune response, because glutamine is an important substrate for optimal lymphocyte[21] and macrophage[22] function. In addition, some reports indicate that glutamine may counteract glutathione depletion by supporting gut glutathione biosynthesis[23] and may influence cytokines production by gut mucosa in rats[24] or in humans[25,26].

Therefore, the aim of this study was to investigate the effect of glutamine supplementation on the integrity of the intestinal mucosa and its glutathione stores and on acute phase response in protein depleted rats during an inflammatory challenge.

MATERIALS AND METHODS

Animals

Guidelines for the handling and care of laboratory animals conformed to the standards established by the Animal Studies Committee of the Rouen University.

Seventy two adult male Sprague-Dawley rats weighing 291 ± 23 g were obtained from Charles River (L'Arbresle, France) and were allowed at least 3 d to acclimatize to laboratory conditions (constant humidity and temperature: 21℃, with a 12 h light-dark cycle) in community cages before being studied. During this time the rats were allowed ad libitum intake of water and standard rat chow (UAR A03, Epinay-sur-Orge, France). Two weeks before the inflammatory challenge (d-14), rats were housed in individual metabolism cages at 21℃ with 12 h periods of dark and light cycles with a free access to food and water. Rats were assigned to 4 groups: a control group (CG) fed with a 23% protein diet (23 g casein/100 g synthetic diet, UAR, Epinay-sur-Orge, France); and 3 groups fed with an isocaloric protein-free (0% casein) diet. The composition of diets is summarized in Table 1. In two protein-restricted groups, rats were supplemented after 7 d of protein-free diet with either glutamine (3 g/100 mL) or protein powder (PolypeptalR, Novartis, 3.75 g/100 mL), and until the end of the study (Gln and PP groups, respectively). These supplements were administered in solution with the drinking water, with adequate dilution to provide isonitrogenous solutions. Equal volumes and thus isonitrogenous supplements were given to the rats of Gln and PP groups. One protein-restricted group received no supplementation later on (PR group).

Diet regimens were maintained until sacrifice day. During the experimental period, rats were weighted weekly, and food and water consumption was monitored daily. After 14 d of regimen, rats received a subcutaneous injection of 3 mL/kg of turpentine oil (TO) to induce an acute-phase response. An experimental inflammation induced by TO may increase intestinal permeability in rats[27]. Rats were sacrificed immediately before TO injection (0 h) or 1, 3, and 7 d after TO. The number of animals

Table 1 Composition of control and protein-deficient diets[1]

Constituent (g/kg)	Control diet (23% casein)	Protein-deficient diet (0% casein)
Protein	230[2]	0
Glucose (+ starch)	580	800
Lipids	50	60
Cellulose	60	60
Mineral salts[3]	70	70
Vitamins[4]	10	10
Total	1000	1000

[1]The energy density of each diet was 18 kJ/g. In the protein-restricted (PR) group, energy was replaced with isocaloric quantities of carbohydrates (glucose + starch in equal amounts); [2]Containing (g/kg): L-Arginine 8.5; L-Cysteine 3.0; L-Lysine 17.4; L-Methionine 7.1; L-Tryptophane 5.0; L-Glycine 1.0; [3]Containing (mg/kg): phosphorus, 7750; calcium, 10000; potassium, 6000; sodium, 4000; magnesium, 1000; manganese, 80; iron, 300; copper, 12.5; zinc, 45; cobalt, 0.09; and iodine, 0.49; [4]Containing (UI/kg): retinyl acetate, 19800; cholecalciferol, 6000; and (mg/kg): thiamin, 20; riboflavin, 15; D-pantothenic acid, 70; pyridoxine, 10; inositol, 150; cyanocobalamine, 0.05; ascorbic acid, 800; dl-α-tocopherol acetate, 170; menadione sodium bisulfite, 40; nicotinic acid, 100; choline, 1360; folic acid, 5; biotin, 0.3. (ND, not detectable).

ranged from 3 to 5 in each group at each time point.

Preparations

The rats were sacrificed and a ventral midline incision was made under sterile conditions and mesenteric lymph nodes were quickly removed and put into a sterile vial kept at 4℃ and transferred to the bacteriology laboratory within 4 h. After excision of lymph nodes and exsanguination, the portal vein was cannulated, the supra hepatic veins were cut, and the liver was rinsed with ice cold normal saline until it appeared blood free. Then, it was rapidly excised and blotted. A sample of liver (about 1 g) was weighed, minced and homogenized in a Braun[R] potter homogenizer with 3 mL of normal saline for 60 s at 4℃. This homogenate was used to determine the liver content of soluble proteins. Another 1 g liver sample was similarly homogenized in 3 mL of perchloric acid (0.4 mol/L). The homogenate was centrifuged at 10000 × g for 20 min at 4℃. The supernatant was kept at -80℃ for glutathione concentration measurement. After removal of the liver, the jejunum was removed and carefully rinsed with ice-cold phosphate buffer saline to eliminate fecal material. This tissue was opened longitudinally and the mucosa was immediately scraped off and prepared as previously described for the liver[28].

Analytical methods

Total reduced glutathione concentration in the supernatant was determined according to a modified spectro-photometric glutathione reductase assay as previously[28]. Glutathione assay was performed twice, with a variation coefficient of less than 10%. Results were expressed as μmoles glutathione per g wet weight tissue. Intracellular glutamine and glutamate levels were determined in the supernatant of jejunal homogenates after protein precipitation by using an amino acid analyzer (Biotronik LC3000; Eppendorf).

For measurement of villus height, additional 1 cm samples of jejunum were rinsed with ice-cold saline

Table 2 Body weight, total energy and nitrogen intake

	CG	PR	Gln	PP
Body weight (g)	295 ± 9	288 ± 31	284 ± 30	296 ± 8
Energy intake (kcal/d. 100 g body weight)				
1st wk	34 ± 2	20 ± 5[a]	22 ± 7[a]	19 ± 7[a]
2nd wk	30 ± 4	30 ± 4	28 ± 10	28 ± 10
Nitrogen intake (g/100 g body weight)	0.28 ± 0.02	0.00	0.05 ± 0.03	0.04 ± 0.01

Body weight (g) before the beginning of the study, total energy intake (powder or powder + supplementation in the drinking water) expressed in kcal/d per 100 g of body weight, and total nitrogen intake (g/100 g body weight) in CG (control group), protein-restricted group (PR) and protein-restricted groups supplemented with glutamine (Gln) or a protein powder (PP). [a]$P < 0.05$ *vs* CG.

Table 3 Positive cultures (colony forming units per gram of organ tissue (CFU) > 100) from cultured lymph nodes/total cultures for (CG), protein-restricted (PR), glutamine-(Gln) and protein powder (PP) supplemented groups

	d 0	d 1	d 3
CG	0/4	2/4	1/4
PR	1/5	1/5	1/5
Gln	2/6	4/7	2/5
PP	3/5	3/4	3/4
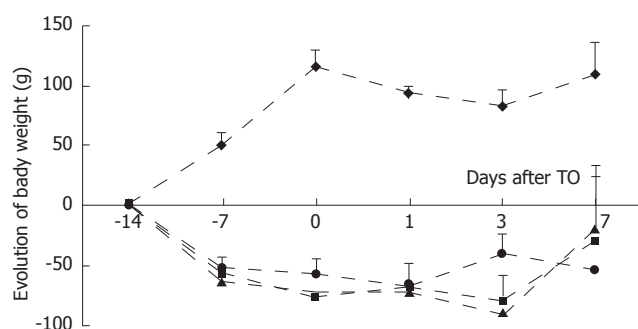
Figure 1 Evolution of body weight from initial weight as a function of time during the feeding period and at each time point studied after turpentine oil (TO) injection (arrow) for control (CG;◆), protein-restricted (PR;■), glutamine (Gln; ▲) and protein-powder (PP; ●) groups. Values are means ± SD. $P < 0.05$, between CG and other groups from d-7 until d7.

and fixed in a 10% formol solution during 24-72 h. The samples were coded and further handled in blinded fashion by the same observer. The samples were cut longitudinally in 3 pieces and embedded in paraffin. The sections (40 μm) were placed on a slide and then stained with hematoxylin. To minimize the variability of measurements, about 20 villi were studied in jejunal samples, and for each villus, epithelial thickness, chorion or lamina propria height and crypt depths were measured in duplicate.

In the bacteriology laboratory, lymph nodes were weighed in sterile conditions and then homogenized in a Teflon potter homogenizer with sterilized NaCl (10% weight/volume). The homogenate was then cultured in aerobic atmosphere on 3 different medium: horse blood Columbia, CLED (Biomérieux, Marcy l'Etoile, France) and nalidixic acid (Pasteur Diagnostics, Marnes-la-Coquette, France) agar plates, during 48 h. Colony counts were expressed as colony forming units per gram of organ tissue (CFU/g tissue), and culture was considered positive for (CFU/g tissue) > 100.

α-1 AGP and α2-macroglobulin plasma concentrations were determined by rocket immunoelectrophoresis as previously described[12] using rat anti-α-1 AGP or anti-α2-macroglobulin (UER Sciences Pharmaceutiques et Biologiques, Chatenay Malabray, France) antibodies.

RT-PCR

Total RNAs were extracted from the liver or intestinal mucosa by a modified-extraction method as previously described[26]. The quality and quantity of total RNA were determined by spectrophotometry using the absorbance at A260/A280 nm. The integrity was also controlled by visualization of 18S and 28S ribosomal bands. RT-PCR was performed as previously reported[26]. The RT products were amplified by PCR using sense and antisense primers (Eurogentec) specific for α-1 AGP and glycerladehyde-3 phosphate deshydrogenase (GAPDH) used as an internal standard: α-1 AGP, 5'-GCAGCTT TCCGAGACCCCGT-3' and 5'-CATGCCCACATCT TTGACAG-3'; GAPDH, 5'-AAAGGGTCATCATCT CCGCC-3' and 5'-GTGGAGGAATGGGAGTTGC T-3'. The relative quantification of the autoradiogram bands represents an integrated area under the curve of densitometric tracing, estimated as the ratio of targeted gene to GAPDH.

Statistical analysis

Values are expressed as the mean ± SD. Data were analyzed by analysis of variance, and differences between means were determined using Scheffe's multiple comparison test. The incidence of bacterial translocation was compared by corrected χ² test. Significance was defined as $P < 0.05$.

RESULTS

Dietary intake and weight of animals

Before starting the specialized regimens, there was no significant body weight difference between the groups (Table 2). Control group's body weight rose during the whole period before TO injection, slightly diminished 24 h after TO (not significant) and then remained unchanged (Figure 1). In contrast, in the three other groups, the animals lost about 60 g of their body weight during the first week of protein deprivation, and about 10 g during the second week, Turpentine oil did not induce an additional loss of weight and no significant difference was observed between these 3 groups (Figure 1).

The mean daily energy intake during the first week of the feeding period was reduced in all the groups fed with 0% protein diets (Table 2). During the second week of the feeding period, the energy intake (powder or powder + supplementation in the drinking water, see the methods section) was not significantly different between the groups (Table 2). During the supplementation period, nitrogen intake of Gln and PP groups represented about 18% and 14% (expressed in g N/d per 100 g body weight, respectively) of the nitrogen intake of CG (Table 3). When the rats were injected with TO, a significant (about 50%)
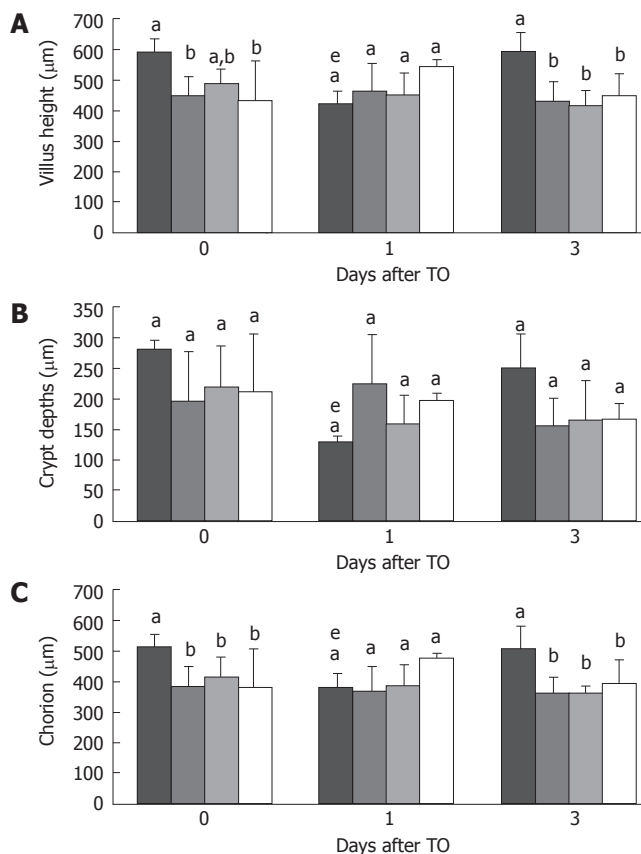
Figure 2 Morphometrics of jejunal villus height (**A**), jejunal crypt depths (**B**), and jejunal lamina propria (**C**), immediately before turpentine oil (TO) injection and 1, and 3 d after TO. Rats received either control (■), protein-restricted (PR; ▥), glutamine (Gln; ▦), or protein-powder (PP; □) supplemented diets. Values are means ± SD. Means without a common letter (a, b or c) differ. $^{e}P < 0.05$ vs d 0.

reduction of food intake was observed in all groups, with no significant difference between groups, and food intake normalized 24 h later.

Intestinal morphology

The morphometric data of the four groups are displayed on Figure 2. After 14 d of 0% protein diet, both the villus and lamina propria heights in the jejunum (446 ± 80 vs 590 ± 43 μm and 388 ± 65 vs 518 ± 39 μm respectively; $P < 0.05$) were significantly decreased in comparison to CG. The jejunal crypt depths were also decreased, although not significantly. There was no significant difference for crypt depths and lamina propria height before injection of TO between Gln and PP-supplemented groups. In contrast, villus heights were maintained in Gln group but not in PP group (Figure 2A). One day after TO injection, a significant decrease was observed in jejunal villus height, crypt depth and lamina propria for CG group (421 ± 36 μm vs 590 ± 43 μm, 130 ± 4 μm vs 282 ± 13 μm, 386 ± 40 μm vs 517 ± 39 μm respectively; $P < 0.05$). In the other groups, morphometrics did not change after TO. Three days after injury, morphometric parameters were restored only in CG group. There was no difference between the 3 protein restricted groups (PR, Gln, PP; Figure 2).

Bacterial translocation

For the CG, no viable bacteria were detectable in cultured

mesenteric lymph nodes before TO injection (Table 3). In contrast, some positive cultures were observed for lymph nodes from PR animals as well as from Gln or PP-supplemented groups. After TO induced inflammation, bacterial translocation was also noted in several animals; however, no significant difference between groups was observed (Table 3).

Glutathione and glutamine concentrations

The glutathione concentration in liver and jejunum is displayed in Figure 3. In both tissues, glutathione concentration significantly decreased after protein restriction (jejunum: 1.72 ± 0.46 vs 4.24 ± 1.40 μmol/g tissue; liver: 2.59 ± 0.38 vs 7.3 ± 0.38 μmol/g tissue, both $P < 0.05$). Glutathione concentration was restored after glutamine supplementation in the jejunum (3.24 ± 1.05 vs 1.72 ± 0.46 μmol/g tissue, $P < 0.05$), while it remained low despite supplementation with protein powder (Figure 3A). In the liver, glutamine supplementation had no significant effect on glutathione concentration (Figure 3B).

After TO injection, glutathione concentration in the jejunum peaked on d 1 and d 3 for CG and PR animals, respectively (Figure 3A). In the Gln group, but not in the PP group, a marked jejunal glutathione concentration peak was also observed on d 3 (Figure 3A, $P < 0.05$ Gln vs PR). Glutathione in the liver was decreased on d 1, and later increased on d 3 in CG and PR animals (Figure 3B, $P < 0.05$ d 1 vs d 0 for CG , and $P < 0.05$ on d 3 vs d 1 for PR). In both groups of supplemented rats, liver glutathione rose markedly on d 1 and peaked on d 3 after TO injection, and returned to initial values on d 7 (Figure 3B). Protein concentrations were similar and did not vary significantly in the both organs.

Intracellular glutamine concentration before inflammation was significantly increased in the Gln group in comparison to CG (2.36 ± 2.93 vs 1.05 ± 0.23 μmol/g tissue; $P < 0.05$), while it was not affected by protein deprivation alone or by supplementation with protein powder. After TO, no significant difference was observed between groups and intracellular glutamate was not modified by any diet nor by TO induced inflammation (data not shown).

Acute phase response

Before TO, α-1 AGP was detected to a low level in the plasma but no difference was observed between the groups (Figure 4A). In contrast, α2-MG was increased in plasma from Gln rats (Figure 4B). After TO, plasma α-1 AGP and α2-MG increased in all groups to a similar extent.

Jejunal α-1 AGP mRNA (Figure 5) was not constitutively expressed in any groups. TO injection induced a weak increase of α-1 AGP mRNA level in CG group only at d 1. This increase was prolonged in PR group until d 7. However, the peak response of α-1 AGP mRNA was higher in the two supplemented groups (Gln and PP, $P < 0.05$, Figure 5). The highest α-1 AGP mRNA peak response was observed in the Gln group at d 1, and was significantly higher than that observed in PR and PP groups ($P < 0.05$). Jejunal α2-MG mRNA level remained not affected by protein restriction, Gln or PP supplementation and TO challenge (data not shown).

A Jejunum
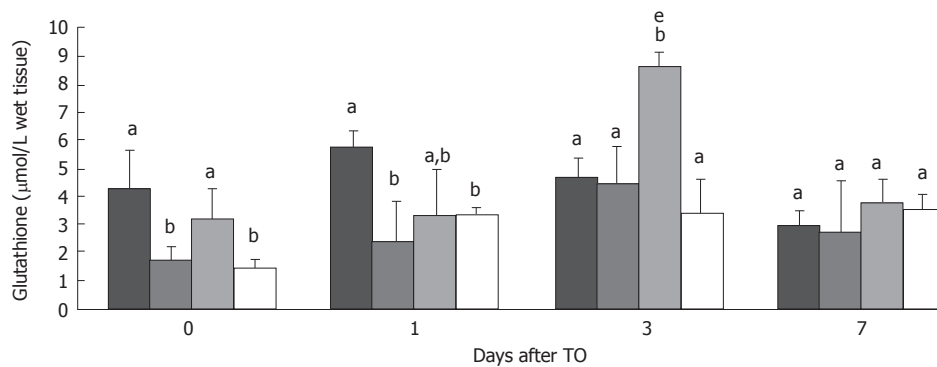
B Liver
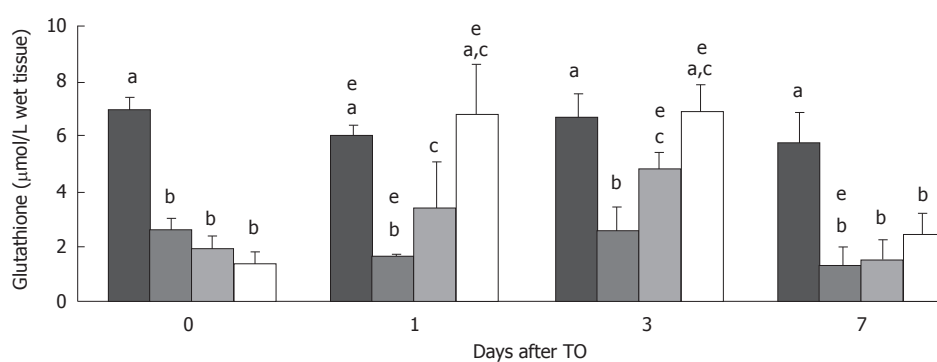
Figure 3 Jejunal (**A**) and liver (**B**) glutathione (μmol/g tissue) immediately before turpentine oil (TO) injection and 1, 3 and 7 d after TO. Rats received either control (■), protein-restricted (PR; ■), glutamine (Gln; ■), or protein-powder (PP; □). Values are means ± SD. Means without a common letter (a, b or c) differ. $^{e}P < 0.05$ *vs* d 0.

A α1-AGP
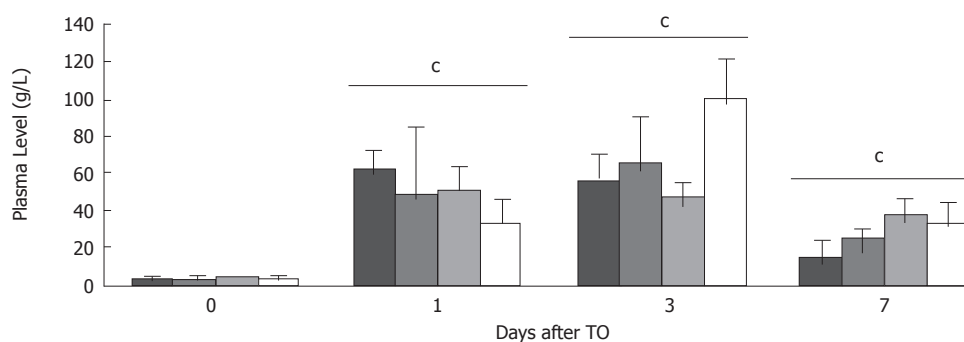
B α2-MG
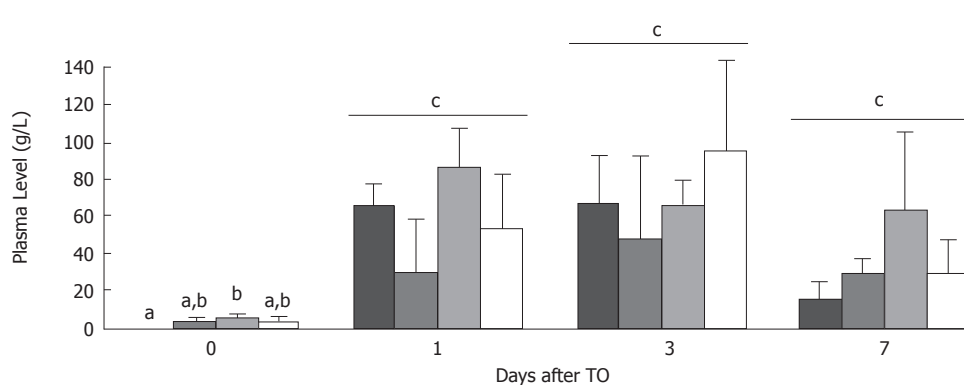
Figure 4 Plasma levels (g/L) for alpha-1 acid glycoprotein (**A**) and alpha-2 macroglobulin (**B**) immediately before turpentine oil (TO) injection and 1, 3 and 7 d after TO. Rats received either control (■), protein-restricted (PR; ■), glutamine (Gln; ■), or protein-powder (PP; □) supplemented diets. Values are means ± SD. Means without a common letter (a, b) differ. $^{c}P < 0.05$ *vs* d 0.

DISCUSSION

In the present study, we measured the effect of glutamine supplementation on gut barrier, glutathione content and acute phase response in severely protein-restricted rats during TO injection. Our results indicate that glutamine restored gut glutathione content and regulated intestinal acute phase response without influencing bacterial translocation in protein-restricted rats.

In the present study, weight gain was severely impaired in rats fed a protein-free diet (PR group). Growth retardation has been reported as a consequence of feeding
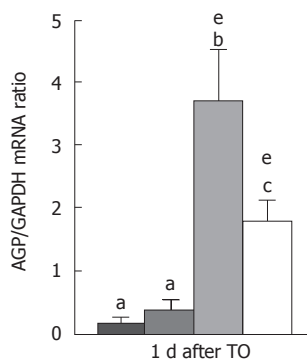
Figure 5 Jejunal mRNA level for alpha-1 acid glycoprotein (AGP/GAPDH mRNA ratio) one day after turpentine oil injection. Rats received either control (■), protein-restricted (PR; ■), glutamine (Gln; ■), or protein-powder (PP; □) supplemented diets. Values are means ± SD. Means without a common letter (a, b or c) differ. $^{e}P < 0.05$ vs d 0.

a poor-protein diet without taking into consideration the anorexia associated with the consumption of low protein diets[29]. In our study, the mean daily energy intake during the first week of the feeding period was also diminished in all the groups fed with 0% protein diets (see results section). Thus, as both diets were isocaloric, this suggests that the absence of proteins may have affected the palatability of the diets or influenced the central regulation of appetite[30]. Neither glutamine nor protein powder supplementation restored a growth rate similar to that of animals fed the normal-protein diet. However, during the second week, the variations in the energy intake between the 4 groups did not reach significance. It may appear not physiological to have used a protein-free diet. However, it is not rare that patients remain with only fluids and glucose for several days in postoperative situations while undergoing inflammatory stress. In addition, this diet was appropriate to test the pharmacological effect of glutamine alone, apart from that of other amino acids.

Inflammation was induced by a subcutaneous injection of 3 mL/kg of body weight of TO. Previous studies have shown that this experimental model elicits hormonal and metabolic changes similar to those observed during the response to injury and infection[12,17,27]. This includes the production of the acute-phase protein α-2 macroglobulin[12,27] but does not lead to the anorexia commonly associated with administration of endotoxin, gavage with bacteria or other injury models[27]. The injection of TO had only a marginal effect upon the rate of weight gain in normally fed animals following the injection. This observation confirms similar findings observed in pigs[31].

The gastrointestinal tract is a major organ of glutamine utilization[32]. In various models of stress-induced injury (cancer, radiation, and chemotherapy) or malnutrition, glutamine supply maintains or restores the normal morphometric values of the small bowel mucosa and supports gut function[33]. However, glutamine deprivation in an otherwise complete diet prior to TO injury had only a marginal detrimental effect on the structural integrity of the small intestinal mucosa[17]. This may be due to the fact that animals were not otherwise protein-depleted, and were thus able to maintain an adequate glutamine endogenous de novo synthesis from several other amino acids i.e. branched-chain amino acids[34].

In our study, the histological assessment of the mucosa in the jejunum was carried out on 4 rats from each dietary group before and 1 and 3 d after TO injection. Protein

restriction induced a marked, significant decrease of jejunal villus and chorion height (Figure 2). In contrast, in Gln group, villus height was only modestly reduced (not significantly different from CG). This is consistent with a beneficial effect of glutamine supplementation on enterocyte proliferation rate as reported in human mucosa in vitro[35]. It may also be explained by a prolongation of cell life[20] or apoptosis inhibition[36,37].

Bacterial translocation occurred in several animals in all protein-restricted rats. This may be due to the passage of viable bacteria through paracellular pathways, as a consequence of altered tight junction selectivity secondary to severely impaired metabolism. None of the supplements had any significant preventive effect on bacterial translocation, which is at variance with some other reports in enterally[1] or parenterally fed rats supplemented with glutamine[19]. This lack of preventive effect may be due to the fact that other factors involved in gut barrier function, such as mucosal immune cells or IgA secretion, had been impaired by severe protein restriction[1,19].

Glutathione plays an important role in detoxification reactions with xenobiotics and oxygen radicals[3] and is also required in large amounts in catabolic states, not only by hepatic and intestinal cells but also by inflammatory cells; thus, impaired mucosal glutathione content increases the susceptibility to oxidative tissue injury[3,5]. Glutathione requires glutamate for its biosynthesis and the main intracellular source of glutamate is derived from glutamine[38]. Some authors reported that glutamine supplementation may increase glutathione concentration both in the liver[39] and in the gut[23,40,41]. In both tissues studied in the present study (jejunum and liver), glutathione concentration decreased markedly in PR rats before TO injection. After the inflammatory shock, liver glutathione slightly decreased in CG and PR groups, and later increased up to values not different from initial values; in contrast, it was markedly increased in Gln and PP groups. The transient initial decrease in CG and PR animals may reflect the short-term reduction of solid food intake after TO, since liver glutathione is very sensitive to food deprivation. Contrastingly, after TO, rats in all groups markedly increased their water intake (data not shown) until d 3; this resulted in an increased intake of both glutamine and protein powder. Accordingly, an increase of liver glutathione was observed after inflammatory shock on d 3 and may have been supported by the increased intake of precursors from glutamine or protein powder. The significant decrease in jejunal glutathione of severely protein-restricted rats in the present study is in accordance with previous results in rats fed a 3% protein diet[31]. Both a decreased synthetic rate of glutathione in the mucosa[23,42] and/or a leakage in the lumen may have contributed to this decreased concentration of glutathione. At most time points, glutamine but not protein powder restored glutathione concentrations in the jejunum and this effect was significant on d 0 and d 3. In contrast, glutathione in the liver was best restored with the amino acid mixture (PP). The specific beneficial effect of glutamine on jejunal glutathione probably reflects the high capacities of uptake, as reflected by intracellular glutamine concentration and of glutamine utilization in the proximal small intestine[43]

for immediate glutathione synthesis. In addition, beneficial effects of glutamine on villus height and GSH content in jejunal mucosa could be related to each other since a negative correlation between GSH content and apoptosis of epithelial cells has been reported[44]. Despite being provided with isonitrogenous drinking solutions, rats in the PP group drank somewhat less water than those in the Gln group, with consequently a lower nitrogen intake in the PP group than in the Gln group. Despite this, jejunal glutathione content in the glutamine group was even higher than in normally fed rats (Figure 3B). Thus, the supply of free glutamine via the oral route may have a distinct kinetic advantage as far as mucosal glutathione synthesis is concerned.

Before the induction of inflammatory shock, the mRNA for α-1 AGP was not expressed in the jejunal mucosa, which is in accordance with data in cultured rat intestinal epithelial cells[45]. In response to TO challenge, mRNA expression for α-1 AGP increased in jejunal mucosa in normally fed rats. However, protein restriction and glutamine-supplementation enhanced jejunal α-1 AGP response without altering plasma APP concentrations. The α-1 AGP has been reported to have an anti-inflammatory effect by increasing the production of IL-1 receptor antagonist[46], by limiting the migration of leukocytes through endothelium[47] and by reducing complement- and neutrophil-mediated intestinal injury[48]. Thus, an enhanced intestinal α-1 AGP production after supplementation with glutamine may contribute to the local protective effects of glutamine, together with the reduction of pro-inflammatory cytokine production[49], as well as the improvement of protein metabolism[50].

In summary, our results indicate that glutamine supports glutathione stores and may support the intestinal acute phase response in the jejunum of malnourished rats during inflammatory shock. Since a marked glutathione depletion has been observed during inflammatory bowel diseases, specially when combined with malnutrition[8], the beneficial effects of glutamine-supplemented diets on antioxidative capacities and gut integrity in inflammatory conditions with associated malnutrition should be evaluated.

ACKNOWLEDGMENTS

REFERENCES

1   **Souba WW**, Herskowitz K, Klimberg VS, Salloum RM, Plumley DA, Flynn TC, Copeland EM 3rd. The effects of sepsis and endotoxemia on gut glutamine metabolism. *Ann Surg* 1990; **211**: 543-549; discussion 549-551

2   **Alexander JW**. Nutrition and translocation. *JPEN J Parenter Enteral Nutr* 1990; **14**: 170S-174S

3   **Meister A**, Anderson ME. Glutathione. *Annu Rev Biochem* 1983; **52**: 711-760

4   **Lash LH**, Hagen TM, Jones DP. Exogenous glutathione protects intestinal epithelial cells from oxidative injury. *Proc Natl Acad Sci USA* 1986; **83**: 4641-4645

5   **Rao RK**, Li L, Baker RD, Baker SS, Gupta A. Glutathione oxidation and PTPase inhibition by hydrogen peroxide in Caco-2 cell monolayer. *Am J Physiol Gastrointest Liver Physiol* 2000; **279**: G332-G340

6   **Kelly FJ**. Glutathione content of the small intestine: regulation and function. *Br J Nutr* 1993; **69**: 589-596

7   **Hum S**, Koski KG, Hoffer LJ. Varied protein intake alters glutathione metabolism in rats. *J Nutr* 1992; **122**: 2010-2018

8   **Miralles-Barrachina O**, Savoye G, Belmonte-Zalar L, Hochain P, Ducrotte P, Hecketsweiler B, Lerebours E, Dechelotte P. Low levels of glutathione in endoscopic biopsies of patients with Crohn's colitis: the role of malnutrition. *Clin Nutr* 1999; **18**: 313-317

9   **Sido B**, Hack V, Hochlehnert A, Lipps H, Herfarth C, Droge W. Impairment of intestinal glutathione synthesis in patients with inflammatory bowel disease. *Gut* 1998; **42**: 485-492

10 **Molmenti EP**, Ziambaras T, Perlmutter DH. Evidence for an acute phase response in human intestinal epithelial cells. *J Biol Chem* 1993; **268**: 14116-14124

11 **Jennings G**, Bourgeois C, Elia M. The magnitude of the acute phase protein response is attenuated by protein deficiency in rats. *J Nutr* 1992; **122**: 1325-1331

12 **Lyoumi S**, Tamion F, Petit J, Dechelotte P, Dauguet C, Scotte M, Hiron M, Leplingard A, Salier JP, Daveau M, Lebreton JP. Induction and modulation of acute-phase response by protein malnutrition in rats: comparative effect of systemic and localized inflammation on interleukin-6 and acute-phase protein synthesis. *J Nutr* 1998; **128**: 166-174

13 **Li JY**, Lu Y, Hu S, Sun D, Yao YM. Preventive effect of glutamine on intestinal barrier dysfunction induced by severe trauma. *World J Gastroenterol* 2002; **8**: 168-171

14 **Martensson J**, Jain A, Meister A. Glutathione is required for intestinal function. *Proc Natl Acad Sci USA* 1990; **87**: 1715-1719

15 **van der Hulst RR**, van Kreel BK, von Meyenfeldt MF, Brummer RJ, Arends JW, Deutz NE, Soeters PB. Glutamine and the preservation of gut integrity. *Lancet* 1993; **341**: 1363-1365

16 **Zhou YP**, Jiang ZM, Sun YH, Wang XR, Ma EL, Wilmore D. The effect of supplemental enteral glutamine on plasma levels, gut function, and outcome in severe burns: a randomized, double-blind, controlled clinical trial. *JPEN J Parenter Enteral Nutr* 2003; **27**: 241-245

17 **Wusteman M**, Tate H, Weaver L, Austin S, Neale G, Elia M. The effect of enteral glutamine deprivation and supplementation on the structure of rat small-intestine mucosa during a systemic injury response. *JPEN J Parenter Enteral Nutr* 1995; **19**: 22-27

18 **Quan ZF**, Yang C, Li N, Li JS. Effect of glutamine on change in early postoperative intestinal permeability and its relation to systemic inflammatory response. *World J Gastroenterol* 2004; **10**: 1992-1994

19 **Alverdy JA**, Aoys E, Weiss-Carrington P, Burke DA. The effect of glutamine-enriched TPN on gut immune cellularity. *J Surg Res* 1992; **52**: 34-38

20 **van der Hulst RR**, von Meyenfeldt MF, Tiebosch A, Buurman WA, Soeters PB. Glutamine and intestinal immune cells in humans. *JPEN J Parenter Enteral Nutr* 1997; **21**: 310-315

21 **Ziegler TR**, Bye RL, Persinger RL, Young LS, Antin JH, Wilmore DW. Effects of glutamine supplementation on circulating lymphocytes after bone marrow transplantation: a pilot study. *Am J Med Sci* 1998; **315**: 4-10

22 **Newsholme P**, Curi R, Pithon Curi TC, Murphy CJ, Garcia C, Pires de Melo M. Glutamine metabolism by lymphocytes, macrophages, and neutrophils: its importance in health and disease. *J Nutr Biochem* 1999; **10**: 316-324

23 **Cao Y**, Feng Z, Hoos A, Klimberg VS. Glutamine enhances gut glutathione production. *JPEN J Parenter Enteral Nutr* 1998; **22**: 224-227

24 **Ameho CK**, Adjei AA, Harrison EK, Takeshita K, Morioka T, Arakaki Y, Ito E, Suzuki I, Kulkarni AD, Kawajiri A, Yamamoto S. Prophylactic effect of dietary glutamine

supplementation on interleukin 8 and tumour necrosis factor alpha production in trinitrobenzene sulphonic acid induced colitis. *Gut* 1997; **41**: 487-493

25   **Coeffier M**, Marion R, Leplingard A, Lerebours E, Ducrotte P, Dechelotte P. Glutamine decreases interleukin-8 and interleukin-6 but not nitric oxide and prostaglandins e(2) production by human gut in-vitro. *Cytokine* 2002; **18**: 92-97

26   **Coeffier M**, Miralles-Barrachina O, Le Pessot F, Lalaude O, Daveau M, Lavoinne A, Lerebours E, Dechelotte P. Influence of glutamine on cytokine production by human gut in vitro. *Cytokine* 2001; **13**: 148-154

27   **Jennings G**, Elia M. Independent effects of protein and energy deficiency on acute-phase protein response in rats. *Nutrition* 1991; **7**: 430-434

28   **Fouin-Fortunet H**, Besnier MO, Colin R, Wessely JY, Rose F. Effects of ketoacids on liver glutathione and microsomal enzymes in malnourished rats. *Kidney Int Suppl* 1989; **27**: S222-S226

29   **Grimble RF**, Jackson AA, Persaud C, Wride MJ, Delers F, Engler R. Cysteine and glycine supplementation modulate the metabolic response to tumor necrosis factor alpha in rats fed a low protein diet. *J Nutr* 1992; **122**: 2066-2073

30   **Hunter EA**, Grimble RF. Dietary sulphur amino acid adequacy influences glutathione synthesis and glutathione-dependent enzymes during the inflammatory response to endotoxin and tumour necrosis factor-alpha in rats. *Clin Sci* (Lond) 1997; **92**: 297-305

31   **Jahoor F**, Wykes LJ, Reeds PJ, Henry JF, del Rosario MP, Frazer ME. Protein-deficient pigs cannot maintain reduced glutathione homeostasis when subjected to the stress of inflammation. *J Nutr* 1995; **125**: 1462-1472

32   **Dechelotte P**, Darmaun D, Rongier M, Hecketsweiler B, Rigal O, Desjeux JF. Absorption and metabolic effects of enterally administered glutamine in humans. *Am J Physiol* 1991; **260**: G677-G682

33   **Inoue Y**, Grant JP, Snyder PJ. Effect of glutamine-supplemented total parenteral nutrition on recovery of the small intestine after starvation atrophy. *JPEN J Parenter Enteral Nutr* 1993; **17**: 165-170

34   **Darmaun D**, Dechelotte P. Role of leucine as a precursor of glutamine alpha-amino nitrogen in vivo in humans. *Am J Physiol* 1991; **260**: E326-E329

35   **Scheppach W**, Loges C, Bartram P, Christl SU, Richter F, Dusel G, Stehle P, Fuerst P, Kasper H. Effect of free glutamine and alanyl-glutamine dipeptide on mucosal proliferation of the human ileum and colon. *Gastroenterology* 1994; **107**: 429-434

36   **Papaconstantinou HT**, Hwang KO, Rajaraman S, Hellmich MR, Townsend CM Jr, Ko TC. Glutamine deprivation induces apoptosis in intestinal epithelial cells. *Surgery* 1998; **124**: 152-159; discussion 159-160

37   **Evans ME**, Jones DP, Ziegler TR. Glutamine prevents cytokine-induced apoptosis in human colonic epithelial cells. *J Nutr* 2003; **133**: 3065-3071

38   **Welbourne TC**. Ammonia production and glutamine incorporation into glutathione in the functioning rat kidney. *Can J Biochem* 1979; **57**: 233-237

39   **Gonzales S**, Polizio AH, Erario MA, Tomaro ML. Glutamine is highly effective in preventing in vivo cobalt-induced oxidative stress in rat liver. *World J Gastroenterol* 2005; **11**: 3533-3538

40   **Basivireddy J**, Jacob M, Balasubramanian KA. Oral glutamine attenuates indomethacin-induced small intestinal damage. *Clin Sci* (Lond) 2004; **107**: 281-289

41   **Prabhu R**, Thomas S, Balasubramanian KA. Oral glutamine attenuates surgical manipulation-induced alterations in the intestinal brush border membrane. *J Surg Res* 2003; **115**: 148-156

42   **Breuille D**, Rose F, Arnal M, Melin C, Obled C. Sepsis modifies the contribution of different organs to whole-body protein synthesis in rats. *Clin Sci* (Lond) 1994; **86**: 663-669

43   **Windmueller HG**, Spaeth AE. Respiratory fuels and nitrogen metabolism in vivo in small intestine of fed rats. Quantitative importance of glutamine, glutamate, and aspartate. *J Biol Chem* 1980; **255**: 107-112

44   **Benard O**, Madesh M, Anup R, Balasubramanian KA. Apoptotic process in the monkey small intestinal epithelium: I. Association with glutathione level and its efflux. *Free Radic Biol Med* 1999; **26**: 245-252

45   **Boudreau F**, Yu SJ, Asselin C. CCAAT/enhancer binding proteins beta and delta regulate alpha1-acid glycoprotein gene expression in rat intestinal epithelial cells. *DNA Cell Biol* 1998; **17**: 669-677

46   **Tilg H**, Vannier E, Vachino G, Dinarello CA, Mier JW. Antiinflammatory properties of hepatic acute phase proteins: preferential induction of interleukin 1 (IL-1) receptor antagonist over IL-1 beta synthesis by human peripheral blood mononuclear cells. *J Exp Med* 1993; **178**: 1629-1636

47   **De Graaf TW**, Van der Stelt ME, Anbergen MG, van Dijk W. Inflammation-induced expression of sialyl Lewis X-containing glycan structures on alpha 1-acid glycoprotein (orosomucoid) in human sera. *J Exp Med* 1993; **177**: 657-666

48   **Williams JP**, Weiser MR, Pechet TT, Kobzik L, Moore FD Jr, Hechtman HB. alpha 1-Acid glycoprotein reduces local and remote injuries after intestinal ischemia in the rat. *Am J Physiol* 1997; **273**: G1031-G1035

49   **Coeffier M**, Marion R, Ducrotte P, Dechelotte P. Modulating effect of glutamine on IL-1beta-induced cytokine production by human gut. *Clin Nutr* 2003; **22**: 407-413

50   **Coeffier M**, Claeyssens S, Hecketsweiler B, Lavoinne A, Ducrotte P, Dechelotte P. Enteral glutamine stimulates protein synthesis and decreases ubiquitin mRNA level in human gut mucosa. *Am J Physiol Gastrointest Liver Physiol* 2003; **285**: G266-G273

Radiofrequency ablation in a porcine liver model: Effects of transcatheter arterial embolization with iodized oil on ablation time, maximum output, and coagulation diameter as well as angiographic characteristics

Motoki Nakai, Morio Sato, Shinya Sahara, Nobuyuki Kawai, Hirohiko Tanihata, Masashi Kimura, Masaki Terada

Motoki Nakai, Department of Radiology, Hidaka General Hospital, 116-2 Sono, Gobo Shi, Wakayama 644-8655, Japan
Morio Sato, Shinya Sahara, Nobuyuki Kawai, Hirohiko Tanihata, Masashi Kimura, Masaki Terada, Department of Radiology, Wakayama Medical University 811-1, Kimiidera, Wakayama Shi, Wakayama 641-8510, Japan
Correspondence to: Motoki Nakai, Department of Radiology, Hidaka General Hospital, 116-2 Sono, Gobo Shi, Wakayama 644-8655, Japan. nakai@hidakagh.gobo.wakayama.jp
Telephone: +81-738-221111 Fax: +81-738-232253
Received: 2007-02-10   Accepted: 2007-04-13

Abstract

AIM: To evaluate the effects of combined radiofrequency ablation and transcatheter arterial embolization with iodized oil on ablation time, maximum output, coagulation diameter, and portal angiography in a porcine liver model.

METHODS: Radiofrequency ablation (RFA) was applied to *in vivo* livers of 10 normal pigs using a 17-gauge 3.0 cm expandable LeVeen RF needle electrode with or without transcatheter arterial embolization (TAE) with iodized oil (*n* = 5). In each animal, 2 areas in the liver were ablated. Direct portography was performed before and after RFA. Ablation was initiated at an output of 30 W, and continued with an increase of 10 W per minute until roll-off occurred. Ablation time and maximum output until roll-off, and coagulated tissue diameter were compared between the 2 groups. Angiographic changes on portography before and after ablation were also reviewed.

RESULTS: For groups with and without TAE with iodized oil, the ablation times until roll-off were 320.6 ± 30.9 seconds and 445.1 ± 35.9 seconds, respectively, maximum outputs were 69.0 ± 7.38 W and 87.0 ± 4.83 W and maximal diameters of coagulation were 41.7 ± 3.85 mm and 33.2 ± 2.28 mm. Significant reductions of ablation time and maximum output, and significantly larger coagulation diameter were obtained with RFA following TAE with iodized oil compared to RFA alone. Portography after RFA following TAE with iodized oil revealed more occlusion of the larger portal branches than with RFA alone.

CONCLUSION: RFA following TAE with iodized oil can increase the volume of coagulation necrosis with lower output and shorter ablation time than RFA alone in normal pig liver tissue.

INTRODUCTION

Percutaneous radiofrequency ablation (RFA) is widely used to treat focal malignant tumors such as hepatocellular carcinoma (HCC) and metastatic liver tumors[1-3]. It has been reported by many authors that this is a satisfactory therapeutic modality because it results in reliable local control and is minimally invasive[4,5]. The greatest disadvantage of RF ablation for treating liver tumors is difficulty of ablating large tumors due to the limited coagulation area, frequently observed in the treatment of large HCC. Inability to reliably creating adequate volumes of complete tumor coagulation limits the adoption of RF ablation for large hepatic tumors.

One characteristic of RF ablation is its susceptibility to the cooling effect of blood flow[6,7], a factor which has a considerable effect on RFA treatment. The reduced efficacy of RF ablation for large tumors reflects the *in vivo* biophysiological limitations imposed by perfusion-mediated vascular cooling, which limits heat-induced coagulation necrosis. HCCs, in particular, are supplied almost entirely by the hepatic arteries, and the abundant tumoral arterial blood flow has a cooling effect, which diminishes radiofrequency wave heating. Several investigators have been able to increase RF-induced coagulation necrosis by occluding blood flow to the liver

during ablation procedures in animal models[7-10].

Transcatheter arterial embolization (TAE) using iodized oil mixed with an anticancer drug has been widely performed to treat HCC[11-13]. TAE can block hepatic arterial blood flow and attenuate the cooling effect of tumoral arterial blood flow. Recently, many clinical studies have shown that RF combined with TAE is effective on large HCC lesions[14,15].

In the present study, we evaluated whether TAE with iodized oil can increase RF-induced coagulation necrosis, and what modifications and effects are added in terms of ablation time, maximum output, and portal angiography by TAE with iodized oil.

MATERIALS AND METHODS

Animals and animal care

Approval of the institutional committee for the care of research animals was obtained before the study was initiated. This study was conducted in accordance with the guideline for the care and use of laboratory animals.

Ten healthy male pigs (weighing 52-59 kg; mean, 56.6 kg) were subjected to laparotomy under general anesthesia. The animals were sedated with an intramuscular injection of ketamine (5 mg/kg weight), xylazine (5 mg/kg weight), and atropine (0.02 mg/kg weight). General anesthesia was maintained with 1.5% fluothane containing a mixture of oxygen and nitrous oxide after tracheal intubation. Cardiac and respiratory parameters were monitored throughout the procedures. A longitudinal midline abdominal incision was made, and the peritoneum was opened. A 4 Fr. catheter (RC2; Clinical Supply, Gifu, Japan) was inserted into the proper hepatic artery *via* the femoral artery. The portal vein was exposed and punctured directly, and the 4 Fr. catheter was inserted. Hepatic arteriography and direct portography were performed before and after RFA. Hepatic arteriography was performed with an injection of contrast agent (Iomeprol 350 Ezai, Tokyo, Japan) at a rate of 3 mL/s for a total volume of 15 mL, and direct portography at a rate of 6 mL/s for a total volume of 24 mL. TAE was performed by selectively introducing a microcatheter (Sniper; Clinical Supply, Gifu, Japan) into the right and left hepatic arteries, and injecting iodized oil (10 mL per body ; lipiodol ultra-fluid: iodine addition products of the ethylesters of the fatty acid obtained from poppyseed oil, Nihon Schering, Osaka Japan) (LP) and 1 mm gelatin sponge particles in 5 animals. Animals were divided into 2 groups of 5 animals each: RFA-alone group and RFA following TAE with iodized oil group (LP-TAE group).

RF procedure

The RF device used was a RF2000 radiofrequency ablation system (Boston Scientific Corporation, Natick, MA, USA) with an expansion-type electrode (LeVeen needle). A 17-gauge, 3.0-cm expandable 10-hook needle electrode was inserted directly into the liver with ultrasound guidance. After the needle position was confirmed with X ray and ultrasound, ablation was started. For each pig, 2 areas of the right and left lobes were ablated, yielding a total of 20 areas.

Table 1 Ablation protocol

Baseline power output	Step up rate	Maximum output	Restart output	Application process
30 W	10 W/min	Until roll-off	70% of the maximum output	Twice

The baseline power output was set at 30 W. Ablation was continued with an increase of 10 W per minute until roll-off occurred. After the first RO, ablation was resumed 30 s later at 70% of the maximum power achieved, and was completed when RO occurred a second time.

The RF 2000 generator monitors system impedance, the level of which determines the extent of tissue necrosis. In this apparatus, an increase of tissue impedance to current flow, which is caused by decreased conductivity of electrical current due to protein denaturation and loss of intracellular fluids, is measured in ohms. When tissue impedance rises above 200 Ω, the power output passively decreases to less than 10 W (roll-off). Roll-off indicates a precipitous drop of power output with a marked increase of tissue impedance because of tissue necrosis, which prohibits the passage of electrical current[16]. For all experiments, impedance and power output status were monitored on the display window of the RF2000 generator, and recorded on paper every 15 s.

A 2-phase application process was performed. The baseline power output was set at 30 W. Ablation was continued with an increase of 10 W per minute until roll-off occurred. After the first RO, ablation was resumed 30 seconds later at 70% of the maximum power achieved, and was completed when RO occurred a second time (Table 1). The total RF application time was calculated as the sum of the duration of the first and second phases of ablation.

Animals were sacrificed using an overdose of pento-barbital immediately after post-RFA angiography, and their livers were removed for gross pathologic analysis. Visible regions of coagulation necrosis were measured with calipers in fresh tissue prior to preservation. Measurements of the diameter of coagulation were based on the consensus of 2 observers. The 2 groups were compared with respect to ablation time and maximum output required for the occurrence of the second RO, as well as maximum coagulation diameter. Angiographic changes on portography before and after ablation were also compared. Data were analyzed using Student's *t*-test with a significance level of 5%.

RESULTS

Both cardiac and respiratory parameters remained stable throughout the experiments. No thermal injuries to adjacent structures or organs occurred. Regions of RF ablation were easily distinguished from untreated tissue.

For the RFA-alone group and LP-TAE group, total ablation times were 445.1 ± 35.9 s and 320.6 ± 30.9 s, maximum outputs were 87.0 ± 4.83 W and 69.0 ± 7.38 W, and maximal diameters of coagulation were 33.2 ± 2.28 mm and 41.7 ± 3.85 mm, respectively (Table 2). Significant reductions of ablation time and maximum output and significantly larger coagulation diameter were obtained with

Table 2 Ablation time to roll-off, maximum output, and coagulation diameter

	Group with RFA alone	Group with RFA following LP-TAE	*P* value
Ablation time to roll-off (s)	445.1 ± 35.9	320.6 ± 30.9	*P* < 0.05
Maximum output (W)	87.0 ± 4.83	69.0 ± 7.38	*P* < 0.05
Coagulation diameter (mm)	33.2 ± 2.28	41.7 ± 3.85	*P* < 0.05

Significant reductions in roll-off time and output and significantly greater coagulation diameter were obtained with RFA following LP-TAE compared with RFA alone. LP-TAE: Transcatheter arterial embolization with iodized oil (Lipiodol); RFA: radiofrequency ablation.

Figure 3 Portography showing large branches of portal veins have disappeared (arrow) after RFA following LP-TAE.
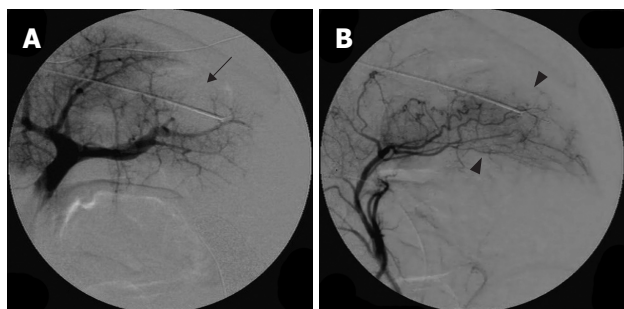
Figure 1 Portography revealing occlusion of distal small portal vein branches in the ablated area (arrow) (**A**) and hepatic arteriography showing a compensatory increase in hepatic arterial blood flow in response to occlusion of the portal vein branches (arrow head) (**B**) in group with RFA **alone**.
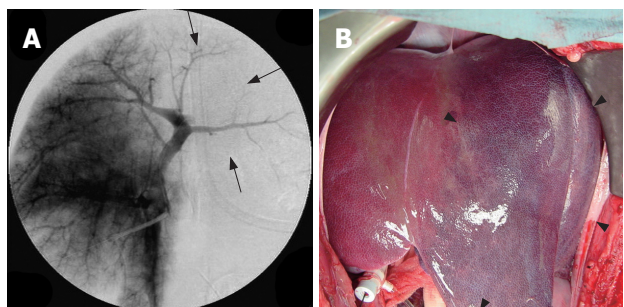
Figure 2 Portography revealing a decrease of portal venous blood flow in the left lobe after LP-TAE before RFA (arrow) (**A**) and photograph of liver showing the dark red left lobe after LP-TAE before RFA (arrow head) (**B**).

Figure 4 Region of necrosis avoiding large vessels (white arrow) in group with RFA alone (**A**), and showing ill-defined boundaries of coagulation necrosis and increase of the necrotic area in the group with RFA following LP-TAE (B).

RFA following LP-TAE compared to RFA alone.

In the RFA-alone group, disappearance of the small distal branches of the portal vein was observed on portography (Figure 1A), and a compensatory increase of hepatic arterial blood flow was noted on hepatic arteriography (Figure 1B). Subsegmental or distal portal branches disappeared in 8 ablated areas (80%), and segmental portal branches disappeared in 2 ablated areas (20%) on portography.

After LP-TAE, portal venous blood flow was decreased (Figure 2A) and the liver- enforced LP-TAE changed to dark red (**Figure 2B**). **Disappearance of blood flow in large portal branches was recognized after RFA following LP-TAE** (Figure 3). Segmental portal branches or larger branches such as the primary branch of the portal vein disappeared in 8 ablated areas (80%) on portography.

Gross examination revealed a gray core of ablated tissue surrounded by a dark rim in all ablation areas. The RFA-alone group exhibited coagulation necrosis with sparing of large vessels (Figure 4A). In the LP-TAE group, the boundaries of coagulation necrosis were ill-defined, and the diameters of necrotic areas were increased (Figure 4B).

DISCUSSION

The results of the present study demonstrate that RF ablation following TAE with iodized oil induce a larger coagulation necrosis with lower output and shorter ablation time than with RFA alone. To our knowledge, this is the first formal animal study evaluating the effects of combined RFA and TAE with iodized oil on ablation time, maximum power output, and portal angiographic changes.

Radiofrequency tumor ablation has been demonstrated to be a reliable method for creating heat-induced coagulation necrosis using a percutaneous approach[17]. A

RF electrode is inserted into the tumor under ultrasound guidance. After attachment to the appropriate generator, a radiofrequency current is emitted from the electrode. RF energy can cause localized cell desiccation and necrosis. Radiofrequency current is emitted from the exposed, non-insulated portion of the electrode, and ion agitation is produced within the tissues surrounding the electrode. This agitation is converted by friction into heat, inducing cellular death *via* coagulation necrosis[18]. When the temperature within the tissue rises above 60℃, a region of necrosis surrounding the electrode begins to develop[19]. The extent of RF-induced coagulation necrosis depends on overall energy deposition, the duration of radiofrequency application, and radiofrequency electrode tip length[20]. A larger coagulation necrosis is formed with a 3.0 cm expandable electrode than with a 2.0 cm expandable electrode.

RF-induced heating is limited by perfusion-mediated vascular cooling[6,7]. A reduction of blood flow during RF application has been shown to increase coagulation necrosis in animal models[7-10]. Goldberg *et al*[7] applied RF to normal *in vivo* porcine liver with and without balloon occlusion of the portal vein and the hepatic artery, and found that greater coagulation could be achieved during portal venous occlusion. Chinn *et al*[9] compared 4 vascular occlusion groups: portal vein, hepatic artery, both hepatic artery and portal vein, and no occlusion, and reported that coagulation volume is the greatest with occlusion of both hepatic artery and portal vein. Sugimori *et al*[21] applied RF to normal pig livers using a 15-gauge LeVeen needle with a 2.0 cm expandable electrode at the maximum output of 60 w after transcatheter arterial infusion (TAI) of iodized oil, TAE with gelatin sponge, and TAE with iodized oil and gelatin sponge. They reported that RF ablation after TAE with iodized oil and gelatin sponge induces the largest coagulation necrosis, but there are no significant differences in RF ablation times with RFA alone and RFA combined TAE. In the present study, we applied RF to normal pig livers using a 17-gauge 3.0 cm expandable electrode until roll-off, and compared ablation time, maximum power output, and coagulation diameter between RFA alone and RFA following TAE with iodized oil and gelatin sponge, demonstrating that RF ablation following TAE with iodized oil and gelatin sponge could induce a larger coagulation necrosis with a lower output and a shorter ablation time than RFA alone with a significant difference. It is suggested that the cooling effects of blood flow are greater, so ablation range and expansion diameter of electrode are large.

Arterioportal communications occur through the sinusoids (transsinusoidal communications) and the peribiliary vascular plexus (transplexal communications)[22,23]. It is postulated that when more than a certain amount of iodized oil (lipiodol) is pooled in the sinusoids, a change occurs in the hepatic microcirculation and iodized oil flows into the portal vein through arterioportal communications after pooling in the sinusoids[24]. Therefore, injection of iodized oil into the hepatic artery results in a retrograde flow to the portal vein through the sinusoids and occlusion of portal vein branches[25]. Both hepatic artery and branches of the portal vein are simultaneously blocked after TAE with iodized oil, and perfusion-mediated vascular cooling

effect limiting RF-induced coagulation necrosis is thus reduced. As a result, a larger coagulation necrosis is formed with lower output and shorter ablation time than with RFA alone. Furthermore, disappearance of blood flow in large portal branches was recognized after RFA following TAE with iodized oil in the present study, however, the necrosis achieved with RFA alone avoided the large vessels, probably due to the cooling effect of blood flow.

Because HCCs are hypervascular tumors and have abundant tumoral arterial blood flow, which diminishes radiofrequency wave heating, higher power output ablation compared to normal liver tissue is required until roll-off in opposition to the cooling effect. However, high-output RF ablation by RFA alone results in boiling and carbonization of the tissue near the electrode[7,19], leaving an incompletely ablated tumor, and increases the frequency of puncture and the risk of dissemination. It is presumed that scattered recurrence or rapid tumor growth after RFA is attributable to a rapid increase of local tissue temperature and intratumoral pressure due to high-output ablation, and bumping (explosion) in the early process of ablation might cause a spreading of incompletely ablated neoplastic cells *via* the portal vein[26-30]. Moreover, with RFA alone, a compensatory increase of hepatic arterial blood flow in r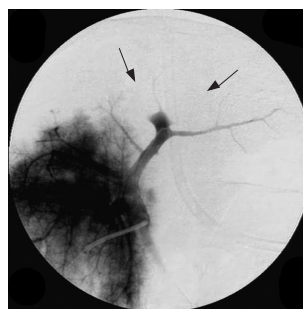esponse to occlusion of the portal vein branches after RFA might be related to a rapid growth of residual tumors. Because TAE with iodized oil can block hepatic arterial and portal blood flow and attenuate the vascular cooling effect, RF ablation with a low output for hypervascular hepatic tumors is enabled by combining TAE with iodized oil. Low output RF ablation combined with TAE with iodized oil can prevent a rapid increase of local tissue temperature and intra-tumoral pressure, and may prevent intraportal disseminations and intrahepatic scattered recurrence. Furthermore, TAE with iodized oil prior to RFA can cause ischemic necrosis of the tumors, thereby decreasing the number of neoplastic cells, which can reduce the risk of dissemination even if bumping (explosion) occurs. Our results strongly suggest that a combination of **low output RFA and TAE with** iodized oil might be efficacious for treating hypervascular large hepatic tumors without complications such as scattered recurrence or rapid tumor growth.

In conclusion, reduction of arterial and portal blood flow due to TAE with iodized oil before RF increases coagulation necrosis with lower output and shorter ablation time than with RFA alone. Strategies for combining RFA with TAE with iodized oil to reduce tumoral blood flow might improve treatment effect on hypervascular large hepatic tumors.

REFERENCES

1   **Livraghi T**, Goldberg SN, Lazzaroni S, Meloni F, Ierace T, Solbiati L, Gazelle GS. Hepatocellular carcinoma: radio-frequency ablation of medium and large lesions. *Radiology* 2000; **214**: 761-768

2   **Rossi S**, Di Stasi M, Buscarini E, Quaretti P, Garbagnati F, Squassante L, Paties CT, Silverman DE, Buscarini L. Percutaneous RF interstitial thermal ablation in the treatment of hepatic cancer. *AJR Am J Roentgenol* 1996; **167**: 759-768

3   **Lencioni R**, Cioni D, Bartolozzi C. Percutaneous radiofrequency thermal ablation of liver malignancies: techniques, indications, imaging findings, and clinical results. *Abdom Imaging*

2001; **26**: 345-360

4   **Rossi S**, Buscarini E, Garbagnati F, Di Stasi M, Quaretti P, Rago M, Zangrandi A, Andreola S, Silverman D, Buscarini L. Percutaneous treatment of small hepatic tumors by an expandable RF needle electrode. *AJR Am J Roentgenol* 1998; **170**: 1015-1022

5   **Goldberg SN**, Gazelle GS, Solbiati L, Livraghi T, Tanabe KK, Hahn PF, Mueller PR. Ablation of liver tumors using percutaneous RF therapy. *AJR Am J Roentgenol* 1998; **170**: 1023-1028

6   **Goldberg SN**, Gazelle GS. Radiofrequency tissue ablation: physical principles and techniques for increasing coagulation necrosis. *Hepatogastroenterology* 2001; **48**: 359-367

7   **Goldberg SN**, Hahn PF, Tanabe KK, Mueller PR, Schima W, Athanasoulis CA, Compton CC, Solbiati L, Gazelle GS. Percutaneous radiofrequency tissue ablation: does perfusion-mediated tissue cooling limit coagulation necrosis? *J Vasc Interv Radiol* 1998; **9**: 101-111

8   **Patterson EJ**, Scudamore CH, Owen DA, Nagy AG, Buczkowski AK. Radiofrequency ablation of porcine liver in vivo: effects of blood flow and treatment time on lesion size. *Ann Surg* 1998; **227**: 559-565

9   **Chinn SB**, Lee FT Jr, Kennedy GD, Chinn C, Johnson CD, Winter TC 3rd, Warner TF, Mahvi DM. Effect of vascular occlusion on radiofrequency ablation of the liver: results in a porcine model. *AJR Am J Roentgenol* 2001; **176**: 789-795

10   **Sugimori K**, Morimoto M, Shirato K, Kokawa A, Tomita N, Saito T, Nozawa A, Hara M, Sekihara H, Tanaka K. Radiofrequency ablation in a pig liver model: effect of transcatheter arterial embolization on coagulation diameter and histologic characteristics. *Hepatol Res* 2002; **24**: 164

11   **Yamada R**, Sato M, Kawabata M, Nakatsuka H, Nakamura K, Takashima S. Hepatic artery embolization in 120 patients with unresectable hepatoma. *Radiology* 1983; **148**: 397-401

12   **Nakamura H**, Hashimoto T, Oi H, Sawada S. Transcatheter oily chemoembolization of hepatocellular carcinoma. *Radiology* 1989; **170**: 783-786

13   **Uchida H**, Ohishi H, Matsuo N, Nishimine K, Ohue S, Nishimura Y, Maeda M, Yoshioka T. Transcatheter hepatic segmental arterial embolization using lipiodol mixed with an anticancer drug and Gelfoam particles for hepatocellular carcinoma. *Cardiovasc Intervent Radiol* 1990; **13**: 140-145

14   **Buscarini L**, Buscarini E, Di Stasi M, Quaretti P, Zangrandi A. Percutaneous radiofrequency thermal ablation combined with transcatheter arterial embolization in the treatment of large hepatocellular carcinoma. *Ultraschall Med* 1999; **20**: 47-53

15   **Rossi S**, Garbagnati F, Lencioni R, Allgaier HP, Marchiano A, Fornari F, Quaretti P, Tolla GD, Ambrosi C, Mazzaferro V, Blum HE, Bartolozzi C. Percutaneous radio-frequency thermal ablation of nonresectable hepatocellular carcinoma after occlusion of tumor blood supply. *Radiology* 2000; **217**: 119-126

16   **Cabassa P**, Donato F, Simeone F, Grazioli L, Romanini L. Radiofrequency ablation of hepatocellular carcinoma: long-term experience with expandable needle electrodes. *AJR Am J Roentgenol* 2006; **186**: S316-S321

17   **McGahan JP**, Browning PD, Brock JM, Tesluk H. Hepatic ablation using radiofrequency electrocautery. *Invest Radiol* 1990; **25**: 267-270

18   **Cosman ER**, Nashold BS, Ovelman-Levitt J. Theoretical aspects of radiofrequency lesions in the dorsal root entry zone. *Neurosurgery* 1984; **15**: 945-950

19   **Goldberg SN**, Gazelle GS, Halpern EF, Rittman WJ, Mueller PR, Rosenthal DI. Radiofrequency tissue ablation: importance of local temperature along the electrode tip exposure in determining lesion shape and size. *Acad Radiol* 1996; **3**: 212-218

20   **Goldberg SN**, Gazelle GS, Dawson SL, Rittman WJ, Mueller PR, Rosenthal DI. Tissue ablation with radiofrequency: effect of probe size, gauge, duration, and temperature on lesion volume. *Acad Radiol* 1995; **2**: 399-404

21   **Sugimori K**, Nozawa A, Morimoto M, Shirato K, Kokawa A, Saito T, Numata K, Tanaka K. Extension of radiofrequency ablation of the liver by transcatheter arterial embolization with iodized oil and gelatin sponge: results in a pig model. *J Vasc Interv Radiol* 2005; **16**: 849-856

22   **Cho KJ**, Lunderquist A. The peribiliary vascular plexus: the microvascular architecture of the bile duct in the rabbit and in clinical cases. *Radiology* 1983; **147**: 357-364

23   **Itai Y**, Matsui O. Blood flow and liver imaging. *Radiology* 1997; **202**: 306-314

24   **Miller DL**, O'Leary TJ, Girton M. Distribution of iodized oil within the liver after hepatic arterial injection. *Radiology* 1987; **162**: 849-852

25   **Nakamura H**, Hashimoto T, Oi H, Sawada S. Iodized oil in the portal vein after arterial embolization. *Radiology* 1988; **167**: 415-417

26   **Nicoli N**, Casaril A, Hilal MA, Mangiante G, Marchiori L, Ciola M, Invernizzi L, Campagnaro T, Mansueto G. A case of rapid intrahepatic dissemination of hepatocellular carcinoma after radiofrequency thermal ablation. *Am J Surg* 2004; **188**: 165-167

27   **Ruzzenente A**, Manzoni GD, Molfetta M, Pachera S, Genco B, Donataccio M, Guglielmi A. Rapid progression of hepatocellular carcinoma after Radiofrequency Ablation. *World J Gastroenterol* 2004; **10**: 1137-1140

28   **Kotoh K**, Enjoji M, Arimura E, Morizono S, Kohjima M, Sakai H, Nakamuta M. Scattered and rapid intrahepatic recurrences after radio frequency ablation for hepatocellular carcinoma. *World J Gastroenterol* 2005; **11**: 6828-6832

29   **Kotoh K**, Morizono S, Kohjima M, Enjoji M, Sakai H, Nakamuta M. Evaluation of liver parenchymal pressure and portal endothelium damage during radio frequency ablation in an in vivo porcine model. *Liver Int* 2005; **25**: 1217-1223

30   **Nakai M**, Shiraki T, Higashi K, Maeda M, Sahara S, Takeuchi N, Kimura M, Terada M, Sato M. Low-output radiofrequency ablation combined with transcatheter arterial oily-chemoembolization for hepatocellular carcinoma. *Nippon Igaku Hoshasen Gakkai Zasshi* 2005; **65**: 124-126

Assessment of hepatic fibrosis in pediatric cases with hepatitis C virus in Egypt

Manal A El-Hawary, Mona S El-Raziky, Gamal Esmat, Hanan Soliman, Amr Abouzied, Maissa El-Raziky,

Wafaa El-Akel, Rokaya El-Sayed, Fatma Shebl, Abdel Aziz Shaheen, Hanaa El-Karaksy

Manal A El-Hawary, Department of Pediatrics, Fayoum University, Egypt
Mona S El-Raziky, Rokaya El-Sayed, Hanaa El-Karaksy, Department of Pediatrics, Cairo University, Egypt
Gamal Esmat, Maissa El-Raziky, Wafaa El-Akel, Department of Tropical Medicine, Cairo University, Egypt
Hanan Soliman, Department of Pathology, Cairo University, Egypt
Amr Abouzied, Abdel Aziz Shaheen, Department of Tropical Medicine, Hepatitis C Project, Egypt
Fatma Shebl, Department of Public Health, National Liver Institute, Egypt
Correspondence to: Manal A EL-Hawary, MD, Associate Professor of Pediatrics, Faculty of Medicine-Fayoum University, Postal address: 3 Mossadak street, Dokki, Cairo, Egypt. manalelhawary@yahoo.com
Telephone: +20-2-7600350 Fax: +20-10-1584525
Received: 2007-02-01   Accepted: 2007-03-01

Abstract

AIM: To assess hepatic fibrosis and factors associated with its progression in children with HCV infection.

METHODS: At the Hepatology Unit, Cairo University Children's Hospital, a single liver biopsy was performed to 43 children with HCV infection after an informed consent between 1998-2004. Their mean age at liver biopsy was 8.67 ± 4.3 years.

RESULTS: Among the 43 patients' biopsies, 12 (27.9%) were having no fibrosis, 20 (46.5%) mild fibrosis and 11 (25.6%) moderate to severe fibrosis. The median time for development of fibrosis was estimated to be 5.5 years. Developing fibrosis was significantly associated with shorter duration from first detected ALT elevation to biopsy (12 mo *vs* 1.2 mo, $P = 0.015$) and having higher levels of direct serum bilirubin (0.3 mg/dL *vs* 0.5 mg/dL, $P = 0.048$). No association was found between fibrosis stage and the presence of co-morbid conditions ($P = 0.33$).

CONCLUSION: Hepatic fibrosis was present in 72.1% of children with HCV infection. The development of fibrosis was associated with higher levels of direct serum bilirubin. There was no significant association between fibrosis and age, duration of infection, risk factors, co-morbid conditions and most biochemical parameters.

INTRODUCTION

Egypt has the highest prevalence of hepatitis C virus (HCV) infection in the world, averaging 12%-24% in the general population[1]. HCV Genotype 4 is the prevailing genotype in Egypt (90%)[2].

Worldwide, the major clinical consequence of chronic hepatitis C infection is the progression to cirrhosis and its potential complications: hemorrhage, hepatic insufficiency, and primary liver cancer[3]. The current understanding of HCV infection has been advanced by the concept of liver fibrosis progression[4].

A main characteristic of HCV infection is the highly variable course of its natural history[5]. A major challenge is to distinguish the disease progression in patients according to those possessing specific risk factors[6]. Higher risk of disease progression is associated with older age, male gender, excessive alcohol consumption, overweight and immunodeficiency[7]. The role of the liver biopsy in chronic hepatitis C would seem, at first, to be unquestioned. After all, a liver biopsy provides much information in such a small package. It provides confirmation of the diagnosis, exclusion of other liver diseases, and assessment of the grade and stage of the disease[8]. Furthermore, the usefulness of the liver biopsy in chronic hepatitis C has received the endorsement of several national and international consensus conferences on the diagnosis and treatment of hepatitis C[9,10].

The outcome of HCV infection acquired in childhood is uncertain as a result of the variation of clinical course of infection and disease in children[11]. HCV infection is not always benign in the childhood period, a recent study in Egypt showed that, ALT levels were elevated in half of the subjects and histological abnormalities were detected in three quarters of HCV-RNA positive cases[12]. Because of the major long-term complications of chronic HCV, and

the development of cirrhosis and end-stage liver disease, the degree of fibrosis on liver biopsy would seem to be an appropriate surrogate marker[13]. Liver biopsy remains the gold standard in assessing the stage and progression of HCV infection[14].

The aim of this work was to assess hepatic fibrosis and identify factors associated with its progression in liver biopsies from a group of Egyptian children with HCV infection. To achieve this goal, we studied factors related to HCV acquisition, co-morbid conditions, demographic factors and biochemical variables related to disease course and finally findings of liver biopsy.

MATERIALS AND METHODS

The study was carried out at the Pediatric Hepatology Unit, Cairo University Children's Hospital, Egypt, between 1998 and 2004. HCV genotype in Egypt is mostly (> 90%) genotype 4[2]. Among a total of 105 HCV infected children, on regular follow-up every 3 mo, 43 cases were fit and consented to do liver biopsy. Twenty children had blood diseases; 18 thalassemics, 1 sickle cell anemia and 1 pure red cell aplasia. Seven were treated in the past for malignancies; 4 Hodgkin lymphoma and 3 acute lymphocytic leukemia (ALL). None of the children received any therapy for HCV.

Study population
Inclusion criteria: Age below 18 years, both sexes included, HCV antibody and HCV-RNA positive, elevation of ALT, at least 1.5 folds, at least once throughout the disease course, informed consent signed by the parent of each patient.

Exclusion criteria: Co-infection with HBV or HIV, coagulopathy, or thrombocytopenia, to a degree which precludes the safe performance of a percutaneous biopsy, therapy for HCV infection, biopsies less than 10 mm long, biopsies including less than 5 portal tracts.

All parents completed a survey regarding possible risk factors for HCV acquisition.

Biochemical assessment of liver function tests (total and direct serum bilirubin, AST, ALT, albumin and prothrombin time and concentration) was done on the same day of liver biopsy which was performed only once for each patient, in addition to a complete blood count. No fresh frozen plasma or blood transfusion was offered to correct these tests prior to biopsy.

Percutaneous liver biopsy was obtained with the Menghini technique using a secure cut biopsy needle 1.6-mm-diameter needle [Hospital Service S.p.A.Via Naro, 81-00040 Pomezia (RM) Italia.

Histological evaluation
Percutaneous liver biopsies were fixed in formalin, embedded in paraffin and cut at 4 microns thickness and stained with haematoxylin and eosin and mason trichrome. Liver sections were evaluated by a single pathologist who was blinded of the patient's clinical and laboratory data. The grade of activity and stage of fibrosis were scored according to Knodell *et al*[15]. The HAI system scores necroinflammatory activity from 0 to 18 assessing periportal necrosis and inflammation (0 to 10), lobular necrosis and

inflammation (0 to 4), and portal inflammation (0 to 4). Fibrosis is staged as 0, 1, 3, or 4, with 1 indicating portal fibrosis only (mild), 3 indicating bridging fibrosis (moderate), and 4 cirrhosis (extensive). The discontinuous scale allows for clear separation of mild (1+) from extensive (3+). The HAI system is simple and has been widely used. We considered moderate and extensive fibrosis as one group because of their small numbers. Liver iron deposition was evaluated by using the scale developed by Deugnier *et al*[16]. This scoring system was defined as the sum of three scores: hepatocytic iron score (0-36), sinusoidal iron score (0-12), and portal iron score (0-12). The sum of these scores defines the total iron score (TIS; range: 0-60). According to Halonen *et al*[17], liver TIS is classified into mild iron overload (TIS 0-14), moderate iron overload (TIS 15-29) and severe iron overload (TIS 30-60). Steatosis was graded based on percent of hepatocytes involved; mild (< 33%), moderate (33%-66%) and severe (> 66%)[18].

Statistical analysis
Frequency analysis of categorical variables was presented as numbers and percentages. Chi square or Fischer's exact tests were used to assess the association between hepatic fibrosis and various categorical factors. Descriptive analysis of continuous variables was presented by median and range. Kruskal Wallis test was used to compare groups of no, moderate and marked fibrosis. Kendall's tau test was used to assess the correlation between fibrosis stage and other continuous variables. Cumulative hazard function for developing fibrosis among patients was done. In all tests, *P* < 0.05 was considered significant.

RESULTS

The present study included 43 HCV infected infants and children (24 boys and 19 girls); their mean age at liver biopsy was 8.67 ± 4.3 years (median age 9 years, range 2 mo-18 years). The estimated median duration of infection was 36 mo.

Twelve biopsies showed no fibrosis, 20 showed mild fibrosis and 11 had moderate to severe fibrosis. Iron staining was not detected in 19 cases, 15 had mild TIS, 9 had moderate TIS and no cases had severe TIS. Steatosis was absent in 30 cases, mild in 5 cases, moderate in 6 cases and severe in 2 cases.

According to the parents' responses to a survey regarding risk factors for HCV acquisition, risk factors were identified in 39 cases (90.7%). Risk factors included blood transfusion (37 cases), injections (11 cases), surgical procedures (8 cases) and (1 case) household contact infected with HCV. Among the 39 patients with known risk factors, a reliable estimate of the duration of infection was possible in only 29 cases.

Analysis of factors that could be associated with development of fibrosis in these patients was performed. Development of fibrosis was not associated with gender, elevated ALT and AST, blood transfusion, injections, surgical procedures, having a family member with HCV or having blood disease. The analysis revealed that all 7 cases that had past malignant disease had fibrosis in their liver

Table 1 Characteristic features of studied patients *n* = 43			
	No Fibrosis (*n* = 12)	Fibrosis (*n* = 31)	*P* value
Sex			
Boys	8	16	0.37 (NS)
Girls	4	15	
High ALT (*n* = 28)	7	21	0.72 (NS)
Injections (*n* = 11)	2	9	0.41 (NS)
Blood transfusion (*n* = 37)	12	25	0.10 (NS)
Frequency of transfusion			
Once	2	6	0.61 (NS)
Multiple	10	19	
Surgical procedures (*n* = 8)	4	4	0.19 (NS)
Household contact infected with HCV (*n* = 1)	0	1	0.53 (NS)
No risk factor (*n* = 4)	1	3	0.86 (NS)
Blood disease (*n* = 20)			
Red cell aplasia	1	0	0.14 (NS)
Sickle cell anemia	0	1	
Thalassemia	8	10	
Malignancy (*n* = 7)			
ALL	0	3	NA
Lymphoma	0	4	

NA: not applicable (as *P* value cannot be calculated).

biopsies (Table 1).

The higher grade of fibrosis was associated with shorter duration from first detected ALT elevation to biopsy (*P* = 0.015) and higher levels of direct bilirubin (*P* = 0.048) (Table 2).

There was no association between the fibrosis stage and the presence of co-morbid condition (having blood disease or previous malignancies) (*P* = 0.33) (Table 3).

The risk for development of fibrosis, from the time of exposure to infection to the time of biopsy, was estimated in only 29 cases with a reliable duration of infection (1-10 years) and was expressed in a hazard function curve. Accordingly, liver biopsy was performed in 9 patients after an estimated duration of infection of one year. 8 of them had fibrosis, which was extensive in 3 patients. Similarly, when 6 of the 29 patients had liver biopsy ten years after exposure to infection, 4 of them had fibrosis (which was extensive in 3 cases, mild in one) and two had no fibrosis. The median time for fibrosis development in liver biopsy was estimated to be 63.7 mo (5.5 years) (Figure 1).

DISCUSSION

This is one of few studies to assess factors associated with fibrosis progression using liver biopsies from HCV infected children. The purpose of the study was to determine whether any baseline demographic, clinical, biochemical or histological factors could be associated with fibrosis stage.

Seventy-two percent of our cases showed some degree of fibrosis, 47% mild fibrosis and 25% moderate to extensive. Guido *et al*[19] reported a similar proportion of fibrosis in their HCV infected children.

Analysis of the risk factors for acquisition of HCV revealed no association with fibrosis. El-Shorbagy *et al*[20] reported that liver fibrosis progression is related to the mechanism of transmission. In contrast, Kage *et al*[21] and Vogt *et al*[22] described a relatively benign course for trans-

fusion associated hepatitis C. Although the studies presented earlier may suggest that the route of transmission may be a contributing factor in the course (mother-to-infant *vs* transfusional), it is not known which patients are most likely to develop end-stage liver disease.

Although we noticed that there was a steady increase in age with increasing fibrosis, the difference did not reach statistical significance. Similar results were reported by Marcellin *et al*[7] where age was not a statistically significant feature associated with progression of fibrosis in patients with chronic HCV. Alternatively, some studies reported age to be an important factor in prediction of fibrosis but were predominantly reported in adults[4,23].

Only three cases had cirrhosis in our study. These results are similar to those reported by Guido *et al*[24] and Badizadegan *et al*[25]. However, 44% of the cases in the latter study had moderate to severe fibrosis as compared to 25% in our series. This might be explained by the older mean age of their cases compared to ours (11.4 *vs* 8.7 years). Kage *et al*[21] reported that 97% of their cases had mild fibrosis and none had cirrhosis. The mean age of their patients was 3.7 years.

Although the hazard of development of fibrosis increased with the duration of the disease (Figure 1), a longer duration of infection does not necessarily mean more extensive fibrosis. Overall, it is thought that hepatic inflammation drives the progression of fibrosis to cirrhosis in a relatively linear manner. However, progression is not linear in all patients[26]. In historical studies, approximately 20% of patients who developed post-transfusion non-A non-B hepatitis, now known to have been HCV, developed cirrhosis within 20 years of infection[27], but these data may have been skewed by selection of those with more severe disease at presentation. More recently large cross-sectional studies have assessed the rate of progression of HCV related hepatic fibrosis retrospectively using a ratio of the stage of hepatic fibrosis to the estimated duration of infection, such as the time from initial exposure to intravenous drugs or from transfusion[4,28]. A median time to cirrhosis of 30 years was observed[4]. However this finding obscured the observation that the median time to cirrhosis was 13 years in those infected over the age of 40. These had consumed alcohol to excess, while those infected at an earlier age and did not abuse alcohol had a median time to cirrhosis of 42 years. Notably, 32% were thought unlikely to develop progressive disease. These findings were based on a single liver biopsy and the rate of fibrosis was calculated assuming a uniform rate of progression, although no data exists to indicate whether progression occurs in a linear fashion or more erratically[29]. Poynard *et al*[30] observed that fibrosis progression was not normally distributed. The distribution suggested at least 3 populations: "rapid fibrosers", "intermediate fibrosers" and "slow fibrosers".

Male gender was not associated with fibrosis in this study. In adults, male gender seems to be associated with fibrosis, particularly in those above 40 years of age who had history of drinking > 50 g alcohol/day[4].Other studies failed to demonstrate the association of male gender with fibrosis stage[31].

Our observation determined that direct serum bilirubin

Table 2 Analysis of data among patients with no, mild and moderate to extensive fibrosis (Kruskal Wallis test)

	No fibrosis (*n* = 12) Median (min-max)	Mild fibrosis (*n* = 20) Median (min-max)	Moderate to extensive fibrosis (*n* = 11) Median (min-max)	*P*
Age at biopsy	9 (3.5 yr-13 yr)	7.3 (1 yr-19 yr)	11 (2 mo-18 yr)	0.394 (NS)
Duration from exposure to biopsy (mo) (*n* = 29)	43.8 (12-144)	36 (12-120)	12 (2.4-144)	0.627 (NS)
Duration from first detected ALT elevation to biopsy (mo)	12 (0-24)	6 (0-24)	1.2 (0-7.2)	0.015 (S)
Duration from exposure to first detected ALT elevation (mo) (*n* = 29)	30 (12-132)	18 (0-119)	12 (1.2-141)	0.411 (NS)
Total bilirubin (mg/dL)	1.65 (0.-5.2)	0.8 (0.3-4.3)	1.5 (0.4-11)	0.270 (NS)
Direct bilirubin (mg/dL)	0.3 (0.1-2.5)	0.2 (0.1-1.3)	0.5 (0.1-10)	0.048 (S)
ALT (IU/L)	77 (17-367)	88 (16-432)	97 (30-1200)	0.649 (NS)
AST (IU/L)	69 (27-273)	84 (28-415)	96 (26-927)	0.912 (NS)
Albumin (mg/dL)	3.6 (2.9-4.7)	4.2 (3.1-5.3)	3.1 (2.8-4.7)	0.119 (NS)
Prothrombin Concentration (%)	80 (66-100)	87 (60-100)	80 (55-97)	0.458 (NS)
Platelets count (thousands/mm^3)	333 (110-284)	266 (138-396)	306 (95-302)	0.329 (NS)
HAI	5 (0-11)	5 (0-10)	4 (0-9)	0.574 (NS)
TIS	9 (0-27)	3 (0-18)	9 (0-18)	0.49 (NS)
Steatosis	*n* = 12	*n* = 20	*n* = 11	
None (*n* = 30)	10	13	7	0.61 (NS)
Mild (*n* = 5)	0	4	1	
Moderate (*n* = 6)	2	2	2	
Severe (*n* = 2)	0	1	1	

Table 3 Association of fibrosis stage with co-morbid condition

	Fibrosis groups			Total
	No fibrosis *n* = 12	Minimal fibrosis *n* = 20	Extensive fibrosis *n* = 11	
Without co-morbid condition	3	7	6	16
With co-morbid condition	9	13	5	27

P = 0.33 (NS).

Figure 1 Cumulative hazard of fibrosis development.

correlated significantly with higher grades of fibrosis as was also reported by Ghany *et al*[13].

The relationship between serum ALT and liver disease progression remains controversial. Although the mean value of ALT appeared to increase hand in hand with degree of fibrosis, yet the results did not reach statistical significance (Table 2). Ghany *et al*[13] found that the magnitude of elevated ALT and AST levels were most predictive of more rapid fibrosis progression. In cross-sectional studies, serum ALT levels have correlated weakly with disease activity and little or not at all with hepatic fibrosis[7]. Recent reports state that it is recognized that even patients with normal ALT do not necessarily have inactive disease by histopathological evaluations. This confirms the value of liver biopsy prior to initiation of antiviral therapy to identify those who will benefit from therapy[10].

What was interesting in our results was the duration from 1st detected ALT elevation to development of fibrosis. This duration was significantly shorter in those developing moderate to extensive fibrosis. This signifies that the earlier the ALT elevation in the course of hepatitis C, the more extensive fibrosis will be. This indirectly points to the importance of ALT elevation in association

with fibrosis. In addition, liver fibrosis was reported to be considerably slower in HCV-infected patients with normal, as compared with elevated, ALT levels[32,33].

In the present study, we could not find an association between fibrosis and necro-inflammation. Similarly, other studies did not show an association between inflammation and fibrosis progression[34,35]. On a single liver biopsy, there is little or no correlation between severity of the necroinflammatory activity and degree of fibrosis[4,36]. In a cohort of 123 patients, Ghany et al[13] identified age, ALT, and periportal inflammation as independent predictors of fibrosis progression from a dataset that included viral, demographic, biochemical, and histologic factors.

Poynard et al[30] found that although fibrosis stage and inflammatory grade were correlated, however, there was discordance in 36% of their patients. Accordingly, they reported that activity grade, which represents necrosis is not a good predictor of fibrosis progression, but fibrosis alone is the best marker of ongoing fibrogenesis.

We reported positive iron staining in 55% of our cases. Iron accumulation was less frequently reported by Badizadegan et al[25] and Guido et al[24] (22% and 8.7% respectively). Forty percent of our cases were thalassemics which explains the high incidence of iron staining in our study. The role of hepatic iron stores in hepatic damage caused by HCV infection is unclear. Transfusional hemosiderosis has been recognized to play a significant role in the development of chronic liver disease, as liver fibrosis and cirrhosis are well-known complications in thalassemia and sickle cell anemia[37]. Among our studied cases, mean TIS showed no statistically significant difference between the various fibrosis groups as previously reported by Haque et al[38] and Boucher et al[39].

Steatosis was present in nearly one-third of our cases, but was severe in only 2 cases one with mild and the other with moderate to extensive fibrosis. Steatosis is a frequent finding in chronic hepatitis C, with between 40% and 70% (mean 55.9%) of such biopsies showing some degree of fibrosis[8,40,41]. It was suggested that the concurrence of steatosis and chronic HCV may be synergistic in causing hepatic fibrosis[7]. Perumalswami et al[42] reported that initial hepatic steatosis did not predict the degree of fibrosis progression on follow up.

Presence of co-morbid condition (blood disease or malignancy) did not affect the grade of fibrosis. Although during treatment of malignancies patients are exposed to periods of immune deficiency, the most pronounced immune deficient state that was reported to be associated with fibrosis progression was co-infection with HIV[4,43] and liver transplant recipients[44,45]. None of our patients was HIV positive.

In conclusion, 72.1% of children with HCV infection have hepatic fibrosis. The development of fibrosis was associated with higher levels of direct serum bilirubin. There was no significant association between fibrosis and age, duration of infection, risk factors, co-morbid conditions and most biochemical parameters.

REFERENCES

1   Abdel-Wahab MF, Zakaria S, Kamel M, Abdel-Khaliq MK, Mabrouk MA, Salama H, Esmat G, Thomas DL, Strickland GT. High seroprevalence of hepatitis C infection among risk groups in Egypt. Am J Trop Med Hyg 1994; 51: 563-567

2   Chamberlain RW, Adams N, Saeed AA, Simmonds P, Elliott RM. Complete nucleotide sequence of a type 4 hepatitis C virus variant, the predominant genotype in the Middle East. J Gen Virol 1997; 78: 1341-1347

3   WHO. Hepatitis C: global prevalence. Wkly Epidemiol Rec 1997; 72: 341–344

4   Poynard T, Bedossa P, Opolon P. Natural history of liver fibrosis progression in patients with chronic hepatitis C. The OBSVIRC, METAVIR, CLINIVIR, and DOSVIRC groups. Lancet 1997; 349: 825-832

5   Seeff LB. Natural history of hepatitis C. Hepatology 1997; 26: 21S-28S

6   Danta M, Dore GJ, Hennessy L, Li Y, Vickers CR, Harley H, Ngu M, Reed W, Desmond PV, Sievert W, Farrell GC, Kaldor JM, Batey RG. Factors associated with severity of hepatic fibrosis in people with chronic hepatitis C infection. Med J Aust 2002; 177: 240-245

7   Marcellin P, Asselah T, Boyer N. Fibrosis and disease progression in hepatitis C. Hepatology 2002; 36: S47-S56

8   Kleiner DE. The liver biopsy in chronic hepatitis C: a view from the other side of the microscope. Semin Liver Dis 2005; 25: 52-64

9   National Institutes of Health Consensus Development Conference Panel statement Management of hepatitis C. Hepatology 1997; 26: 2S-10S

10   National Institutes of Health Consensus Development Conference Statement Management of Hepatitis C--June10-12, 2002. Hepatology 2002; 36: S3–S20

11   Jara P, Resti M, Hierro L, Giacchino R, Barbera C, Zancan L, Crivellaro C, Sokal E, Azzari C, Guido M, Bortolotti F. Chronic hepatitis C virus infection in childhood: clinical patterns and evolution in 224 white children. Clin Infect Dis 2003; 36: 275-280

12   El-Raziky MS, El-Hawary M, El-Koofy N, Okasha S, Kotb M, Salama K, Esmat G, El-Raziky M, Abouzied AM, El-Karaksy H. Hepatitis C virus infection in Egyptian children: single centre experience. J Viral Hepat 2004; 11: 471-476

13   Ghany MG, Kleiner DE, Alter H, Doo E, Khokar F, Promrat K, Herion D, Park Y, Liang TJ, Hoofnagle JH. Progression of fibrosis in chronic hepatitis C. Gastroenterology 2003; 124: 97-104

14   Bedossa P. Morphological aspects of the normal and pathological liver. Pathol Biol (Paris) 1999; 47: 879-885

15   Knodell RG, Ishak KG, Black WC, Chen TS, Craig R, Kaplowitz N, Kiernan TW, Wollman J. Formulation and application of a numerical scoring system for assessing histological activity in asymptomatic chronic active hepatitis. Hepatology 1981; 1: 431-435

16   Deugnier YM, Loreal O, Turlin B, Guyader D, Jouanolle H, Moirand R, Jacquelinet C, Brissot P. Liver pathology in genetic hemochromatosis: a review of 135 homozygous cases and their bioclinical correlations. Gastroenterology 1992; 102: 2050-2059

17   Halonen P, Mattila J, Suominen P, Ruuska T, Salo MK, Makipernaa A. Iron overload in children who are treated for acute lymphoblastic leukemia estimated by liver siderosis and serum iron parameters. Pediatrics 2003; 111: 91-96

18   Brunt EM, Janney CG, Di Bisceglie AM, Neuschwander-Tetri BA, Bacon BR. Nonalcoholic steatohepatitis: a proposal for grading and staging the histological lesions. Am J Gastroenterol 1999; 94: 2467-2474

19   Guido M, Bortolotti F, Leandro G, Jara P, Hierro L, Larrauri J, Barbera C, Giacchino R, Zancan L, Balli F, Crivellaro C, Cristina E, Pucci A, Rugge M. Fibrosis in chronic hepatitis C acquired in infancy: is it only a matter of time? Am J Gastroenterol 2003; 98: 660-663

20   El-Shorbagy E, Afefy AF, Ibrahem IA, Mangoud AM, Eissa MH, Sabee EI, Mahrous S, Abdel-Monem A, Ismail A, Morsy TA, Etewa S, Nor Edin E, Mostafa Y, Abouel-Magd Y, el-Sedawy M, Ragab H, el-Tokhy H, Hassan MI, Lakouz K, Abdel-Aziz K, el-Hady G, Saber M. Non-invasive markers and predictors of severity of hepatic fibrosis in HCV patients

at Sharkia Governorate, Egypt. *J Egypt Soc Parasitol* 2004; **34**: 459-478

21 **Kage M**, Fujisawa T, Shiraki K, Tanaka T, Fujisawa T, Kimura A, Shimamatsu K, Nakashima E, Kojiro M, Koike M, Tazawa Y, Abukawa D, Okaniwa M, Takita H, Matsui A, Hayashi T, Etou T, Terasawa S, Sugiyama K, Tajiri H, Yoden A, Kajiwara Y, Sata M, Uchimura Y. Pathology of chronic hepatitis C in children. Child Liver Study Group of Japan. *Hepatology* 1997; **26**: 771-775

22 **Vogt M**, Lang T, Frosner G, Klingler C, Sendl AF, Zeller A, Wiebecke B, Langer B, Meisner H, Hess J. Prevalence and clinical outcome of hepatitis C infection in children who underwent cardiac surgery before the implementation of blood-donor screening. *N Engl J Med* 1999; **341**: 866-870

23 **Bain VG**, Bonacini M, Govindarajan S, Ma M, Sherman M, Gibas A, Cotler SJ, Deschenes M, Kaita K, Jhangri GS. A multicentre study of the usefulness of liver biopsy in hepatitis C. *J Viral Hepat* 2004; **11**: 375-382

24 **Guido M**, Rugge M, Jara P, Hierro L, Giacchino R, Larrauri J, Zancan L, Leandro G, Marino CE, Balli F, Bagni A, Timitilli A, Bortolotti F. Chronic hepatitis C in children: the pathological and clinical spectrum. *Gastroenterology* 1998; **115**: 1525-1529

25 **Badizadegan K**, Jonas MM, Ott MJ, Nelson SP, Perez-Atayde AR. Histopathology of the liver in children with chronic hepatitis C viral infection. *Hepatology* 1998; **28**: 1416-1423

26 **Afdhal NH**. The natural history of hepatitis C. *Semin Liver Dis* 2004; **24** Suppl 2: 3-8

27 **Di Bisceglie AM**, Goodman ZD, Ishak KG, Hoofnagle JH, Melpolder JJ, Alter HJ. Long-term clinical and histopathological follow-up of chronic posttransfusion hepatitis. *Hepatology* 1991; **14**: 969-974

28 **Roudot-Thoraval F**, Bastie A, Pawlotsky JM, Dhumeaux D. Epidemiological factors affecting the severity of hepatitis C virus-related liver disease: a French survey of 6,664 patients. The Study Group for the Prevalence and the Epidemiology of Hepatitis C Virus. *Hepatology* 1997; **26**: 485-490

29 **Collier JD**, Woodall T, Wight DG, Shore S, Gimson AE, Alexander GJ. Predicting progressive hepatic fibrosis stage on subsequent liver biopsy in chronic hepatitis C virus infection. *J Viral Hepat* 2005; **12**: 74-80

30 **Poynard T**, Ratziu V, Benmanov Y, Di Martino V, Bedossa P, Opolon P. Fibrosis in patients with chronic hepatitis C: detection and significance. *Semin Liver Dis* 2000; **20**: 47-55

31 **Wong V**, Caronia S, Wight D, Palmer CR, Petrik J, Britton P, Alexander GJ. Importance of age in chronic hepatitis C virus infection. *J Viral Hepat* 1997; **4**: 255-264

32 **Mathurin P**, Moussalli J, Cadranel JF, Thibault V, Charlotte F, Dumouchel P, Cazier A, Huraux JM, Devergie B, Vidaud M, Opolon P, Poynard T. Slow progression rate of fibrosis in hepatitis C virus patients with persistently normal alanine transaminase activity. *Hepatology* 1998; **27**: 868-872

33 **Shiffman ML**, Stewart CA, Hofmann CM, Contos MJ, Luketic VA, Sterling RK, Sanyal AJ. Chronic infection with hepatitis C virus in patients with elevated or persistently normal serum alanine aminotransferase levels: comparison of hepatic histology and response to interferon therapy. *J Infect Dis* 2000; **182**: 1595-1601

34 **Zarski JP**, Mc Hutchison J, Bronowicki JP, Sturm N, Garcia-Kennedy R, Hodaj E, Truta B, Wright T, Gish R. Rate of natural disease progression in patients with chronic hepatitis C. *J Hepatol* 2003; **38**: 307-314

35 **Ryder SD**, Irving WL, Jones DA, Neal KR, Underwood JC. Progression of hepatic fibrosis in patients with hepatitis C: a prospective repeat liver biopsy study. *Gut* 2004; **53**: 451-455

36 **Poynard T**, Ratziu V, Charlotte F, Goodman Z, McHutchison J, Albrecht J. Rates and risk factors of liver fibrosis progression in patients with chronic hepatitis c. *J Hepatol* 2001; **34**: 730-739

37 **Angelucci E**, Muretto P, Nicolucci A, Baronciani D, Erer B, Gaziev J, Ripalti M, Sodani P, Tomassoni S, Visani G, Lucarelli G. Effects of iron overload and hepatitis C virus positivity in determining progression of liver fibrosis in thalassemia following bone marrow transplantation. *Blood* 2002; **100**: 17-21

38 **Haque S**, Chandra B, Gerber MA, Lok AS. Iron overload in patients with chronic hepatitis C: a clinicopathologic study. *Hum Pathol* 1996; **27**: 1277-1281

39 **Boucher E**, Bourienne A, Adams P, Turlin B, Brissot P, Deugnier Y. Liver iron concentration and distribution in chronic hepatitis C before and after interferon treatment. *Gut* 1997; **41**: 115-120

40 **Brunt EM**, Ramrakhiani S, Cordes BG, Neuschwander-Tetri BA, Janney CG, Bacon BR, Di Bisceglie AM. Concurrence of histologic features of steatohepatitis with other forms of chronic liver disease. *Mod Pathol* 2003; **16**: 49-56

41 **Sanyal AJ**, Contos MJ, Sterling RK, Luketic VA, Shiffman ML, Stravitz RT, Mills AS. Nonalcoholic fatty liver disease in patients with hepatitis C is associated with features of the metabolic syndrome. *Am J Gastroenterol* 2003; **98**: 2064-2071

42 **Perumalswami P**, Kleiner D, Lutchman G, et al. Hepatitis C infection and hepatic steatosis; Fibrosis is not forged in the flame of fat. *Gastroenterology* 2004; **126** (suppl 2): A-672 (Abstract 176)

43 **Sulkowski MS**, Mast EE, Seeff LB, Thomas DL. Hepatitis C virus infection as an opportunistic disease in persons infected with human immunodeficiency virus. *Clin Infect Dis* 2000; **30** Suppl 1: S77-S84

44 **Prieto M**, Berenguer M, Rayon JM, Cordoba J, Arguello L, Carrasco D, Garcia-Herola A, Olaso V, De Juan M, Gobernado M, Mir J, Berenguer J. High incidence of allograft cirrhosis in hepatitis C virus genotype 1b infection following transplantation: relationship with rejection episodes. *Hepatology* 1999; **29**: 250-256

45 **Berenguer M**, Ferrell L, Watson J, Prieto M, Kim M, Rayon M, Cordoba J, Herola A, Ascher N, Mir J, Berenguer J, Wright TL. HCV-related fibrosis progression following liver transplantation: increase in recent years. *J Hepatol* 2000; **32**: 673-684

RAPID COMMUNICATION

Experience with gemcitabine and cisplatin in the therapy of inoperable and metastatic cholangiocarcinoma

Chaiyut Charoentum, Sumitra Thongprasert, Busyamas Chewaskulyong, Sutthirak Munprakan

Chaiyut Charoentum, Sumitra Thongprasert, Busyamas Chewaskulyong, Sutthirak Munprakan, Chiang Mai University, Chiang Mai, Thailand
Correspondence to: Chaiyut Charoentum, MD, Maharaj Nakorn Chiang Mai Hospital, Department of Medicine, Faculty of Medicine, Chiang Mai University, 110 Intawaroros Road, Maung district, Chiang Mai 50200,
Thailand. ccharoen@mail.med.cmu.ac.th
Telephone: +66-53-946488 Fax: +66-53-945481
Received: 2007-02-15   Accepted: 2007-03-21

Abstract

AIM: To study the activity of gemcitabine and cisplatin in a cohort of patients with inoperable or metastatic cholangiocarcinoma.

METHODS: Chemotherapy-naive patients with pathologically proven cholangiocarcinoma, receiving treatment that consisted of gemcitabine at 1250 mg/m^2 in a 30-min infusion on d 1 and 8, and cisplatin at 75 mg/m^2 at every 21-d cycle, were retrospectively analyzed.

RESULTS: From June 2003 to December 2005, 42 patients were evaluated. Twelve patients (28%) had unresectable disease and 30 (72%) had metastatic disease. There were 28 males and 14 females with a median age of 51 years (range 33-67) and median ECOG PS of 1 (range 0-2). A total of 171 cycles were given with a median number of cycles of 4 (range 1-6). There were 0 CR, 9 PR, 11 SD and 13 PD (response rate 21%). Grade 3-4 hematologic toxicities were: anemia in 33%, neutropenia in 22% and thrombocytopenia in 5%. Non-hematologic toxicity was generally mild. No cases of febrile neutropenia or treatment-related death were noted. The median survival was 10.8 mo (range 8.4-13 mo) and progression free survival was 8.5 mo. One-year survival rate was 40%.

CONCLUSION: Our results indicate that the combination of gemcitabine and cisplatin had consistent efficacy in patients with unresectable or metastatic cholangiocarcinoma.

© 2007 The WJG Press. All rights reserved.

Key words: Gemcitabine; Cisplatin; Cholangiocarcinoma

INTRODUCTION

Cholangiocarcinoma once known as an endemic cancer in the northeastern part of Thailand is now an increasingly recognized common malignancy in the north of the country. It is one of the most difficult malignancies to diagnose and it presents late with unresectable disease. Consequently, an effective and well tolerated systemic therapy is urgently needed in the battle against this deadly disease. To date, chemotherapy has played a limited role because of its lack of activity and the overall toxicity of treatment in this high risk population. As with other gastrointestinal cancers, 5-fluorouracil (5-FU) as a single agent or in combination is the most tested drug for this disease. The wide range of activity of a 5-FU based regimen had been reported to range from 0% to 30%[1-3]. Many studies included a heterogeneous group of patients, with tumors arising from different anatomic sites along the biliary tract such as gall bladder cancer, periampullary cancer and cholangiocarcinoma, which may have a different biology and sensitivity to chemotherapy. Different chemotherapeutic agents have been evaluated in small uncontrolled studies with generally poor results. Among the lists, the nucleoside analog gemcitabine seems to be the most promising new agent with consistent data supporting efficacy and tolerability in biliary tract cancer[4,5]. We previously reported a phase II study of gemcitabine and cisplatin combination in 40 patients (38 with cholangiocarcinoma, 1 with periampullary cancer and 1 with gall bladder cancer) which produced an overall response rate of 27.5% with a median survival of 36 wk[6]. This combination has been well tolerated with predictably mild hematologic toxicity. After the completion of that study in July 2002, we continued to treat cholangiocarcinoma patients at our institution with this regimen. We hereby report the results after treatment of gemcitabine and cisplatin combination in 42 chemo-naive cholangiocarcinoma patients.

MATERIALS AND METHODS

Patients

The retrospective analysis included patients with histologically or cytologically proven unresectable or metastatic cholangiocarcinoma, seen at Maharaj Nakorn Chiang Mai Hospital. Eligibility, schema of chemotherapy, dose of medication and evaluation criteria were similar to previous reports and briefly outlined here.

Only patients with measurable disease and an ECOG performance status of 0-2 were included. All patients had to have adequate baseline organ functions, as stated in the following: absolute neutrophil count (ANC) > 1500/μL, platelet count > 100 000/μL, total serum bilirubin of 5.0 mg/dL, serum AST/ALT < 2.5 above twice the institution's normal upper limit and creatinine of less than 1.5 mg/dL. Patients who received prior chemotherapy for unresectable or metastatic cholangiocarcinoma were not included in this analysis.

Treatment

Patients received gemcitabine at 1250 mg/m^2 by short 30-min infusion on d 1 and 8, and cisplatin at 75 mg/m^2 by 1 to 2 h intravenous infusion on d 1 of every 3-wk interval for a maximum of 6 cycles. Patients were given pretreatment intravenous hydration of at least 1 L over 2 to 3 h. The patients also received mannitol diuresis and post treatment hydration. Appropriate antiemetic regimens (e.g. ondansetron and dexamethasone) were given before and after the administration of cisplatin.

Dose modification

The d 8 dose of gemcitabine was reduced by 20% if an ANC > 1000-1500/μL and platelets of > 50 000-100 000/μL were observed. If ANC and platelets were lower than the above, the d 8 dose of gemcitabine was omitted. The dose adjustment criteria also based on the worst toxicity observed during the previous course. The dose of gemcitabine was reduced by 20% for neutropenic fever or a sustained ANC of less than 500/μL or platelets less than 50 000/μL for more than 5 d. Granulocyte colony-stimulating factor (G-CSF) was generally not used.

Treatment was repeated at every 3-wk interval for a maximum of 6 cycles and was discontinued when unacceptable toxicities occurred, disease progressed or patients had intermittent illness that prevented further administration of treatment.

Patients' evaluation

Before each chemotherapy administration, the following assessments were performed and recorded: medical history with toxicity assessment, physical examination, body weight, and PS, complete blood count and differential, and serum chemistries. The patients were seen on d 1 and 8 of each treatment cycle by a physician in the outpatient clinic; toxicities were assessed at this time. Toxicities were graded according to the NCIC CTG Expanded Common Toxicity Criteria version 2.0. Tumor response was assessed according to the WHO criteria, with a CT scan or ultrasound evaluation of the indicator lesions after the second cycle of chemotherapy.

Table 1 Patient characteristics

Characteristics	No. of patients (n = 42)
Age (yr)	
Median	51
(range)	(33-67)
Sex	
Female	14 (33%)
Male	28 (67%)
ECOG performance status	
0-1	35 (83%)
2	7 (17%)
Disease	
Unresectable	12 (28%)
Metastatic disease	30 (72%)

Table 2 Major toxicity

Toxicity	%
Anemia grade 3/4	31/2
Neutropenia grade 3/4	19/2
Thrombocytopenia grade 3/4	5/0
Nephrotoxicity (Creatinine) grade $\geqslant$ 2	0
Nausea/vomiting grade $\geqslant$ 2	0
Neuropathy grade $\geqslant$ 2	0
AST/ALT grade $\geqslant$ 2	0

Statistical analysis

The patients were monitored and recorded for treatment-related toxicity, response and time to death. Those who received two or more cycles were evaluated for response, while those who received at least 1 cycle were evaluated for toxicity and survival. The purpose of this analysis was to determine whether the activity of this chemotherapy is reproducible in an expanded cohort of patients with cholangiocarcinoma. The primary endpoint of the analysis was the overall response rate (complete plus partial responses). A secondary objective was to document toxicity and survival. Overall survival was estimated using the method of Kaplan and Meier.

RESULTS

From June 2003 to December 2005, 42 patients were evaluated retrospectively in the same institution. Patient demographics are listed in Table 1. There were 28 males (67%) and 14 females (33%). The median age was 51 years (range, 33 to 67) and the median ECOG performance status was 1 (range 0-2). Twelve patients (28%) had unresectable disease and 30 (72%) had metastatic disease. A total of 171 cycles of therapy were delivered and the median number of cycles was 4 (range 1-6). There were no complete responses, 9 patients (22%) achieved partial response, 11 patients (26%) had stable disease and the remaining 22 patients (52%) had PD disease progression. Severe toxicities are listed in Table 2. Grade 3 toxicities were observed in the following: anemia in 31%, neutropenia in 19% and thrombocytopenia in 5%. One patient (2%) had grade 4 neutropenia and the others had grade 4 anemia. Non-hematologic toxicity was generally mild including nausea, vomiting and fatigue. There was
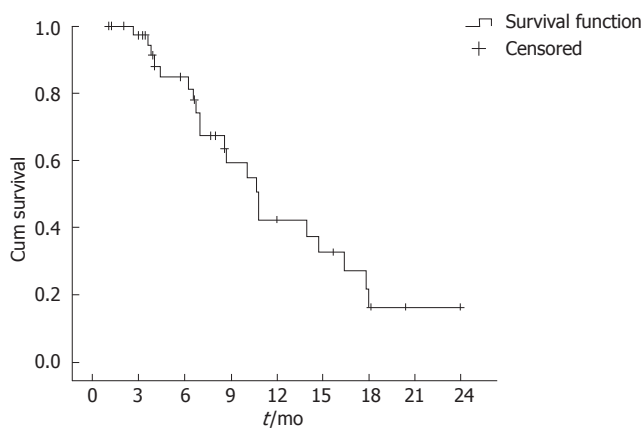
Figure 1 Overall survival.

no episode of neutropenic fever or treatment-related death. The median time to progression was 8.5 mo and the median survival was 10.8 mo (range 8.4-13 mo) (Figure 1). One-year survival rate was 40%.

DISCUSSION

We report here one of the largest case series in cholangiocarcinoma. The combination of gemcitabine and cisplatin achieved a response rate of 22% plus an additional disease stabilization rate of 26% giving an overall disease control rate of 48%. The median survival was 10.8 mo with a 1-year survival rate of 40% which were encouraging in the majority of patients with metastatic disease. These efficacy data compared favorably with our previous report and other trials using this gemcitabine and cisplatin combination, with slightly different doses and schedules[6-8]. However, grade 3 anemia occurred more frequently in this patient cohort. Anemia was not in the exclusion criteria for receiving or delaying the initiation of chemotherapy and about 28% of the patients already had grade 1 anemia at baseline. This could explain the high incidence of severe anemia during treatment in this analysis.

Single agent gemcitabine also demonstrated a response rate of 22% to 30% in previous reports with generally mild toxicity[4,5]. A randomized study comparing single agent gemcitabine or gemcitabine plus cisplatin, similar to our regimen in the biliary cancer, is warranted and ongoing in the United Kingdom. The results of this large trial from a cooperative group will provide more definite conclusions on tolerability and efficacy between these regimens and potentially set a new reference regimen for this disease. Many new chemotherapy agents including oxaliplatin and capecitabine have also been tested in combination with gemcitabine and they were shown as well to be active regimens with a response rate ranging from 22% to 36% that make a reasonable comparative arm with the single

agent gemcitabine[9,10]. Moreover, recent data suggest a therapeutic benefit of targeted agents with different mechanisms of action and toxicity such as epidermal growth factor receptor (EGFR) blockade, i.e. erlotinib, which warrants further study in combination with other existing active agents to take another step forward in treating this disease[11].

In conclusion, therapy with gemcitabine and cisplatin as seen here has consistent activity and is a well tolerated therapeutic option for patients with unresectable and metastatic cholangiocarcinoma. Further study is warranted to determine the optimal dose and schedule. To clarify the survival advantage, a randomized study needs to be performed.

REFERENCES

1   **Falkson G**, MacIntyre JM, Moertel CG. Eastern Cooperative Oncology Group experience with chemotherapy for inoperable gallbladder and bile duct cancer. *Cancer* 1984; **54**: 965-969
2   **Takada T**, Kato H, Matsushiro T, Nimura Y, Nagakawa T, Nakayama T. Comparison of 5-fluorouracil, doxorubicin and mitomycin C with 5-fluorouracil alone in the treatment of pancreatic-biliary carcinomas. *Oncology* 1994; **51**: 396-400
3   **Choi CW**, Choi IK, Seo JH, Kim BS, Kim JS, Kim CD, Um SH, Kim JS, Kim YH. Effects of 5-fluorouracil and leucovorin in the treatment of pancreatic-biliary tract adenocarcinomas. *Am J Clin Oncol* 2000; **23**: 425-428
4   **Kubicka S**, Rudolph KL, Tietze MK, Lorenz M, Manns M. Phase II study of systemic gemcitabine chemotherapy for advanced unresectable hepatobiliary carcinomas. *Hepatogastroenterology* 2001; **48**: 783-789
5   **Penz M**, Kornek GV, Raderer M, Ulrich-Pur H, Fiebiger W, Lenauer A, Depisch D, Krauss G, Schneeweiss B, Scheithauer W. Phase II trial of two-weekly gemcitabine in patients with advanced biliary tract cancer. *Ann Oncol* 2001; **12**: 183-186
6   **Thongprasert S**, Napapan S, Charoentum C, Moonprakan S. Phase II study of gemcitabine and cisplatin as first-line chemotherapy in inoperable biliary tract carcinoma. *Ann Oncol* 2005; **16**: 279-281
7   **Park BK**, Kim YJ, Park JY, Bang S, Park SW, Chung JB, Kim KS, Choi JS, Lee WJ, Song SY. Phase II study of gemcitabine and cisplatin in advanced biliary tract cancer. *J Gastroenterol Hepatol* 2006; **21**: 999-1003
8   **Kim ST**, Park JO, Lee J, Lee KT, Lee JK, Choi SH, Heo JS, Park YS, Kang WK, Park K. A Phase II study of gemcitabine and cisplatin in advanced biliary tract cancer. *Cancer* 2006; **106**: 1339-1346
9   **Andre T**, Tournigand C, Rosmorduc O, Provent S, Maindrault-Goebel F, Avenin D, Selle F, Paye F, Hannoun L, Houry S, Gayet B, Lotz JP, de Gramont A, Louvet C. Gemcitabine combined with oxaliplatin (GEMOX) in advanced biliary tract adenocarcinoma: a GERCOR study. *Ann Oncol* 2004; **15**: 1339-1343
10 **Cho JY**, Paik YH, Chang YS, Lee SJ, Lee DK, Song SY, Chung JB, Park MS, Yu JS, Yoon DS. Capecitabine combined with gemcitabine (CapGem) as first-line treatment in patients with advanced/metastatic biliary tract carcinoma. *Cancer* 2005; **104**: 2753-2758
11 **Philip PA**, Mahoney MR, Allmer C, Thomas J, Pitot HC, Kim G, Donehower RC, Fitch T, Picus J, Erlichman C. Phase II study of erlotinib in patients with advanced biliary cancer. *J Clin Oncol* 2006; **24**: 3069-3074

New concept of ileocecal junction: Intussusception of the terminal ileum into the cecum

Burin Awapittaya, Jirawat Pattana-arun,Tanwa Tansatit, Prapon Kanjanasilpa, Chucheep Sahakijrungruang, Arun Rojanasakul

Burin Awapittaya, Colorectal Division, Department of Surgery, Rajavithi Hospital, Bangkok 10400, Thailand
Jirawat Pattana-arun , Colorectal Division, Department of Surgery, Faculty of Medicine, King Chulalongkorn Memorial Hospital, Chulalongkorn University, Bangkok 10330, Thailand
Tanwa Tansatit, Department of Anatomy, Faculty of Medicine, Chulalongkorn University, Bangkok 10330, Thailand
Prapon Kanjanasilpa, Department of Anatomy, Faculty of Medicine, Chulalongkorn University, Bangkok 10330, Thailand
Chucheep Sahakijrungruang, Colorectal Division, Department of Surgery, Faculty of Medicine, King Chulalongkorn Memorial Hospital, Chulalongkorn University, Bangkok 10330, Thailand
Arun Rojanasakul, Colorectal Division, Department of Surgery, Faculty of Medicine, King Chulalongkorn Memorial Hospital, Chulalongkorn University, Bangkok 10330, Thailand
Correspondence to: Burin Awapittaya, MD, Colorectal Division, Department of Surgery, Rajavithi Hospital, Bangkok 10400, Thailand. burinmail@gmail.com
Telephone: +66-2-3458080 Fax: +66-2-3548080
Received: 2007-02-09   Accepted: 2007-03-08

Abstract

AIM: To prove that the terminal ileum is intussuscepted into the cecum creating the ileocecal junction, contrary to previous valvular concept which has been widely believed.

METHODS: This study is based on gross and microscopic examinations of fresh specimens derived from colonic operations (right hemicolectomy or subtotal colectomy). Data compiled from observing and dissecting of specimens of seven patients are used to examine both gross and microscopic appearance of ileocecal junction.

RESULTS: Intussusception of the terminal ileum was found in every specimen. However, the length of intussusception was different in each specimen.

CONCLUSION: Gross and microscopic appearance studies suggest that the terminal ileum is intussuscepted into the cecum.

Awapittaya B, Pattana-arun J, Tansatit T, Kanjanasilpa P, Sahakijrungruang C, Rojanasakul A. New concept of ileocecal junction: Intussusception of the terminal ileum into the cecum. *World J Gastroenterol* 2007; 13(20): 2855-2857

INTRODUCTION

The anatomy of the ileocecal junction (IC junction) was first described as ileocecal valve concept; fold of mucosa into the lumen of cecum[1,2]. Later studies described a thickened muscular eminence, and the concept of sphincter at IC junction was emerged. Manometric studies had shown characteristic of IC junction[3-8]. A four-centimeter zone of elevated pressure was demonstrated at the junction[3]. Physiological study of the IC junction has suggested that "ceco-ileal excitatory reflex", initiated by Ileal distension stimulate the reflex relaxation of IC junction and cecal, is the main mechanism in allowing the chime to pass into the cecum. Cecal distension appears to evoke reflex ileal and IC junction, thus preventing ceco-ileal reflux[4]. Kumar and Phillips[1,8] proposed that competency of IC junction is facilitated by angulation of the ileum on the cecum, an anatomic arrangement which maintained by external (superior and inferior ileocecal) ligaments.

However, from our observation, during the operation and examination of specimens reveal that the appearance of ileocecal junction as the terminal ileum was intussuscepted into the cecum, of which is the point that this study attempts to prove.

MATERIALS AND METHODS

Seven specimens of colon and terminal ileum (including ileocecal junction) from seven patients were collected for this study.

Inclusion criteria

(1) Specimens derived from right hemicolectomy or extended right hemicolectomy; (2) Specimens derived from subtotal colectomy.

Exclusion criteria

(1) Specimens of patients who had disease or pathology of ileocecal junction; (2) Specimens of patients who

Table 1 Details of patients and operations

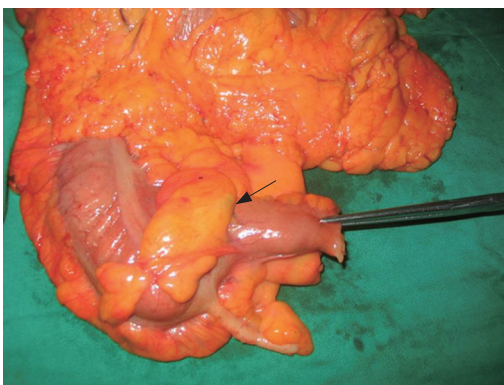| Patient's diagnosis	Age (yr)	Gender	Operation
Colonic cancer of the ascending colon	58	Male	Right hemicolectomy
Colonic cancer of the hepatic flexure	64	Male	Right hemicolectomy
Colonic cancer of the sigmoid colon	53	Male	Subtotal colectomy
Bleeding diverticulosis	70	Female	Subtotal colectomy
Colonic cancer of the hepatic flexure	74	Male	Extended right hemicolectomy
Colonic cancer of the hepatic flexure	64	Female	Extended right hemicolectomy
Colonic cancer of the transverse colon	64	Male	Extended right hemicolectomy

Table 2 Findings of specimen examination and the length of the intussusception of the terminal ileum

Specimen	Intussusception	Length of intussusception (cm)
Patient 1's specimen	Yes	1.6
Patient 2's specimen	Yes	1
Patient 3's specimen	Yes	0.5
Patient 4's specimen	Yes	2
Patient 5's specimen	Yes	1.4
Patient 6's specimen	Yes	1.6
Patient 7's specimen	Yes	1.9

Figure 1 Intussusception of the terminal ileum into the cecum.
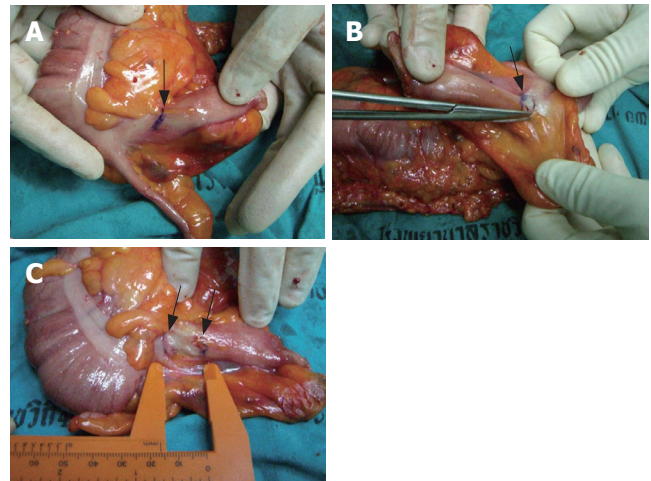
Figure 2 Reduction of the intussusceptum part of the terminal ileum from the cecal wall (blue marker). **A**: Point of intussusception; **B**: Dissection and reduction of intussusception; **C**: Length of intussusception, after reduction.

underwent appen-dectomy.

Methods of studying the ileocecal junction from specimens

Gross anatomy examination is conducted to investigate the possibility of terminal ileum intussuscepted into the cecum. In case of detecting the intussusception, the length of the terminal ileum which is intussuscepted in to the cecum will be measured.

Microscopic examination with H&E staining is conducted to determine the intussusception of terminal ileum into the cecum by dissecting specimens from the ileocecal junction area.

RESULTS

Seven specimens from seven patients were used in this study. Details of patients are shown in Table 1.

Findings of gross appearance reveal that the terminal ileum is intussuscepted into the cecum in all seven specimens (Figures 1 and 2). However, the length of the intussusception is different as shown in Table 2.

The microscopic examination supports our postulation that there is the intussusception of the terminal ileum into the cecum at the ileocecal junction. Figures 3 and 4 show both muscular layers of the terminal ileum and the cecum in the area of intussusception.

Figure 3 Cross section of the specimen reveals wall of the terminal ileum intussuscepted into the cecum (arrow).

DISCUSSION

In 1859 John Hunter proposed his valvular concept of the ileocecal junction of which the mucosa fold extending into the cecum (Flap-valve)[1]. However, our findings from the observation during the operation of the ileocecal junction area and examination of specimens, revealed that there is an intussusception of the terminal ileum into the cecum in every specimen. Cross section of ileocecal junction display both muscular and mucosal layers of the terminal ileum fold
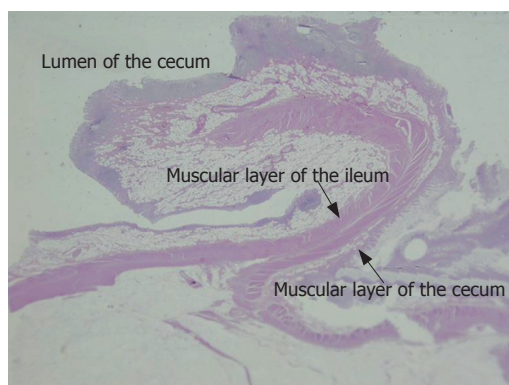
Figure 4 Microscopic appearance of the ileocecal junction displays the muscular layer of the terminal ileum fold extending into the cecum.

into the cecum wall (Figuers 3 and 4). The intussusceptum can be reduced from the cecum by dissection between layers of the terminal ileum and cecum. These findings further refute the flap-valve concept previously believed. Moreover, additional microscopic study reveals that the terminal ileum and cecum are bundled together. Muscle fibers of the cecum and terminal ileum can be depicted separately though bundled up together in the ileocecal junction.

According to these findings, our impression that all layers of the terminal ileum is intussuscepted into the cecum wall is the important role in the anatomy of ileocecal junction which contrary to the previous belief of merely the mucosa.

We will later explore the relationship between the intussusception of the terminal ileum into the cecum and the competency for the ileocecal junction.

REFERENCES

1   **Kumar D**, Phillips SF. The contribution of external ligamentous attachments to function of the ileocecal junction. *Dis Colon Rectum* 1987; **30**: 410-416
2   **Rosenberg JC**, DiDio LJ. Anatomic and clinical aspects of the junction of the ileum with the large intestine. *Dis Colon Rectum* 1970; **13**: 220-224
3   **Cohen S**, Harris LD, Levitan R. Manometric characteristics of the human ileocecal junctional zone. *Gastroenterology* 1968; **54**: 72-75
4   **Shafik A**, El-Sibai O, Shafik AA. Physiological assessment of the function of the ileocecal junction with evidence of ileocecal junction reflexes. *Med Sci Monit* 2002; **8**: CR629-CR635
5   **Corazziari E**, Barberani F, Tosoni M, Boschetto S, Torsoli A. Perendoscopic manometry of the distal ileum and ileocecal junction in humans. *Gastroenterology* 1991; **101**: 1314-1319
6   **Barberani F**, Corazziari E, Tosoni M, Badiali D, Materia E, Ribotta G, Montesani C, Boschetto S, Torsoli A. Perendoscopic manometry of the distal ileum and ileocecal junction: technique, normal patterns, and comparison with transileostomy manometry. *Gastrointest Endosc* 1994; **40**: 685-691
7   **Nasmyth DG**, Williams NS. Pressure characteristics of the human ileocecal region--a key to its function. *Gastroenterology* 1985; **89**: 345-351
8   **Nivatvongs S**, Gordon PH. Surgical anatomy. In: Gordon PH, Nivatvongs S, editors. Principles and practice of surgery for colon, rectum and anus. 2nd ed. St.Louis: Quality Medical Publishing, 1999: 33-39

S- Editor Wang J   **L- Editor** Alpini GD   **E- Editor** Zhou T

Clinical features of familial adenomas polyps in Chinese and establishment of its immortal lymphocyte cell lines

Shan-Rong Cai, Su-Zhang Zhang, Shu Zheng

Shan-Rong Cai, Su-Zhang Zhang, Shu Zheng, Cancer Institute, 2nd Affiliated Hospital, School of Medicine, Zhejiang University, Hangzhou 310009, Zhejiang Province, China
Supported by National 863 Program of China, No. 2004AA227070
Correspondence to: Dr Shu Zheng, Cancer Institute, 2nd Affiliated Hospital, School of Medicine, Zhejiang University, Hangzhou 310009, Zhejiang Province, China. caisr2007@yahoo.com.cn
Telephone: +86-571-87784528 Fax: +86-571-87214404
Received: 2007-01-19   Accepted: 2007-03-01

Abstract

AIM: To reserve the rare Chinese familial adenomas polyp (FAP) family resource and to investigate the clinical features of FAP in Chinese for its diagnosis.

METHODS: Clinical features of patients with FAP were investigated. If there is any question, their medical records were verified. Blood sample was taken and lymphocyte immortal cell lines were established with modified EB-transformation methods. Congenital hypertrophy of retinal pigment epithelium (CHRPE) was checked by an experienced ophthalmologist.

RESULTS: Twenty seven families including 21 classical FAP (CFAP) families, 3 attenuated FAP (AFAP) families, and 3 suspected AFAP families were investigated. A total of 116 lymphocyte immortal cell lines were established from 26 families. In all the FAP families, colorectal cancer occurred at the mean age of 42.84 years. Of the 16 families checked, 15 (93.75%) had CHRPE. The mean number of patients suffering from colorectal neoplasm was 3.14 in CFAP families and 2.0 in AFAP families ($P < 0.01$). The mean oldest age at diagnosis of FAP was 41.75 years in CFAP families, and 58.67 years in AFAP families, respectively ($P < 0.01$). Mean age of development of colorectal cancer was 42.23 in CFAP and 57.33 years old in AFAP ($P < 0.01$). Mean of the earliest age at diagnosis of FAP was 29.95 years in the FAP families with a positive family history and 46.80 years in the FAP families with a negative family history ($P < 0.01$). The ratio of extra-intestinal tumors to colorectal neoplasms was different in the two kinds of families with positive and negative family history ($P < 0.01$).

CONCLUSION: Additional use of ciclosporin will effectively improve to establish lymphocyte immortal cell lines with modified EB- transformation methods. In Chinese FAP, there was a high frequency of CHRPE , and

a later age at diagnosis and a later age of development of colorectal cancer in AFAP. And earlier age at diagnosis in FAP with positive family history was also found that will help to diagnose various kinds of FAP in Chinese.

INTRODUCTION

Familial adenomatous polyposis (FAP) is one of the two commonest familial syndromes that predispose to colorectal cancer in China. Classically, FAP is characterized by the occurrence of hundreds to thousands of colorectal polyps, which give rise to colorectal cancer if left untreated. The disease is caused by mutations in the adenomatous polyposis coli (*APC*) tumor suppressor gene. Approximately 50% of offsprings in FAP family will be affected, and prophylactic surgical intervention is fundamental to avoid the development of colorectal cancer[1]. Classical FAP is defined clinically by the finding of at least 100 colorectal adenomas polyps. Another different kind of FAP named attenuated FAP (AFAP) in which adenomas are less than one hundreds, and the average age of cancer onset is also older (55 years old) than that of classical FAP (39 years old)[2,3]. However, little is known about the clinical manifestations of these two kinds of FAP in Chinese. It is also of vital importance to collect and reserve FAP family resource and to analyze FAP's phenotype that will extend our understanding of FAP and its diagnosis in Chinese.

MATERIALS AND METHODS

Methods

All FAP families were collected from the People's Republic of China, mainly from Zhejiang Province (24 families). Classical FAP (CFAP) is defined clinically by the finding of
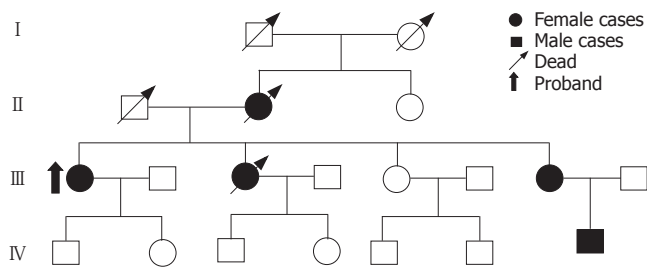
Figure 1 Classical FAP pedigrees.

Figure 2 Established lymphocyte immortal cell lines (× 40).

at least 100 colorectal adenoma polyps. In attenuated FAP (AFAP), less than 100 adenomas could be found at the age of over 40 years, and at least one of the following has a family history of FAP or colorectal cancer, congenital hypertrophy of retinal pigment epithelium (CHRPE). If a proband was found in less than 100 adenomas and the age was less than 40 years, this family was defined as suspected AFAP. The clinical features of patients in one FAP family were investigated. If there is any question, medical records in hospital were verified. Blood samples were taken to establish immortal lymphocyte cell lines with informed consent.

Lymphocyte separation and cultivation: About 5 mL blood was drawn into two BD vacutainers containing 3.6 mg k2 EDTA, and 2-2.5 mL blood was doubly diluted with wash media such as RPMI 1640 culture, and added into one tube containing Ficoll-plaque, then centrifuged at 2400 r/min for 13 min. The lymphocytes at the interface were collected and washed with RPMI 1640.

EB virus transformation (immortalization)[4,5]**:** B95-8 cell line producing Epstein-barr virus (EBV) was cultured and 1000 mL cell mixture was centrifuged at 2000 r/min for 5 min at 4℃. The supernatants were collected and centrifuged at 10 000 r/min for 2 h at 4℃. After the supernatants were discarded, EBV was stayed in the tube and resolved in 10 mL RPMI 1640 culture through a 0.45 μm filter and stored at -80℃. Lymphocytes after separation were resolved in an initiation medium (RPMI 1640, + 10%-15% heat-inactivated fetal bovine serum, + 2 μg/mL ciclosporin) in 24-well plates (Falcon), and 50 μL EB virus suspension was added. The lymphocytes were incubated at 37℃ in an atmosphere containing 5% CO_2 for one week without changing the medium. Then, the medium was replaced with about half of the total volume of the initiation medium every 2-3 d. After 10-15 d, clones apppeared and grew rapidly. If the cell density was over $5 × 10^5$, they transfomed into another 25 mL plate and cultured for 10-15 d and freezed in liquid nitrogen.

Statistical analysis

Student's *t* test was used to analyze the mean between different kinds of FAP, and chi-square test was used to compare the ratio of extra-intestinal tumors and colorectal neoplasms with SPSS 10.0 software.

RESULTS

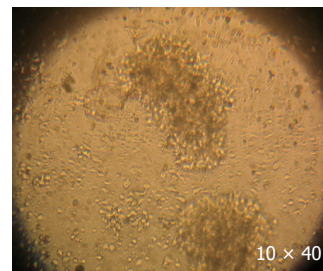Twenty-seven FAP families were investigated. Pedigrees such as classical FAP were plotted (Figure 1).

In the 27 families, one family refused to afford blood samples although its members received investigation. One hundred and thirty-two blood samples were taken from 26 FAP families and 125 blood samples were used to establish EB-transformed cell lines, in which 116 lymphocyte immortal cell lines were successfully established (Figure 2) and 9 relatives' lymphocytes failed to set up immortal cell lines due to epiphyte contamination. The rate of successfully transformed cell lines was 92.8% (116/125).

In the 27 families, there were 80 cases of colorectal neoplasm (including adenoma and cancer). Among them, colorectal cancer was diagnosed in 29 members from 19 FAP families at the age of 19-67 years, and colorectal cancer occurred at the mean age of 42.84 years. Six families were diagnosed with AFAP and suspected AFAP in which the number of polyps in probands was less than 100. Of the 6 families, 5 had 8 persons suffering from extra colonic cancer including 3 lung cancers, 2 live cancers, 1 vocal, stomach and small intestine cancer, respectively.

The phenotype in the three different FAP families is listed in Table 1A and 1B, and the phenotype in FAP families with positive and negative family history is listed in Table 2A and B.

There was a difference in the number of colorectal neoplasms (due to their definitions) between CFAP and AFAP families and the mean oldest age at diagnosis of FAP and colorectal cancer. The mean oldest age at diagnosis of FAP and the mean age of colorectal cancer development in AFAP families were later than those in CFAP families.

There was a difference in the mean number of colorectal neoplasms (due to classification), the mean youngest age at diagnosis of FAP and the ratio of extra-intestinal tumors to colorectal neoplasms in the FAP families with a different family history. In the FAP families with a positive history, onset of FAP was 15 years earlier than which in the FAP families with a negative family history.

DISCUSSION

In Western countries, there is a national or international collection net of FAP. In China, no national net for collection of FAP has been established. However, more attention is paid to the collection and reservation of the rare resource of hereditary cancer families such as FAP and hereditary nonpolyposis colorectal cancer families than before. We have established 116 lymphocyte immortal cell

Table 1A Phenotype of different kinds of FAP families mean ± SD

Kinds of FAP families	Number of families	Families withpositive family history	Mean number of colorectal neoplasms[b]	Mean number of colorectal cancer	Mean of the earliest age at diagnosis in one family
CFAP	21	16	3.14 ± 1.59	1.29 ± 1.10	32.9 ± 10.31
AFAP	3	3	2.00 ± 0.00	1.50 ± 0.71	42.0 ± 14.0
Suspected AFAP	3	3	2.67 ± 0.58	0.67 ± 0.58	25.0 ± 3.61

CFAP: Classical familial adenomatous polyposisp; AFAP: attenuated familial adenomatous polyposisp. [b]$P < 0.01$, comparison between CFAP and AFAP.

Table 1B Phenotype of different kinds of FAP families

Kinds of FAP families	Mean of the latest age at diagnosis in one family[b]	Mean age of symptom appearing	Mean age of colorectal cancer development[b]	Extra colonic cancers/colorectal neoplasms	Positive CHRPE families/total checked families
CFAP	41.75 ± 7.75	26.56 ± 12.36	42.23 ± 9.24	6/66	11/12
AFAP	58.67 ± 7.37	37.50 ± 21.92	57.33 ± 8.39	2/6	2/2
Suspected AFAP	41.6 ± 10.02	18.00 ± 4.24	33.67 ± 13.58	0	2/2

CFAP: Classical familial adenomatous polyposisp; AFAP: attenuated familial adenomatous polyposisp. [b]$P < 0.01$, comparison between CFAP and AFAP.

Table 2A Phenotype in FAP families with a different family history mean ± SD

Status of family history	Number of families	Mean number of colorectal neoplasms[b]	Mean number of colorectal cancers	Mean of the youngest age at diagnosis of FAP in one family[b]
Positive	22	3.41 ± 1.22	1.68 ± 0.82	29.95 ± 8.25
Negative	5	1.00 ± 0.00	0	46.80 ± 9.91

[b]$P < 0.01$, comparison between CFAP and AFAP.

Table 2B Phenotype in FAP families with different family history mean ± SD

Status of family history	Mean of the latest age at diagnosis in one family	Mean age of symptom appearing	Mean age of colorectal cancer development	Extra colonic cancers/colorectal neoplasms[b]	Positive CHRPE families/total checked families
Positive	44.05 ± 9.64	25.64 ± 12.36	43.15 ± 11.48	5/75	12/13
Negative		33.33 ± 17.01		3/5	3/3

[b]$P < 0.01$, comparison between CFAP and AFAP.

lines (92.8%) with modified EB-transformation method for the reservation of FAP family resource. Additional use of 2 μg/mL ciclosporin can effectively prevent T lymphocytes to attack B lymphocytes.

The phenotypic variability in patients with FAP has been recognized for many years[6]. However, it is uncertain whether FAP clinical manifestations are different in Chinese and Western individuals. It was reported that colorectal cancer occurs at the age of 39 years in Western populations[3] and in Chinese at the mean age of 42.23 years. It was also reported that, in AFAP families, colorectal cancer occurs at the age of 55 years in Western populations[2] and at the age of 57.33 years in Chinese. In Chinese, Symptoms of colorectal cancer appear 10 years later in AFAP families than in CFAP families, while symptoms of colorectal cancer appear in Western population at the age of 33 years[5]. In addition, some items are different in the two kinds of FAP families in Chinese. In the present study, the mean number of colorectal neoplasms was higher in CFAP families (3.14) than in AFAP families (2.0, $P < 0.01$), the

mean oldest age at diagnosis of FAP in one family was later in AFAP than in CFAP ($P < 0.01$). All these findings may further improve our ability to predict AFAP and CFAP. Based on these data, it may be concluded that the development time of colorectal cancer may be later in Chinese than which in Western populations. To confirm these hypotheses may need a larger sample of Chinese FAP families.

In Chinese FAP families, the mean youngest age at diagnosis of FAP in one family was 29.95 and 46.8 years, respectively in the two groups with positive (22 families) and negative (5 families) family history ($P < 0.01$), indicating that a positive FAP family history is a high-risk factor for developing colorectal cancer at a young age. The ratio of extra-intestinal tumors to colorectal neoplasms was 5/75 and 3/5 in the two kinds of families with a different family history ($P < 0.01$).

CHRPE is a common symptom of FAP. It was reported that there is no association between CHRPE characteristics and FAP phenotype variants[7]. It was reported that the rate of CHRPE is 75%-80% in Western

FAP patients[8] and 93.75% in Chinese FAP families. CHRPE is more frequent in Chinese FAP families. In the present study, 8 asymptomatic family members with CHRPE were diagnosed with FAP, indicating that CHRPE is a good marker for the diagnosis of FAP in Chinese.

Clinicians must be aware of the broad range of variable clinical features of FAP due to its different variants. In China, it is of vital importance to establish a national net to collect FAP families and to analyze its phenotype characteristics and its association with genotype.

REFERENCES

1   **Lynch HT**, Smyrk TC. Classification of familial adenomatous polyposis: a diagnostic nightmare. *Am J Hum Genet* 1998; **62**: 1288-1289

2   **Spirio L**, Olschwang S, Groden J, Robertson M, Samowitz W, Joslyn G, Gelbert L, Thliveris A, Carlson M, Otterud B. Alleles of the APC gene: an attenuated form of familial polyposis. *Cell* 1993; **75**: 951-957

3   **Lynch HT**, Smyrk T, McGinn T, Lanspa S, Cavalieri J, Lynch J, Slominski-Castor S, Cayouette MC, Priluck I, Luce MC. Attenuated familial adenomatous polyposis (AFAP). A phenotypically and genotypically distinctive variant of FAP. *Cancer* 1995; **76**: 2427-2433

4   **Miller G**, Lipman M. Release of infectious Epstein-Barr virus by transformed marmoset leukocytes. *Proc Natl Acad Sci USA* 1973; **70**: 190-194

5   **Sugimoto M**, Tahara H, Ide T, Furuichi Y. Steps involved in immortalization and tumorigenesis in human B-lymphoblastoid cell lines transformed by Epstein-Barr virus. *Cancer Res* 2004; **64**: 3361-3364

6   **Howe JR**, Guillem JG. The genetics of colorectal cancer. *Surg Clin North Am* 1997; **77**: 175-195

7   **Tourino R**, Conde-Freire R, Cabezas-Agricola JM, Rodriguez-Aves T, Lopez-Valladares MJ, Otero-Cepeda JL, Capeans C. Value of the congenital hypertrophy of the retinal pigment epithelium in the diagnosis of familial adenomatous polyposis. *Int Ophthalmol* 2004; **25**: 101-112

8   **Hamilton SR**, Aaltonen LA. World Health Organization Classification of Tumours (Pathology and Gennetics of Tumors of the Digestive System). Lyon (France): International Agency for Research on Cancer Press, 2000: 120-125

RAPID COMMUNICATION

Elevation of vascular endothelial growth factor production and its effect on revascularization and function of graft islets in diabetic rats

Ying Cheng, Yong-Feng Liu, Jia-Lin Zhang, Tie-Min Li, Ning Zhao

Ying Cheng, Yong-Feng Liu, Jia-Lin Zhang, Tie-Min Li, Ning Zhao, Organ Transplant Unit of First Hospital of China Medical University, Shenyang 110001, Liaoning Province, China
Correspondence to: Ying Cheng, Organ Transplant Unit of First Affiliated Hospital of China Medical University, 155 Nanjingbei Street, Heping District, Shenyang 110001, Liaoning Province, China. chengying75@sina.com
Telephone: +86-24-83282452

Abstract

AIM: To determine whether the elevated vascular endothelial growth factor (VEGF) expression produced by the transfected vascular endothelial cells (VECs) could stimulate angiogenesis of the graft islets and exert its effect on the graft function.

METHODS: Thirty diabetic recipient rats were divided into three groups (n = 10 per group). In the control group, 300 IEQ islets were transplanted in each rat under the capsule of the right kidney, which were considered as marginal grafts. In the VEC group, VEC together with the islets were transplanted in each rat. In the VEGF group, VEC transfected by pIRES2-EGFP/VEGF165 plasmid and the islets were transplanted in each rat. Blood glucose and insulin levels were evaluated every other day after operation. Intravenous glucose tolerance test (IVGTT) was performed 10 d after the transplantation. Hematoxylin and eosin (HE) staining was used to evaluate the histological features of the graft islets. Immunohistochemical staining was used to detect insulin-6, VEGF and CD34 (MVD) expression in the graft islets.

RESULTS: Blood glucose and insulin levels in the VEGF group restored to normal 3 d after transplantation. In contrast, diabetic rats receiving the same islets with or without normal VECs displayed moderate hyperglycemia and insulin, without a significant difference between these two groups. IVGTT showed that both the amplitude of blood glucose induction and the kinetics of blood glucose in the VEGF group restored to normal after transplantation. H&E and immunohistochemical staining showed the presence of a large amount of graft islets under the capsule of the kidney, which were positively stained with insulin-6 and VEGF antibodies in the VEGF group. In the cell masses, CD34-stained VECs were observed. The similar masses were also seen in the other two groups, but with a fewer positive cells stained with insulin-6 and CD34 antibodies. No VEGF-positive cells appeared in these groups. Microvessel density (MVD) was significantly higher in the VEGF group compared to the other two groups.

CONCLUSION: Elevated VEGF production by transfected vascular endothelial cells in the site of islet transplantation stimulates angiogenesis of the islet grafts. The accelerated islet revascularization in early stage could improve the outcome of islet transplantation, and enhance the graft survival.

http://www.wjgnet.com/1007-9327/13/2862.asp

INTRODUCTION

Islet transplantation is considered a potentially curative treatment for diabetes mellitus. However, the protocol depends on the sufficiently large amounts of graft islets, requiring two to four cadaveric pancreas. The native islet vascular network has been ruined during the isolation[1]. It is estimated that > 70% of islet mass becomes stably engrafted[2]. So apart from immune rejection, another critical limitation to islet transplantation is the rate and extent of islet revascularization[3]. In this study, we used rat vascular endothelial cells (VECs) transfected with VEGF165 to elevate the production of vascular endothelial growth factor (VEGF) in the site of islet transplantation, and then determined whether the elevated VEGF expression could stimulate the angiogenesis in the grafts. These results would provide proof-of-principle that

local expression of angiogenic molecules may enhance islet revascularization, thereby improving the outcome of marginal islet transplantation with better glycemic control in diabetic rats.

MATERIALS AND METHODS

Animals and materials

Wistar rats (body weight, 150 ± 20 g) were purchased from Animal Center of China Medical University. Diabetic rats were induced by streptozocin (STZ, IP, 60 mg/kg), and diabetes mellitus was defined when the non-fasting blood glucose level was greater than 16.8 mmol/L on two consecutive measurement[4]. Then the diabetic recipients were randomly divided into three groups ($n = 10$ in each group). In the control group, the islets were transplanted under the capsule of the right kidney. In the VEC group, vascular endothelial cells (VECs) were transplanted together with the islets. In the VEGF group, VECs transfected with pIRES2-EGFP/VEGF165 plasmid were transplanted together with the islets.

pIRES2-EGFP/VEGF165 was propagated in permissive cells and purified by CsCl density gradient centrifugation as previously described[5]. The titer of pIRES2-EGFP/VEGF165 was 1.1×10^{11} plaque-forming unit (pfu)/mL.

Islet isolation and transplant

Islets were isolated and purified according to the modified Minnesota program[6]. Briefly, after intraductal infusion of 10-12 mL of cold Hank's balanced solution containing 1.5 mg/mL type V collagenase (C9263, Sigma), the pancreas was surgically procured and digested at 37℃ for 15-20 min. During the digestion, the pancreas was observed closely, and digestion was stopped by RPMI1640 containing 200 mL/L serum when the emulsion appeared. The islets were purified by discontinuous Ficoll density gradient (25%, 23%, 20.5% and 11%) centrifugation at 3000 r/min for 10 min at 4℃. The distinct islets were collected and washed, and finally the 300 IEQ islets free of acinar cells, vessels, lymph nodes and ducts, which were considered as marginal grafts, were used for transplantation.

For the islet transduction by vectors, aliquots of the islets were incubated with VEGF vector at a defined multiplicity of infection (MOI) in 2 mL of serum-free RPMI1640 medium at 37℃ for 2 h. After washing with Hanks' balanced salt solution, transduced islets were used for transplantation.

Detection of islet function

Blood glucose and insulin levels were evaluated every other day after operation. The intravenous glucose tolerance test (IVGTT) was performed 10 d after transplantation. Rats were fasted for 5 h and injected intravenously with 500 g/L dextrose solution at a dose of 0.5 g/kg body weight, as previously described[7]. Blood glucose levels were measured before and at 1, 5, 10, 15, 30, 60 and 90 min after glucose infusion.

Histological observation

Hematoxylin and eosin (H&E) and immunohistochemical
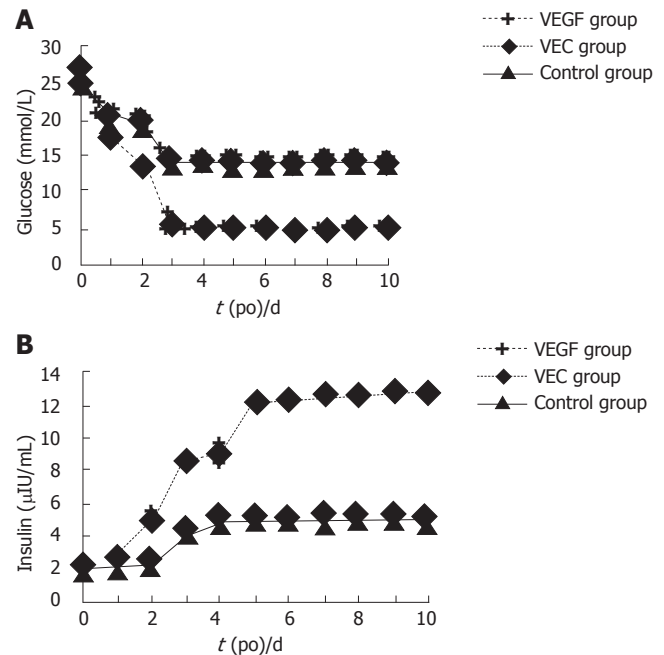
Figure 1 Glucose (**A**) and insulin (**B**) levels in the diabetic rats after transplantation.

staining of islet grafts were performed. Briefly, animals were killed 14 d after transplantation, and islet grafts were retrieved from individual animals. After fixing in 10% phosphate-buffered formalin overnight, islet grafts were embedded in paraffin. The paraffin-embedded islet grafts were cut into consecutive sections (4-μm thick), which were immunostained with anti-insulin-6, rat anti-CD31 and rabbit anti-VEGF165 antibodies, respectively. Microvessel density (MVD) was determined under light microscopy after sections were immunostained with anti-CD34 antibodies, as previously described[8]. Clusters of stained endothelial cells were counted as a single microvessel. MVD expressed as average number of three highest area identified within a single 200 × field.

Statistical analysis

Data were expressed as mean $\pm$ SE. Statistical analyses of data were performed by ANOVA. Unpaired ANOVA analysis of variance was used to compare between two different treatment groups. P value < 0.05 was considered statistically significant.

RESULTS

Graft islet function after transplantation

The blood glucose and plasma insulin levels in the diabetic recipients of the VEGF group restored to normal 3 d after transplantation. In contrast, diabetic rats receiving the same islets with or without normal VECs displayed moderate hyperglycemia (13-14 mmol/L), and insulin (? μIU/mL), without a significant difference between these two groups (Figure 1). We observed a significant difference in both the amplitude of blood glucose induction and kinetics of blood glucose decline between VEGF group and the other two groups, but no obvious difference between the control and VEC groups. In response to injection of
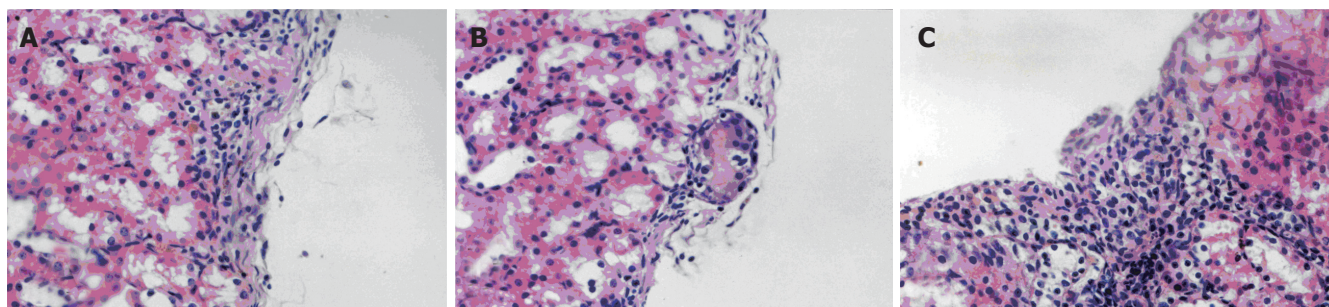
Figure 2 HE staining of the graft islets under the kidney capsule (× 400). **A**: Control group; **B**: VEC group; **C**: VEGF group.
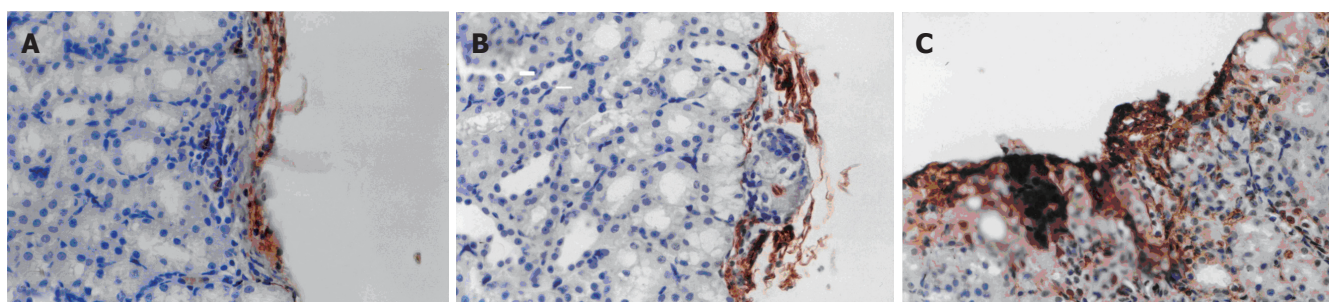
Figure 3 Immunohistochemical staining of insulin-6 in graft islets transplanted under the kidney capsule (× 400). **A**: Control group; **B**: VEC group; **C**: VEGF group.
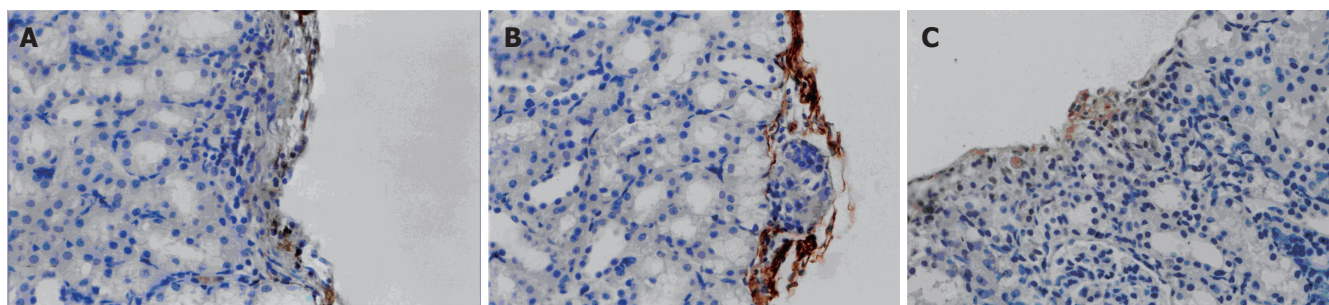
Figure 4 Immunohistochemical staining of VEGF in graft islets transplanted under the kidney capsule (× 400). **A**: Control group; **B**: VEC group; **C**: VEGF group.

a high dose of glucose, elevated blood glucose levels in the VEGF group were restored to a normal range within 90 min, whereas blood glucose levels in the control and VEC groups were increased to a significantly higher amplitude after glucose infusion and remained at the hyperglycemic level.

Histological findings

HE staining showed that a large amount of cell masses, which were different from the kidney native cells, were seen under the capsule of the kidney in the VEGF group. There were some vascular endothelial cells around and in the center of the masses. In the control and VEC groups, the similar cell masses were observed, but more fibrosis was seen in the center of the masses, where no vascular endothelial cells were seen (Figure 2).

Immunohistochemistry showed a large amount of insulin-6-positive cells in cell masses of the VEGF group, whereas insulin-6-positive cells were seldom seen in the other two groups (Figure 3).

VEGF165 was expressed in the VEGF group but not in the control and VEC groups (Figure 4). As shown in Figure 5, a significant difference in the relative intensity of immunostaining for anti-CD34 antibody was observed between the VEGF and the other two groups, thereby indicating an increased degree of revascularization of transplanted islets in the VEGF group. MVD in the islet grafts was significantly higher in the VEGF group (74.3 ± 6.74) compared to the VEC group (11.43 ± 2.22) and control groups (10.9 ± 2.45) ($P < 0.05$).

DISCUSSION

Pancreatic islet transplantation has been proposed as a treatment for diabetic patients in order to restore physiological insulin secretion, to reduce hyper-/hypogly-cemia events and consequently to improve the quality of life. Successful islet transplantation depends on the infusion of sufficiently large quantities of islets, but more than 70% islets would become inactive in the early
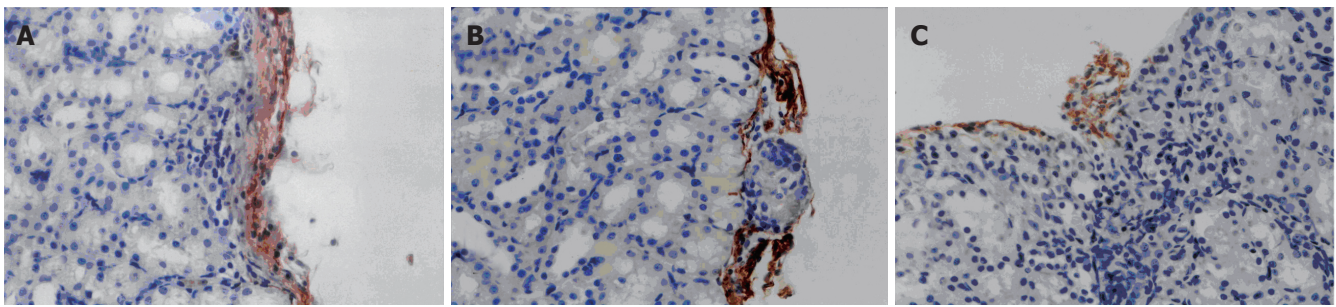
Figure 5 Immunohistochemical staining of CD34 in graft islets transplanted under the kidney capsule (× 400). **A**: Control group; **B**: VEC group; **C**: VEGF group.

stage (7-14 d after transplantation)[9]. Many factors may contribute to islet death, including initial blood-mediated inflammation reaction (IBMIR), immunoattack, and ischemic injury due to insufficient blood supply[10-12]. Islet survival depends on the diffusion of oxygen and nutrients. Pancreatic islets are heavily vascularized, and they receive their blood supply from an afferent arteriole that branches into a glomerular-like network of microvessels, which forms a local intra-islet portal system through which blood flows from the central core of β cells to the non-β cell mantle. Islet capillaries are fenestrated, which may be important for the efficient release of secreted products into the bloodstream[13]. Moreover, β cells may require more oxygen than most other cell types, as suggested by the finding that islets constitute only 1% of the pancreatic mass but receive 10% of the pancreatic blood supply[14].

During the process of islet isolation, the circulation within the islets and the extra-islet vascularization are disrupted. Formation of new vessels may be too slow to allow survival of an optimal number of cells. Furuya *et al*[15] demonstrated that the native endothelial cell in the graft islets reduced gradually, and disappeared 5 d after the transplantation. New blood vessels develop over a period of about 14 d, or even 4 wk which is not fast enough to prevent the marked loss of islet cells occurring during the first few days after transplantation[16]. The mechanisms that regulate the revascularization of islets are poorly understood. Some studies[16] have suggested that the reduction of the endothelial cells from the donors may contribute to the poor revascularization. However, in our experiment, a large number of endothelial cells were transplanted together with the graft islets. We observed that in the early stage after transplantation, the process of revascularization was not changed and no vessels were formed although the endothelial cells survived.

It has been suggested that growth factors may be important in this process. VEGF is known to be one of the most important factors associated with angiogenesis[17,18]. Therapeutic angiogenesis has been used for treating coronary and peripheral artery diseases by facilitating new vessel formation using plasmid or adenoviral vector-mediated VEGF gene delivery in a number of clinical trials[19-21]. VEGF may be a mediator in islets because it increases vascular permeability[22], which is important for the maintenance of normal endocrine function in highly vascularized organs and in devascularized islets[23]. VEGF may play a role in the

maintenance of the islet capillary system[24] and initiate the revascularization of islets during transplantation[25]. VEGF expression is increased in the graft islets, but significantly reduced 2-3 d after transplantation and is not sufficient for revascularization[26,27]. Therefore, evaluation of local VEGF expression may provide a crucial clue for improving revascularization and survival of graft islets.

Our study aimed to investigate the effect of VEGF production on islet revascularization and function by transplanting the endothelial cells transducted by VEGF165 together with 300 IEQ islets, which is considered a marginal mass for diabetic rats. In the presence of islet impairment, revascularization appears to ensue irrespective of whether islets are transplanted intra-portally in the liver, retrogradely into the spleen, or under the kidney capsule. In our experiment, the islets were transplanted under the kidney capsule in order to facilitate histological observations. Unlike previous studies, we used endothelial cells, not the graft islets, as the "target cells" in our experiment. Endothelial cells take part in the revascularization, and are easy to obtain and be transducted. Our results validated the concept that elevated local production of VEGF helps facilitate islet revascularization, as reflected by the significantly increased CD34 immunostaining under the kidney capsule that was grafted with the VEGF vector-transduced endothelial cells.

The newly transplanted islets are hypoxic, causing islet cells to undergo apoptosis and/or necrosis, which contribute to the loss of functional β-cell mass after transplantation[28]. Our results also showed that the elevated VEGF expression contributed to the increased islet masses as reflected by H&E and immunohistochemical staining for insulin, which was associated with improved glycemic control in the diabetic recipient rats. Taken together, these results demonstrate that local VEGF production significantly enhances islet revascularization and improve glycemic control in STZ-induced diabetic rats. Our study may provide a novel strategy to accelerate islet revascularization and improve long-term survival of functional islet masses after transplantation.

REFERENCES

1   **Stagner JI**, Samols E. Altered microcirculation and secretion in transplanted islets. *Transplant Proc* 1994; **26**: 1100-1102
2   **Shapiro AM**, Ryan EA, Lakey JR. Diabetes. Islet cell transplantation. *Lancet* 2001; **358** Suppl: S21
3   **Boker A**, Rothenberg L, Hernandez C, Kenyon NS, Ricordi

C, Alejandro R. Human islet transplantation: update. *World J Surg* 2001; **25**: 481-486

4   **Dehghani GA**, Sotoodeh M, Omrani GR. Trophic effects of vanadium on beta-cells of STZ-induced insulin dependent diabetic rats & evidence for long-term relief of diabetes mellitus. *Indian J Med Res* 1999; **110**: 70-75

5   **Yu M**, Qian YQ, Lu SY, Chen GS, Ye J. Construction of VEGF eukaryotic expression vector and its expression in endothelial cells and cardiac myocytes in-vitro. *Xibao Yufen Zimian Yixue ZaZhi* 2003; **19**: 223-224

6   **Hering BJ**, Matsumoto I, Sawada T, Nakano M, Sakai T, Kandaswamy R, Sutherland DE. Impact of two-layer pancreas preservation on islet isolation and transplantation. *Transplantation* 2002; **74**: 1813-1816

7   **Russell JC**, Graham SE, Dolphin PJ. Glucose tolerance and insulin resistance in the JCR: LA-corpulent rat: effect of miglitol (Bay m1099). *Metabolism* 1999; **48**: 701-706

8   **Imao T**, Egawa M, Takashima H, Koshida K, Namiki M. Inverse correlation of microvessel density with metastasis and prognosis in renal cell carcinoma. *Int J Urol* 2004; **11**: 948-953

9   **Fontaine MJ**, Fan W. Islet cell transplantation as a cure for insulin dependent diabetes: current improvements in preserving islet cell mass and function. *Hepatobiliary Pancreat Dis Int* 2003; **2**: 170-179

10   **Ozmen L**, Ekdahl KN, Elgue G, Larsson R, Korsgren O, Nilsson B. Inhibition of thrombin abrogates the instant blood-mediated inflammatory reaction triggered by isolated human islets: possible application of the thrombin inhibitor melagatran in clinical islet transplantation. *Diabetes* 2002; **51**: 1779-1784

11   **Gainer AL**, Suarez-Pinzon WL, Min WP, Swiston JR, Hancock-Friesen C, Korbutt GS, Rajotte RV, Warnock GL, Elliott JF. Improved survival of biolistically transfected mouse islet allografts expressing CTLA4-Ig or soluble Fas ligand. *Transplantation* 1998; **66**: 194-199

12   **Fotiadis C**, Xekouki P, Papalois AE, Antonakis PT, Sfiniadakis I, Flogeras D, Karampela E, Zografos G. Effects of mycophenolate mofetil vs cyclosporine administration on graft survival and function after islet allotransplantation in diabetic rats. *World J Gastroenterol* 2005; **11**: 2733-2738

13   **Jansson L**, Carlsson PO. Graft vascular function after transplantation of pancreatic islets. *Diabetologia* 2002; **45**: 749-763

14   **Barshes NR**, Wyllie S, Goss JA. Inflammation-mediated dysfunction and apoptosis in pancreatic islet transplantation: implications for intrahepatic grafts. *J Leukoc Biol* 2005; **77**: 587-597

15   **Furuya H**, Kimura T, Murakami M, Katayama K, Hirose K, Yamaguchi A. Revascularization and function of pancreatic islet isografts in diabetic rats following transplantation. *Cell Transplant* 2003; **12**: 537-544

16   **Brissova M**, Fowler M, Wiebe P, Shostak A, Shiota M, Radhika A, Lin PC, Gannon M, Powers AC. Intraislet endothelial cells contribute to revascularization of transplanted pancreatic islets. *Diabetes* 2004; **53**: 1318-1325

17   **Brown LF**, Detmar M, Claffey K, Nagy JA, Feng D, Dvorak AM, Dvorak HF. Vascular permeability factor/vascular endothelial growth factor: a multifunctional angiogenic cytokine. *EXS* 1997; **79**: 233-269

18   **Shimizu H**, Mitsuhashi N, Ohtsuka M, Ito H, Kimura F, Ambiru S, Togawa A, Yoshidome H, Kato A, Miyazaki M. Vascular endothelial growth factor and angiopoietins regulate sinusoidal regeneration and remodeling after partial hepatectomy in rats. *World J Gastroenterol* 2005; **11**: 7254-7260

19   **Isner JM**. Myocardial gene therapy. *Nature* 2002; **415**: 234-239

20   **Koransky ML**, Robbins RC, Blau HM. VEGF gene delivery for treatment of ischemic cardiovascular disease. *Trends Cardiovasc Med* 2002; **12**: 108-114

21   **Khan TA**, Sellke FW, Laham RJ. Gene therapy progress and prospects: therapeutic angiogenesis for limb and myocardial ischemia. *Gene Ther* 2003; **10**: 285-291

22   **Sigrist S**, Mechine-Neuville A, Mandes K, Calenda V, Braun S, Legeay G, Bellocq JP, Pinget M, Kessler L. Influence of VEGF on the viability of encapsulated pancreatic rat islets after transplantation in diabetic mice. *Cell Transplant* 2003; **12**: 627-635

23   **Gorden DL**, Mandriota SJ, Montesano R, Orci L, Pepper MS. Vascular endothelial growth factor is increased in devascularized rat islets of Langerhans *in vitro*. *Transplantation* 1997; **63**: 436-443

24   **Kuroda M**, Oka T, Oka Y, Yamochi T, Ohtsubo K, Mori S, Watanabe T, Machinami R, Ohnishi S. Colocalization of vascular endothelial growth factor (vascular permeability factor) and insulin in pancreatic islet cells. *J Clin Endocrinol Metab* 1995; **80**: 3196-3200

25   **Vasir B**, Aiello LP, Yoon KH, Quickel RR, Bonner-Weir S, Weir GC. Hypoxia induces vascular endothelial growth factor gene and protein expression in cultured rat islet cells. *Diabetes* 1998; **47**: 1894-1903

26   **Vasir B**, Jonas JC, Steil GM, Hollister-Lock J, Hasenkamp W, Sharma A, Bonner-Weir S, Weir GC. Gene expression of VEGF and its receptors Flk-1/KDR and Flt-1 in cultured and transplanted rat islets. *Transplantation* 2001; **71**: 924-935

27   **Okuda T**, Azuma T, Ohtani M, Masaki R, Ito Y, Yamazaki Y, Ito S, Kuriyama M. Hypoxia-inducible factor 1 alpha and vascular endothelial growth factor overexpression in ischemic colitis. *World J Gastroenterol* 2005; **11**: 1535-1539

28   **Carlsson PO**, Mattsson G. Oxygen tension and blood flow in relation to revascularization in transplanted adult and fetal rat pancreatic islets. *Cell Transplant* 2002; **11**: 813-820

Expression of ornithine decarboxylase in precancerous and cancerous gastric lesions

Xin-Pu Miao, Jian-Sheng Li, Hui-Yan Li, Shi-Ping Zeng, Ye Zhao, Jiang-Zheng Zeng

Xin-Pu Miao, Shi-ping Zeng, Department of Gastroenterology, the Affiliated Hospital of Hainan Medical College, Haikou 570102, Hainan Province, China

Jian-Sheng Li, Ye Zhao, Department of Gastroenterology, the First Affiliated Hospital of Zhengzhou University, Zhengzhou 450052, Henan Province, China

Hui-Yan Li, Department of Chemotherapy for Cancer, West China Hospital of Sichuan University, Chengdu 610041, Sichuan Province, China

Jiang-zheng Zeng, Department of Cancer, the Affiliated Hospital of Hainan Medical College, 31 Longhua Avenue, Haikou 570102, Hainan Province, China

Supported by Miao Pu Foundation of Hainan Medical College, No. 2004108 and Natural Science Foundation of Hainan Province, No. 80582

Correspondence to: Dr. Xin-Pu Miao, Department of Gastroenterology, West China Hospital of Sichuan University, 17 Renmin Avenue, Chengdu 610041, Sichuan Province, China. miaoxinpu@163.com

Telephone: +86-13438913825

Received: 2007-01-29   Accepted: 2007-02-14

Abstract

AIM: To investigate the expression of ornithine decarboxylase (ODC) in precancerous and cancerous gastric lesions.

METHODS: We studied the expression of ODC in gastric mucosa from patients with chronic superficial gastritis (CSG, n = 32), chronic atrophic gastritis [CAG, n = 43; 15 with and 28 without intestinal metaplasia (IM)], gastric dysplasia (DYS, n = 11) and gastric cancer (GC, n = 48) tissues using immunohistochemical staining. All 134 biopsy specimens of gastric mucosa were collected by gastroscopy.

METHODS: The positive rate of ODC expression was 34.4%, 42.9%, 73.3%, 81.8% and 91.7% in cases with CSG, CAG without IM, CAG with IM, DYS and GC, respectively (P < 0.01), The positive rate of ODC expression increased in the order of CSG < CAG (without IM) < CAG (with IM) < DYS and finally, GC. In addition, ODC positive immunostaining rate was lower in well-differentiated GC than in poorly-differentiated GC (P < 0.05).

CONCLUSION: The expression of ODC is positively correlated with the degree of malignity of gastric mucosa and development of gastric lesions. This finding indicates that ODC may be used as a good biomarker in the screening and diagnosis of precancerous lesions.

INTRODUCTION

Ornithine decarboxylase (ODC) is the first-rate limiting enzyme in the polyamine biosynthesis pathway[1]. ODC plays a critical role in cell proliferation[2], and it is implicated as an essential promoter in normal cell cycles. The activation of ODC is similarly related to tumor promotion and progression[3,4]. ODC activity appears to be directly coupled to the expression of ODC protein and increases with eukaryotic cell division in neoplasia and fetal development. Convincing evidence has confirmed that ODC plays an important role in the chemical carcinogenesis of mouse skin, and tumor formation can be blocked by the irreversible inhibitor of ODC, α-difluoromethylornithine[5-7]. ODC is overexpressed in a variety of cancers. Elevated levels of ODC have been found in gastric cancer[8], gliomas[9], breast cancer[10,11], colon cancer[12], pancreatic cancer[13], lung cancer[14], and prostate cancer[15]. In addition, increased expression of ODC has been found associated with gastric atrophy[16].

Although ODC overexpression is clearly associated with cancer development, a definitive causal role for ODC overexpression in carcinogenesis has only been shown in NIH/3T3 fibroblast cells[17]. Overexpression of ODC is sufficient to transform fibroblast cells *in vitro*, causing increased frequency of skin tumors in a transgenic mouse model[5,17].

Although several studies have evaluated ODC expression in gastric cancer, to date, no one has investigated its associations with precancerous gastric lesions, namely, in chronic atrophic gastritis (CAG), intestinal metaplasia (IM) and gastric dysplasia (DYS). There is no information

presently available about the protein status of ODC in stomach mucosa collected by gastroscopy. A detailed study comparing the expression patterns of ODC in gastric carcinoma and precancerous tissues has not been conducted. Furthermore, whether overexpression of ODC is involved in the initiation or promotion of gastric cancer (GC) has not been established. Therefore, the aim of the present study was to investigate the expression of ornithine decarboxylase (ODC) in precancerous and cancerous gastric lesions.

MATERIALS AND METHODS

Tissue samples

We collected gastric mucosal specimens from 134 patients including 32 with chronic superficial gastritis (CSG), 43 with CAG (15 with and 28 without IM), 11 with DYS and 48 with antral GC, during gastroscopy. These specimens were obtained from symptom-free subjects who volunteered to participate in gastroscopic screening for gastric cancer in the Department of Gastroenterology of the First Affiliated Hospital of Zhengzhou University. The 48 GC patients had not received any radiation therapy or chemotherapy. GC tissues could be further separated on the basis of differentiation grade. Histopathologically, all the 48 gastric specimens were confirmed as adenocarcinoma. All of the biopsies were taken from gastric antrum. The tumors were histologically graded as well-differentiated (17 patients, 35%), moderately-differentiated (10 patients, 21%) and poorly-differentiated (21 patients, 44%).The study protocol was approved by the Ethics Committee of the First Affiliated Hospital of Zhengzhou University.

Immunohistochemical staining for anti-ODC antibody

Tissues were fixed in 96% ethanol for 6 h at 4℃, embedded in paraffin, and cut into 5-mm thick sections. For Immunohistochemical (IHC) analysis, endogenous peroxidase activity was neutralized by treating the section in 1% hydrogen peroxide in phosphate-buffered saline for 20 min. For the microwave antigen retrieval procedure, slides were immersed in 10 mmol/L citrate buffer (pH 6.0) in a clean polyethylene chamber and placed inside a full-powered microwave, then heated for 10 min at 95℃ to repair antigens, and subsequently cooled for 10-20 min. After being washed 3 times with phosphate-buffered saline, the sections were blocked in 10% mouse serum for 30-60 min to suppress nonspecific binding of IgG. Each tissue section was then incubated with primary mouse antihuman ODC monoclonal antibody (1:1000, Westbury, NY) for 2 h at room temperature. The slides were washed 3 times with phosphate-buffered saline and incubated with anti-mouse biotinylated secondary antibody (Vector, Burlingame, CA). The slides were colorized by DAB Reagent (Vectastain) and counterstained with hematoxylin. Negative controls were established by replacing the primary antibody with PBS supplemented with normal mouse or rabbit serum.

The staining results were evaluated according to the immunodetection of stain intensity and positive cells by

Table 1 Immunohistochemical assay of ODC protein in gastric precancerous and cancerous lesions

Histological grade	ODC protein expression (n)				Total	Positive rate (%)[a]
	−	+	+ +	+ + +		
CSG	21	9	2	0	32	34.4[b]
CAG (without IM)	16	9	1	2	28	42.9[b,c]
CAG (with IM)	4	2	6	3	15	73.3
DYS	2	1	4	4	11	81.8
GC	4	4	23	17	48	91.7

[a]$P < 0.01$, by treand; [b]$P < 0.01$, CSG vs CAG (with IM), CSG vs DYS, CSG vs GC, CAG (without IM) vs DYS and CAG (without IM) vs GC; and [c]$P < 0.05$, CAG (without IM) vs CAG (with IM). CSG: chronic superficial gastritis; CAG: chronic atrophic gastritis; IM: intestinal metaplasia; DYS: dysplasia; GC: gastric cancer.

two pathologists (Z Tan and L H Jiao), who discussed each case until they reached a consensus. Stain intensity is up to the standard of the relative stain intensity of most cells. The stain intensity could be from 0 to 3 (0, no staining; 1, shallow brown; 2, brown; 3, dark brown); and the positive cells in the observed stomach mucous cells ranged from 0 to 3 in percentage (0,no staining; 1, < 30%; 2, 30%-70%; and 3 > 70%). The samples were scored by their summation: 0-1 (-); 2-3 (+); 4 (++); 5-6 (+++).Any staining score ≥ 2 (+) was considered as positive expression.

Histopathological diagnosis for gastric epithelia was made according to the cellular morphological changes and tissue architecture using previously established criteria[18,19]. In brief, SCG, an inflammation manifested by mild lymphocyte and plasma-cell infiltration; CAG, glandular morphology disappeared partially or completely absent in the mucosa and replaced by connective tissues, inter-glandular space was infiltrated mainly by plasma cells and lymphocytes; IM, confirmed by the presence of goblet cells in gastric mucosa; and DYS, characterized by nuclear atypia with or without architectural abnormalities in the gastric epithelium without invasion. GC is characterized by invasion of neoplastic gastric cells through the basement membrane. Carcinomas were classified according to the histological classification of WHO and the Japanese Gastric Cancer Association[20,21].

Statistical analysis

The χ^2 test was used for the percentage of samples with positive staining among lesions of different severities. SPSS 12.0 was used for statistical analyses. $P < 0.05$ was considered statistically significant.

RESULTS

Positive immunostaining for ODC was observed in the gastric epithelial cells and cancer cells with different rates in the lesions of CSG, CAG (without IM), CAG (with IM), DYS and GC. To estimate the difference, staining for ODC was carried out on whole sections. The positive immunostaining rate for ODC was 34.4% (11 of 32), 42.9% (12 of 28), 73.3% (11 of 15), 81.8% (9 of 11), and 91.7% (44 of 48), respectively ($P < 0.001$) (Table 1). ODC
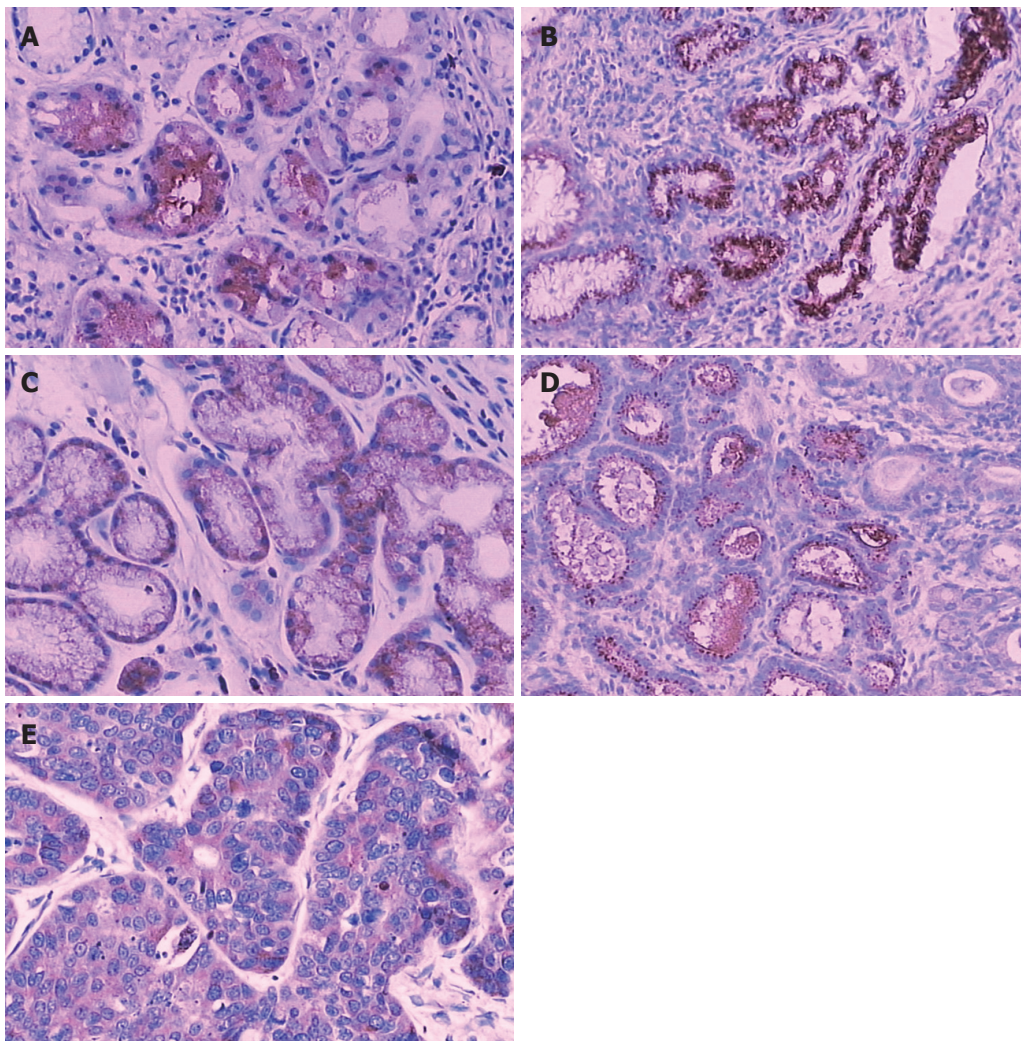
Figure 1 Immunoreactivity of ODC protein in gastric precancerous and cancerous lesions. **A**: Immunostaining of ODC in CSG, SP × 200; **B**: Immunostaining of ODC in CAG (Without IM). SP × 200; **C**: Immunostaining of ODC in CAG (with IM) SP × 200; **D**: Immunostaining of ODC in DYS, SP × 200; **E**: Immunostaining of ODC in GC, SP × 200. CSG: chronic superficial gastritis; CAG: chronic atrophic gastritis; IM: intestinal metaplasia; DYS: dysplasia; GC: gastric cancer.

Table 2 IHC assay of ODC protein in gastric cancer

Histological grade	ODC protein expression (*n*)				Total	Positive rate (%)
	-	+	+ +	+ + +		
Well differentiated	9	1	5	2	17	47.1[a]
Moderately differentiated	1	3	2	4	10	90
Poorly differentiated	1	5	6	9	21	95.2

[a]*P* < 0.05, well differentiated tissue *vs* either moderately or poorly differentiated tissues.

immunoreactivity was located mainly in the cytoplasm and cell membrane (Figure 1A-E).

The positive immunostaining rate for ODC was very low in CSG and CAG (without IM), and slightly increased in CAG (with IM) and DYS, and significantly increased in GC. ODC protein accumulation was higher in the GC than in CSG and CAG (without IM). In the cases of CAG (with IM) and DYS, it was also higher than in CSG and CAG (without IM). But it did not show significant difference among the groups with CAG (with IM), DYS and GC (Table 1). ODC positive immunostaining rate in

the well-differentiated GC was lower than that in poorly-differentiated GC (Table 2).

DISCUSSION

Gastric cancer has a high incidence in China and around the world. Gastric carcinogenesis is considered as a multistage, progressive process. It is of great importance to understand the biological processes of cancer initiation for early cancer detection. An early indicator for a patient predisposed to GC is abnormal hyperproliferation of gastric epithelial cells, such as in CAG, DYS and IM, which have all been considered as precancerous lesions for GC[22,23]. However, information about the mechanism of gastric carcinogenesis is very limited. Studies of ODC protein expression levels at different stages of gastric carcinogenesis may help answer why different stages of cancerous development occur.

Polyamines, such as putrescine, spermidine and spermine, play important roles in cell proliferation and differentiation. ODC is a rate-limiting enzyme in the biosynthesis of polyamines, and the ODC gene is considered as an immediate early gene as well as an oncogene[2,23,24]. The expression rate of ODC is invariably associated with a cell's proliferate activity. ODC protein is 50 kDa monomer and about 100 kDa as the active

homodimer is formed. It has a rapid turnover rate with a half-life at 15 min[25]. While ODC activity may be correlated with the oncogenesis and progression of gastric cancer, the expression pattern of ODC in precancerous gastric lesions have not yet been elucidated.

In the present study, we conducted a detailed IHC comparison between precancerous and cancerous gastric lesions. The expression of ODC is positively correlated with the degree of malignity of gastric mucosa and the development of gastric lesions. With the likelihood of malignant lesions progressed from normal to CSG < CAG < DYS < GC, the positive immunostaining rates for ODC similarly increased, showing a good linear correlation between ODC expression and lesion progression. We found that the positive immunostaining rate of ODC is abnormally high in CAG (with IM), DYS and GC, indicative of abnormally high cell proliferation activity. This indicates that ODC expression may be related to the proliferative status of gastric mucosa epithelial cells. These data are consistent with the views of Patchett and others who have suggested that the presence of atrophy and intestinal metaplasia are strongly associated with increased levels of ODC activity[26]. The present results indicate that increased expression of ODC may be an important molecular event, involved in the early stages of gastric carcinogenesis. The high coincidental expression of ODC protein accumulation may be an important event to enhance GC and a useful biomarker to assess risk for the development of GC[27]. This conclusion differs from Patchett's, which suggested that measurement of mucosal ODC activity may not be a valuable clinical marker of increased cancer risk [28]. We believe that variations in technique, materials and methods may partly explain these distinctions.

Another interesting observation is that the expression of ODC directly correlates with the differentiable condition of GC. The ODC positive immunostaining rate in well-differentiated GC was lower than in both the poorly-differentiated and moderately-differentiated GC. This result is consistent with findings in human colon carcinomas[29]. The present results indicate that increased expression of ODC may reflect the differentiated condition of stomach mucosa.

The regulation of ODC expression can occur at multiple levels including transcription, translation and protein degradation[30-32]. The ODC antizyme is a major factor in the regulation of ODC[33,34]. ODC antizyme binds to monomeric ODC, stimulating the degradation of ODC, and therefore, decreasing the exogenous level of ODC protein[35]. We presume that gastric mucosa epithelial cells may have different intrinsic ODC antizyme levels. ODC antizyme levels may decrease significantly while the degree of malignity of the gastric mucosa increases. This hypothesis requires careful investigation in follow-up studies.

In conclusion, the expression of ODC is positively correlated with the degree of malignity of gastric mucosa and development of gastric lesions. This finding indicates that ODC may be used as a good biomarker in the screening and diagnosis of precancerous lesions.

COMMENTS

Background

Ornithine decarboxylase (ODC) catalyzes the first step in the polyamine biosynthetic pathway forming putrescine, which is then converted into the polyamines spermidine and spermine. Polyamine content plays an important role in both normal and neoplastic growth and alterations of polyamine synthesis via changes in ODC content occur in response to tumor promoters and carcinogens. The amount of ODC is altered in response to many growth factors, oncogenes, and tumor promoters and to changes in polyamine levels. ODC is overexpressed in a variety of cancers. Gastric cancer has a high incidence in China and around the world. Gastric carcinogenesis is considered as a multistage, progressive process. It is of great importance to understand the biological processes of cancer initiation for early cancer detection. An early indicator for a patient predisposed to GC is abnormal hyperproliferation of gastric epithelial cells, such as in CAG, DYS and IM, which have all been considered as precancerous lesions for GC. Studies of ODC protein expression levels at different stages of gastric carcinogenesis may help answer why different stages of cancerous development occur.

Research frontiers

It can be seen in the following four aspects: (1) expression of ODC in cancers; (2)regulation of ornithine decarboxylase; (3) inhibitor of ODC-antizyme; and (4)role of ODC and antizyme in carcinogenesis

Innovations and breakthroughs

Although several studies have evaluated ODC expression in gastric cancer, to date, no one has investigated its associations with precancerous gastric lesions, namely, in chronic atrophic gastritis (CAG), intestinal metaplasia (IM) and gastric dysplasia (DYS). The authors found the expression of ODC is positively correlated with the degree of malignity of gastric mucosa and the development of gastric lesions. The positive immunostaining rates for ODC similarly increased, showing a good linear correlation between ODC expression and lesion progression. This finding indicates that ODC may be used as a good biomarker in the screening and diagnosis of precancerous lesions.

Applications

The authors found the expression of ODC is positively correlated with the degree of malignity of gastric mucosa and the development of gastric lesions. With the likelihood of malignant lesions progressed from normal to CSG < CAG < DYS < GC, the positive immunostaining rates for ODC similarly increased, showing a good linear correlation between ODC expression and lesion progression. Therefore, ODC may be used as a good biomarker in future in screening and diagnosing precancerous and cancerous gastric lesions

Terminology

ODC: ornithine decarboxylase; CAG: chronic atrophic gastritis; IM: intestinal metaplasia; DYS: gastric dysplasia; GC: gastric cancer.

Peer review

This paper investigates the expression and diagnostic value of ODC, a key rate-limiting enzyme in polyamine biosynthesis, in gastric precursor and cancer. The expression of ODC is positively correlated with the degree of malignancy of gastric mucosa, in the order of chronic superficial gastritis, chronic atrophic gastritis (without intestinal metaplasia), chronic atrophic gastritis (with intestinal metaplasia), gastric dysplasia and gastric cancer. They concluded that ODC can be a good indicator in the screening and diagnosis of gastric precursor and cancerous lesions.

REFERENCES

1   **Thomas T**, Thomas TJ. Polyamine metabolism and cancer. *J Cell Mol Med* 2003; **7**: 113-126

2   **Auvinen M**, Paasinen A, Andersson LC, Holtta E. Ornithine decarboxylase activity is critical for cell transformation. *Nature* 1992; **360**: 355-358

3   **Pegg AE**. Polyamine metabolism and its importance in neoplastic growth and a target for chemotherapy. *Cancer Res* 1988; **48**: 759-774

4   **Tabib A**, Bachrach U. Role of polyamines in mediating malignant transformation and oncogene expression. *Int J Biochem Cell Biol* 1999; **31**: 1289-1295

5   **O'Brien TG**, Megosh LC, Gilliard G, Soler AP. **Ornithine** decarboxylase overexpression is a sufficient condition for tumor promotion in mouse skin. *Cancer Res* 1997; **57**: 2630-2637

6   **Soler PA,** Gilliard G, Megosh L, George K, O'Brien TG. Polyamine regulates expression of the neoplastic phenotype in mouse skin. *Cancer Res* 1988; **58**:1654-1659

7   **Megosh LC**, Hu J, George K, O'Brien TG. Genetic control of polyamine-dependent susceptibility to skin tumorigenesis. *Genomics* 2002; **79**: 505-512

8   **Mori M**, Honda M, Shibuta K, Baba K, Nakashima H, Haraguchi M, Koba F, Ueo H, Sugimachi K, Akiyoshi T. Expression of ornithine decarboxylase mRNA in gastric carcinoma. *Cancer* 1996; **77**: 1634-1638

9   **Ernestus RI**, Rohn G, Schroder R, Els T, Klekner A, Paschen W, Klug N. Polyamine metabolism in brain tumours: diagnostic relevance of quantitative biochemistry. *J Neurol Neurosurg Psychiatry* 2001; **71**: 88-92

10   **Mimori K**, Mori M, Shiraishi T, Tanaka S, Haraguchi M, Ueo H, Shirasaka C, Akiyoshi T. Expression of ornithine decarboxylase mRNA and c-myc mRNA in breast tumours. *Int J Oncol* 1998; **12**: 597-601

11   **Canizares F**, Salinas J, de las Heras M, Diaz J, Tovar I, Martinez P, Penafiel R. Prognostic value of ornithine decarboxylase and polyamines in human breast cancer: correlation with clinicopathologic parameters. *Clin Cancer Res* 1999; **5**: 2035-2041

12   **Berdinskikh NK**, Ignatenko NA, Zaletok SP, Ganina KP, Chorniy VA. Ornithine decarboxylase activity and polyamine content in adenocarcinomas of human stomach and large intestine. *Int J Cancer* 1991; **47**: 496-498

13   **Subhi AL**, Tang B, Balsara BR, Altomare DA, Testa JR, Cooper HS, Hoffman JP, Meropol NJ, Kruger WD. Loss of methylthioadenosine phosphorylase and elevated ornithine decarboxylase is common in pancreatic cancer. *Clin Cancer Res* 2004; **10**: 7290-7296

14   **Tian H**, Huang Q, Li L, Liu XX, Zhang Y. Gene expression of ornithine decarboxylase in lung cancers and its clinical significance. *Acta Biochim Biophys Sin* (Shanghai) 2006; **38**: 639-645

15   **Young L**, Salomon R, Au W, Allan C, Russell P, Dong Q. Ornithine decarboxylase (ODC) expression pattern in human prostate tissues and ODC transgenic mice. *J Histochem Cytochem* 2006; **54**: 223-229

16   **Konturek PC**, Rembiasz K, Konturek SJ, Stachura J, Bielanski W, Galuschka K, Karcz D, Hahn EG. **Gene expression of** ornithine decarboxylase, cyclooxygenase-2, and gastrin in atrophic gastric mucosa infected with Helicobacter pylori before and after eradication therapy. *Dig Dis Sci* 2003; **48**: 36-46

17   **Moshier JA**, Dosescu J, Skunca M, Luk GD. Transformation of NIH/3T3 cells by ornithine decarboxylase overexpression. *Cancer Res* 1993; **53**: 2618-2622

18   **Wang LD**, Shi ST, Zhou Q, Goldstein S, Hong JY, Shao P, Qiu SL, Yang CS. Changes in p53 and cyclin D1 protein levels and

cell proliferation in different stages of human esophageal and gastric-cardia carcinogenesis. *Int J Cancer* 1994; **59**: 514-519

19   **Rugge M**, Correa P, Dixon MF, Hattori T, Leandro G, Lewin K, Riddell RH, Sipponen P, Watanabe H. Gastric dysplasia: the Padova international classification. *Am J Surg Pathol* 2000; **24**: 167-176

20   **Fenoglio-Preiser C,** Muñoz N, Carneiro F. Tumors of the stomach. In: Hamilton SR, Aaltonen LA. World Health Organization classification of tumours, Pathology and genetics of tumours of the digestive system. 1st ed. Lyon: International Agency for Research on Cancer, 2000: 37-38

21   Japanese Gastric Cancer Association, Japanese classification of gastric carcinoma, 2nd ed, Tokyo: Kanehara & Co. Ltd Pub, 1998; 10-24

22   **You WC**, Blot WJ, Li JY, Chang YS, Jin ML, Kneller R, Zhang L, Han ZX, Zeng XR, Liu WD. Precancerous gastric lesions in a population at high risk of stomach cancer. *Cancer Res* 1993; **53**: 1317-1321

23   **Correa P**. Human gastric carcinogenesis: a multistep and multifactorial process--First American Cancer Society Award Lecture on Cancer Epidemiology and Prevention. *Cancer Res* 1992; **52**: 6735-6740

24   **Rousseau D**, Kaspar R, Rosenwald I, Gehrke L, Sonenberg N. Translation initiation of ornithine decarboxylase and nucleocytoplasmic transport of cyclin D1 mRNA are increased in cells overexpressing eukaryotic initiation factor 4E. *Proc Natl Acad Sci USA* 1996; **93**: 1065-1070

25   **Pendeville H**, Carpino N, Marine JC, Takahashi Y, Muller M, Martial JA, Cleveland JL. The ornithine decarboxylase gene is essential for cell survival during early murine development. *Mol Cell Biol* 2001; **21**: 6549-6558

26   **Patchett SE**, Katelaris PH, Zhang ZW, Alstead EM, Domizio P, Farthing MJ. Ornithine decarboxylase activity is a marker of premalignancy in longstanding Helicobacter pylori infection. *Gut* 1996; **39**: 807-810

27   **Okuzumi J**, Yamane T, Kitao Y, Tokiwa K, Yamaguchi T, Fujita Y, Nishino H, Iwashima A, Takahashi T. Increased mucosal ornithine decarboxylase activity in human gastric cancer. *Cancer Res* 1991; **51**: 1448-1451

28   **Patchett SE**, Alstead EM, Butruk L, Przytulski K, Farthing MJ. Ornithine decarboxylase as a marker for premalignancy in the stomach. *Gut* 1995; **37**: 13-16

29   **Pegg AE**. Recent advances in the biochemistry of polyamines in eukaryotes. *Biochem J* 1986; **234**: 249-262

30   **Hu HY**, Liu XX, Jiang CY, Zhang Y, Bian JF, Lu Y, Geng Z, Liu SL, Liu CH, Wang XM, Wang W. Cloning and expression of ornithine decarboxylase gene from human colorectal carcinoma. *World J Gastroenterol* 2003; **9**: 714-716

31   **Pegg AE**, Shantz LM, Coleman CS. Ornithine decarboxylase: structure, function and translational regulation. *Biochem Soc Trans* 1994; **22**: 846-852

32   **Shantz LM**, Pegg AE. Translational regulation of ornithine decarboxylase and other enzymes of the polyamine pathway. *Int J Biochem Cell Biol* 1999; **31**: 107-122

33   **Ivanov IP**, Matsufuji S, Murakami Y, Gesteland RF, Atkins JF. Conservation of polyamine regulation by translational frameshifting from yeast to mammals. *EMBO J* 2000; **19**: 1907-1917

34   **Coffino P**. Regulation of cellular polyamines by antizyme. *Nat Rev Mol Cell Biol* 2001; **2**: 188-194

35   **Ivanov IP**, Rohrwasser A, Terreros DA, Gesteland RF, Atkins JF. Discovery of a spermatogenesis stage-specific ornithine decarboxylase antizyme: antizyme 3. *Proc Natl Acad Sci USA* 2000; **97**: 4808-4813

RAPID COMMUNICATION

5-aminosalicylic acid in combination with nimesulide inhibits proliferation of colon carcinoma cells *in vitro*

Hai-Ming Fang, Qiao Mei, Jian-Ming Xu, Wei-Juan Ma

Hai-Ming Fang, Qiao Mei, Jian-Ming Xu, Wei-Juan Ma, Department of Gastroenterology, The First Affiliated Hospital, Anhui Medical University; The Key Laboratory of Digestive Diseases of Anhui Province, Hefei 230032, Anhui Province, China
Hai-Ming Fang, Department of pharmacology, Anhui Medical University, Hefei 230032, Anhui Province, China
Supported by The Key Laboratory of Digestive Diseases of Anhui Province and colleagues from Department of Gastroenterology, The First Affiliated Hospital, Anhui Medical University, China
Correspondence to: Jian-Ming Xu, Department of Gastroenterology, The First Affiliated Hospital, Anhui Medical University, Hefei 230032, Anhui Province,
China. funhemon@163.com
Telephone: +86-551-2922039 Fax: +86-551-2922382
Received: 2007-01-27   Accepted: 2007-02-14

Abstract

AIM: To investigate the effects of 5-aminosalicylic acid (5-ASA) in combination with nimesulide on the proliferation of HT-29 colon carcinoma cells and its potential mechanisms.

METHODS: Inhibitory effects of drugs (5-ASA, nimesulide and their combination) on HT-29 colon carcinoma cells were investigated by thiazolyl blue tetrazolium bromide (MTT) assay. Cellular apoptosis and proliferation were detected by TUNEL assay and immunocytochemical staining, respectively.

RESULTS: Pretreatment with 5-ASA or nimesulide at the concentration of 10-1000 μmol/L inhibited proliferation of HT-29 colon carcinoma cells in a dose-dependent manner *in vitro* ($t = 5.122$, $P < 0.05$; $t = 3.086$, $P < 0.05$, respectively). The inhibition rate of HT-29 colon carcinoma cell proliferation was also increased when pretreated with 5-ASA (100 μmol/L) or nimesulide (100 μmol/L) for 12-96 h, which showed an obvious time-effect relationship ($t = 6.149$, $P < 0.05$; $t = 4.159$, $P < 0.05$, respectively). At the concentration of 10-500 μmol/L, the apoptotic rate of HT-29 colon carcinoma cells significantly increased ($t = 18.156$, $P < 0.001$; $t = 19.983$, $P < 0.001$, respectively), while expression of proliferating cell nuclear antigen (PCNA) was remarkably decreased ($t = 6.828$, $P < 0.05$; $t = 14.024$, $P < 0.05$, respectively). 5-ASA in combination with nimesulide suppressed the proliferation of HT-29 colon carcinoma cells more than either of these agents in a dose-dependent and time-dependent manner ($t = 5.448$, $P < 0.05$; $t = 4.428$, $P < 0.05$, respectively).

CONCLUSION: 5-ASA and nimesulide may inhibit the proliferation of HT-29 colon carcinoma cells and coadministration of these agents may have additional chemopreventive potential.

INTRODUCTION

Inflammatory bowel disease (IBD) is associated with an increased risk of developing colorectal cancer (CRC)[1-5]. Primary prevention of CRC in IBD has received more attention in recent years. Epidemiological, experimental and preliminary clinical work strongly suggests that 5-aminosalicylic acid (5-ASA) may have potentially chemopreventive properties against CRC[6-10]. On the other hand, aspirin, sulindac and other non-steroid anti-inflammatory drugs (NSAIDs) are also known to reduce the risk of developing colon cancer[6,11-13]. However, the potential mechanisms of either 5-ASA or NSAIDs underlying chemoprevention of CRC in IBD remain largely unexplored.

Inhibition of inflammatory cascades involved in cell growth is the popular putative actions of 5-ASA. Arachidonic acid (AA) metabolism has obtained popular attention and can be metabolized in two major pathways including cycloxygenase (COX) pathway and lipoxygenase (LOX) pathway. Metabolites of the former are prostaglandins which regulate cell proliferation and those of the latter are responsible for the subsequent expression of pro-inflammatory molecules[14-16]. 5-LOX and COX-2 activities have recently attracted considerable interest in CRC and data demonstrate that 5-LOX and COX-2 are both up-regulated in CRC[17,18]. It was reported that

COX-2 inhibitors or 5-LOX inhibitors may suppress CRC development[13,17]. Lots of studies[13,15,19-21] indicate that the chemopreventive effect of 5-ASA on CRC is correlated with inhibiting 5-LOX activity and COX-2 is the main target of NSAIDs to suppress CRC development. 5-LOX and COX-2 are the key enzymes for AA metabolism. Since inhibition of one pathway alone, especially the 5-LOX pathway, may change the metabolism of the other, just inhibiting the activity of 5-LOX or COX-2 may not suppress CRC development effectively. However, few studies[22] are available on the chemopreventive effect of coadministration of these agents. It makes this method an interesting new alternative to CRC chemoprevention. This study was performed to investigate the effect of 5-ASA and a selective COX-2 inhibitor, nimesulide, on the proliferation of human colon carcinoma cells (HT-29) in vitro and its potential mechanisms.

MATERIALS AND METHODS

Cell culture
HT-29 colon carcinoma cells were obtained from Institute of Biochemistry and Cell Biology, Shanghai Institutes for Biological Sciences.The cells were maintained in RPMI 1640 medium, supplemented with 10% heat-inactivated fetal calf serum (FCS), 50 U/mL penicillin, 50 μg/mL streptomycin, in a humidified atmosphere containing 95% air and 5% CO_2 at 37℃ and routinely trypsinized with 0.25% trypsin solution.

Reagents
5-ASA, nimesulide, MTT were purchased from Sigma Corp (Steinheim, Germany). FCS was purchased from Hangzhou Sijiqing Biological Corp (Hangzhou, China). Dimethylcarbinol was purchased from Bengbu Chemical Corp (Bengbu, China). TUNEL assay kits for apoptosis were purchased from Nanjing Keygen Corp (Nanjing, China). PCNA polyclonal antibody was purchased from Santa Cruz Biotechnology Corp (California, USA). S-P immunocytochemical assay kits were purchased from Fuzhou Maixin Reagent Corp (Fuzhou, China). Other reagents used in the present study were of analytical grade.

Cell proliferation assay
Cytostatic effects were measured by MTT assay. The cells were detached with a 0.25% trypsin solution for 5 min. Subsequently, the cells were seeded onto 96-well plates (1×10^6 cells/well), supplemented with 10% FCS and allowed to attach for 24 h before the addition of test compounds (5-ASA, nimesulide, and their combination). Test compounds were diluted in serum-free culture medium. Then the cells were incubated in a medium or at different concentrations of drugs for 48 h, 20 μL of MTT solution (5 g/L) in PBS was added. Four hours later, the medium in each well was removed, and 120 μL of 0.04 mmol/L muriatic isopropanol was added, slightly concussed for 10 min. Dye uptake was measured at 490 nm with an ELISA reader. Five wells were used for each concentration or as a control group. On the other hand, the cells were seeded onto 96-well plates (1×10^6 cells/well) according to the method described above and allowed to attach for 24 h, then treated with test compounds (5-ASA, nimesulide, and their combination). The final concentration was 100 μmol/L. The same medium was added into the control group and dye uptake was then measured according to the method described above. Five wells were used for each test compound or control group.

Immunocytochemical determination of cellular proliferation and apoptosis in cells
The procedure for the determination of cell proliferation has been described elsewhere[23]. In brief, exponentially growing cells (3×10^5/mL) were trypsinized and seeded onto 24-well plates with a 10 mm × 10 mm sterile slide, supplemented with 10% FCS, allowed to attach for 24 h. The cells were then treated with different doses of drugs (5-ASA, nimesulide, and their combination). After 48-h incubation, the slides were washed twice with PBS. After blocked with normal serum, polyclonal PCNA antibody (1:200) was applied to the slides overnight at 4℃. The following steps were performed in kits following the manufacturer's introductions. Negatively expressed cells were manifested as blue-stained nuclei and the positive cells had brown-yellow cytoplasma or nuclear membrane. The expression of target protein was further semi-quantitated according to the percentage of positively-stained cells and evaluated by two blinded investigators. Negative cells were scored as 0, positive cells less than 25% were scored as 1, 25%-50% as 2, 51%-75% as 3, and higher than 75% as 4, respectively.

Apoptotic cells were visualized with the terminal deoxytransferase (TdT)-mediated dUTP biotin nick end labeling (TUNEL) method[24]. In brief, cell slides were subjected to digestion by proteinase K. TdT buffer solution was added to the slides together with 50 U TdT and 5 nmol/L dUTP and incubated at 37℃ for 90 min. The reaction was then terminated by adding 30 mmol/L sodium citrate buffer. Peroxidase-conjugated streptavidin from the DAKO kit was added, followed by the addition of DAB. The number of apoptotic cells was counted under a microscope (× 400) and negatively expressed cells were manifested as blue-stained nuclei and the positive cells gad brown-yellow cytoplasma or nuclear membrane. Apoptotic index was determined by counting the number of positive cells among 200 cells and indicated as percentages, less than 25% was graded as 1, 26%-50% as 2, 51%-75% as 3, and higher than 76% as 4, respectively.
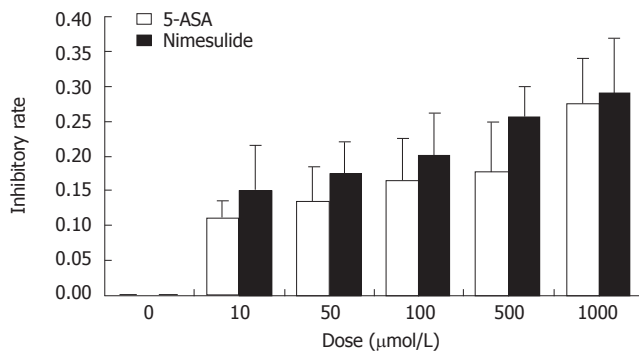
Statistical analysis
Experimental results were analyzed by ANOVA and *t*-test for multiple comparisons between groups. Data were expressed as mean ± SD. $P < 0.05$ was considered statistically significant.
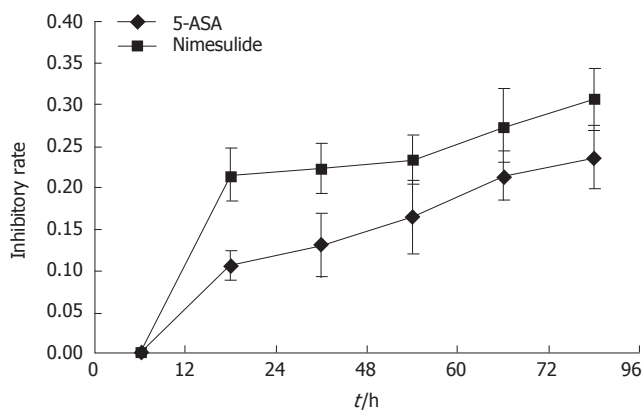
RESULTS

Effect of 5-ASA and nimesulide on growth of HT-29 colon carcinoma cells
Pretreatment with 5-ASA or nimesulide at different

Figure 1 Dose-dependent inhibitory effect of 5-ASA and nimesulide on proliferation of HT-29 colon carcinoma cells. The cells were pretreated with different doses of 5-ASA or nimesulide respectively (10, 50, 100, 500, 1000 μmol/L) for 48 h, then dye uptake was measured at 490 nm using an ELISA reader. Data were expressed as mean $\pm$ SE of five independent samples. Compared with the control group, the inhibitory rate was markedly increased in a dose-dependent manner ($P < 0.05$).

Figure 3 Inhibitory effect of 5-ASA in combination with nimesulide on proliferation of HT-29 colon carcinoma cells. The cells were pretreated with 100 μmol/L 5-ASA (final concentration) in combination with different doses of nimesulide (10,100, 500, 1000 μmol/L) for 48 h, then dye uptake was measured at 490 nm using an ELISA reader. The inhibitory rate was markedly increased in a dose-dependent manner. Data were expressed as mean $\pm$ SE of three independent samples. [a,c,e]$P < 0.05$ vs the corresponding concentration of nimesulide.
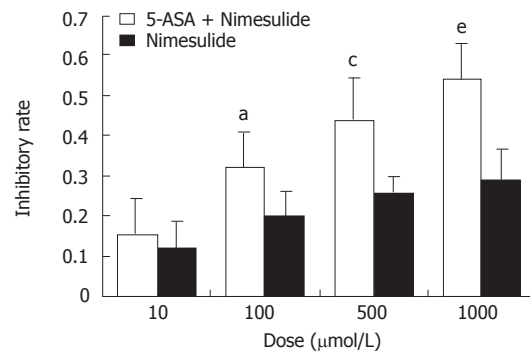

Figure 2 Time-dependent inhibitory effect of 5-ASA or nimesulide on proliferation of HT-29 colon carcinoma cells. The cells were pretreated with 100 μmol/L 5-ASA or 100 μmol/L Nimesulide respectively for 12, 24, 48, 72, 96 h), then dye uptake was measured at 490 nm using an ELISA reader. Data were expressed as mean $\pm$ SE of five independent samples. The inhibitory rate was markedly increased in a time-dependent manner.

Figure 4 Dose-dependent inhibitory effect of nimesulide in combination with 5-ASA on proliferation of HT-29 colon carcinoma cells. The cells were pretreated with 100 μmol/L nimesulide (final concentration) in combination with different doses of 5-ASA (10, 100, 500,1000 μmol/L) for 48 h, then dye uptake was measured at 490 nm using an ELISA reader. The inhibitory rate was markedly increased in a dose-dependent manner. Data were expressed as mean $\pm$ SE of three independent samples. [a,c,e]$P < 0.05$ vs the corresponding concentration of 5-ASA .
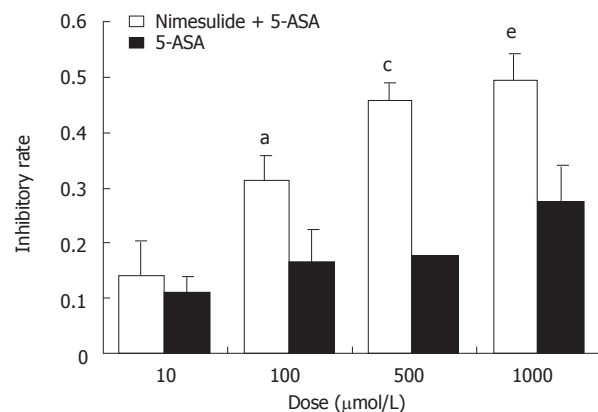
concentration (10-1000 μmol/L) for 12-96 h, inhibited the growth of HT-29 colon carcinoma cells in a dose and time-dependent manner (Figures 1 and 2). However, the suppression of 5-ASA or nimesulide had no statistical significance.

Effect of combined 5-ASA and nimesulide on the growth of HT-29 colon carcinoma cells

Interestingly, the growth of HT-29 colon carcinoma cells was inhibited dose-dependently when pretreated with different doses of combined 5-ASA and nimesulide. Combined 5-ASA (final concentration 100 μmol/L) and nimesulide (final concentration 10-1000 μmol/L) inhibited the proliferation of HT-29 colon carcinoma cells in a dose-dependent manner, being more potent than corresponding dose of nimesulide (Figure 3). Similarly, combined nimesulide (final concentration 100 μmol/L) and 5-ASA (final concentration 10-1000 μmol/L) also inhibited the proliferation of these cells dose-dependently, being more

potent than corresponding dose of 5-ASA (Figure 4).

Pretreatment with combined 5-ASA and nimesulide (final concentration 100 μmol/L) for 12-96 h, inhibited the growth of HT-29 colon carcinoma cells in a time-dependent manner (Figure 5).

Effect of 5-ASA or nimesulide alone or their combination on proliferation and apoptosis of HT-29 colon carcinoma cells

The proliferation of HT-29 carcinoma cells was significantly inhibited when pretreated with different doses of 5-ASA. The expression of PCNA was remarkably down-regulated while cell apoptosis was remarkably up-regulated in a dose-dependent manner. Similarly, nimesulide inhibited the proliferation of HT-29 carcinoma cells and promoted cell apoptosis significantly (Table 1). Co-administration of 5-ASA and nimesulide inhibited the proliferation of HT-29 colon carcinoma cells and promoted cell apoptosis
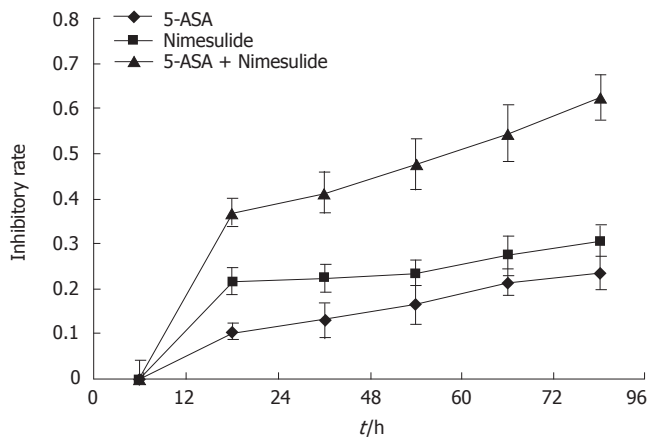
Figure 5 Time-dependent inhibitory effect of 5-ASA in combination with nimesulide on proliferation of HT-29 colon carcinoma cells. The cells were pretreated with 5-ASA in combination with nimesulide at the final dose of 100 μmol/L for different times (0, 12, 24, 48, 72, 96 h), then dye uptake was measured at 490 nm using an ELISA reader. Data were expressed as mean ± SE of five independent samples.
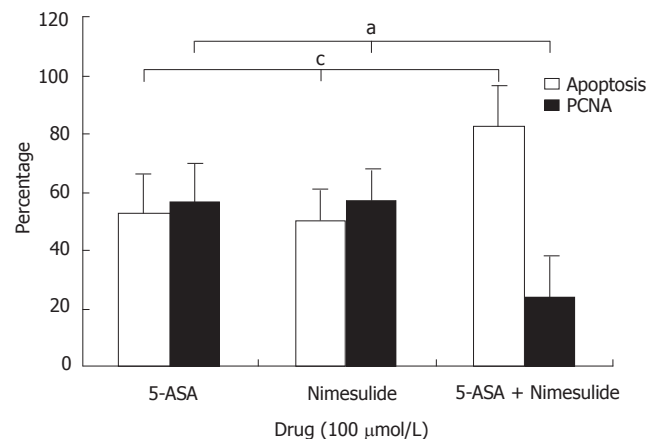
Figure 6 Inhibitory effect of 5-ASA in combination with nimesulide on proliferation and apoptosis of HT-29 colon carcinoma cells. The cells were pretreated with 5-ASA in combination with nimesulide (the final concentration was 100 μmol/L) for 48 h, then the expression of PCNA and apoptosis was detected with kits according the manufacturer's introductions. Data were expressed as mean ± SE of three independent samples. [a]$P < 0.05$, [c]$P < 0.05$, *vs* 5-ASA or nimesulide alone.

Table 1 Effect of 5-ASA and nimesulide administrated alone on apoptosis and proliferation of HT-29 colon carcinoma cells

Group	Dose (μmol/L)	Percentage of apoptosis (%)	PCNA label index (%)
Control	0	22.12 ± 3.61	75.13 ± 2.55
5-ASA	10	31.82 ± 2.61	61.73 ± 7.51
	100	52.96 ± 3.73[a]	56.47 ± 3.21[a]
	500	75.76 ± 3.28[a]	31.13 ± 1.96[a]
Nimesulide	10	29.13 ± 2.73	63.37 ± 3.23
	100	50.46 ± 1.83[a]	57.42 ± 2.14[a]
	500	70.54 ± 2.33[a]	33.15 ± 1.87[a]

The cells were pretreated with different doses of 5-ASA and nimesulide respectively (10-500 μmol/L) for 48 h, then the expression of PCNA and apoptosis were detected with kits according the the manufacturer's introductions. Data were expressed as mean ± SE of three independent samples. [a]$P < 0.001$ *vs* control group.

significantly, being more potent than the corresponding dose of 5-ASA and nimesulide (Figure 6).

DISCUSSION

IBD is associated with an increased risk of developing CRC at sites of chronic colon inflammation[1-5]. Primary prevention of CRC in IBD has received more attention in recent years. A body of evidence now suggests that 5-ASA can protect against development of CRC in individuals with IBD[6-10]. Eaden *et al*[8] performed a case-control study comparing 102 cases of CRC in ulcerative colitis (UC) with matched IBD controls, and found that a history of regular 5-ASA use significantly reduces the risk of CRC by 75%. When the results were adjusted for other variables, the protective effect of 5-ASA reduced the risk of CRC by 81% at a dose of 1.2 g/d or greater. In the present study, 5-ASA inhibited the proliferation of HT-29 carcinoma cells and promoted cell apoptosis *in vitro* in a dose- and time- dependent manner, indicating 5-ASA has significant chemopreventive properties against CRC, which is also

consistent with previous reports[18,25,26].

5-ASA is the most commonly prescribed anti-inflammatory agents for IBD and exerts its action on IBD by inhibiting 5-LOX activity. Wang *et al*[18] performed a follow-up study of 99 patients with CRC, and found that 5-LOX expression is significantly higher in colon carcinoma cells than in normal colon mucosa, and correlates with Duke's staging, diversion and infiltration of CRC. The biological functions of 5-LOX in cancer cells have been examined using pharmacological inhibitors and/or antisense technology[15,17]. It was reported that 5-LOX and its metabolites, especially LTB4 are over-expressed in colon cancer, the inhibitors of 5-LOX activity may remarkably inhibit the proliferation of colon carcinoma cells[17]. It also showed in our other study that 5-ASA may down-regulate 5-LOX expression in HT-29 carcinoma cells in a dose-depend manner (data not shown), indicating that 5-ASA anticancer property may be correlated with inhibiting 5-LOX activity.

On the other hand, many studies over the past decade have demonstrated that NSAIDs, including indomethacin, piroxicam and sulindac as well as aspirin, have a potent inhibitory effect on the growth of colorectal cancer[6,11-13]. It is postulated that this antitumor effect is mediated by inhibiting the COX-2 activity[20,21,27]. Over-expression of COX-2 in CRC may activate epidermal growth factor receptor, up-regulate the bcl-2 gene to promote cell proliferation, and inhibit cell apoptosis[28]. Being consistent with these effects, nimesulide, a selective COX-2 inhibitor, could down-regulate COX-2 expression in a dose-depend manner (data not shown) and significantly inhibit the proliferation of HT-29 carcinoma cells and promote cell apoptosis *in vitro* in a dose- and time- dependent manner.

In the present study, 5-ASA or nimesulide suppressed the proliferation of HT-29 carcinoma cells and promoted cell apoptosis *in vitro* remarkably, the possible mechanism may correlate with the inhibition of 5-LOX or COX-2 activity when pretreated with 5-ASA or nimesulide alone.

However, both 5-LOX and COX-2 were up-regulated in colon cancer cells. Ye et al[22] demonstrated that inhibition of COX-2 or 5-LOX reduces the tumor size. Treatment with a COX-2 inhibitor could decrease the PGE2 level and increase the LTB4 level. In contrast, treatment with a 5-LOX-inhibitor reduced the LTB4 level and did not change the PGE2 level, suggesting that just inhibiting 5-LOX or COX-2 activity alone may not suppress CRC development effectively[22]. However, treatment with COX-2 and 5-LOX inhibitors further could inhibit the tumor growth[29-32], which was accompanied with the down regulation of PGE2 and LTB4 simultaneously[22]. Both 5-ASA and nimesulide, which are the most commonly prescribed anti-inflammatory agents in clinic, could suppress colon cancer proliferation by inhibiting 5-LOX or COX-2 activity. Can we hypothesize that co-administration of 5-ASA and nimesulide may inhibit colon cancer cell proliferation more effectively? Co-administration of these agents has more chemopreventive properties against the proliferation of HT-29 carcinoma cells *in vitro* than administration of 5-ASA or nimesulide alone, showing a dose and time dependent correlation.

In conclusion, co-administration of 5-ASA and NSAIDs, especially at a low dose may have chemopreventive effect on CRC, which may reduce the side effect of theses agents when administrated alone. This approach should present a superior anticancer profile, and a new therapy for cancers associated with IBD.

REFERENCES

1   Ekbom A, Helmick C, Zack M, Adami HO. Ulcerative colitis and colorectal cancer. A population-based study. *N Engl J Med* 1990; **323**: 1228-1233

2   Pinczowski D, Ekbom A, Baron J, Yuen J, Adami HO. Risk factors for colorectal cancer in patients with ulcerative colitis: a case-control study. *Gastroenterology* 1994; **107**: 117-120

3   Hanauer SB. Inflammatory bowel disease. *N Engl J Med* 1996; **334**: 841-848

4   Podolsky DK. Inflammatory bowel disease. *N Engl J Med* 2002; **347**: 417-429

5   Munkholm P. Review article: the incidence and prevalence of colorectal cancer in inflammatory bowel disease. *Aliment Pharmacol Ther* 2003; **18** Suppl 2: 1-5

6   Janne PA, Mayer RJ. Chemoprevention of colorectal cancer. *N Engl J Med* 2000; **342**: 1960-1968

7   Moody GA, Jayanthi V, Probert CS, Mac Kay H, Mayberry JF. Long-term therapy with sulphasalazine protects against colorectal cancer in ulcerative colitis: a retrospective study of colorectal cancer risk and compliance with treatment in Leicestershire. *Eur J Gastroenterol Hepatol* 1996; **8**: 1179-1183

8   Eaden J. Review article: the data supporting a role for aminosalicylates in the chemoprevention of colorectal cancer in patients with inflammatory bowel disease. *Aliment Pharmacol Ther* 2003; **18** Suppl 2: 15-21

9   Cheng Y, Desreumaux P. 5-aminosalicylic acid is an attractive candidate agent for chemoprevention of colon cancer in patients with inflammatory bowel disease. *World J Gastroenterol* 2005; **11**: 309-314

10   Ryan BM, Russel MG, Langholz E, Stockbrugger RW. Aminosalicylates and colorectal cancer in IBD: a not-so bitter pill to swallow. *Am J Gastroenterol* 2003; **98**: 1682-1687

11   Sandler RS, Galanko JC, Murray SC, Helm JF, Woosley JT. Aspirin and nonsteroidal anti-inflammatory agents and risk for colorectal adenomas. *Gastroenterology* 1998; **114**: 441-447

12   Giardiello FM, Hamilton SR, Krush AJ, Piantadosi S, Hylind LM, Celano P, Booker SV, Robinson CR, Offerhaus GJ. Treatment of colonic and rectal adenomas with sulindac in familial adenomatous polyposis. *N Engl J Med* 1993; **328**: 1313-1316

13   Jacoby RF, Seibert K, Cole CE, Kelloff G, Lubet RA. The cyclooxygenase-2 inhibitor celecoxib is a potent preventive and therapeutic agent in the min mouse model of adenomatous polyposis. *Cancer Res* 2000; **60**: 5040-5044

14   Marnett LJ. Generation of mutagens during arachidonic acid metabolism. *Cancer Metastasis Rev* 1994; **13**: 303-308

15   Hong SH, Avis I, Vos MD, Martinez A, Treston AM, Mulshine JL. Relationship of arachidonic acid metabolizing enzyme expression in epithelial cancer cell lines to the growth effect of selective biochemical inhibitors. *Cancer Res* 1999; **59**: 2223-2228

16   Hong J, Bose M, Ju J, Ryu JH, Chen X, Sang S, Lee MJ, Yang CS. Modulation of arachidonic acid metabolism by curcumin and related beta-diketone derivatives: effects on cytosolic phospholipase A(2), cyclooxygenases and 5-lipoxygenase. *Carcinogenesis* 2004; **25**: 1671-1679

17   Romano M, Claria J. Cyclooxygenase-2 and 5-lipoxygenase converging functions on cell proliferation and tumor angiogenesis: implications for cancer therapy. *FASEB J* 2003; **17**: 1986-1995

18   Wang JL, Xu JM, Mei Q, Bao JJ. Expression of 5-lipoxygenase and cyclooxygenase-2 in colonic carcinoma and its relationship with pathological characteristics. *Anhui Yikedaxue Xuebao* 2006; **41**: 58-60

19   Allgayer H. Review article: mechanisms of action of mesalazine in preventing colorectal carcinoma in inflammatory bowel disease. *Aliment Pharmacol Ther* 2003; **18** Suppl 2: 10-14

20   Fujimura T, Ohta T, Oyama K, Miyashita T, Miwa K. Role of cyclooxygenase-2 in the carcinogenesis of gastrointestinal tract cancers: a review and report of personal experience. *World J Gastroenterol* 2006; **12**: 1336-1345

21   Sinicrope FA. Targeting cyclooxygenase-2 for prevention and therapy of colorectal cancer. *Mol Carcinog* 2006; **45**: 447-454

22   Ye YN, Wu WK, Shin VY, Bruce IC, Wong BC, Cho CH. Dual inhibition of 5-LOX and COX-2 suppresses colon cancer formation promoted by cigarette smoke. *Carcinogenesis* 2005; **26**: 827-834

23   Samaha HS, Kelloff GJ, Steele V, Rao CV, Reddy BS. Modulation of apoptosis by sulindac, curcumin, phenylethyl-3-methylcaffeate, and 6-phenylhexyl isothiocyanate: apoptotic index as a biomarker in colon cancer chemoprevention and promotion. *Cancer Res* 1997; **57**: 1301-1305

24   Clahsen PC, van de Velde CJ, Duval C, Pallud C, Mandard AM, Delobelle-Deroide A, van den Broek L, Sahmoud TM, van de Vijver MJ. p53 protein accumulation and response to adjuvant chemotherapy in premenopausal women with node-negative early breast cancer. *J Clin Oncol* 1998; **16**: 470-479

25   Bus PJ, Nagtegaal ID, Verspaget HW, Lamers CB, Geldof H, Van Krieken JH, Griffioen G. Mesalazine-induced apoptosis of colorectal cancer: on the verge of a new chemopreventive era? *Aliment Pharmacol Ther* 1999; **13**: 1397-1402

26   Reinacher-Schick A, Schoeneck A, Graeven U, Schwarte-Waldhoff I, Schmiegel W. Mesalazine causes a mitotic arrest and induces caspase-dependent apoptosis in colon carcinoma cells. *Carcinogenesis* 2003; **24**: 443-451

27   Brown JR, DuBois RN. COX-2: a molecular target for colorectal cancer prevention. *J Clin Oncol* 2005; **23**: 2840-2855

28   Sheng H, Shao J, Morrow JD, Beauchamp RD, DuBois RN. Modulation of apoptosis and Bcl-2 expression by prostaglandin E2 in human colon cancer cells. *Cancer Res* 1998; **58**: 362-366

29   Parente L. Pros and cons of selective inhibition of cyclooxygenase-2 versus dual lipoxygenase/cyclooxygenase inhibition: is two better than one? *J Rheumatol* 2001; **28**: 2375-2382

30   Rao CV, Indranie C, Simi B, Manning PT, Connor JR, Reddy BS. Chemopreventive properties of a selective inducible nitric oxide synthase inhibitor in colon carcinogenesis, administered

alone or in combination with celecoxib, a selective cyclooxygenase-2 inhibitor. *Cancer Res* 2002; **62**: 165-170

31   **Kovarikova M**, Hofmanova J, Soucek K, Kozubik A. The effects of TNF-alpha and inhibitors of arachidonic acid metabolism on human colon HT-29 cells depend on differentiation status. *Differentiation* 2004; **72**: 23-31

32   **Cianchi F**, Cortesini C, Magnelli L, Fanti E, Papucci L, Schiavone N, Messerini L, Vannacci A, Capaccioli S, Perna F, Lulli M, Fabbroni V, Perigli G, Bechi P, Masini E. Inhibition of 5-lipoxygenase by MK886 augments the antitumor activity of celecoxib in human colon cancer cells. *Mol Cancer Ther* 2006; **5**: 2716-2726

Intrahepatic HBV DNA as a predictor of antivirus treatment efficacy in HBeAg-positive chronic hepatitis B patients

Hai-Ying Lu, Li-Wei Zhuang, Yan-Yan Yu, Hadad Ivan, Chong-Wen Si, Zheng Zeng, Jun Li, Dong-Ming Hou, Xin-Yue Chen, Zhong-Hou Han, Yong Chen

Hai-Ying Lu, Li-Wei Zhuang, Yan-Yan Yu, Chong-Wen Si, Zheng Zeng, Jun Li, Department of Infectious Diseases, Peking University First Hospital, Beijing 100034, China
Hadad Ivan, Dong-Ming Hou, Indiana University School of Medicine, Indianapolis, IN 46202, United States
Xin-Yue Chen, Beijing You'an Hospital, Beijing 100054, China
Zhong-Hou Han, Qinhuangdao Third Hospital, Qinhuangdao 066000, Hebei Province, China
Yong Chen, Huai'an Infectious Disease Hospital, Huai'an 223300, Jiangsu Province, China
Supported by Beijing Municipal Science & Technology Commission, No. H020920020690
Correspondence to: Professor Chong-Wen Si, Department of Infectious Diseases, Peking University First Hospital, Beijing 100034, China. bjsichongwen@sina.com
Telephone: +86-10-66551122-2370
Received: 2006-12-25   Accepted: 2007-01-14

Abstract

AIM: To evaluate the effect of antiviral agents on intrahepatic HBV DNA in HBeAg-positive chronic hepatitis B patients.

METHODS: Seventy-one patients received treatment with lamivudine, interferon alpha (IFN-α2b) or sequential therapy with lamivudine-IFN-α2b for 48 wk. All subjects were followed up for 24 wk. Serum and intrahepatic HBV DNA were measured quantitatively by PCR. HBV genotypes were analyzed by PCR-RFLP.

RESULTS: At the end of treatment, the intrahepatic HBV DNA level in 71 patients decreased from a mean of (6.1 ± 1.0) log10 to (4.9 ± 1.4) log10. Further, a larger decrease was seen in the intrahepatic HBV DNA level in patients with HBeAg seroconversion. Intrahepatic HBV DNA level (before and after treatment) was not significantly affected by the patients' HBV genotype, or by the probability of virological flare after treatment.

CONCLUSION: Intrahepatic HBV DNA can be effectively lowered by antiviral agents and is a significant marker for monitoring antivirus treatment. Low intrahepatic HBV DNA level may achieve better efficacy of antivirus treatment.

© 2007 The WJG Press. All rights reserved.

Key words: Intrahepatic HBV DNA; Histology; Antiviral

therapy; HBV genotype

INTRODUCTION

Hepatitis B virus (HBV) is one of the major causes of liver disease worldwide. Approximately more than 350 million people in the world are chronic carriers, and eventually 15%-25% of them could progress to end-stage liver disease and hepatocellular carcinoma, ranking ninth globally among all causes of mortality (up to 1 million deaths annually)[1]. Fortunately, several therapies have been developed for chronic hepatitis B. Anti-viral therapy is believed to be the most important strategy. Currently available anti-viral drugs include interferon-alpha[2-4] and nucleoside analogue agents[5-9]. It was reported that long-term anti-viral treatment can improve fibrosis and cirrhosis, increase survival rate and decrease the incidence of hepatocellular carcinoma in patients with chronic hepatitis B[10,11]. Nonetheless, when the treatment with anti-viral drugs is stopped, relapse occurs in a great majority of patients, even if they have undetectable serum HBV DNA, normal serum alanine aminotransferase level and HBeAg seroconversion.

Therefore, it is important to determine which end points should be used to judge the success or failure of treatment and assist in determining how long therapy should be maintained. Since biopsy specimens from chronic HBV patients are not easy to obtain, intrahepatic HBV DNA level is not often studied. The aim of the present study was to analyze the effect of anti-viral drugs on intrahepatic HBV DNA and the relationship between intrahepatic HBV DNA and the long-term efficacy of antivirus treatment.

MATERIALS AND METHODS

Subjects

Between March 2003 and March 2005, 71 patients (59

Table 1 Histological and virological characteristics of 71 patients with chronic HBV infection mean ± SD

Parameter	Total (*n* = 71)	HBeAg positive (*n* = 54)	HBeAg seroconversion (*n* = 17)
Knodell score: pretreatment	8.2 ± 4.1	8.4 ± 4.1	7.1 ± 4.2
post-treatment	5.8 ± 3.4[a]	6.0 ± 3.6	5.1 ± 3.1[a]
Intrahepatic HBV DNA (log10): pretreatment	6.1 ± 1.0	6.3 ± 0.8	5.6 ± 1.2
post-treatment	4.9 ± 1.4[a]	5.1 ± 1.5	4.1 ± 0.8[a]
Serum HBV DNA (log10): pretreatment	7.7 ± 1.1	7.9 ± 0.9	7.5 ± 1.0
post-treatment	4.0 ± 1.3[a]	4.4 ± 1.4[a]	3.0 ± 0.2[a]
ALT (nkat/L): pretreatmen	3390 ± 2321	3206 ± 2354	3841 ± 2371
post-treatment	868 ± 885[a]	9853 ± 985	618 ± 659[a]

[a]*P* < 0.05 *vs* pretreatment.

males and 12 females) with HBeAg-positive chronic hepatitis B were recruited. Their age was 19-47 (mean 32 ± 9) years. Informed consent was obtained from all patients. The patients were matched according to the following criteria: positive for HBsAg and HBeAg, serum HBV DNA $\geq 1 \times 10^5$ copies/L, serum alanine aminotransferase (ALT) level above at least two-fold the normal range (normal range 0-667 nkat/L) for more than 6 mo. Exclusion criteria were as follows: alcoholism, pregnancy, cirrhosis, chronic renal failure, concurrent autoimmune disease, serious neurological disorders, human immunodeficiency virus (HIV) infection and viral hepatitis A, C, delta or E. Patients treated with interferon or other anti-viral therapies for 6 mo prior to enrollment in this study were also excluded. Patients were treated with 100 mg oral lamivudine daily (*n* = 35), or lamivudine during the first 8 mo and IFN-α from mo 7 to 12 (*n* = 24) or 5 million units of interferon-alpha (IFN-α), three times per week (*n* = 12). Treatment groups were randomized at the ratio 3:2:1. The total duration of therapy was 12 mo. All subjects were followed up for 24 wk after the 12 mo of treatment. Presence of serum HBV DNA level $\leq 1 \times 10^3$ and normalization of serum ALT level were assessed as treatment response.

Measurement of hepatitis B virus markers and biochemical tests

Blood samples were obtained before and after treatment and at the 24 wk follow-up visit. Liver biochemistry and HBV marker test (enzyme-linked immunosorbant assay) were performed on these samples.

Liver biopsy specimens were collected by needle biopsies (0.5 cm-1.5 cm) before and after treatment. The tissue was washed several times in cold phosphate buffered saline (PBS) and stored at -70℃. Total DNA was extracted from liver tissue with Qiaamp DNA tissue Mini DNA kit (Qiagen, Germany). Serum and intrahepatic HBV DNA were measured quantitatively by real-time polymerase chain reaction (PCR) (Model 5700, ABI Company, USA) with a lower limit of detection of 1×10^3 HBV DNA copies/L and 1×10^3 copies/g total DNA, respectively. HBV genotypes were determined by PCR restriction fragment length polymorphism (PCR-RFLP) analysis[12].

Detection of histological inflammatory score

Histological inflammatory score was detected with the Knodell scoring system. Histological response was defined as a decrease by at least two points in the Knodell scoring system[13].

Statistical analysis

Data were analyzed with the Statistical Program for Social Sciences (SPSS 13.0 for Windows). Categorical variables were tested using chi-square test or Fisher's exact test. Normally distributed variables were tested using *t*-test or ANOVA, whereas continuous variables with skewed distribution were tested using the Kruskal Wallis test. A regression model was used for univariate and multivariate analysis. *P* < 0.05 was considered statistically significant.

RESULTS

Histological, biochemical and virological data

At the end of treatment, the mean values of Knodell score, serum HBV DNA level, intrahepatic HBV DNA level, and serum ALT level in all the 71 patients declined significantly (*P* < 0.05). HBeAg seroconversion occurred in 17 out of the 71 patients. There was no significant difference in above mentioned parameters between HBeAg seroconversion group and HBeAg positive group before treatment (*P* > 0.05), except for the baseline intrahepatic HBV DNA levels (5.6 ± 1.2) log10 and (6.3 ± 0.8) log10, respectively (*P* = 0.02). After treatment, HBeAg seroconversion group had better improvement than HBeAg positive group. The mean intrahepatic HBV DNA decreased to (4.1 ± 0.8) log10 in seroconversion group (*P* = 0.0124), and to (5.1 ± 1.5) log10 (*P* = 0.0872) in HBeAg positive group (Table 1).

Intrahepatic HBV DNA level and HBV genotype

At the end of treatment, the intrahepatic HBV DNA load was less than 5 log10 in 38 patients, and higher than 5 log10 in 33 patients (*P* < 0.05). The difference was not statistically significant in serum HBV DNA load, histology and serum ALT level before treatment. After treatment, compared with the patients with intrahepatic HBV DNA load greater than 5 log10, greater reduction in above mentioned parameters was seen in patients with intrahepatic HBV DNA load less than 5 log10. After 24 wk of treatment, sustained virological response rate and ALT normalization rate were very similar between two groups (*P* > 0.05) (Table 2). Regression analysis showed that virological flares after antiviral treatment were not correlated with the baseline or post-treatment level of

Table 2 Intrahepatic HBV DNA level in chronic HBV patients and HBV genotypes mean ± SD

Parameter	Intrahepatic HBV DNA < 5 log10 (n = 38)	Intrahepatic HBV DNA ≥ 5 log10 (n = 33)	HBV genotypes Genotype C group (n = 61)	Genotype B (n = 10)
Knodell score: pretreatment	7.6 ± 4.0	8.2 ± 4.1	8.1 ± 4.1	5.7 ± 3.2
post-treatment	4.8 ± 2.2[a]	7.4 ± 4.1	6.0 ± 3.4[a]	5.4 ± 3.1
Intrahepatic HBV DNA (log10): pretreatment	5.8 ± 1.0	6.3 ± 0.9	6.1 ± 0.9	5.6 ± 1.5
post-treatment	3.8 ± 0.9[a]	6.1 ± 0.7	4.9 ± 1.4[a]	4.7 ± 1.2
Serum HBV DNA (log10): pretreatment	7.6 ± 1.0	7.8 ± 1.3	7.7 ± 1.2	7.6 ± 0.8
post-treatment	3.3 ± 0.7[a]	4.7 ± 1.4[a]	4.05 ± 1.3[a]	4.9 ± 1.2[a]
Off- treatment 24 wk	5.1 ± 1.4	5.2 ± 1.7	5.1 ± 1.6	4.3 ± 1.3
ALT (nkat/L): pretreatment	4342 ± 2788	2571 ± 1519	3390 ± 2438	4509 ± 2338
post-treatment	634 ± 567[a]	1135 ± 1052	912 ± 918[a]	551 ± 236[a]
Off-treatment 24 wk	1519 ± 1519	1637 ± 1369	1503 ± 1336	1987 ± 1720
Off-treatment 24 wk virological response rate	23.7% (9/38)	27.3% (9/33)	31.1% (19/51)	30% (3/10)
Off-treatment 24 wk ALT normalization rate	16.7% (15/38)	13.3% (10/33)	39.3% (24/51)	30% (3/10)

[a]$P < 0.05$ *vs* pretreatment.

intrahepatic HBV DNA load ($P > 0.05$).

HBV genotype C accounted for 85.9% (n = 61), and genotype B for 14.1% (n = 10). The mean intrahepatic HBV DNA loads in genotype C patients before and after treatment were (6.1 ± 0.9) log10 and (4.9 ± 1.4) log10 ($P < 0.05$), and (5.6 ± 1.5) log10 and (4.7 ± 1.2) log10 in genotype B patients, respectively ($P > 0.05$). There was no statistically significant difference in serum intrahepatic HBV DNA load and ALT level between the two groups at the end of treatment and in any of the parameters measured after 24 wk of treatment ($P > 0.05$). After 24 wk of treatment, sustained virological response rate and ALT normalization rate were similar (Table 2).

Antiviral outcome

There was no significant difference in all the parameters among the three groups before treatment ($P > 0.05$). At the end of treatment, the antiviral effect of sequential lamivudine-INF-α therapy and lamivudine monotherapy was similar ($P > 0.05$), which was superior to that of INF-α monotherapy ($P < 0.05$). Reduction of intrahepatic HBV DNA was greater in lamivudine-INF-α therapy group and lamivudine monotherapy group than in INF-α monotherapy group, suggesting that the nucleoside analogue agents might play a stronger role than INF-α in inhibiting intrahepatic HBV DNA (data not shown).

DISCUSSION

Due to recent advancements, chronic hepatitis B has become a treatable disease. The short-term efficacy of IFN-α is about 40%-60%[12,17]. Peginterferon-alpha (PEG IFN-α) is more effective against HBeAg-positive chronic hepatitis B than either lamivudine or standard IFN-α monotherapy[3,4]. Nucleoside analogue agents markedly suppress HBV DNA polymerase, and have numerous advantages, such as minimal side effects, ease of administration. Furthermore, they show good effects on chronic hepatitis B, liver decompensation, cirrhosis, or other coexisting conditions. It was reported that serum HBV DNA is undectable in 80% of patients, HBeAg is eliminated in 20%-25% of them, and 60% ALT level becomes normal in 60% of them after treatment with

lamivudine[14-16].

Nonetheless, the efficacy of antiviral treatment is far from perfect. IFN-α can achieve a sustained response after one year in only 20%-30% of chronic HBV infection patients[17]. Relapse occurs in the majority of patients after therapy. The main reason is that HBV covalently closed circular DNA (cccDNA) in infected hepatocytes cannot be eliminated by antiviral agents, leading to rebound of HBV DNA after antiviral therapy[18]. The life cycle of HBV relies on a covalently closed circular form of the viral genome, which provides the template for viral pregenomic messenger RNA. Replication of cccDNA is not semi-conservative, and needs viral DNA cycling back to the nuclei to amplify and maintain the pool of cccDNA[19,20]. It was reported that intrahepatic HBV cccDNA correlates positively with the total intrahepatic HBV DNA[21], suggesting that intrahepatic HBV DNA should be eliminated first in order to clear HBV cccDNA and intrahepatic HBV DNA level can be taken as a reasonable parameter in evaluating the efficacy of antiviral therapy, thus helping decide the duration of therapy.

The results of our study show that antiviral treatment decreased the serum and intrahepatic HBV DNA as well as alanine aminotransferase levels in 71 patients ($P < 0.05$). HBeAg seroconversion occurred in 17 out of the 71 patients at the end of treatment. There was no significant difference in the baseline levels of Knodell score, serum ALT and HBV DNA levels between HBeAg seroconversion and HBeAg positive groups ($P > 0.05$). Only the intrahepatic HBV DNA level was obviously lower in HBeAg seroconversion group than in HBeAg positive group ($P = 0.02$). After treatment, greater improvement in above mentioned parameters was seen in patients with HBeAg seroconversion than in HBeAg positive patients. The mean intrahepatic HBV DNA level was lower in the HBeAg seroconversion group than in the HBeAg positive group ($P = 0.010$), suggesting that intrahepatic HBV DNA can be effectively lowered by antiviral agents and a lower intrahepatic HBV DNA level is able to predict the efficacy of antiviral therapy.

At the end of treatment, the intrahepatic HBV DNA load was less than 5 log10 in 38 patients and greater than 5 log10 in 33 patients. The mean intrahepatic HBV DNA

load before and after treatment was obviously lower in the patients with intrahepatic HBV DNA load less than 5 log10 than in the patients with intrahepatic HBV DNA load greater than 5 log10 ($P < 0.05$), and the difference was not statistically significant in the other parameters. At the end of treatment, greater reduction in the measured parameters was seen in patients with intrahepatic HBV DNA load less than 5 log10, indicating that reduction in intrahepatic HBV DNA load is also very important in antiviral treatment. After 24 wk of treatment, sustained virus response rate and ALT normalization rate for the two groups were very similar (23.7% and 16.7%, 27.3% and 13.3%, respectively, $P > 0.05$). Regression analysis showed that virus flares after antiviral treatment were not correlated with the baseline or with the post-treatment level of serum and intrahepatic HBV DNA load ($r < 0.05$, $P > 0.05$). A possible reason is that the duration of antiviral treatment in this study was too short to eliminate or largely lessen the intrahepatic HBV DNA load. Therefore, once the antiviral drugs are withdrawn, the majority of patients would experience virus rebound. Intrahepatic HBV DNA was undetectable even if the patients had undetectable serum HBV DNA, indicating that intrahepatic HBV DNA is more useful than serum HBV DNA in monitoring the efficacy of antivirus therapy, and loss of intrahepatic HBV DNA might be crucial for the patients to achieve sustained antiviral response.

HBV is classified into 8 genotypes (A-H), each showing a distinct geographical distribution and disease progression. HBV genotype C is believed to be associated with a higher risk of reactivation and progression to cirrhosis compared to HBV genotype B[22,23]. Whether hepatitis B virus (HBV) genotypes influence the response to antiviral treatment remains controversial. It was reported that HBV genotypes do not influence the development of resistance to lamivudine, but influence the severity of liver disease[24]. In the present study, 85.9% of patients were infected with the HBV genotype C and 14.1% with the HBV genotype B. There was no significant difference in intrahepatic HBV DNA load, serum ALT and HBV DNA level, as well as in histological findings before and after treatment between the two groups ($P > 0.05$). After 24 wk of treatment, both sustained virological response rate and ALT normalization rate for the two groups were very similar ($P > 0.05$), indicating that HBV genotypes have no influence on intrahepatic HBV DNA load. In this study, there was no statistically significant difference in the long-term effect of antiviral therapy between HBV genotypes B and C.

In conclusion, antiviral therapy can effectively suppress intrahepatic HBV DNA replication. Better efficacy of antivirus treatment can be achieved in patients with a low intrahepatic HBV DNA level. Intrahepatic HBV DNA level at the end of antiviral treatment is correlated with the effect of antiviral therapy, suggesting that loss of intrahepatic HBV DNA may induces less virus flare and can be taken as the optimal endpoint of antiviral treatment. There is no significant difference in intrahepatic HBV DNA level between HBV genotypes C and B.

ACKNOWLEDGMENTS

REFERENCES

1   **Fact sheets**: Hepatutus B. Geneva: World Health Organization, October 2000

2   **Lok AS**, Heathcote EJ, Hoofnagle JH. Management of hepatitis B: 2000--summary of a workshop. *Gastroenterology* 2001; **120**: 1828-1853

3   **Lau GK**, Piratvisuth T, Luo KX, Marcellin P, Thongsawat S, Cooksley G, Gane E, Fried MW, Chow WC, Paik SW, Chang WY, Berg T, Flisiak R, McCloud P, Pluck N. Peginterferon Alfa-2a, lamivudine, and the combination for HBeAg-positive chronic hepatitis B. *N Engl J Med* 2005; **352**: 2682-2695

4   **Marcellin P**, Lau GK, Bonino F, Farci P, Hadziyannis S, Jin R, Lu ZM, Piratvisuth T, Germanidis G, Yurdaydin C, Diago M, Gurel S, Lai MY, Button P, Pluck N. Peginterferon alfa-2a alone, lamivudine alone, and the two in combination in patients with HBeAg-negative chronic hepatitis B. *N Engl J Med* 2004; **351**: 1206-1217

5   **Dienstag JL**, Schiff ER, Wright TL, Perrillo RP, Hann HW, Goodman Z, Crowther L, Condreay LD, Woessner M, Rubin M, Brown NA. Lamivudine as initial treatment for chronic hepatitis B in the United States. *N Engl J Med* 1999; **341**: 1256-1263

6   **Marcellin P**, Chang TT, Lim SG, Tong MJ, Sievert W, Shiffman ML, Jeffers L, Goodman Z, Wulfsohn MS, Xiong S, Fry J, Brosgart CL. Adefovir dipivoxil for the treatment of hepatitis B e antigen-positive chronic hepatitis B. *N Engl J Med* 2003; **348**: 808-816

7   **Hadziyannis SJ**, Tassopoulos NC, Heathcote EJ, Chang TT, Kitis G, Rizzetto M, Marcellin P, Lim SG, Goodman Z, Ma J, Arterburn S, Xiong S, Currie G, Brosgart CL. Long-term therapy with adefovir dipivoxil for HBeAg-negative chronic hepatitis B. *N Engl J Med* 2005; **352**: 2673-2681

8   **Chang TT**, Gish RG, de Man R, Gadano A, Sollano J, Chao YC, Lok AS, Han KH, Goodman Z, Zhu J, Cross A, DeHertogh D, Wilber R, Colonno R, Apelian D. A comparison of entecavir and lamivudine for HBeAg-positive chronic hepatitis B. *N Engl J Med* 2006; **354**: 1001-1010

9   **Lai CL**, Shouval D, Lok AS, Chang TT, Cheinquer H, Goodman Z, DeHertogh D, Wilber R, Zink RC, Cross A, Colonno R, Fernandes L. Entecavir versus lamivudine for patients with HBeAg-negative chronic hepatitis B. *N Engl J Med* 2006; **354**: 1011-1020

10 **Lok AS**, Lai CL, Leung N, Yao GB, Cui ZY, Schiff ER, Dienstag JL, Heathcote EJ, Little NR, Griffiths DA, Gardner SD, Castiglia M. Long-term safety of lamivudine treatment in patients with chronic hepatitis B. *Gastroenterology* 2003; **125**: 1714-1722

11 **Han HL**, Lang ZW. Changes in serum and histology of patients with chronic hepatitis B after interferon alpha-2b treatment. *World J Gastroenterol* 2003; **9**: 117-121

12 **Tanaka Y**, Orito E, Yuen MF, Mukaide M, Sugauchi F, Ito K, Ozasa A, Sakamoto T, Kurbanov F, Lai CL, Mizokami M. Two subtypes (subgenotypes) of hepatitis B virus genotype C: A novel subtyping assay based on restriction fragment length polymorphism. *Hepatol Res* 2005; **33**: 216-224

13 **Bayraktar Y**, Koseoglu T, Temizer A, Kayhan B, Van Thiel DH, Uzunalimoglu B. Relationship between the serum alanine aminotransferase level at the end of interferon treatment and histologic changes in wild-type and precore mutant hepatitis B virus infections. *J Viral Hepat* 1996; **3**: 137-142

14 **Dienstag JL**, Perrillo RP, Schiff ER, Bartholomew M, Vicary C, Rubin M. A preliminary trial of lamivudine for chronic hepatitis B infection. *N Engl J Med* 1995; **333**: 1657-1661

15 **Lai CL**, Chien RN, Leung NW, Chang TT, Guan R, Tai DI, Ng KY, Wu PC, Dent JC, Barber J, Stephenson SL, Gray DF. A one-year trial of lamivudine for chronic hepatitis B. Asia Hepatitis Lamivudine Study Group. *N Engl J Med* 1998; **339**: 61-68

16 **Dienstag JL**, Goldin RD, Heathcote EJ, Hann HW, Woessner M, Stephenson SL, Gardner S, Gray DF, Schiff ER.

Histological outcome during long-term lamivudine therapy. *Gastroenterology* 2003; **124**: 105-117

17   **Wong DK**, Cheung AM, O'Rourke K, Naylor CD, Detsky AS, Heathcote J. Effect of alpha-interferon treatment in patients with hepatitis B e antigen-positive chronic hepatitis B. A meta-analysis. *Ann Intern Med* 1993; **119**: 312-323

18   **Nicoll AJ**, Angus PW, Chou ST, Luscombe CA, Smallwood RA, Locarnini SA. Demonstration of duck hepatitis B virus in bile duct epithelial cells: implications for pathogenesis and persistent infection. *Hepatology* 1997; **25**: 463-469

19   **Yang W**, Summers J. Integration of hepadnavirus DNA in infected liver: evidence for a linear precursor. *J Virol* 1999; **73**: 9710-9717

20   **Zoulim F**. New insight on hepatitis B virus persistence from the study of intrahepatic viral cccDNA. *J Hepatol* 2005; **42**: 302-308

21   **Wong DK**, Yuen MF, Yuan H, Sum SS, Hui CK, Hall J, Lai CL. Quantitation of covalently closed circular hepatitis B virus DNA in chronic hepatitis B patients. *Hepatology* 2004; **40**: 727-737

22   **Watanabe K**, Takahashi T, Takahashi S, Okoshi S, Ichida T, Aoyagi Y. Comparative study of genotype B and C hepatitis B virus-induced chronic hepatitis in relation to the basic core promoter and precore mutations. *J Gastroenterol Hepatol* 2005; **20**: 441-449

23   **Yuen MF**, Sablon E, Tanaka Y, Kato T, Mizokami M, Doutreloigne J, Yuan HJ, Wong DK, Sum SM, Lai CL. Epidemiological study of hepatitis B virus genotypes, core promoter and precore mutations of chronic hepatitis B infection in Hong Kong. *J Hepatol* 2004; **41**: 119-125

24   **Kao JH**. Hepatitis B virus genotypes and hepatocellular carcinoma in Taiwan. *Intervirology* 2003; **46**: 400-407

Detection of let-7a microRNA by real-time PCR in gastric carcinoma

Hong-He Zhang, Xian-Jun Wang, Guo-Xiong Li, En Yang, Ning-Min Yang

Hong-He Zhang, Xian-Jun Wang, Guo-Xiong Li, Diagnostic Laboratory, Hangzhou First People's Hospital, Hangzhou 310006, Zhejiang Province, China
En Yang, Ning-Min Yang, Zhiyuan Medical Laboratory, Hangzhou 310006, Zhejiang Province, China
Correspondence to: Hong-He Zhang, Diagnostic Laboratory, Hangzhou First People's Hospital, Hangzhou 310006, Zhejiang Province, China. honghezhang@tom.com
Telephone: +86-571-87065701-30826 Fax: +86-571-87914773
Received: 2007-02-14   Accepted: 2007-03-21

Abstract

AIM: To establish an accurate and rapid stem-loop reverse transcriptional real-time PCR (RT-PCR) method to quantify human let-7a miRNA in gastric cancer.

METHODS: According to the sequence of let-7a miRNA, the stem-loop reverse transcriptional primer, the primers and quantitative MGB probes of real-time PCR were designed and synthesized. The dynamic range and the sensitivity of quantitative reverse transcriptional real-time PCR were determined. The levels of let-7a miRNA were examined in 32 gastric carcinoma samples by stem-loop RT-PCR method.

RESULTS: The dynamic range and sensitivity of the let-7a miRNA quantification scheme were evaluated, the result showed the assay could precisely detect 10 copies of mature let-7a miRNA in as few as 0.05 ng of total RNA of gastric mucosa. The results of specificity analysis showed no fluorescence signal occurred even though 50 ng of human genomic DNA was added to the reverse transcription (RT) reaction. The expression level of let-7a miRNA in gastric tumor tissues was significantly lower compared to normal tissues in 14 samples from 32 patients.

CONCLUSION: The stem-loop RT-PCR is a reliable method to detect let-7a miRNA which may play an important role in the development of gastric carcinoma.

Zhang HH, Wang XJ, Li GX, Yang E, Yang NM. Detection of let-7a microRNA by real-time PCR in gastric carcinoma.

INTRODUCTION

Mature microRNAs (miRNAs) were a recently discovered class of endogenous, small non-encoding RNAs with the length of 21-25 nucleotides[1]. Their primary function was believed as translational repression of protein coding mRNAs at post-transcriptional level[2-4]. miRNAs were found in the genomes of animals[5,6] and plants[7,8]. There are about 4000 unique transcripts, including 462 human miRNAs in the Sanger Center miRNA registry[9]. Otherwise, it is estimated that human genome has more than 1000 miRNAs[10].

Although the biological functions and the target genes of miRNAs are poorly understood, it has been confirmed that they regulate complicated biological behaviors, such as cell differentiation, proliferation and death, *etc*[11]. Recent studies have shown that miRNA is closely related to tumor genesis and differentiation[12], especially, the expression level of let-7a miRNA was reduced in human lung cancer and colon cancer[13,14], and it was shown to be anticancer miRNA that repressed Ras and c-myc expression at translational level[15]. As Ras and c-myc are universal pathways of several tumors, let-7a miRNA may be the target of tumor genesis.

Since miRNAs are very different from other traditional RNAs, different methods are needed to quantify their expression. We, therefore, established an accurate and rapid real-time PCR fluorescence quantitative method to quantify human let-7a miRNA in human gastric carcinoma and normal tissue. Based on this method, we preliminarily discussed the relationship between let-7a expression level and gastric carcinoma genesis.

MATERIALS AND METHODS

Patients and specimens

All human tissue samples were obtained from surgical specimens of 32 patients with gastric carcinoma from 2005 to 2006 at Hangzhou First People's Hospital, China. All tissues, including gastric carcinoma and corresponding adjacent normal tissue, were divided into two parts and preserved in liquid nitrogen for 30 min after removing

Table 1 Oligonucleotides used in this study

let-7aPRT: GTCGTATCCAGTGCAGGGTCCGAGGTATTCGCACTGGAT
          ACGACAACTA
let-7aPf: GCCGCTGAGGTAGTAGGTTGTA
let-7aPr: GTGCAGGGTCCGAGGT
let-7aT: (6-FAM) TGGATACGACAACTATAC (MGB)
let-7aSeq: 6-ugagguaguagguuguauaguu-27 (MIMAT0000062)

from the body. Informed consent was taken from all subjects.

Total RNA and genomic DNA preparation

Total RNA and genomic DNA were extracted from the gastric carcinoma tissues and normal gastric mucous tissues. Total RNA was extracted by using Trizol (Invitrogen, Carlsbad CA) and genomic DNA was extracted by using QIAamp DNA Mini Kit (Qiagene, Germany) according to the manufacturer's instructions. The total RNA and genomic DNA were quantified by ultraviolet spectrophotometer (UVPC2401, SHIMADZU) at a wavelength of 260 nm. Total RNA from normal gastric mucosa was quantified to 5 μg, and then diluted to 500 ng, 50 ng, 5 ng, 0.5 ng, 0.05 ng, 0.005 ng, respectively.

Stem-loop RT primer and TaqMan MGB probe

All of the oligonucleotides described are displayed in Table 1. The stem-loop RT primer, real-time PCR primes and TaqMan MGB probe were designed as previously described by Chen et al[16]. The let-7a miRNA template sequence was accessed from http://microrna.sanger.ac.uk/cgi-bin/sequences/mirna_entry.pl? acc = MI0000060. All primers, and probes were synthesized by Shanghai GeneCore Biotechnologies Co., Ltd.

Reverse transcription

The miRNAs were reverse transcribed into cDNAs by SuperScript Ⅲ reverse transcription kits (Invitrogen). Ten microliters of the total RNA or artificially synthesized let-7a miRNA template, 1.0 μL of 1.0 μmmol/μL stem-loop RT primer (let-7aP$_{RT}$), 1.0 μL of 10 mmol/L dNTPs (Promega) and 1.0 μL of H$_2$O were mixed and heated at 65℃ for 5 min. The mixture was immediately placed on ice for 2 min. Then 4.0 μL of 5 × First-Strand buffer, 1.0 μL of 0.1 mol/L DTT, 1.0 μL of RNase inhibitor (Invitrogen) and 1.0 μL of SuperScript Ⅲ reverse transcriptase were added and mixed. The 20 μL of reaction volume was incubated for 60 min at 55℃, 15 min at 70℃ and then held at 4℃. All reverse transcriptions as well as no-template controls were run at the same time.

Real-time PCR

Real-time PCR was performed using a standard TaqMan PCR protocol on an Applied Biosystems 7000 Sequence Detection System (Applied Biosystems). The 50 μL of PCR mixture included 5.0 μL of RT product, 5.0 μL of 10 × PCR buffer (Takara), 1.0 μL of 10 mmol/L dNTPs (Takara), 7.0 μL of 25 mmol/L Mg^{2+} (Takara), 0.6 μL of AmpliTaq DNA polymerase (5 U/μL, Takara),

0.2 μL of TaqMan probe (let-7aT, 10 μmol/μL), 1.5 μL of amplification primer I (let-7aPf, 10 μmol/μL), 0.7 μL of amplification primer Ⅱ (let-7aPr, 10 μmol/μL) and 29 μL of autoclaved distilled water. The reaction mixtures were incubated at 95℃ for 10 min, followed by 40 amplification cycles of 95℃ for 15 s and 60℃ for 1 min. The threshold cycle (CT) is defined as the fractional cycle number at which the fluorescence passes the fixed threshold. TaqMan CT values were converted into absolute copy numbers using a standard curve from synthetic let-7a miRNA. We also quantified transcripts of beta-actin as the endogenous RNA control, and each sample was normalized on the basis of its beta-actin content[17].

RESULTS

Sensitivity and dynamic range

The dynamic range and the sensitivity of the let-7a miRNA quantification scheme were evaluated using synthesized let-7a miRNA. The synthesized let-7a miRNA was quantified at the ultraviolet (UV) wavelength of 260 nm (A_{260}) and diluted by ten orders of magnitude, including 10^{10}, 10^9, 10^8, 10^7, 10^6, 10^5, 10^4, 10^3, 10^2, 10^1 and 1 copies/μL. The real-time PCR assay showed excellent linearity between the log of target input and CT value, suggesting that the assay has a dynamic range of at least 8 logs and is capable of detecting as few as ten copies let-7a in the reaction (Figure 1), and the correlation coefficient was 0.996. The total RNA input ranged from 0.005 ng to 5 μg, and the result showed the method could detect the let-7a miRNA as few as 0.05 ng of total RNA from gastric mucosa (Figure 2).

Specificity analysis

The effect of non-specific genomic DNA on let-7a miRNA assay was tested. The results showed that no fluorescence signal occurred even though 50 ng of human genomic DNA was added to the RT reaction, indicating that the method has a good specificity without disturbance of genome.

Expression of let-7a miRNA in gastric carcinoma

In order to confirm whether the level of let-7a miRNA was reduced in human gastric cancer, we examined the expression of mature let-7a miRNA and beta-actin in the samples from 32 patients with gastric cancer. As shown in Table 2 and Figure 3, the expression level of let-7a miRNA in tumors was significantly lower (down-regulation rate over 2-fold) in 14 patients tested. However, in the other 18 patients, no significant difference in let-7a miRNA expression was observed between tumors and normal tissues, and the up- or down-regulation rates were within two-fold.

DISCUSSION

MicroRNAs are endogenous short non-coding RNA molecules that regulate cell differentiation, proliferation, and apoptosis through post-transcriptional suppression of gene expression by binding to the complementary sequence in the 3'-untranslated region (3'-UTR) of target messenger
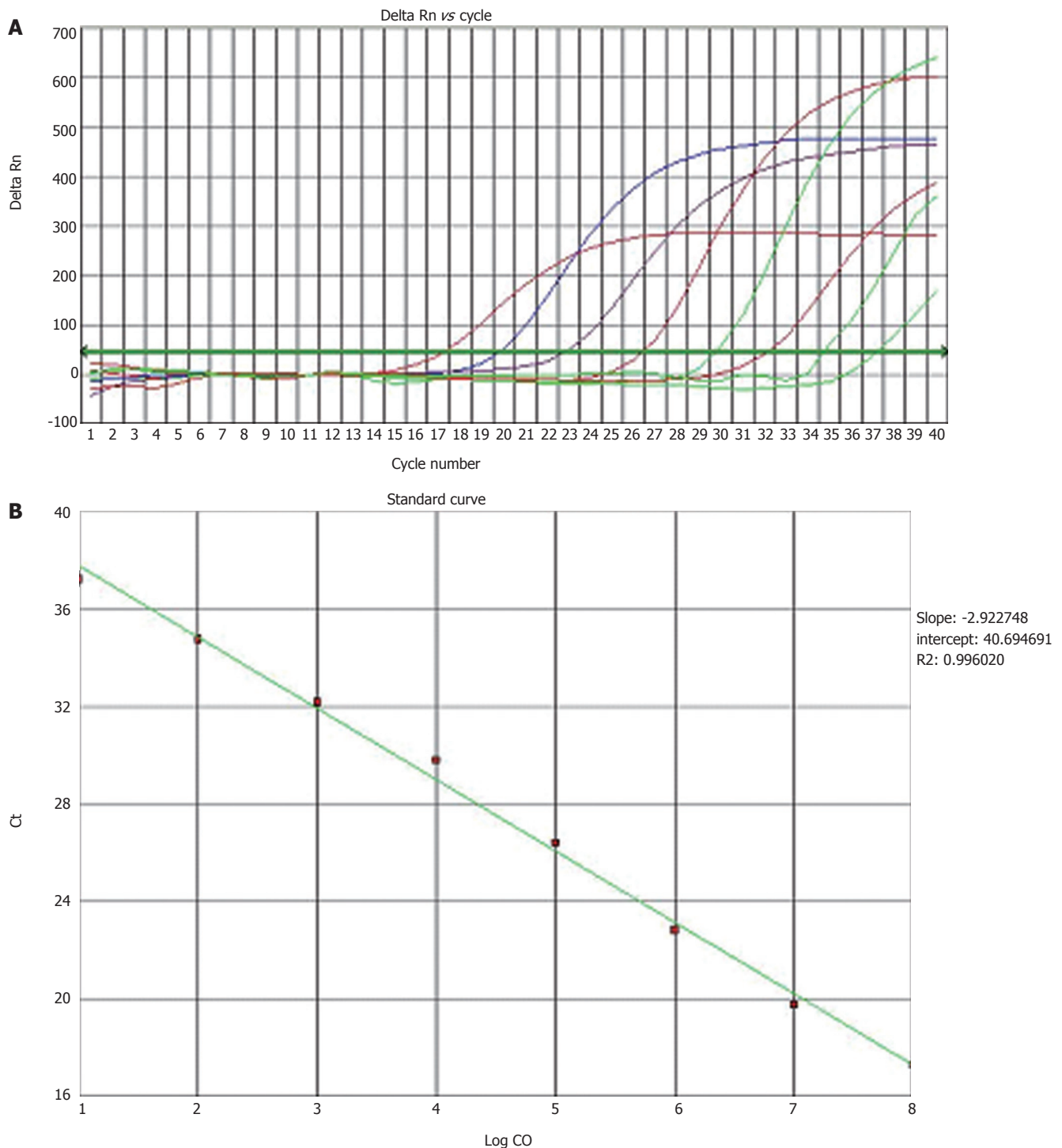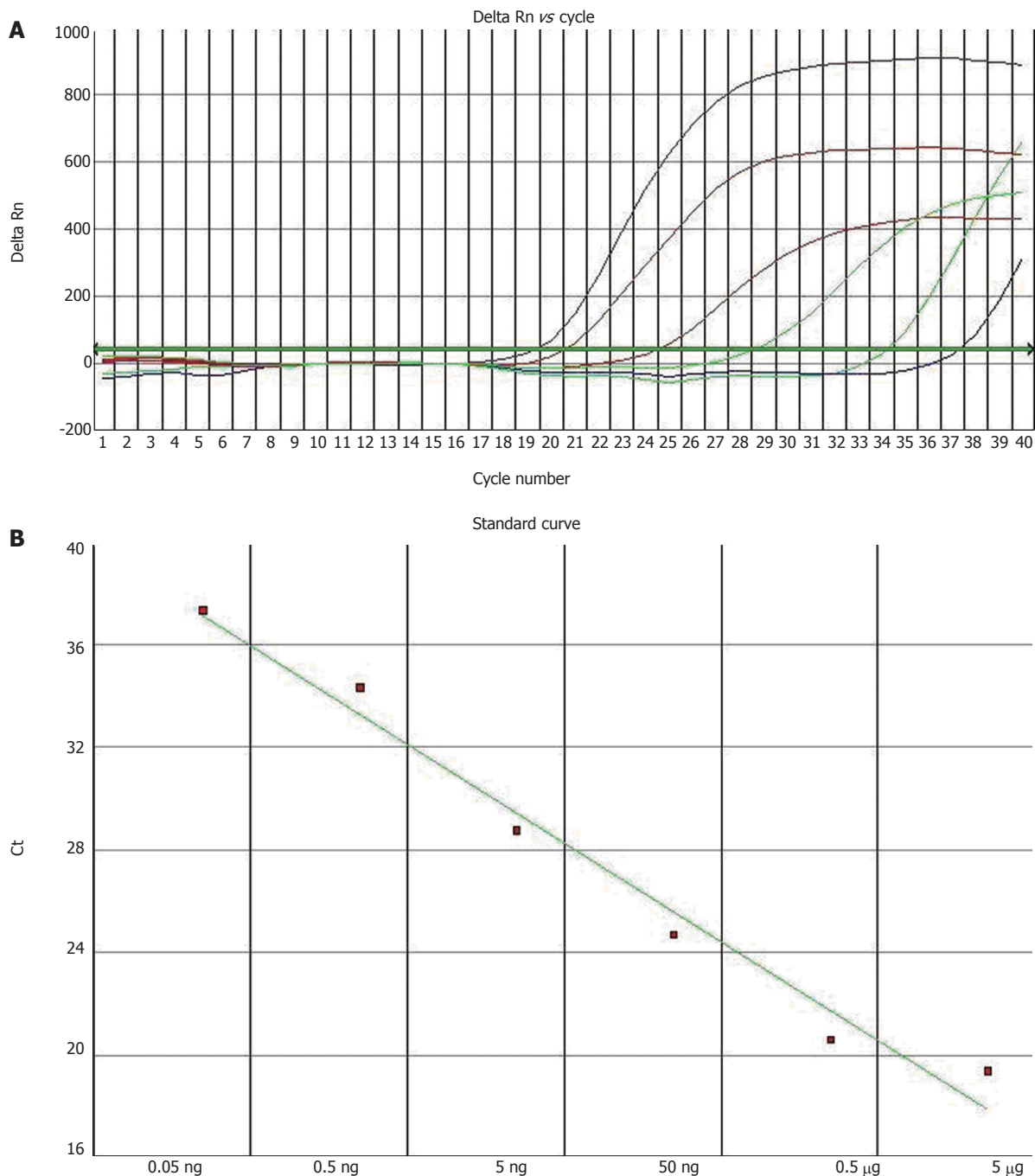
Figure 1 Sensitivity and dynamic range of let-7a miRNA assay. **A**: Amplification curve of the synthesized let-7a miRNA, the well-behaved assay exhibited high sensitivity and broad dynamic range between the signal of 10 copies and 10^8 copies input template and the no-template-control background; **B**: Standard curve of the let-7a miRNA (r^2 = 0.996, slope = -2.92).

RNAs (mRNAs)[3]. Recently, it has been revealed that the change of miRNA expressions contributes to the initiation and progression of carcinoma. More than 50% of miRNAs are located in cancer-associated genomic regions or in fragile sites[18]. The relationship between miRNA and tumor has currently become the focus of many scientists. Current methods for detection and quantification of let-7a miRNA are largely based on cloning, Northern blotting[19], or primer extension[20]. Although microarrays could improve the throughput of miRNA profiling, the

method is relatively limited in terms of sensitivity and specificity[21,22]. Low sensitivity becomes a problem for miRNA quantification because it is difficult to amplify these short RNA targets. Furthermore, low specificity may lead to a false-positive signal. They are not only low-sensitive, but also low-specific, because of the non-specificity of let-7a pre-miRNA and genome.

Real-time PCR is the gold standard for gene expression quantification[23,24]. It has been a long challenge for scientists to design a conventional PCR assay from

Figure 2 Total RNA sensitivity and dynamic range of let-7a miRNA assay. **A**: Amplification plot of total RNA from gastric mucosa at six orders of magnitude. The total RNA input ranged from 50 pg to 5 μg in per stem-loop RT-PCR reaction; **B**: Correlation of total RNA input with the threshold of cycle (Ct) values for let-7a miRNA assays.

miRNAs with 22 nt in length on average. We specifically quantified the let-7a miRNA expression levels in gastric carcinoma using TaqMan PCR assays designed by Chen *et al*[16]. This assay can precisely detect 10 copies let-7a in 50 pg of total RNA. Furthermore, the results showed this method could detect let-7a miRNA without disturbance of genome.

Gastric carcinoma develops through the accumulation of multiple genetic lesions that involve oncogenes, tumor suppressor genes and DNA mismatch repair genes. The relationship between gastric carcinoma genesis and the expression of let-7a miRNA is rarely reported. In the present study, we examined, using real-time PCR, the expression of let-7a mature miRNA in 32 matched pairs of gastric tumoral and non-tumoral tissues from patients. The results showed let-7a miRNA was significantly down-regulated in 14 of 32 patients with gastric cancer. Similarly, the expression of let-7a miRNA was reduced in lung cancer[13] and colon cancer[14]. The 3'UTRs of the human *Ras* genes contain multiple let-7a complementary sites (LCSs), allowing let-7a to regulate Ras expression. It has been reported that the expression of let-7a is lower in gastric tumors than in normal gastric tissue, while Ras protein is significantly higher in gastric tumors, which provides a possible mechanism for the association of let-7a in gastric cancer. Further studies on relationship between

Table 2 Expression of let-7a miRNA in gastric carcinoma tissue

Sample No.	T (copies/μg)			N (copies/μg)			T/N
	let-7a	β-actin	let-7a/β-actin	let-7a	β-actin	let-7a/β-actin	
50901	7.37×10^4	1.05×10^5	0.7	2.15×10^5	1.43×10^5	1.5	0.47
51005	1.15×10^4	3.83×10^4	0.3	4.35×10^4	2.90×10^4	1.5	0.20
51006	1.03×10^5	5.15×10^5	0.2	8.57×10^5	4.76×10^5	1.8	0.11
51208	6.30×10^5	1.26×10^6	0.5	1.98×10^6	1.65×10^6	1.2	0.42
06031	1.03×10^3	8.58×10^2	1.2	2.63×10^3	1.05×10^3	2.5	0.48
60412	1.35×10^5	2.70×10^5	0.5	5.88×10^5	2.45×10^5	2.4	0.21
60418	6.53×10^5	1.09×10^6	0.6	2.74×10^6	1.37×10^6	2.0	0.30
60519	6.31×10^4	2.10×10^5	0.3	4.94×10^5	2.35×10^5	2.1	0.14
60524	3.05×10^5	7.63×10^5	0.4	6.22×10^5	6.91×10^5	0.9	0.44
60625	1.53×10^5	5.10×10^5	0.3	5.78×10^5	4.82×10^5	1.2	0.25
60726	8.24×10^4	1.03×10^5	0.8	2.55×10^5	9.46×10^4	2.7	0.30
60729	5.61×10^6	5.61×10^7	0.1	3.49×10^7	4.36×10^7	0.8	0.13
60731	4.35×10^4	8.70×10^4	0.5	1.32×10^5	9.41×10^4	1.4	0.36
60832	7.28×10^5	3.64×10^6	0.2	3.78×10^6	3.15×10^6	1.2	0.17

T: Gastric carcinoma tissue; N: Normal tissue; T/N: Difference in let-7a expression between tumor and normal tissue.
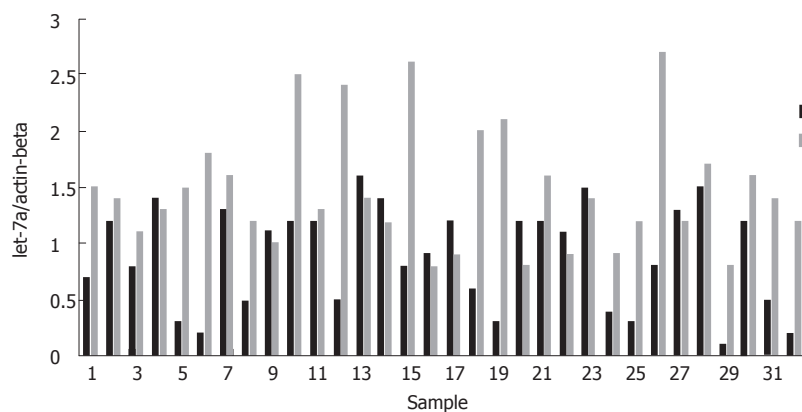
Figure 3 Expression of let-7a miRNA in gastric cancer. Difference in let-7a miRNA expression between in tumor tissues (T) and the adjacent non-tumor tissues (N). The patient numbers correspond to those in Table 2. Compared to normal tissues, let-7a miRNAs expression in tumor tissue from 14 patients was significantly down-regulated.

gastric carcinoma and let-7a are currently underway in our laboratory.

REFERENCES

1   **Ambros V**. microRNAs: tiny regulators with great potential. *Cell* 2001; **107**: 823-826
2   **Ambros V**. The functions of animal microRNAs. *Nature* 2004; **431**: 350-355
3   **Bartel DP**. MicroRNAs: genomics, biogenesis, mechanism, and function. *Cell* 2004; **116**: 281-297
4   **Zhang L**, Huang J, Yang N, Greshock J, Megraw MS, Giannakakis A, Liang S, Naylor TL, Barchetti A, Ward MR, Yao G, Medina A, O'brien-Jenkins A, Katsaros D, Hatzigeorgiou A, Gimotty PA, Weber BL, Coukos G. microRNAs exhibit high frequency genomic alterations in human cancer. *Proc Natl Acad Sci USA* 2006; **103**: 9136-9141
5   **Rajewsky N**. microRNA target predictions in animals. *Nat Genet* 2006; **38** Suppl: S8-S13
6   **Lagos-Quintana M**, Rauhut R, Lendeckel W, Tuschl T. Identification of novel genes coding for small expressed RNAs. *Science* 2001; **294**: 853-858
7   **Bonnet E**, Van de Peer Y, Rouze P. The small RNA world of plants. *New Phytol* 2006; **171**: 451-468
8   **Reinhart BJ**, Weinstein EG, Rhoades MW, Bartel B, Bartel DP. MicroRNAs in plants. *Genes Dev* 2002; **16**: 1616-1626
9   **miRBase Sequence database**. http://microrna.sanger.ac.uk/sequences/index.shtml (Version current at August 9, 2006)
10 **Zamore PD**, Haley B. Ribo-gnome: the big world of small RNAs. *Science* 2005; **309**: 1519-1524
11 **Krutzfeldt J**, Poy MN, Stoffel M. Strategies to determine the biological function of microRNAs. *Nat Genet* 2006; **38** Suppl: S14-S19
12 **McManus MT**. MicroRNAs and cancer. *Semin Cancer Biol* 2003; **13**: 253-258
13 **Takamizawa J**, Konishi H, Yanagisawa K, Tomida S, Osada H, Endoh H, Harano T, Yatabe Y, Nagino M, Nimura Y, Mitsudomi T, Takahashi T. Reduced expression of the let-7 microRNAs in human lung cancers in association with shortened postoperative survival. *Cancer Res* 2004; **64**: 3753-3756
14 **Akao Y**, Nakagawa Y, Naoe T. let-7 microRNA functions as a potential growth suppressor in human colon cancer cells. *Biol Pharm Bull* 2006; **29**: 903-906
15 **Johnson SM**, Grosshans H, Shingara J, Byrom M, Jarvis R, Cheng A, Labourier E, Reinert KL, Brown D, Slack FJ. RAS is regulated by the let-7 microRNA family. *Cell* 2005; **120**: 635-647
16 **Chen C**, Ridzon DA, Broomer AJ, Zhou Z, Lee DH, Nguyen JT, Barbisin M, Xu NL, Mahuvakar VR, Andersen MR, Lao KQ, Livak KJ, Guegler KJ. Real-time quantification of microRNAs by stem-loop RT-PCR. *Nucleic Acids Res* 2005; **33**: e179
17 **Xie D**, Nakachi K, Wang H, Elashoff R, Koeffler HP. Elevated levels of connective tissue growth factor, WISP-1, and CYR61 in primary breast cancers associated with more advanced features. *Cancer Res* 2001; **61**: 8917-8923
18 **Calin GA**, Sevignani C, Dumitru CD, Hyslop T, Noch E, Yendamuri S, Shimizu M, Rattan S, Bullrich F, Negrini M, Croce CM. Human microRNA genes are frequently located at fragile sites and genomic regions involved in cancers. *Proc Natl Acad Sci USA* 2004; **101**: 2999-3004
19 **Kloosterman WP**, Steiner FA, Berezikov E, de Bruijn E, van de Belt J, Verheul M, Cuppen E, Plasterk RH. Cloning and expression of new microRNAs from zebrafish. *Nucleic Acids*

Res 2006; **34**: 2558-2569

20   **Zeng Y**, Cullen BR. Sequence requirements for micro RNA processing and function in human cells. *RNA* 2003; **9**: 112-123

21   **Krichevsky AM**, King KS, Donahue CP, Khrapko K, Kosik KS. A microRNA array reveals extensive regulation of microRNAs during brain development. *RNA* 2003; **9**: 1274-1281

22   **Liu CG**, Calin GA, Meloon B, Gamliel N, Sevignani C, Ferracin M, Dumitru CD, Shimizu M, Zupo S, Dono M, Alder H, Bullrich F, Negrini M, Croce CM. An oligonucleotide microchip for genome-wide microRNA profiling in human and mouse tissues. *Proc Natl Acad Sci USA* 2004; **101**: 9740-9744

23   **Livak KJ**, Schmittgen TD. Analysis of relative gene expression data using real-time quantitative PCR and the 2 (-Delta Delta C(T)) Method. *Methods* 2001; **25**: 402-408

24   **Heid CA**, Stevens J, Livak KJ, Williams PM. Real time quantitative PCR. *Genome Res* 1996; **6**: 986-994

CASE REPORT

Successful endoscopic repair of an unusual colonic perforation following polypectomy using an endoclip device

Francesco Barbagallo, Giorgio Castello, Saverio Latteri, Emanuele Grasso, Salvatrice Gagliardo, Gaetano La Greca, Michele Di Blasi

Francesco Barbagallo, Giorgio Castello, Saverio Latteri, Emanuele Grasso, Salvatrice Gagliardo, Gaetano La Greca, Department of Surgical Sciences, Transplantation and Advanced Technologies, University of Catania, Padiglione 29, Policlinico Universitario, Via S. Sofia, Catania 95100, Italy
Michele Di Blasi, Digestive Endoscopic Unit, University of Catania, P.O. Cannizzaro, Via Messina 829, Catania 95126, Italy
Correspondence to: Gaetano La Greca, MD, PhD, Department of Surgical Sciences, Transplantation and Advanced Technologies, University of Catania, *Via* Messina 354 95126 Catania, Italy. glagreca@unict.it
Telephone: +39-95-7223914 Fax: +39-95-7122221
Received: 2007-02-09   Accepted: 2007-03-08

Abstract

Colonic perforation during endoscopic diagnostic or therapeutic procedures, represents an uncommon occurrence even if, together with haemorrhage, it is still the most common complication of colonoscopy, with an incidence ranging between 0.1% and 2% of all colonoscopic procedures. The ideal treatment in these cases remains elusive as the endoscopist and the surgeon have to make a choice case by case, depending on many factors such as how promptly the rupture is identified, the condition of the patient, the degree of contamination and the evidence of peritoneal irritation. Surgical interventions both laparotomic and laparoscopic, and other medical non-operative solutions are described in the literature. Only three cases have been reported in the literature in which the endoscopic apposition of endoclips was used to repair a colonic perforation during colonoscopy. Ours is the first case that the perforation itself was caused by the improper functioning of a therapeutic device.

Barbagallo F, Castello G, Latteri S, Grasso E, Gagliardo S, La Greca G, Di Blasi M. Successful endoscopic repair of an unusual colonic perforation following polypectomy using an endoclip device. *World J Gastroenterol* 2007; 13(20): 2889-2891

INTRODUCTION

Colonic perforation, together with haemorrhage, represents the most common complication of therapeutic colonoscopy, although its incidence is very low and ranges between 0.1% and 2% of all colonoscopic procedure[1]. The occurrence of colonic perforations during polypectomy can depend on several factors alone or in association with each other. Some of these risk factors are from physicians, and others depend on the polyp and the shape of its peduncle. There are few cases in which the main risk factor is represented by a malfunctioning therapeutic device. We report a case of a perforation of the colonic wall during an endoscopic polypectomy, caused by a defective device, which was promptly treated endoscopically by the apposition of endoclips.
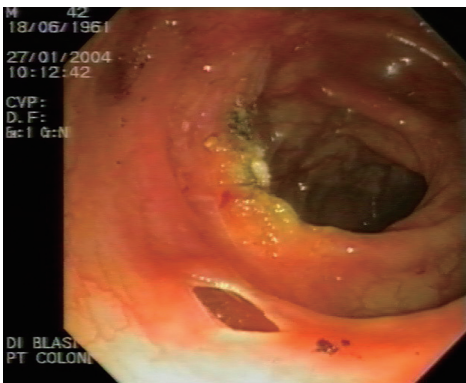
CASE REPORT

A 48-year-old male patient was admitted complaining of rectal bleeding for the past two months accompanied with frequent episodes of constipation and diarrhoea. The patient underwent colonoscopy after preparation with 4 L PEG-Electrolyte solution. Endoscopy was performed after light sedation with intravenous 10 mg benzodiazepine (Valium®). The procedure showed a 1 cm in diameter sigmoid polyp with a short peduncle, and two other polyps of about 3 cm in diameter. One of these was larger with a 1.5 cm peduncle on the left flexure of the colon and the other was a sessile polyp on the right flexure. Endoscopic resection was started with the polyp at the right flexure after a submucosal injection of 12 mL 0.9% saline. Using an oval diathermic loop and electrocautery Olympus EUS 30®, the peduncle was sectioned with a mixed current (cutting 40W, coagulating 35W). During the initial section of the peduncle, the diathermy loop broke at one of its roots because of a manufacturing defect (Figure 1) so that its elastic tension was discharged on the colonic wall producing a transmural perforation. This was about 2 cm long and 3 cm away from the polyp and not bleeding possibly because of the high temperature of the device (Figure 2). The perforation was immediately noticed and promptly closed using two endoclips Olympus® (Figure 3). As the closure seemed stable and resistant, the patient was in good condition. Considering the bleeding risk of the partially excised polyp, the polypectomy was successfully and easily completed with a new diathermy loop as the
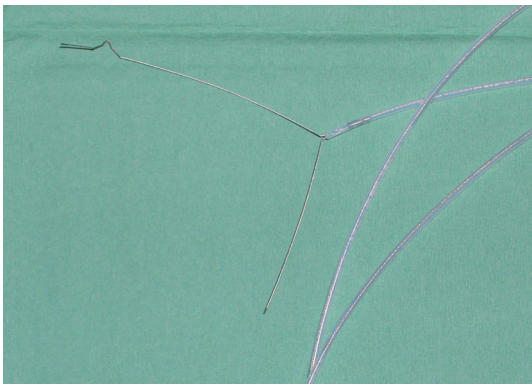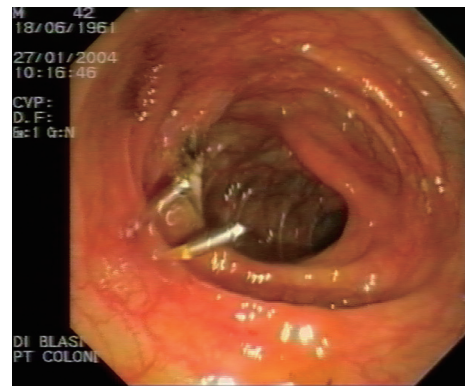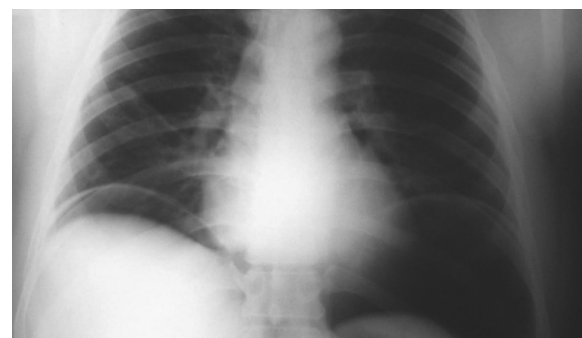
Figure 1 Defective device captured after the offending procedure.

Figure 3 Two endoclips Olympus® are endoscopically positioned to repair the perforation of the colonic wall.

Figure 2 Transmural perforation of the colon, about 2 cm long and 3 cm from the polyp.

Figure 4 Abdominal X-ray examination performed soon after the successful conclusion of the endoscopic procedure, showing bilateral sub-diaphragmatic free air.

other two polypectomies, simpler and more distal, not needing further air insufflations. After the procedure, the patient reported modest right hypochondria pain, with no signs of shock, or peritonism. An abdominal X-ray examination was performed (Figure 4) and showed bilateral sub-diaphragmatic free air. Based on the stable general condition of the patient, his age and the very good colonic preparation, we decided to adopt a conservative attitude. The patient was kept with fluids and peripheral parenteral nutrition, and two doses of metronidazole 500 mg and amoxycillin-clavulonic acid 1 g were administered. The general condition of the patient consistently remained good without any increase of temperature, variation of haemodynamic parameters, or increase of WBC count. A second abdominal X-ray examination three days after the procedure showed a significant resorption of the sub-diaphragmatic air. Since there were no sufficient experiences in literature, we preferred to extend the hospital stay of the patient even if she was already dischargeable. The modest abdominal pain disappeared slowly and intestinal motility became normal after the 4th post-procedural day so that a light diet was introduced. The patient was finally discharged in good condition eight days after the procedure. A further X-ray examination 18 d later showed the complete resorption of the intra-peritoneal air and the patient was completely asymptomatic. The histopathological examination of

all the resected polyps were classified as tubulo-villous adenomas with moderate dysplasia and free peduncles, requiring no more surgical procedure.

DISCUSSION

The ideal management of colonic perforation following colonoscopic polypectomy remains elusive because its incidence is very low and estimated to be between 0.1% and 2% of all colonoscopic procedures[1]. The possibility of such a rare occurrence can be related to several factors, some depending on the experience and the training of the endoscopist. Colonic perforation can be due to technical errors with consequent direct perforation of the colonic wall, or to the use of the wrong cutting current causing extensive necrotic damage of the wall. Other important risk factors are related to the pathology, the polyp itself, its shape and dimensions, and the type and size of its peduncle. Sessile polyps and polyps with short and thick peduncle are certainly associated with a higher risk of colonic perforation, as the procedures required for the endoscopic excision are not always simple. Rare but still possible, there are cases of perforation resulting from the improper functioning of a therapeutic device which is not related to the type of the polyp or the experience of the endoscopist. The treatment of colonic perforation during polypectomy is still controversial and

there are different treatment options to evaluate: the surgical treatment, either laparoscopic or laparotomic, the conservative non-operative treatment, and the endoscopic treatment. An endoscopist must maintain a high index of suspicion despite minimal or atypical symptoms and negative radiological studies, because perforation can be a complication with a high morbidity and mortality[2]. The research of the best possible management is mandatory in all cases and immediate surgical consultation should always be sought. The trend is to be less invasive, using no surgery given the advantages in ICU care and antibiotics. Laparoscopically or laparoscopically assisted (minilaparotomy) surgery is also being increasingly used, with outcomes comparable to conventional laparotomy. Moreover, experience and advantages in accessories have enabled the endoscopic repair of iatrogenic perforation in recent years[2]. There are only three cases in the English literature (PubMed) which report the endoscopic apposition of endoclips to repair a colonic perforation[3-5], and all of them obtained as good results as ours. In our opinion, an individualized approach must be taken to manage the patient with an iatrogenic perforation, and several factors should be taken into consideration before making a choice of the treatment. Local factors such as the suspected septic contamination, the localization of the polyp, the dimensions of the lesion and the quality of colonic preparation before the procedure, are important in order to make the right treatment choice. Other factors are the general condition of the patient, the symptoms and the eventual peritoneal irritation. In case of a risk of peritoneal septic contamination, especially in a patient with uncertain conditions, the surgical treatment on an emergency basis has to be considered the only reasonable choice. In these cases, according to the literature, a laparoscopic repair, other than minimally invasive, can be also safe, effective and fast[6], while a delayed surgery may sometimes prove fatal[7]. The main benefit of the laparoscopic approach, compared to the traditional laparotomy, is seen in a more favourable postoperative status and in the possibility of definitive injury management[8]. The possibility of a conservative or endoscopic solution by apposition of endoclips should also be considered in the patient in good general condition and when colonic preparation before the procedure is performed properly to minimize the risk of septic contamination. The case we reported is the fourth case described in the English literature of perforation following colonoscopy treated endoscopically

as a definitive treatment. There are also a few cases of endoclip apposition to treat duodenal perforation[9,10] and colocutaneous fistula[11]. To our knowledge, ours is the first case due to the improper functioning of a therapeutic device. Although a very careful consideration of the case is required, endoscopic repair may represent a feasible, simple, fast and successful procedure, which meets with the satisfaction of both patient and surgeon, with a high favorable cost-benefit ratio and a relatively short hospital stay of the patients when compared to an urgent surgical procedure after colonic perforation. The reported procedure is clearly considered to be neither always feasible nor a gold standard. In our opinion, a non-surgical endoscopic repair of iatrogenic rupture of the colonic wall during endoscopic manoeuvres in this case should be taken into high consideration.

REFERENCES

1   **Clements RH**, Jordan LM, Webb WA. Critical decisions in the management of endoscopic perforations of the colon. *Am Surg* 2000; **66**: 91-93
2   **Putcha RV**, Burdick JS. Management of iatrogenic perforation. *Gastroenterol Clin North Am* 2003; **32**: 1289-1309
3   **Dhalla SS**. Endoscopic repair of a colonic perforation following polypectomy using an endoclip. *Can J Gastroenterol* 2004; **18**: 105-106
4   **Mana F**, De Vogelaere K, Urban D. Iatrogenic perforation of the colon during diagnostic colonoscopy: endoscopic treatment with clips. *Gastrointest Endosc* 2001; **54**: 258-259
5   **Yoshikane H**, Hidano H, Sakakibara A, Ayakawa T, Mori S, Kawashima H, Goto H, Niwa Y. Endoscopic repair by clipping of iatrogenic colonic perforation. *Gastrointest Endosc* 2001; **53**: 841-842
6   **Miyahara M**, Kitano S, Shimoda K, Bandoh T, Chikuba K, Maeo S, Kobayashi M. Laparoscopic repair of a colonic perforation sustained during colonoscopy. *Surg Endosc* 1996; **10**: 352-353
7   **Biandrate F**, Piccolini M, Francia L, Quarone M, Rosa C, Battaglia A, Pandolfi U. Colonic perforation after colonoscopy: our experience. *Chir Ital* 2003; **55**: 617-620
8   **Martinek L**, Vavra P, Andel P, Mazur M. A laparoscopic management of an iatrogenic lesion of the colon during a colonoscopy. *Rozhl Chir* 2004; **83**: 559-561
9   **Charabaty-Pishvaian A**, Al-Kawas F. Endoscopic treatment of duodenal perforation using a clipping device: case report and review of the literature. *South Med J* 2004; **97**: 190-193
10 **Seibert DG**. Use of an endoscopic clipping device to repair a duodenal perforation. *Endoscopy* 2003; **35**: 189
11 **Familiari P**, Macri A, Consolo P, Angio L, Scaffidi MG, Famulari C, Familiari L. Endoscopic clipping of a colocutaneous fistula following necrotizing pancreatitis: case report. *Dig Liver Dis* 2003; **35**: 907-910

CASE REPORT

Ampullary adenomyoma presenting as acute recurrent pancreatitis

Tae-Hee Kwon, Do Hyun Park, Kwang Yeon Shim, Hyun-Deuk Cho, Jeong Hoon Park, Suck-Ho Lee, Il-Kwun Chung, Hong-Soo Kim, Sang-Heum Park, Sun-Joo Kim

Tae-Hee Kwon, Do Hyun Park, Kwang Yeon Shim, Jeong Hoon Park, Suck-Ho Lee, Il-Kwun Chung, Hong-Soo Kim, Sang-Heum Park, Sun-Joo Kim, Division of Gastroenterology, Department of Internal Medicine, Soon Chun Hyang University Cheonan Hospital, Cheonan, Choongnam 330-721, Korea
Hyun-Deuk Cho, Division of Gastroenterology, Department of Pathology, Soon Chun Hyang University Cheonan Hospital, Cheonan, Choongnam 330-721, Korea
Correspondence to: Do Hyun Park, MD, PhD, Division of Gastroenterology, Department of Internal Medicine, Soon Chun Hyang University Cheonan Hospital 23-20 Bongmyung-dong, Cheonan, Choongnam 330-721, Korea. dhpark@schch.co.kr
Telephone: +82-41-5703675 Fax: +82-41-5745762
Received: 2007-02-11   Accepted: 2007-03-15

Abstract

Adenomyoma is a term generally applied to nodular lesions showing proliferation of both epithelial and smooth muscle components. Despite its benign nature, ampullary adenomyoma is usually presented as biliary obstruction. Most cases are misdiagnosed as carcinoma or adenoma by preoperative endoscopic or radiologic procedure. Therefore, it is frequently treated with extensive surgery. To our knowledge, this is the first reported case in English literature of adenomyoma located in the peripancreatic orifice resulting in intermittent pancreatic duct obstruction and recurrent pancreatitis diagnosed by the endoscopic piecemeal resection.

© 2007 The WJG Press. All rights reserved.

Key words: Ampulla; Adenomyoma; Acute recurrent pancreatitis; Endoscopic resection

INTRODUCTION

Ampullary tumors, both benign and malignant, may present as acute recurrent pancreatitis[1]. The most common benign cause of this situation is adenoma of the major papilla[2,3]. Other benign masses of the major papilla presenting as acute recurrent pancreatitis are extremely rare[4-6]. We describe a rare case of unexposed type ampullary adenomyoma presenting as acute recurrent pancreatitis.

CASE REPORT

A 74-year-old woman was admitted to our department due to severe epigastric pain for one day. She denied alcohol intake and use of any drugs or medications. Five years ago, she was admitted to our hospital for similar symptoms. At the time, serum chemistry analysis revealed 37/11 U/L (0-40 U/L) aspartate/alanine aminotransferase, 85 U/L (39-117 U/L) alkaline phosphatase, 1.3 mg/dL (0.2-1.2 mg/dL) total bilirubin, 4290 IU/L (60-160 IU/L) amylase, and 1526 IU/L (0-60 IU/L) lipase. Abdominal CT scan showed acute pancreatitis and multiple peripancreatic fluid collections. For personal reasons she refused further evaluation and was discharged after receiving conservative treatment for 1 mo. During the second admission, laboratory data revealed 47/49 U/L (0-40 U/L) aspirate/alanine amino transferase, 90 U/L (39-117 U/L) alkaline phosphatase, 0.7 mg/dL (0.2-1.2 mg/dL) total bilirubin, 1417 IU/L (60-160 IU/L) amylase, and 1353 U/L (0-60 IU/L) lipase. Other laboratory results were within normal range. Abdominal CT scan showed acute pancreatitis with peripancreatic fluid collections presenting as grade E. Magnetic resonance cholangiopancreatography (MRCP) showed a diffuse dilated common bile duct without any signal void. The pancreatic duct was unremarkable (Figure 1). Because the terminal common bile duct (CBD) narrowing was suspicious, endoscopic retrograde choledochopancreatography (ERCP) was performed. Duodenoscopy showed the major papilla bulging into the duodenal lumen. The overlying mucosa was intact (Figure 2A). After endoscopic biliary sphincterotomy, an even and firm nodular mass with a granular and villous mucosa was seen originating from the peripancreatic orifice (Figure 2B). Multiple biopsies were taken from the mass. Though the distal common bile duct was diffusely dilated, there was no definite delay of passage after contrast injection. Subsequent endoscopic ultrasonography (EUS) showed slightly elevated echogenic lesions on the major papilla (Figure 3). There was no definite echogenic lesion in the
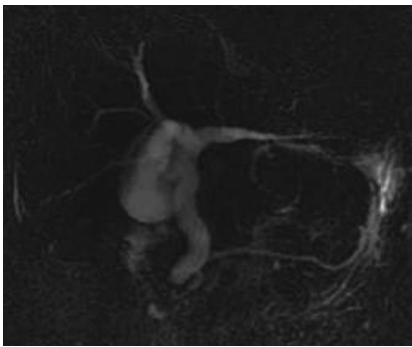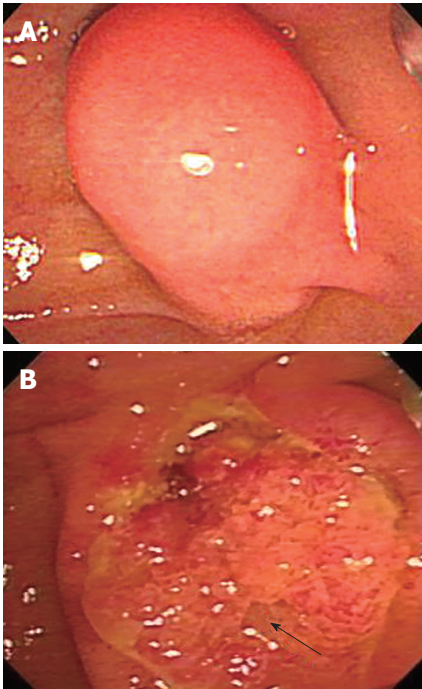
Figure 1 MRCP showing a diffuse dilated common bile duct without signal void and the remarkable pancreatic duct.
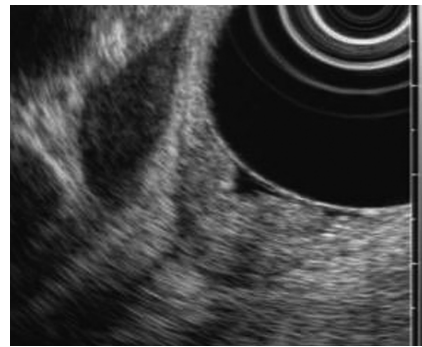
Figure 3 EUS showing slightly elevated echogenic lesions on major papilla.

Figure 2 Duodenoscopy showing a bulged major papilla with overlying intact mucosa (**A**) and an even and firm nodular mass with mucosal and villous granularities origionating from the peripancreatic orifice after endoscopic biliary sphinctertomy (**B**) (the arrow indicates the main pancreatic duct orifice).
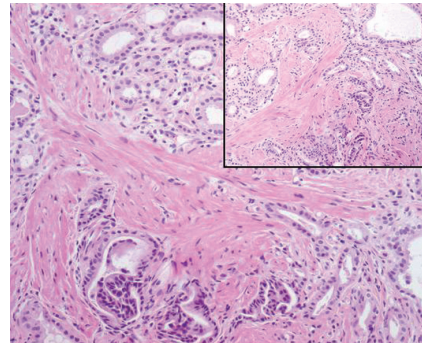
Figure 4 Histology of the resected specimen showing numerous ductules in association with prominent proliferation of smooth muscle in the submucosa of the duodenum (insert, HE, × 2). The ductules were lined by columnar epithelial cells (HE, × 200).

gallbladder. Tentative pathologic diagnosis showed muscle proliferation without atypia. To confirm the diagnosis of unexposed type adenoma we performed a large-particle biopsy (piecemeal resection) using an electrocautery snare. After piecemeal resection, endoscopic pancreatic duct sphincterotomy was performed and a prophylactic pancreatic stent was inserted. Additional argon plasma coagulation (APC) was applied to obliterate remnant villous mucosa. No procedure-related complication occurred following the procedure. Histopathologic analysis of the resected specimen showed an admixture of numerous ductules and a prominent proliferation of smooth muscle in the duodenal submucosa. The ductules were lined by columnar epithelial cells (Figure 4). There were no definite pancreatic acini in the pathologic findings. Based on the pathologic findings, the diagnosis of unexposed type ampullary adenomyoma was confirmed. Follow-up duodenoscopy showed a normal looking of major papilla orifice with scar change. The patient was doing well at the 1 year follow-up.

DISCUSSION

Adenomyoma is a term generally applied to nodular lesions

showing proliferation of both epithelial and smooth muscle components[7,8]. It can occur anywhere in the gastrointestinal tract. Although it is most commonly found in the fundus of the gallbladder, it rarely occurs in the extrahepatic biliary tract, including the ampulla of Vater[8].

Despite its benign nature, in previous reports, ampullary adenomyoma is usually presented as biliary obstruction[9,10]. Most cases are misdiagnosed as carcinoma or adenoma by preoperative endoscopic or radiologic procedure. Therefore, it is frequently treated with extensive surgery[8,9]. To our knowledge, this is the first reported case in English literature of adenomyoma located in the peripancreatic orifice resulting in intermittent pancreatic duct obstruction and recurrent pancreatitis diagnosed by the endoscopic piecemeal resection.

Unexposed type ampullary adenomyoma should be differentiated from chronic papillitis associated with benign conditions such as gallstones and duodenitis. Chronic papillitis may present as adenomatoid ductal hyperplasia with fibrosis and chronic inflammation[10]. In contrast, the intraampullary mass in our case showed admixture of numerous ductules and prominent proliferation of smooth muscle in the submucosa of the duodenum, which was devoid of definite fibrosis.

It may be difficult to detect small ampullary lesions, especially if they do not protrude into the ampulla[1]. Thus, endoscopic biliary sphincterotomy may be helpful in detection of the unexposed types of ampullary tumors, especially in cases of common bile duct dilatation in the absence of gallstones or in cases of unexplained recurrent pancreatitis[1,11]. On endoscopic inspection, the unexposed type ampullary adenomyoma showed lobulated, firm, villous, and mucosal granularities. These endoscopic findings are rather nonspecific and may be observed in nonneoplastic conditions such as a

choledochocele, impacted ampullary stones, or papillitis[12]. Thus, endoscopic findings are by no means pathognomic, and tissue diagnosis is essential for accurate diagnosis[12]. However, tissue samples obtained using conventional biopsy forceps may have a low diagnostic yield[11]. Large-particle biopsy using an electric cautery snare has been shown to increase diagnostic accuracy as shown in previous studies[12] and the patient discussed in this report.

In summary, unexposed type ampullary adenomyoma may be added to the list of rare entities causing recurrent pancreatitis.

REFERENCES

1   **Kim MH**, Lee SK, Seo DW, Won SY, Lee SS, Min YI. Tumors of the major duodenal papilla. *Gastrointest Endosc* 2001; **54**: 609-620

2   **Guzzardo G**, Kleinman MS, Krackov JH, Schwartz SI. Recurrent acute pancreatitis caused by ampullary villous adenoma. *J Clin Gastroenterol* 1990; **12**: 200-202

3   **Berk T**, Friedman LS, Goldstein SD, Marks GP, Rosato FE. Relapsing acute pancreatitis as the presenting manifestation of an ampullary neoplasm in a patient with familial polyposis coli. *Am J Gastroenterol* 1985; **80**: 627-629

4   **Usui M**, Matsuda S, Suzuki H, Hirata K, Ogura Y, Shiraishi T. Somatostatinoma of the papilla of Vater with multiple gastrointestinal stromal tumors in a patient with von Recklinghausen's disease. *J Gastroenterol* 2002; **37**: 947-953

5   **Sriram PV**, Weise C, Seitz U, Brand B, Schroder S, Soehendra N. Lymphangioma of the major duodenal papilla presenting as acute pancreatitis: treatment by endoscopic snare papillectomy. *Gastrointest Endosc* 2000; **51**: 733-736

6   **Mayoral W**, Salcedo J, Al-Kawas F. Ampullary carcinoid tumor presenting as acute pancreatitis in a patient with von Recklinghausen's disease: case report and review of the literature. *Endoscopy* 2003; **35**: 854-857

7   **Ulich TR**, Kollin M, Simmons GE, Wilczynski SP, Waxman K. Adenomyoma of the papilla of Vater. *Arch Pathol Lab Med* 1987; **111**: 388-390

8   **Handra-Luca A**, Terris B, Couvelard A, Bonte H, Flejou JF. **Adenomyoma and adenomyomatous hyperplasia** of the Vaterian system: clinical, pathological, and new immunohistochemical features of 13 cases. *Mod Pathol* 2003; **16**: 530-536

9   **Hammarstrom LE**, Holmin T, Stenram U. Adenomyoma of the ampulla of Vater: an uncommon cause of bile duct obstruction. *Surg Laparosc Endosc* 1997; **7**: 388-393

10 **Narita T**, Yokoyama M. Adenomyomatous hyperplasia of the papilla of Vater: A sequela of chronic papillitis? *Ann Diagn Pathol* 1999; **3**: 174-177

11 **Menzel J**, Poremba C, Dietl KH, Bocker W, Domschke W. Tumors of the papilla of Vater--inadequate diagnostic impact of endoscopic forceps biopsies taken prior to and following sphincterotomy. *Ann Oncol* 1999; **10**: 1227-1231

12 **Venu RP**, Rolny P, Geenen JE, Hogan WJ, Komorowski RA. Ampullary hamartoma: endoscopic diagnosis and treatment. *Gastroenterology* 1991; **100**: 795-798

Standing on the shoulders of giants

Peter McDonald

Peter McDonald, Gastroenterological Surgeon, Northwick Park and St. Mark's Hospitals, Harrow, Middx HA13UJ, United Kingdom
Correspondence to: Peter McDonald, MBBS, MS, FRCS, Consultant Gastroenterological Surgeon, Northwick Park and St. Mark's Hospitals, Harrow, Middx HA13UJ, United Kingdom. pmcdo69277@aol.com

The cover of this well-illustrated, monochrome book has mini-portraits of eight surgical pioneers that suggest the scope of this coffee table sized hardback. Andreas Vesalius rubs shoulders with Lister, Wangensteen, Pasteur and Ambroise Paré. Indeed this multi-author publication is the most comprehensive tome of the history of what is the core of general surgery (i.e. surgery of the gastrointestinal tract) published to date and browsing through it was an utter delight.

I was particularly pleased to find, in an English language publication, not just contributors from the UK, the US and Australia but also from France, the Netherlands and Uruguay. Their scholarly efforts are well referenced, well-edited and hardly ever repetitive. Each chapter is written by obvious experts in their fields in which they describe their chose sub-specialty in great historical detail. I enjoyed the Biographical Notes in the appendix detailing the life histories of the hundred or so most important pioneers (all men!) in gastrointestinal surgery. These vignettes only partly made up for the absence of an index which I think the book deserves. The chapters detail the history of how the anatomy of the intestines was revealed, the battle against infection and pain, the development of anaesthesia and then cover the GI tract organ by organ from oesophagus to anus. Specific topics such as bariatric surgery, intestinal obstruction and the use of mechanical staplers are well covered and it was especially pleasing to see how the pioneers in the Soviet Union were given due credit for the mechanical devices.

The chapter on alimentary tract disorders in infants and children is extraordinarily detailed and throughout this book I came across snippets of knowledge that had until now passed me by such as the fact that the word *pancreas* is derived from the Greek *pan-kreas* ("all-meat") and that Professor (later Lord) Lister migrated from Glasgow (where he trained my great-grandfather) to Edinburgh (which he loved) to King's College London (which he did reluctantly) in order to take his message of antisepsis to that sceptical southern metropolis.

Between the chapters there are a few more detailed biographical footnotes on some of the pioneers and these seem to have been chosen somewhat at random (e.g. On Billroth, Ravitch, Wangensteen, Sir Alan Parks and others). However, this bit of serendipity does not detract from the overall impression of a book of high scholarship which is easy to read and will probably remain the best historical reference book in this subject for many years to come. If Winston Churchill was right when he stated that "The further you look back the easier it is to look forward!" then every student and practitioner of gastroenterological chirurgery must purchase a copy of Pioneers In Surgical Gastroenterology as soon as possible!

Acknowledgments to Reviewers of *World Journal of Gastroenterology*

Simon D Taylor-Robinson, MD
Department of Medicine A, Imperial College London, Hammersmith Hospital, Du Cane Road, London W12 0HS, United Kingdom

Christa Buechler, PhD
Regensburg University Medical Center, Internal Medicine I, Franz Josef Strauss Allee 11, 93042 Regensburg, Germany

Julia Butler Greer, MD, MPH
Department of Gastroenterology, Hepatology and Nutrition, University of Pittsburgh Medical Center, M2, Presbyterian University Hospital, 200 Lothrop Street, Pittsburgh, Pa 15213, United States

Tom Hemming Karlsen, MD
Institute of Immunology, Rikshospitalet University Hospital, N-0027 Oslo, Norway

Florian Obermeier
Internal Medicine I, University of Regensburg, Franz-Josef-Strauss Allee11, Regensburg 93053, Germany

Stefan G Hübscher, MD, Professor
Department of Pathology, University of Birmingham, Birmingham B15 2TT, United Kingdom

Frank A Anania, Professor
Emory University School of Medicine, Division of Division Digestive Diseases, 615 Michael Street, Room 255 Whitehead Biomedical Research Building, Atlanta, GA 30322, United States

Limas Kupcinskas
Gastroenterology of Kaunas University of Medicine, Mickevicius 9, Kaunas LT 44307, Lithuania

Kunissery Ananthasubramanian Balasubramanian, Professor
Christian Medical College, Gastrointestinal Sciences, Ida Scudder Road, Vellore 632004, India

Stefan Wirth, Professor, Dr
Children's Hospital, Heusnerstt. 40, Wuppertal 42349, Germany

Francoise Lunel Fabiani, Professor
Laboratoire De Bacteriologie Virologie Et Hygiene, 4 Rue Larrey, Angers 49933, France

Ramsey Chi-man Cheung, MD, Professor
Division of GI & Hepatology, VAPAHCS(154C), 3801 Miranda Ave, Stanford University School of Medicine, Palo Alto, CA 94304, United States

Hongjin Huang, PhD
Celera Diagnostics, 1401 Harbor Bay Parkway, Alameda, California 94502, United States

Ravi S Chari, MD, Associate Professor
Division of Hepatobiliary Surgery and Liver Transplantation, Departments of Surgery and Cancer Biology,1313 21st Avenue South Suite 801 Oxford House, Vanderbilt University Medical Center,Nashville, TN 37232-4753, United States

Liping Su, MD, PhD
Department of Pathology, The University of Chicago, 5841 S. Maryland, MC 1089, Chicago, IL 60637, United States

Khalid Ahnini Tazi, PhD, Assistant Professor
Laboratoire d'Hemodynamique Splanchnique et de Biologie Vasculaire, Inserm, Hopital Beaujon., Clichy 92118, France

Serdar Karakose, Dr, Professor
Department of Radiology, Meram Medical Faculty, Selcuk University, Konya 42080, Turkey

Shu Zheng, Professor
Scientific Director of Cancer Institute, Zhejiang University, Secondary Affiliated Hospital, Zhejiang University, 88# Jiefang Road, Hangzhou 310009, Zhejiang Province, China

Giorgina Mieli-Vergani, Professor
Institute of Liver Studies, King's College Hospital, Denmark Hill, London, SE5 9RS, United Kingdom

Dieter Glebe, PhD
Institute for Medical Virology, Justus Liebig University Giessen, Frankfurter Str. 107, Giessen 35392, Germany

Serdar Karakose, Dr, Professor
Department of Radiology, Meram Medical Faculty, Selcuk University, Konya 42080, Turkey

Ulf Hindorf, MD, PhD
Division of Gastroenterology, Department of Clinical Sciences, Faculty of Medicine, Lund University, SE-22185 Lund, Sweden

Giovanni D De Palma, Professor
Department of Surgery and Advanced Technologies, University of Naples Federico II, School of Medicine, Naples 80131, Italy

Indra Neil Guha, MD
Liver Group, University of Southampton, Mail Point 805, Level C, Southampton General Hospital, Southampton, SO16 6YD, United Kingdom

Richard A Rippe, Dr
Department of Medicine, The University of North Carolina at Chapel Hill, Chapel Hill, NC 27599-7038, United States

Mark A Feitelson, Dr
Pathology, Anatomy and Cell Biology of Thomas Jefferson University, Philadelphia 19107, United States

Ton Lisman, PhD
Thrombosis and Haemostasis Laboratory, Department of Haematology G.03.550, University Medical Centre, Heidelberglaan 100, 3584 CX Utrecht, The Netherlands

Jean Louis Frossard, Dr
Division of gastroenterology, Geneva University Hospital, Rue Micheli du Crest, 1211 Geneva 14, Switzerland

Paul Jonathan Ciclitira, Professor
The Rayne Institute (GKT), St Thomas' hospital, London NW32QG, United Kingdom

Francesco Feo, Professor
Dipartimento di Scienze Biomediche, Sezione di Patologia Sperimentale e Oncologia, Università di Sassari, Via P, Manzella 4, 07100 Sassari, Italy

Sri Prakash Misra, Professor
Gastroenterology, Moti Lal Nehru Medical College, Allahabad 211001, India

Anthony P Moran, Professor
Department of Microbiology, National University of Ireland Galway University Road Galway, Ireland

Leonidas G Koniaris, Professor
Alan Livingstone Chair in Surgical Oncology, 3550 Sylvester Comprehensive Cancer Center (310T), 1475 NW 12th Ave., Miami, FL 33136, United States

Meetings

MAJOR MEETINGS COMING UP

Meeting Falk Research Workshop: Morphogenesis and Cancerogenesis of the Liver
25-26 January 2007
Goettingen
symposia@falkfoundation.de

Meeting Canadian Digestive Diseases Week (CDDW)
16-20 February 2007
Banff-AB
cagoffice@cag-acg.org
www.cag-acg.org/cddw/cddw2007.htm

Meeting Falk Symposium 158: Intestinal Inflammation and Colorectal Cancer
23-24 March 2007
Sevilla
symposia@falkfoundation.de

Meeting BSG Annual Meeting
26-29 March 2007
Glasgow
www.bsg.org.uk/

NEXT 6 MONTHS

Meeting 42nd Annual Meeting of the European Association for the Study of the Liver
11-15 April 2007
Barcelona
easl2007@easl.ch
www.easl.ch/liver-meeting/

Meeting Falk Symposium 159: IBD 2007 - Achievements in Research and Clinical Practice
4-5 May 2007
Istanbul
symposia@falkfoundation.de

Meeting European Society for Paediatric Gastroenterology, Hepatology and Nutrition Congress 2007
9-12 May 2007
Barcelona
espghan2007@colloquium.fr

Digestive Disease Week
19-24 May 2007
Washington Convention Center, Washington DC

Meeting Gastrointestinal Endoscopy Best Practices: Today and Tomorrow, ASGE Annual Postgraduate Course at DDW
23-24 May 2007
Washington-DC
tkoral@asge.org

Meeting ESGAR 2007 18th Annual Meeting and Postgraduate Course
12-15 June 2007
Lisbon
fca@netvisao.pt

Meeting Falk Symposium 160: Pathogenesis and Clinical Practice in

Gastroenterology
15-16 June 2007
Portoroz
symposia@falkfoundation.de

Meeting ILTS 13th Annual International Congress
20-23 June 2007
Rio De Janeiro
www.ilts.org

Meeting 9th World Congress on Gastrointestinal Cancer
27-30 June 2007
Barcelona
meetings@imedex.com

EVENTS AND MEETINGS IN 2007

Meeting Falk Research Workshop: Morphogenesis and Cancerogenesis of the Liver
25-26 January 2007
Goettingen
symposia@falkfoundation.de

Meeting Canadian Digestive Diseases Week (CDDW)
16-20 February 2007
Banff-AB
cagoffice@cag-acg.org
www.cag-acg.org/cddw/cddw2007.htm

Meeting Falk Symposium 158: Intestinal Inflammation and Colorectal Cancer
23-24 March 2007
Sevilla
symposia@falkfoundation.de

Meeting BSG Annual Meeting
26-29 March 2007
Glasgow
www.bsg.org.uk/

Meeting 42nd Annual Meeting of the European Association for the Study of the Liver
11-15 April 2007
Barcelona
easl2007@easl.ch
www.easl.ch/liver-meeting/

Meeting Falk Symposium 159: IBD 2007 - Achievements in Research and Clinical Practice
4-5 May 2007
Istanbul
symposia@falkfoundation.de

Meeting European Society for Paediatric Gastroenterology, Hepatology and Nutrition Congress 2007
9-12 May 2007
Barcelona
espghan2007@colloquium.fr

Meeting Gastrointestinal Endoscopy Best Practices: Today and Tomorrow, ASGE Annual Postgraduate Course at DDW
23-24 May 2007
Washington-DC
tkoral@asge.org

Meeting ESGAR 2007 18th Annual Meeting and Postgraduate Course
12-15 June 2007
Lisbon
fca@netvisao.pt

Meeting Falk Symposium 160: Pathogenesis and Clinical Practice in Gastroenterology
15-16 June 2007
Portoroz
symposia@falkfoundation.de

Meeting ILTS 13th Annual International Congress
20-23 June 2007
Rio De Janeiro
www.ilts.org

Meeting 9th World Congress on Gastrointestinal Cancer
27-30 June 2007
Barcelona
meetings@imedex.com

Meeting 15th International Congress of the European Association for Endoscopic Surgery
4-7 July 2007
Athens
info@eaes-eur.org
congresses.eaes-eur.org/

Meeting 39th Meeting of the European Pancreatic Club
4-7 July 2007
Newcastle
www.e-p-c2007.com

Meeting XXth International Workshop on Heliobacter and related bacteria in cronic degistive inflammation
20-22 September 2007
Istanbul
www.heliobacter.org

Meeting Falk Workshop: Mechanisms of Intestinal Inflammation
10 October 2007
Dresden
symposia@falkfoundation.de

Meeting Falk Symposium 161: Future Perspectives in Gastroenterology
11-12 October 2007
Dresden
symposia@falkfoundation.de

Meeting Falk Symposium 162: Liver Cirrhosis - From Pathophysiology to Disease Management
13-14 October 2007
Dresden
symposia@falkfoundation.de

American College of Gastroenterology Annual Scientific Meeting
12-17 October 2007
Pennsylvania Convention Center Philadelphia, PA

Meeting APDW 2007 - Asian Pacific Digestive Disease Week 2007
15-18 October 2007
Kobe
apdw@convention.co.jp
www.apdw2007.org

15th United European Gastroenterology Week, UEGW
27-31 October 2007
Le Palais des Congrès de Paris, Paris, France

Meeting The Liver Meeting® 2007 - 57th Annual Meeting of the American Association for the Study of Liver Diseases

2-6 November 2007
Boston-MA
www.aasld.org

Gastro 2009, World Congress of Gastroenterology and Endoscopy London, United Kingdom 2009

Instructions to authors

GENERAL INFORMATION

World Journal of Gastroenterology (*WJG, World J Gastroenterol* ISSN 1007-9327 CN 14-1219/R) is a weekly journal of more than 48 000 circulation, published on the 7th, 14th, 21st and 28th of every month.

Original Research, Clinical Trials, Reviews, Comments, and Case Reports in esophageal cancer, gastric cancer, colon cancer, liver cancer, viral liver diseases, *etc.*, from all over the world are welcome on the condition that they have not been published previously and have not been submitted simultaneously elsewhere.

Indexed and abstracted in
Current Contents®/Clinical Medicine, Science Citation Index Expanded (also known as SciSearch®) and Journal Citation Reports/Science Edition, *Index Medicus*, MEDLINE and PubMed, Chemical Abstracts, EMBASE/ Excerpta Medica, Abstracts Journals, *Nature Clinical Practice Gastroenterology and Hepatology*, CAB Abstracts and Global Health. ISI JCR 2003-2000 IF: 3.318, 2.532, 1.445 and 0.993.

Published by
The WJG Press

SUBMISSION OF MANUSCRIPTS

Manuscripts should be typed double-spaced on A4 (297 mm × 210 mm) white paper with outer margins of 2.5 cm. Number all pages consecutively, and start each of the following sections on a new page: Title Page , Abstract, Introduction, Materials and Methods, Results, Discussion, acknowledgements, References, Tables, Figures and Figure Legends. Neither the editors nor the Publisher is responsible for the opinions expressed by contributors. Manuscripts formally accepted for publication become the permanent property of The WJG Press, and may not be reproduced by any means, in whole or in part without the written permission of both the authors and the Publisher. We reserve the right to put onto our website and copy-edit accepted manuscripts. Authors should also follow the guidelines for the care and use of laboratory animals of their institution or national animal welfare committee.

Authors should retain one copy of the text, tables, photographs and illustrations, as rejected manuscripts will not be returned to the author(s) and the editors will not be responsible for the loss or damage to photographs and illustrations in mailing process.

Online submission
Online submission is strongly advised. Manuscripts should be submitted through the Online Submission System at: http://www.wjgnet.com/index.jsp. Authors are highly recommended to consult the ONLINE INSTRUCTIONS TO AUTHORS (http://www.wjgnet.com/wjg/help/instructions.jsp) before attempting to submit online. Authors encountering problems with the Online Submission System may send an email you describing the problem to wjg@ wjgnet.com for assistance. If you submit your manuscript online, do not make a postal contribution. A repeated online submission for the same manuscript is strictly prohibited.

Postal submission
Send 3 duplicate hard copies of the full-text manuscript typed double-spaced on A4 (297 mm × 210 mm) white paper together with any original photographs or illustrations and a 3.5 inch computer diskette or CD-ROM containing an electronic copy of the manuscript including all the figures, graphs and tables in native Microsoft Word format or *.rtf format to:

Editorial Office
World Journal of Gastroenterology
Editorial Department: Apartment 1066, Yishou Garden,
58 North Langxinzhuang Road,
PO Box 2345, Beijing 100023, China
E-mail: wjg@wjgnet.com
http: //www.wjgnet.com
Telephone: +86-10-85381892
Fax: +86-10-85381893

MANUSCRIPT PREPARATION

All contributions should be written in English. All articles must be submitted using a word-processing software. All submissions must be typed in 1.5 line spacing and in word size 12 with ample margins. The letter font is Tahoma. For authors from China, one copy of the Chinese translation of the manuscript is also required (excluding references). Style should conform to our house format. Required information for each of the manuscript sections is as follows:

Title page
Full manuscript title, running title, all author(s) name(s), affiliations, institution(s) and/or department(s) where the work was accomplished, disclosure of any financial support for the research, and the name, full address, telephone and fax numbers and email address of the corresponding author should be included. Titles should be concise and informative (removing all unnecessary words), emphasize what is new, and avoid abbreviations. A short running title of less than 40 letters should be provided. List the author(s)' name(s) as follows: initial and/or first name, middle name or initial(s) and full family name.

Abstract
An informative, structured abstract of no more than 250 words should accompany each manuscript. Abstracts for original contributions should be structured into the following sections: AIM: Only the purpose should be included. METHODS: The materials, techniques, instruments and equipments, and the experimental procedures should be included. RESULTS: The observatory and experimental results, including data, effects, outcome, *etc*. should be included. Authors should present *P* value where necessary, and the significant data should accompany. CONCLUSION: Accurate view and the value of the results should be included.

The format of structured abstracts is at: http://www.wjgnet.com/wjg/ help/11.doc

Key words
Please list 5-10 key words that could reflect content of the study mainly from *Index Medicus*.

Text
For most article types, the main text should be structured into the following sections: INTRODUCTION, MATERIALS AND METHODS, RESULTS and DISCUSSION, and should include in appropriate Figures and Tables. Data should be presented in the body text or in Figures and Tables, but not in both.

Illustrations
Figures should be numbered as 1, 2, 3 and so on, and mentioned clearly in the main text. Provide a brief title for each figure on a separate page. No detailed legend should be involved under the figures. This part should be added into the text where the figures are applicable. Digital images: black and white photographs should be scanned and saved in TIFF format at a resolution of 300 dpi; color images should be saved as CMYK (print files) but not as RGB (screen-viewing files). Place each photograph in a separate file. Print images: supply images of size no smaller than 126 mm × 85 mm printed on smooth surface paper; label the image by writing the Figure number and orientation using an arrow. Photomicrographs: indicate the original magnification and stain in the legend. Digital Drawings: supply files in EPS if created by freehand and illustrator, or TIFF from photoshops. EPS files must be accompanied by a version in native file format for editing purposes. Existing line drawings should be scanned at a resolution of 1200 dpi and as close as possible to the size where they will appear when printed. Please use uniform legends for the same subjects. For example: Figure 1 Pathological changes of atrophic gastritis after treatment. A: ...; B: ...; C: ...; D: ...; E: ...; F: ...; G: ...

Tables
Three-line tables should be numbered as 1, 2, 3 and so on, and mentioned clearly in the main text. Provide a brief title for each table. No detailed legend should be included under the tables. This part should be added into the text where the tables are applicable. The information should complement but not duplicate that contained in the text. Use one horizontal line under the title, a second under the column heads, and a third below the Table, above any footnotes. Vertical and italic lines should be omitted.

Notes in tables and illustrations
Data that are not statistically significant should not be noted. $^aP<0.05$, $^bP<0.01$ should be noted ($P>0.05$ should not be noted). If there are other series of *P* values, $^cP<0.05$ and $^dP<0.01$ are used. Third series of *P* values can be expressed as $^eP<0.05$ and $^fP<0.01$. Other notes in tables or under

illustrations should be expressed as ^1F, ^2F, ^3F; or some other symbols with a superscript (Arabic numerals) in the upper left corner. In a multi-curve illustration, each curve should be labeled with ●, ○, ■, □, ▲, △, *etc.* in a certain sequence.

Acknowledgments

Brief acknowledgments of persons who have made genuine contributions to the manuscripts and who endorse the data and conclusions are included. Authors are responsible for obtaining written permission to use any copyrighted text and/or illustrations.

REFERENCES

Coding system

The author should code the references according the citation order in text in Arabic numerals, put references codes in square brackets, superscript it at the end of citation content or the author name of the citation. For those citation content as the narrate part, the coding number and square brackets should be typeset normally. For example, Crohn's disease (CD) is associated with increased intestinal permeability[1,2]. If references are directly cited in the text, they would be put together with the text, for example, from references [19,22-24], we know that...

When the authors code the references, please ensure that the order in text is the same as in reference part and also insure the spelling accuracy of the first author's name. Do not code the same citation twice.

PMID requirement

PMID roots in the abstract serial number indexed by PubMed (http://www.ncbi.nlm.nih.gov/entrez/query.fcgi?db=PubMed). The author should supply the PMID for journal citation. For those references that have not been indexed by PubMed, a printed copy of the first page of the full reference should be submitted.

The accuracy of the information of the journal citations is very important. Through reference testing system, the authors and editor could check the authors name, title, journal title, publication date, volume number, start page, and end page. We will interlink all references with PubMed in ASP file so that the readers can read the abstract of the citations online immediately.

Style for journal references

Authors: the first author should be typed in bold-faced letter. The surname of all authors should be typed with the initial letter capitalized and followed by their name in abbreviation (For example, Lian-Sheng Ma is abbreviated as Ma LS, Bo-Rong Pan as Pan BR). Title of the cited article and italicized journal title (Journal title should be in its abbreviation form as shown in PubMed), publication date, volume number (in black), start page, and end page [PMID: 11819634]

Note: The author should test the references through reference testing system (http://www.wjgnet.com/cgi-bin/index.pl)

Style for book references

Authors: the first author should be typed in bold-faced letter. The surname of all authors should be typed with the initial letter capitalized and followed by their name in abbreviation (For example, Lian-Sheng Ma is abbreviated as Ma LS, Bo-Rong Pan as Pan BR) Book title. Publication number. Publication place: Publication press, Year: start page and end page.

Format
Journals
English journal article (list all authors and include the PMID where applicable)

1   **Grover VP**, Dresner MA, Forton DM, Counsell S, Larkman DJ, Patel N, Thomas HC, Taylor-Robinson SD. Current and future applications of magnetic resonance imaging and spectroscopy of the brain in hepatic encephalopathy. *World J Gastroenterol* 2006; **12**: 2969-2978 [PMID: 16718775]

Chinese journal article (list all authors and include the PMID where applicable)

2   **Lin GZ**, Wang XZ, Wang P, Lin J, Yang FD. Immunologic effect of Jianpi Yishen decoction in treatment of Pixu-diarrhoea. *Shijie Huaren Xiaohua Zazhi* 1999; **7**: 285-287

In press

3   **Tian D**, Araki H, Stahl E, Bergelson J, Kreitman M. Signature of balancing selection in Arabidopsis. *Proc Natl Acad Sci U S A* 2006; In press

Organization as author

4   **Diabetes Prevention Program Research Group**. Hypertension, insulin, and proinsulin in participants with impaired glucose tolerance. *Hypertension* 2002; **40**: 679-686 [PMID: 12411462]

Both personal authors and an organization as author

5   **Vallancien G**, Emberton M, Harving N, van Moorselaar RJ; Alf-One Study Group. Sexual dysfunction in 1, 274 European men suffering from lower urinary tract symptoms. *J Urol* 2003; **169**: 2257-2261 [PMID: 12771764]

No author given

6   21st century heart solution may have a sting in the tail. *BMJ* 2002; **325**: 184 [PMID: 12142303]

Volume with supplement

7   **Geraud G**, Spierings EL, Keywood C. Tolerability and safety of frovatriptan with short- and long-term use for treatment of migraine and in comparison with sumatriptan. *Headache* 2002; **42** Suppl 2: S93-99 [PMID: 12028325]

Issue with no volume

8   **Banit DM**, Kaufer H, Hartford JM. Intraoperative frozen section analysis in revision total joint arthroplasty. *Clin Orthop Relat Res* 2002; (**401**): 230-238 [PMID: 12151900]

No volume or issue

9   Outreach: bringing HIV-positive individuals into care. *HRSA Careaction* 2002; 1-6 [PMID: 12154804]

Books
Personal author(s)

10   **Sherlock S**, Dooley J. Diseases of the liver and billiary system. 9th ed. Oxford: Blackwell Sci Pub, 1993: 258-296

Chapter in a book (list all authors)

11   **Lam SK**. Academic investigator's perspectives of medical treatment for peptic ulcer. In: Swabb EA, Azabo S. Ulcer disease: investigation and basis for therapy. New York: Marcel Dekker, 1991: 431-450

Author(s) and editor(s)

12   **Breedlove GK**, Schorfheide AM. Adolescent pregnancy. 2nd ed. Wieczorek RR, editor. White Plains (NY): March of Dimes Education Services, 2001: 20-34

Conference proceedings

13   **Harnden P**, Joffe JK, Jones WG, editors. Germ cell tumours V. Proceedings of the 5th Germ Cell Tumour Conference; 2001 Sep 13-15; Leeds, UK. New York: Springer, 2002: 30-56

Conference paper

14   **Christensen S**, Oppacher F. An analysis of Koza's computational effort statistic for genetic programming. In: Foster JA, Lutton E, Miller J, Ryan C, Tettamanzi AG, editors.   Genetic programming. EuroGP 2002: Proceedings of the 5th European Conference on Genetic Programming; 2002 Apr 3-5; Kinsdale, Ireland. Berlin: Springer, 2002: 182-191

Electronic journal (list all authors)

    Morse SS. Factors in the emergence of infectious diseases. Emerg Infect Dis serial online, 1995-01-03, cited 1996-06-05; 1(1): 24 screens. Available from: URL: http//www.cdc.gov/ncidod/EID/eid.htm

Patent (list all authors)

16   **Pagedas AC**, inventor; Ancel Surgical R&D Inc., assignee. Flexible endoscopic grasping and cutting device and positioning tool assembly. United States patent US 20020103498. 2002 Aug 1

Inappropriate references

Authors should always cite references that are relevant to their article, and avoid any inappropriate references. Inappropriate references include those that are linked with a hyphen and the difference between the two numbers at two sides of the hyphen is more than 5. For example, [1-6], [2-14] and [1, 3, 4-10, 22] are all considered as inappropriate references. Authors should not cite their own unrelated published articles.

Statistical data

Present as mean ± SD or mean ± SE.

Statistical expression

Express t test as t (in italics), F test as F (in italics), chi square test as χ^2 (in Greek), related coefficient as r (in italics), degree of freedom as γ (in Greek), sample number as n (in italics), and probability as P (in italics).

Units

Use SI units. For example: body mass, m (B) = 78 kg; blood pressure, p(B) = 16.2/12.3 kPa; incubation time, t (incubation) = 96 h, blood glucose concentration, c (glucose) 6.4 ± 2.1 mmol/L; blood CEA mass concentration, p (CEA) = 8.6 24.5 μg/L; CO_2 volume fraction, 50 mL/L CO_2 not 5% CO_2; likewise for 40 g/L formaldehyde, not 10% formalin; and mass fraction, 8 ng/g, *etc.* Arabic numerals such as 23, 243, 641 should be read 23 243 641.

The format about how to accurately write common units and quantum is at: http://www.wjgnet.com/wjg/help/15.doc

Abbreviations

Standard abbreviations should be defined in the abstract and on first mention in the text. In general, terms should not be abbreviated unless they are used repeatedly and the abbreviation is helpful to the reader. Permissible abbreviations are listed in Units, Symbols and Abbreviations: A Guide for Biological and Medical Editors and Authors (Ed. Baron DN, 1988) published by The Royal Society of Medicine, London. Certain commonly used abbreviations, such as DNA, RNA, HIV, LD50, PCR, HBV, ECG, WBC, RBC, CT, ESR, CSF, IgG, ELISA, PBS, ATP, EDTA, mAb, can be used directly without further mention.

Italics

Quantities: t time or temperature, c concentration, A area, l length, m mass, V volume.
Genotypes: *gyr*A, *arg* 1, *c myc, c fos, etc.*
Restriction enzymes: *Eco*RI, *Hin*dI, *Bam*HI, *Kbo* I, *Kpn* I, *etc.*
Biology: *H pylori, E coli, etc.*

SUBMISSION OF THE REVISED MANUSCRIPTS AFTER ACCEPTED

Please revise your article according to the revision policies of *WJG*. The revised version including manuscript and high-resolution image figures (if any) should be copied on a floppy or compact disk. Author should send the revised manuscript, along with printed high-resolution color or black and white photos, copyright transfer letter, the final check list for authors, and responses to reviewers by a courier (such as EMS) (submission of revised manuscript by e-mail or on the *WJG* Editorial Office Online System is NOT available at present).

Language evaluation

The language of a manuscript will be graded before sending for revision. (1) Grade A: priority publishing; (2) Grade B: minor language polishing; (3) Grade C: a great deal of language polishing; (4) Grade D: rejected. The revised articles should be in grade B or grade A.

Copyright assignment form

Please downloaded CAF from http://www.wjgnet.com/wjg/help/9.doc.
    We certify that the material contained in this manuscript:

Ms:

Title:

is original, except when appropriately referenced to other sources, and that written permission has been granted by any existing copyright holders. We agree to transfer to WJG all rights of our manuscript, including: (1) all copyright ownership in all print and electronic formats; (2) the right to grant permission to republish or reprint the stated material in whole or in part, with or without a fee; (3) the right to print copies for free distribution or sale; (4) the right to republish the stated material in a collection of articles or in any other format. We also agree that our article be put on the Internet.

Criteria for authorship: The WJG requests and publishes information about contributions of each author named to the submitted study. Authorship credit should be based on (1)direct participation in the study, including substantial contributions to conception and design of study, or acquisition of data, or analysis and interpretation of data; (2) manuscript writing, including drafting the article, or revising it critically for important intellectual content; (3)supportive work, including statistical analysis of data, or acquisition of funding, or administration, technology and materials support, or supervision, or supportive contributions. Authors should meet at least one of the three conditions. The WJG does not publish co-first authors and co-corresponding authors.

    We hereby assign copyright transfer to WJG if this paper is accepted.

    Author Name in full (Full names should be provided, with first name first, followed by middle names and family name at the last, eg, Eamonn MM Quigley). Handwritten names are not accepted.

    Author Name in abbreviation (Family name is put first in full, followed by middle names and first name in abbreviation with first letter in capital, eg, Quigley EMM). Handwritten names are not accepted.

Final check list for authors

The format is at: http://www.wjgnet.com/wjg/help/13.doc

Responses to reviewers

Please revise your article according to the comments/suggestions of reviewers. The format for responses to the reviewers' comments is at: http://www.wjgnet.com/wjg/help/10.doc

1 Full Name: _____
   Abbreviation Name: _____
   Signed: _____
   Date: _____

2 Full Name: _____
   Abbreviation Name: _____
   Signed: _____
   Date: _____

3 Full Name: _____
   Abbreviation Name: _____
   Signed: _____
   Date: _____

4 Full Name: _____
   Abbreviation Name: _____
   Signed: _____
   Date: _____

5 Full Name: _____
   Abbreviation Name: _____
   Signed: _____
   Date: _____

6 Full Name: _____
   Abbreviation Name: _____
   Signed: _____
   Date: _____

7 Full Name: _____
   Abbreviation Name: _____
   Signed: _____
   Date: _____

8 Full Name: _____
   Abbreviation Name: _____
   Signed: _____
   Date: _____

9 Full Name: _____
   Abbreviation Name: _____
   Signed: _____
   Date: _____

10 Full Name: _____
   Abbreviation Name: _____
   Signed: _____
   Date: _____

Proof of financial support

For paper supported by a foundation, authors should provide a copy of the document and serial number of the foundation.

Publication fee

Authors of accepted articles must pay publication fee.
EDITORIAL and LETTERS TO THE EDITOR are free of change.